5-2005

Relating Bedrock Strength to Hydraulic Driving Forces along the Large-Scale Profile of the Colorado River in Glen and Grand Canyons

Rob D. Mackley
Utah State University

RELATING BEDROCK STRENGTH TO HYDRAULIC DRIVING FORCES ALONG

THE LARGE-SCALE PROFILE OF THE COLORADO RIVER

IN GLEN AND GRAND CANYONS

by

Rob D. Mackley

A thesis submitted in partial fulfillment
of the requirements for the degree

of

MASTER OF SCIENCE

in

Geology

UTAH STATE UNIVERSITY
Logan, Utah

2005

ABSTRACT

Relating Bedrock Strength to Hydraulic Driving Forces along

the Large-Scale Profile of the Colorado River

in Glen and Grand Canyons

by

Rob D. Mackley, Master of Science

Utah State University

Major Professor: Dr. Joel L. Pederson
Department: Geology

The role of bedrock on the longitudinal profile of the Colorado River has

intrigued workers for over a century. The river's profile exhibits large-scale (10 to 100

km) variations in geomorphology that are qualitatively associated with changes in rock

type. This study provides the first bedrock-strength data to quantitatively test the relation

of bedrock-resisting to hydraulic-driving forces in Glen and Grand canyons. The intent

of this study is to explore the role, if any, that bedrock has on large-scale geomorphic

variations along the profile of the Colorado River. Rock-strength data collected at 84

sites along the river corridor in Glen and Grand canyons include intact-rock strength,

fracture spacing, and other characteristics associated with Selby rock-mass strength

(RMS). These strength data were statistically related to measurements of channel width,

gradient, and calculations of unit stream power.

At the canyon scale (100 km), rocks in Grand Canyon have significantly higher intact-rock strength, lower fracture spacing, and higher RMS than those in Glen Canyon. These observations correspond to the fact that Grand Canyon is steeper and narrower, and has greater mean unit stream power. Furthermore, smaller scale, reach-average values of rock strength correlate significantly to width, gradient, and unit stream power, although there are outliers related to local-scale effects such as rapids. The Colorado River runs in a narrower and steeper channel in reaches confined by resistant bedrock (e.g., Upper Granite Gorge, RM 77-114). In contrast, reaches floored in weaker bedrock (e.g., lower Marble Canyon, river miles 37 to 58) are associated with wider channels and lower gradient.

This study confirms previous research linking rock type to the geomorphology of the Colorado River. Results imply that knickzones in the profile are persistent features that reflect a dynamic equilibrium between hydraulic-driving and bedrock-resisting forces, rather than transient waves of incision due to tectonics or drainage integration. They support the hypothesis that bedrock sets the long-term, large-scale template for the Colorado River. Bedrock hypothetically acts as a direct control on the river's width and gradient, particularly when the river is in contact with bedrock. Rock-strength and weathering properties of bedrock within tributary catchments, where debris flows initiate, act as an indirect control through their influence on hillslope-to-river sediment production during episodes, such as today, when the river is not on bedrock.

(173 pages)

ACKNOWLEDGMENTS

CONTENTS

LIST OF TABLES

LIST OF FIGURES

INTRODUCTION

The longitudinal profile of the Colorado River records the dynamic interplay between fluvial driving and resisting forces and provides insight on the erosion of the Colorado Plateau. The river's profile is broadly convex from upper Glen Canyon to lower Grand Canyon and is marked by smaller-scale variations in gradient (Figure 1). Powell (1876) made a general observation that the river's "mood" closely corresponded to the type of bedrock encountered at river-level. He hypothesized that harder and more resistant bedrock imposes a control on the river, causing certain canyons and reaches to be to be relatively narrower and steeper. Subsequent workers have not directly tested Powell's hypothesis; however they have stressed the importance of debris fans and coarse bed material in explaining the gradient of the Colorado River in Grand Canyon, particularly at the rapid-pool scale (0.1 to 1 km). Despite the excellent work thus far on the geomorphology of the Colorado River, the degree to which river-level bedrock either directly or indirectly influences the Colorado River at large spatial scales (10 to 100 km) is still unresolved and deserves further attention.

Some of the confusion and debate over the controls on gradient may be due, in part, to differences in the time and space scales at which various workers consider processes. For example, local-scale (1 km) variations that take place from rapids to pools are controlled by coarse debris from tributary side-canyons (e.g., Leopold, 1969; Howard and Dolan, 1981; Kieffer, 1985; Webb et al., 1989). However, on a larger spatial scale, the profile has variations in gradient, width, and other geomorphic parameters at 10 to 100 km reach lengths.
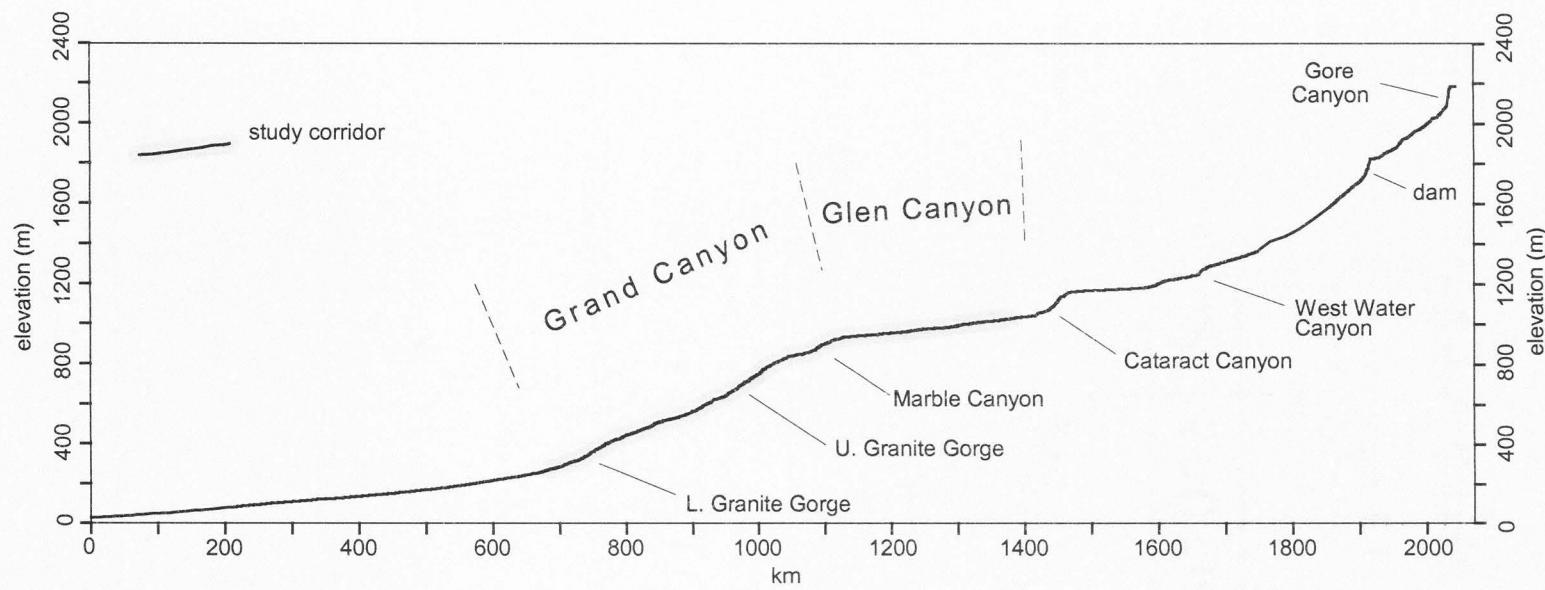
Figure 1. Longitudinal profile of the Colorado River from the Arizona-Sonora, Mexico border to Kremmling, CO. Note difference in gradient between Glen and Grand canyons. The data for this profile were obtained and digitized from multiple surveys conducted by the USGS during the 1920's and 1950's. The density of data varies, but has an average horizontal spacing of 1.5 km (0.9 mi).

The controls on these large-scale variations remain undefined, with some arguing that large-scale variations are due to broad aggradation (e.g., Grams and Schmidt, 1999; Hanks and Blair, 2003), while others attribute it to drainage integration, tectonics, or spatially varying rock-types (e.g., Wagner and Karlstrom, 2002; Coblentz and Karlstrom, 2003; Pederson et al., 2003; Karlstrom and Kirby, 2004; Wolkowinsky and Granger, 2004).

It is possible that the principal controls on the river's profile might also likely vary with the time scale being considered. It is unclear what the role has been, if any, for coarse debris input in the more distant geologic past during fluctuations in climate-controlled sediment production and transport (e.g., Webb et al., 2003; Hanks and Blair, 2003; Pederson et al., 2003). Sequences of inset Pleistocene fill terraces show that the river has gone through high amplitude changes that involve geomorphic and sedimentological conditions different than today (Lucchitta et al., 2000; Anders, 2003). The river has oscillated between being an alluvial system undergoing valley-filling to an incising bedrock river over glacial-interglacial cycles. During these bedrock river episodes, the mechanical properties of river-level bedrock would be important and may set the large-scale profile template for the river. Laboratory and field observations support this notion, showing that bedrock resistance exerts a measurable control on erosion rates and the form of bedrock streams (e.g., Wohl and Merritt, 2001; Sklar and Dietrich, 2001).

The overall goal of this study was to explore the role, if any, that river-level bedrock has on large-scale (10-100 km) gradient variations in the long-profile of the

Colorado River. This is the first, direct testing of Powell's qualitative hypothesis. This was tested across both Glen and Grand canyons, which have contrasting rock types, channel gradients, and widths. Data sets were generated through the gathering of multiple hydraulic (driving) and bedrock (resisting) data through field and laboratory work (GIS). This research quantitatively links geologic controls to geomorphic variables at regional-scales. Furthermore, it tests the possibility that the template of reach and canyon-scale gradients is set during episodes of bedrock incision when the river is adjusted to the bedrock that confines it (Pederson et al., 2003).

TOPICAL BACKGROUND

Longitudinal Stream Profiles

The longitudinal profile of a stream reflects its adjustment to tectonic, geologic, and climatic conditions imposed on it. The modern view of long profiles began with the concept of the "graded" stream. Mackin (1948) originally championed the concept of a graded river, one in which river gradient is adjusted to provide sufficient transport of its sediment load such that the river neither aggrades nor incises, but is said to maintain a state of dynamic equilibrium through time under steady boundary conditions (Leopold and Bull, 1979). Equilibrium or graded profiles were originally thought of as those with a concave-up profile; however, the graded condition does not require longitudinal profiles to be concave (Miller, 1991). Knox (1976, p. 194) suggested that a graded stream be redefined as "one in which the relationship between process and form is stationary and the morphology of the system remains relatively constant over time." This definition does not specify that any particular channel geometry or profile is required for a graded stream, only that there is a balance between erosion and deposition (Knox, 1976).

Field observations and modeling results have demonstrated profiles are more concave when there are downstream decreases in bed-material size and/or increases in water discharge (e.g., Hack, 1957: Snow and Slingerland, 1987). In alluvial rivers, discharge, sediment load, and sediment size are the dominant influences on stream gradient.

Lane (1955) summarized the relation between slope, (S), sediment load, (Q_s), median grain diameter of bed-material, (D_{50}), and discharge, (Q) as:

$$S \sim \frac{Q_s D_{50}}{Q} \qquad (1)$$

Discharge has been empirically shown to have a crude negative correlation to channel gradient (Bray, 1982; Hey and Thorn, 1986). The most direct control on an alluvial river's gradient is bed-material size, with increases in slope corresponding to increases in grain size (e.g., Hack, 1957; Knighton, 1998). For example, the Colorado River's gradient increases at debris fan constrictions (rapids) in Grand Canyon to adjust for coarser bed material (e.g., Kieffer, 1985; Webb et al., 1989).

The concept of the graded stream and other prevalent views of long-profile controls have been most frequently cast in the context of alluvial streams, where adjustments in channel gradient are a response to generate sufficient competence (critical shear stress) to transport the supplied bedload. Pazzaglia et al. (1998) make the point that bedrock and mixed-bedrock rivers, in contrast, must generate the shear stress to maintain incision across variably resistant rocks in addition to transporting their sediment. For this reason, bedrock is a major influence on channel gradient for bedrock streams, even when they contain patches of alluvium and alluvial reaches (e.g., Hack, 1957; Knighton, 1976; Gardner, 1983; Miller, 1991; Wohl et al., 1994; Pazzaglia et al., 1998, Whipple et al., 2000a; Snyder et al., 2003). Brush (1961) and Hack (1957) both found systematic differences in streams in the eastern United States flowing across different rock types, with more intuitively resistant bedrock associated with lower profile concavity and steeper gradient. The lower Susquehanna River and neighboring streams in the eastern

United States exhibit steeper gradients where they encounter resistant amphibolite-grade

metamorphic rocks (Pazzaglia et al., 1998). These ideas are analogous to Powell's

(1876) hypothesis that variations in rock type and erodibility influence the gradient of the

Colorado River in Grand Canyon.

Knickzones

Many rivers, including the Colorado River, do not have smooth profiles, but have

knickzones or knickpoints. These can be caused by baselevel fall, resistant bedrock, or

locally coarse bedload. Physical modeling of knickpoint behavior by Gardner (1983)

illustrated that the upstream migration of knickpoints through the fluvial system over

time is dependent on the characteristics of the bedrock encountered. Knickzones can also

be observed in areas where there has been no recent tectonic activity. Miller (1991)

related knickpoints developed along streams in an area of tectonic quiescence in south

central Indiana to changes in stratigraphic and structural characteristics. This highlights

the fact that knickpoints do not necessary reflect disturbances (e.g., faulting), but can be

stable features of a river's profile reflecting a dynamic equilibrium between driving and

resisting forces.

Recently Coblentz and Karlstrom (2003) proposed that the steep increase in

gradient downstream of Lees Ferry, AZ is a knickzone formed by tectonic baselevel drop.

They speculate that it is a transient feature, slowly working its way up the Colorado River

drainage (Coblentz and Karlstrom, 2003). Pederson et al. (2002) argue, however, that

this is geometrically impossible in the case of the Hurricane and Toroweap faults located

in western Grand Canyon. Faulting in western Grand Canyon has not increased incision

rates upstream of the fault, but rather, it has dampened incision downstream of the fault since background incision rates outpace the rate of slip (Pederson et al., 2002).

Hanks and Blair (2003) argue that reach-scale (10 km) convexities, or reaches of relatively lower gradient, within Grand Canyon (Figure 1) are the result of broad aggradation within reaches containing tributaries that have more debris flows during late Holocene time (Hanks and Blair, 2003). This is consistent with the recognition by Grams and Schmidt (1999) that large-scale convexities along the Green River's profile within Lodore Canyon, Utah are caused by coarse debris fans. On the other hand, Pederson et al. (2003) point out that the Colorado River's gradient seems to change in a logically consistent manner as the river flows between reaches floored in different rock types (Figure 2), an echo of Powell's original hypothesis. Thus, several explanations exist for gradient variations along the Colorado River's profile.

Hydraulic Driving and Bedrock Resisting Forces

It is useful in the discussion of fluvial incision to speak in terms of driving and resisting forces. One expression of the hydraulic driving forces that erode and transport sediment in the fluvial system is unit stream power:

$$\Omega = \frac{\gamma Q S}{w} \tag{2}$$

where ω is stream power per unit area [watt/m^2], γ is the specific weight of the fluid [N/m^3], Q is discharge [m^3/s], S is slope [m/m], and w is bed width [m]. The ability to transport bed material or erode the channel's substrate increases exponentially once a threshold for motion is exceeded.
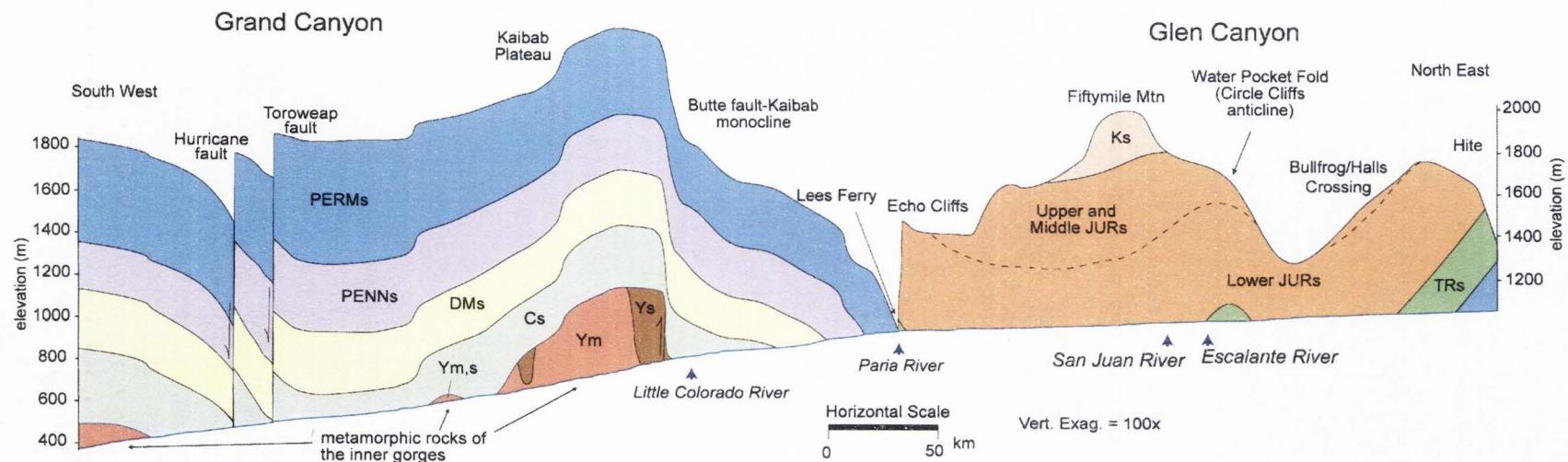
Figure 2. Schematic cross-section showing major structures and simplified bedrock geology encountered by the Colorado River along the study corridor. The longitudinal profile (solid blue line) and major tributary rivers are included (blue arrows). Note, the geology is grouped according to period, with sedimentary and metamorphic/igneous units designated with an "s" or "m" suffix, respectively (e.g. Permian sedimentary rocks = PERMs). Key: Cretaceous (K), Jurassic (JUR), Triassic (TR), Permian (PERM), Pennsylvanian (PENN), Devonian – Mississippian (DM), Cambrian (C), undifferentiated Precambrian (Y).

Several components combine to control a river's ability to flow, transport sediment, and erode into bedrock. First of all, internal fluid shear, the roughness of the bed grains (skin friction), energy loss due to separation of flow from bedforms (form loss), irregularities in channel geometry, and vegetation all contribute to the overall flow resistance (Knighton, 1998). Size and amount of sediment in transport exerts a strong, but nonlinear, control on erosion. Theoretical (Slingerland et al., 1997; Sklar and Dietrich, 1998) and experimental (Sklar and Dietrich, 2001) observations both confirm G.K. Gilbert's (1877) original hypothesis: there is an optimum flux and caliber of bedload acting as abrasive tools which maximize erosion of the bed. In reverse, too much or too coarse sediment in relation to available transporting capacity is predicted to shield the bed with alluvium, reducing incision.

In the case of bedrock and mixed bedrock-alluvial channels, channel substrate properties play an important role in resisting both vertical and lateral erosion (Pazzaglia et al., 1998; Whipple et al., 2000a; Wohl and Merritt, 2001). There is a growing body of literature presenting evidence for the relation between fracture spacing, cementation, and rock strength to bedrock channel form and resistance (e.g., Wohl et al., 1994; Hancock et al., 1998; Sklar and Dietrich, 1998; Whipple et al., 2000a; Wohl and Merritt, 2001; Sklar and Dietrich; 2001; Snyder et al., 2003). Bedrock that is well-cemented, dense, and has widely-spaced fractures exhibits increased resistance to plucking and abrasion, as blocks are either immovably large or wear down more slowly. In essence, resistant rocks require greater energy expenditure to maintain erosion, resulting in increased gradient or channel narrowing.

11

A common approach to quantifying rock erodibility for rivers is adapted from the Selby rock-mass strength (RMS) scale, a method originally employed for analyzing hillslopes (e.g., Allison et al., 1993; Moon, 1984; Selby, 1980,1982, 1993). It is an adaptation from previous rock-mass classification systems used by engineers for mining, tunneling, and quarrying (e.g., Bieniawski, 1976) where classifications are made in the field and don't require drilling or testing core samples. Selby's RMS index semi-quantitatively summarizes the collective effects of weathering, joint spacing, joint orientation, joint continuity, joint width, groundwater outflow, and intact-rock strength. Intact-rock strength is measured with a Schmidt hammer, an *in situ* non-destructive instrument originally used to measure the strength of concrete (Schmidt, 1951).

The Schmidt hammer measures the rebound distance of a known mass impacting on a rock surface, and these are correlated with laboratory measured values of Young's modulus, uniaxial compressive strength, and density for a variety of rock types (e.g., Day and Goudie, 1977; Pool and Farmer, 1980; Goktan and Ayday; 1993; Katz et al., 2000). Values obtained near discontinuities or on thinly bedded rocks dramatically underestimate the true intact-rock strength. In addition, Sklar and Dietrich (2001) contend that tensile strength, rather than compressive strength, is a better measure of a rock's resistance to erosion, especially when the dominant erosion process is abrasion. However, abrasion is not generally considered to be as effective in fluvial erosion as hydraulic plucking – a process limited more by the spacing of discontinuities in the rock rather than its strength (e.g., Hancock et al., 1998; Whipple et al., 2000a). In terms of modeling abrasion, the Schmidt hammer, involving the rapid impacting of a rigid object

against a rock surface, might be considered superior over tensional tests conducted in a laboratory. In any case, hydraulic plucking or abrasion by suspended grains or bedload bashing are mechanically complex processes that likely depend upon the combined tensional and compressional properties of all objects involved.

The Selby RMS scoring involves ranking bedrock units semi-quantitatively according to classifications based on field measurements. This system has advantages over methods in which rock-units are not ranked according to field or laboratory data. Relevant both topically and regionally, Harden (1990) studied the controls on the geometry and distribution of incised meanders on the central Colorado Plateau by the Green, San Juan, and Colorado Rivers. Bedrock resistance was included as a potential factor, organized into an ordinal scale from 1 to 9. Shales and other rocks considered "easily erodible" were ranked lower relative to "harder" limestones, massive sandstones, and quartzites. The results indicated a statistical correlation between strength rankings and meander form. However, ranking bedrock units without field or laboratory data introduces an unquantifiable amount of error and is not the best scenario for running rigorous statistical tests. It may also be biased toward intact strength rather than fracturing, in that rocks perceived to be hard actually may be very erodible if fractured or weathered.

Stream Power Erosion Models

There is an increasing need to quantify bedrock resistance variables for landscape evolution studies. Many numerical landscape evolution models employ a detachment-limited bedrock incision rate (E) that is based on a stream power erosion rule, setting

incision into bedrock proportional to excess stream power (e.g., Howard and Kerby, 1983; Howard et al., 1994; Whipple et al., 2000b). This is commonly expressed as:

$$E = KA^m S^n \qquad (3)$$

where A is contributing drainage area, S is channel slope, and K is the so-called bedrock erodibility factor. K, a dimensional coefficient, lumps an unknown number of resistive factors such as bedrock strength and alluvial armoring of the bed. It is usually parameterized by numerical solution rather than from field or laboratory data (e.g., Stock and Montgomery, 1999).

Several studies have successfully employed stream power models to reproduce reasonable river profiles (e.g., Howard and Kerby, 1983; Howard et al., 1994; Stock and Montgomery, 1999; Whipple et al., 2000b). However, some modeled profiles do not match observed profiles in nature using a single value for K, due to changes in bedrock, sediment input, structural trends, and the location of tectonic knickpoints (Stock and Montgomery, 1999; Whipple et al., 2000b). Stock and Montgomery (1999) present a comparative list of K values for rivers eroded into various rock types in different regions of the world. Easily erodible mudstones in Japan have K values five orders of magnitude lower than granitoids and metamorphic rocks in California (Stock and Montgomery, 1999). The comparisons also show a 2-3 order-of-magnitude range for K in rocks of similar type sampled in a single region. This may be because 1) K values are influenced by different parameterizations of m and n despite their assumed independence, 2) K lumps an unknown number of unspecified variables, or 3) rock-strength properties in these units vary significantly within the same region. This has lead some workers to ask

which parameters are necessary to calibrate *K* in a consistent and independent manner

(e.g., Whipple et al., 2000b). An improved understanding of landscape evolution,

including numerical models of incision, requires a more rigorous quantification of rock

strength.
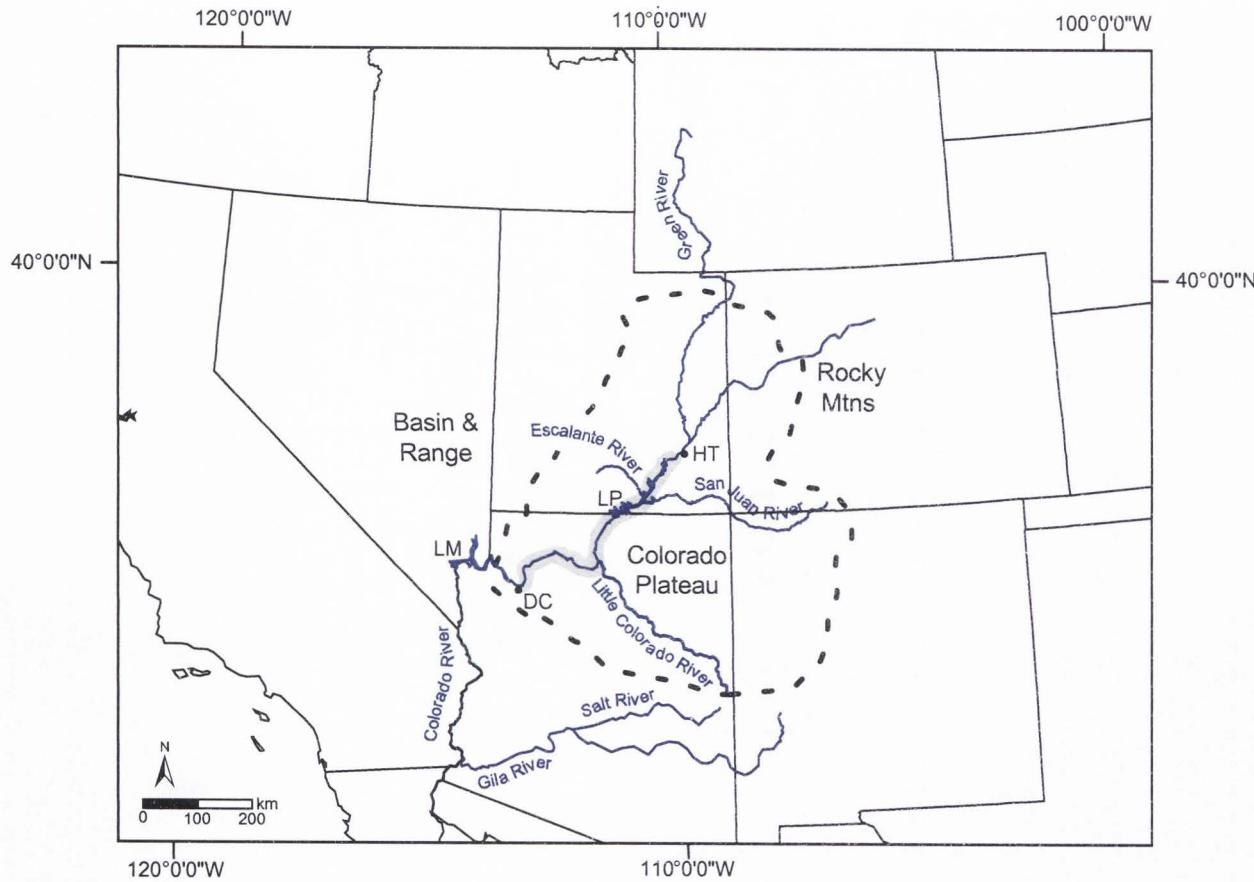
Figure 3. Regional map of the interior-western United States showing the Colorado River, major tributaries, physiographic provinces, and Lake Mead (LM) and Lake Powell (LP). The study area, outlined in gray, includes the river corridor in Glen and Grand canyons, beginning at Hite, UT and ending near the mouth of Diamond Creek (DC) in western Grand Canyon (RM 225).

GEOLOGIC SETTING

The Colorado Plateau physiographic province is bordered on the west by the Basin and Range province and on the east by the Rocky Mountains (Figure 3). The plateau was a long-lived Paleozoic and Mesozoic basin underlain by Precambrian metamorphic rock, and it is typified by relatively subtle structural deformation compared to neighboring areas. The Colorado River encounters Laramide faults, monoclines, and basins in its course across the plateau. This study focuses on the Colorado River corridor between Hite Crossing in southern Utah and the mouth of Diamond Creek (RM 225) in western Grand Canyon, northwestern Arizona (Figure 3). Studying both Glen and Grand canyons provides a contrast between two canyon-scale reaches with different longitudinal profiles, rock types, and structural characteristics.

Bedrock Geology

The geology of the plateau in the vicinity of the study area consists of very thick sequences of slightly deformed Paleozoic and Mesozoic sedimentary units lying unconformably over Precambrian crystalline and subordinate sedimentary rocks. The basement rocks exposed in the inner gorges of Grand Canyon include Proterozoic granites, metavolcanic, and metasedimentary rocks (Figure 4). Ilg et al. (1996) proposed the name of Granite Gorge Metamorphic Suite for the variety of quartz, mica, and felsdspar bearing schists in Grand Canyon and subdivided them into the Brahma Schist, Rama Schist, and Vishnu Schist based on protolith and composition.

Intrusive rocks make up the other half of the crystalline basement, consisting mostly of granites, granodiorites, and granitic pegmatites (Karlstrom et al., 2003). Some of the syncollisional intrusives contain weak to moderate foliation of minerals related to deformation events, and are commonly referred to as "gneisses."

Ilg et al. (1996) have stressed the need to subdivide the crystalline basement units based on petrology, geochemistry, and age for tectonic significance (Ilg et al., 1996); however reconnaissance field investigations suggest they have very similar mechanical properties. For the purposes of this study, all metamorphic and intrusive rocks were grouped into the Vishnu Schist and Zoroaster Granite, respectively, after early references to these same rocks (e.g., Walcott, 1889; Campbell and Maxson, 1938; Brown et al., 1979).

The Grand Canyon Supergroup, lies unconformably over the crystalline basement in some places, and is separated by a 700 million year unconformity (Figure 4). It is a thick sequence (~ 4 km) of siliciclastic and carbonate sedimentary rocks that are generally tilted to the northwest and subdivided into the Unkar Group, Nankoweap Formation, Chuar Group, and Sixtymile Formation. The Unkar Group consists of the Bass Limestone, Hakatai Shale, Shinumo Quartzite, Dox Formation, and Cardenas Basalt. The basal Bass Limestone is chiefly dolomite, generally forming cliffs. The Hakatai Shale is a red, purple, and orange colored unit composed of slope-forming mudstones, shales, and cliff-forming sandstones (Ford and Dehler, 2003). The Shinumo Quartzite forms massive cliffs of resistant sandstones and quartzites.
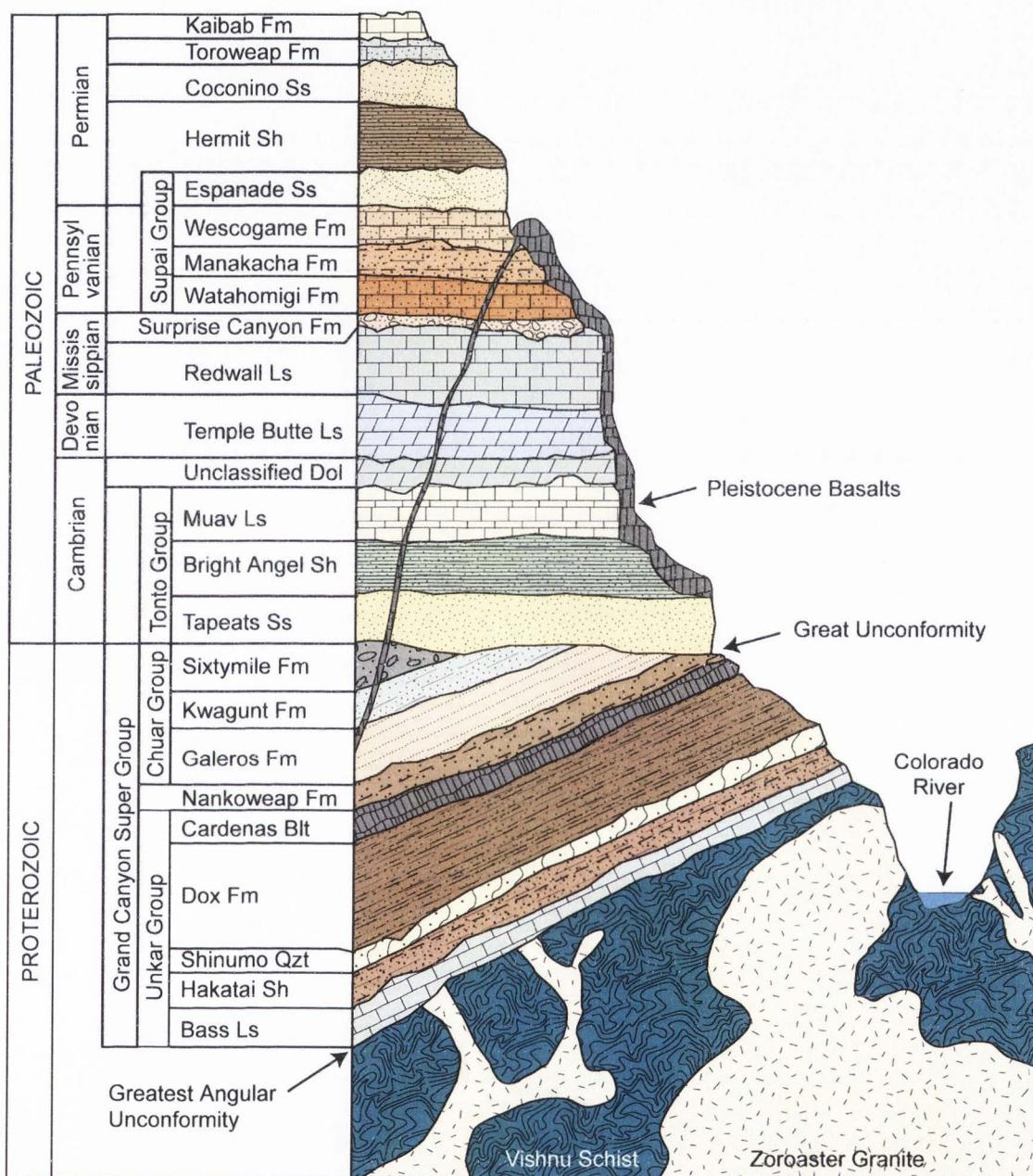
Figure 4. Generalized stratigraphy of rocks exposed along Colorado River corridor in Grand Canyon (after Melis, 1997)

The Dox Formation, the uppermost and thickest formation of the Unkar Group, is a lithologically heterogeneous unit consisting mainly of slope and cliff-forming siltstones, mudstones, shales, sandstones (Figure 4). The Cardenas Basalt is a series of basalt and basaltic andesite flows. Although highly altered, the Cardenas forms cliffs and steep slopes.

It is important to note that although the Nankoweap Formation, Chuar Group, and Sixtymile Formation are exposed just west of the main-stem of the river, they are not stratigraphically preserved along the Colorado River study corridor due to Precambrian erosion (Ford & Dehler, 2003; Hendricks & Stevenson, 2003).

The Tonto Group of Cambrian sandstones, shales, and limestones unconformably overlie either the Unkar Group or Proterozoic crystalline basement, depending upon the amount of Precambrian erosion (Figure 4). Formations in the Tonto Group include the Tapeats Sandstone, Muav Limestone, and Bright Angel Shale. The Tapeats contains fluvial sandstone and conglomerates that form ledgy cliffs, whereas the Muav and Bright Angel are composed of limey shales and shaley limestones, respectively (Middleton and Elliott, 2003).

Uppermost Cambrian, Ordovician, and Silurian rocks are missing in northern Arizona. The remainder of the Paleozoic rocks preserved in the vicinity of Grand Canyon begins at the base of the middle Devonian Temple Butte Formation where an erosion surface truncates the Cambrian section (Figure 4). The dolomite of the Temple Butte Formation, which thickens considerably to the west, conformably merges into the overlying Redwall Limestone, making it a relatively inconspicuous unit (Beus, 2003a).

The Redwall Limestone, on the other hand, is a very visually and topographically prominent rock-unit of Mississippian age. It forms massive vertical cliffs ~200 m high, stained red by iron oxides washing down from the overlying Supai Group (Beus, 2003b).

The Pennsylvanian to early Permian Supai Group is subdivided into four formations, the Watahomigi, Manakacha, Wescogame, and Esplanade (Blakey, 2003). The Watahomigi Formation, generally a slope former, is composed of intercalated red mudstones and siltstones with a few ledges of gray carbonate. The Manakacha Formation forms alternating slopes and cliffs, consisting of fluvial and eolian quartz sandstones (ledges) and red mudstones (slopes). The Wescogame Formation, stratigraphically next, is very similar in lithology and topographic expression to the Manakacha Formation. The Esplanade Sandstone, interpreted as eolian in origin, forms prominent cliffs below the overlying smooth slopes of the Hermit Formation (Blakey, 2003).

The Hermit Formation is a thick (60-200 m) package of Permian-aged siltstones and mudstones that are poorly exposed (Figure 4). It forms a distinctive broad slope between resistant cliffs of underlying Esplanade Sandstone and the overlying Coconino Sandstone. The Coconino Sandstone is a conspicuous layer of cross-bedded sandstones deposited as a series of eolian dunes (Blakey, 2003). The Toroweap and Kaibab formations, both Permian-aged units dominated by carbonates, are the uppermost Paleozoic units in the region. The Toroweap Formation is lithologically diverse unit, with the lower half forming massive gray cliffs of limestone and dolomite, whereas the upper portion is slope-forming gypsum, limestone, and sandstone (Turner, 2003).
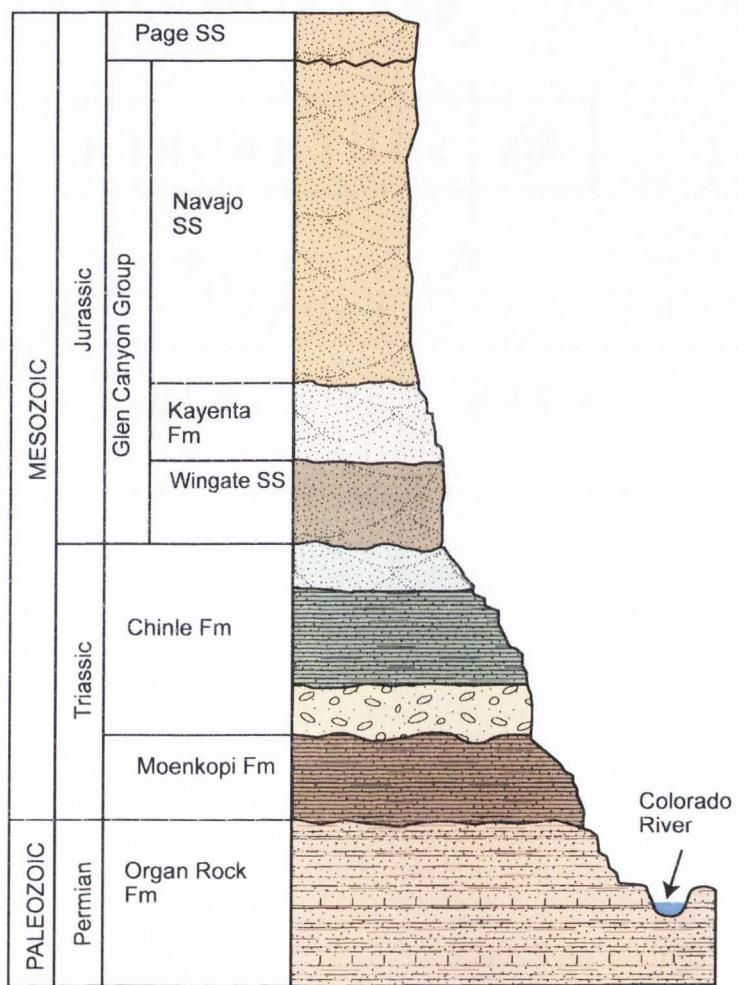
Figure 5. Generalized stratigraphy of rocks exposed along Colorado River corridor in Glen Canyon.

The Kaibab Formation forms the physiographic rim of the Grand Canyon. The lower to middle Kaibab in eastern Grand Canyon is predominantly dolomite with nodules of chert, forming prominent cliffs, while the upper Kaibab is a series of receding ledges of cherty dolomite and limestone with lesser amounts of gypsum and sandstone (Hopkins and Thompson, 2003).

Mesozoic sedimentary rocks begin to outcrop between Glen and Grand Canyon near Lees Ferry, Arizona. The variegated shales and siltstones of the Triassic Moenkopi, and Chinle Formations form unstable slopes near Lees Ferry. From the Vermillion Cliffs north to Hall's Crossing, Glen Canyon is dominated by the Jurassic Glen Canyon Group of eolian and fluvial sandstones (Figure 5). This includes the Wingate and Kayenta Formations and the massive, cross-bedded Navajo and Page sandstones. In the far northeastern study area near Hite Crossing, UT, the Permian Organ Rock Formation underlies the Moenkopi Formation instead of the Kaibab, as in the Grand Canyon area. It is dominated by shales, siltstones, and sandstones that form steep slopes and cliffs.

The structural template of the region is chiefly the expression of Laramide uplift and compression (Late Cretaceous through Eocene), which is responsible for several north-south trending monoclines and anticlines. Laramide monoclines are cored by high-angle reverse faults developed on reactivated Precambrian normal faults, having up to 750 meters of reverse offset along the East Kaibab monocline (Huntoon, 2003). Laramide structures in the vicinity of Grand Canyon, from west to east, include the Meriwhitica, Lone Mountain, Hurricane, Toroweap, Aubrey, Supai, Fossil-Monument-Erimeta, West Kaibab, Phantom-Grandview, East Kaibab, and Echo Cliffs faults/monoclines. The

Waterpocket Fold and the Monument Upwarp are two important Laramide structures in the river corridor of Glen Canyon.

Workers have proposed that Late Cenozoic faulting has played a role in the differential incision of Grand Canyon by the Colorado River. Basin and Range extension was first manifest on the western margin of the Colorado Plateau by down-to-the-west normal faulting along the Grand Wash Fault, a west-dipping fault that forms the boundary between the Colorado Plateau and the Basin and Range province (Lucchitta, 1979). Field relations between the fault, extensional basin sediments, and volcanic tuffs provide evidence for middle to late Miocene slip initiation (e.g., Young and Brennan, 1974; Faulds et al., 1997). The Hurricane and Toroweap faults in western Grand Canyon are associated with recurrent Basin-and-Range extension and account for 580 meters of combined displacement (Huntoon, 2003). These still-active faults may be affecting incision rates up and downstream of the fault zones (e.g., Machette and Rosholt, 1991; Lucchitta et al., 2000; Fenton et al., 2001; Pederson et al., 2002).

In summary, the bedrock geology of the study area can be generalized as a thick sequence of relatively undeformed (at the regional scale) late Proterozoic to Jurassic sedimentary rocks floored in middle Proterozoic crystalline basement. The most abundant rock types among more than twenty different rock formations are sandstones, igneous/metamorphic rocks, carbonates, and shales.

Geomorphology

Perhaps the most spectacular feature of the Colorado Plateau is Grand Canyon, extraordinary for its high rim-to-floor relief, narrow width, and world-class rapids. The

incision of Grand Canyon is driven by base-level lowering related to the combined effects of regional uplift and the integration of the ancestral Colorado River to drain off the plateau to the Gulf of California. Integration of the Colorado River into a through-flowing drainage was established about 5-6 million years ago (e.g., Lucchitta and Young, 1986; Lucchitta, 2003). As previously mentioned, some speculate that the effects of the original late Miocene to early Pliocene drainage integration are still present in the Colorado River's system, one manifestation being the steep reaches or knickzones in the river's profile (Coblentz and Karlstrom, 2003; Wolkowinsky and Granger, 2004).

The alternating steep riffles-rapids and low-gradient pools of the Colorado River in Grand Canyon are caused by debris flows (e.g., Howard and Dolan, 1981; Webb et al., 1989), and is not an endogenic response of the river to maintain hydraulic equilibrium along the profile, as originally hypothesized by Leopold (1969). The location of nearly all rapids is structurally controlled by the occurrence of tributaries running preferentially along fracture zones or faults (Dolan et al., 1978; Howard and Dolan, 1981). The maintenance of rapids is linked to the magnitude and frequency of debris flow forming events in their tributaries and the erosive reworking of debris fans by the river (e.g., Dolan et al., 1978; Howard and Dolan, 1981; Kieffer, 1985; Webb et al., 1989).

Howard and Dolan (1981) classified the Colorado River in Grand Canyon into multiple channel types, based on changes in valley width associated with certain rock types. These channel types included: 1) wide valleys with freely meandering channels in shale, 2) valleys of intermediate width in sandstone or limestone, 3) narrow valleys in fractured igneous and metamorphic rocks, and 4) narrow valleys in massive limestone.

Although their channel type – lithology model captures the dependence of channel type on lithology and structure, Howard and Dolan (1981) did not specify river-mile designations for reaches having these channel type characteristics. This was done first by Schmidt and Graf (1990), who broke Grand Canyon into 11 geomorphic reaches according to specific rock units observed to be covariant with changes in channel width. Melis (1997) statistically refined Schmidt and Graf's (1990) reaches into a shorter list of 6 based on geomorphic parameters which relate to groupings of similar rock-types, rather than on individual formal geologic units.

Typical deposits associated with the Colorado River include poorly sorted gravel and boulders from side-canyon tributaries, Pleistocene fill terraces of gravel and sand, bars of well rounded and well sorted cobbles of intra-canyon lithology, and fine-grained terraces composed of sand and silt deposited in eddies, alcoves, and along banks (e.g., Howard and Dolan, 1981; Hereford et al., 1993, 1996; Schmidt and Graf, 1990; Burke et al., 2003).

METHODS

Mechanical Reaches

Eighteen reaches or sample units were defined within Glen and Grand canyons (650 km) in order to explore reach-scale (10 km) covariation in geomorphic and bedrock variables. As mentioned above, the Colorado River has been previously divided into a number of reaches (Schmidt and Graf 1990; Melis, 1997). However, neither of these efforts have created subdivisions based on mechanical properties, rather they were based on changes in either changes in specific rock units (Schmidt and Graf, 1990) or a combination of geomorphic metrics (e.g., width and gradient; Melis, 1997).

The 18 reaches defined in this study are composed of stratigraphically neighboring and mechanically similar rock-types and allow statistical comparison of rock strength to the hydraulic parameters. For example, thinly-bedded shales and siltstones were grouped separately from more massive sandstones and limestones (Harden, 1990). Igneous and metamorphic rocks, relatively harder and more resistant to erosion and weathering were grouped together. Among the 18 reaches, the minimum, average, and maximum lengths are 3.2, 36.4, and 145.2 km, respectively (Table 1).

Sample Sites

Field investigations were conducted at a total of 84 sites along the ~650 km Colorado River corridor within the 18 study reaches (Figure 6). Study sites were chosen to attain a representative distribution of the mechanical heterogeneity of the rock units.

TABLE 1. STUDY REACH DESCRIPTIONS

Reach ID	Age (Period)	Rock units	Dominant rock type	Study sites (n)	River mile* Start (mi)	River mile* End (mi)	River mile* Length (mi)
Glen Canyon							
GL1	Permian, Triassic	Organ Rock, Moenkopi, Chinle	Shale, siltstone	7	-172.6	-146.6	26.0
GL2	Jurassic	Wingate, Kayenta, Navajo, Page	Sandstone	5	-146.7	-104.0	42.7
GL3	Triassic	Moenkopi, Chinle	Shale, siltstone	0	-104.1	-91.3	12.8
GL4	Jurassic	Wingate, Kayenta, Navajo, Page	Sandstone	7	-91.4	-1.2	90.2
GL5	Triassic	Moenkopi, Chinle	Shale, siltstone	1	-1.3	0.7	2.0
Grand Canyon							
GR1	Permian, Triassic	Toroweap, Kaibab	Carbonate	4	0.8	4.4	3.6
GR2	Pennsylvanian, Permian	Suapi Group	Sandstone, siltstone	14	4.5	23.0	18.5
GR3	Mississippian	Redwall	Carbonate	5	23.1	36.8	13.7
GR4	Cambrian	Muav, Bright Angel	Shale, carbonate	6	36.9	58.1	21.2
GR5	Cambrian	Tapeats	Sandstone	1	58.2	65.3	7.1
GR6	Proterozoic	Bass, Hakatai, Shinumo, Dox, Cardenas	Shale, quartzite, carbonate, basalt	8	65.4	77.1	11.7
GR7	Proterozoic	Zoroaster, Vishnu	Granite, schist, gneiss, pegmatite	16	77.2	117.4	40.2
GR8	Cambrian	Tapeats	Sandstone	2	117.5	126.7	9.2
GR9	Proterozoic	Zoroaster, Vishnu	Granite, schist, gneiss, pegmatite	0	126.8	136.3	9.5
GR10	Cambrian	Muav, Bright Angel, Tapeats	Shale, sandstone, carbonate	2	136.4	178.9	42.5
GR11	Cambrian, Pleistocene	Pleistocene Basalts, Bright Angel, Tapeats	Basalt, shale, sandstone	2	179.0	190.7	11.7
GR12	Cambrian	Muav, Bright Angel, Tapeats	Shale, sandstone, carbonate	4	190.8	214.6	23.8
GR13	Proterozoic	Zoroaster, Vishnu	Granite, schist, gneiss, pegmatite	0	214.7	234.9	20.2

Note: Distance units are river miles in keeping with the convention of previous Grand Canyon workers (e.g. Howard and Dolan, 1981; Schmidt and Graf, 1990).

* River miles are referenced to Lees Ferry, AZ.
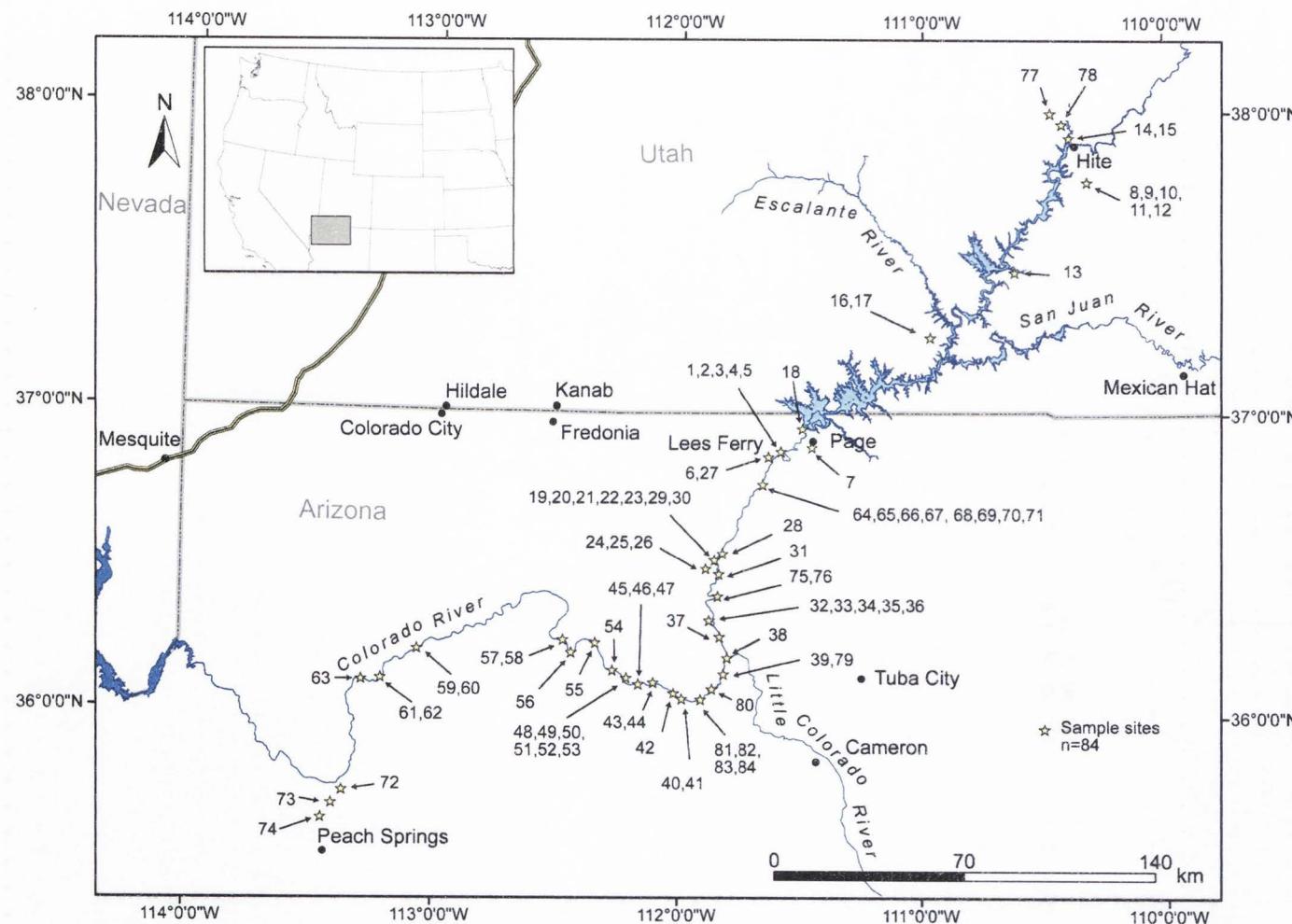
Figure 6. Map of sample sites (stars) within study area of Glen and Grand canyons. Intact-rock strength, fracture spacing, and Selby rock mass strength (RMS), were conducted at a total of 84 outcrops. See Table 1 for sample site details.

There was also an effort to sample major rock units at multiple sites separated by distances of 10 to 100 km to allow for variation and uncertainty within a single unit. For example, the Navajo Sandstone was sampled at 5 different locations within Glen Canyon, with as much as 70 km between sites.

Colorado River Longitudinal Profile

The longitudinal profile of the Colorado River through the study area is one of the basic datasets in this study (Figure 1). Pre-Glen Canyon Dam U.S.G.S. topographical maps (1:62,500 scale; 1953) were used to produce a profile for the Colorado River in Glen Canyon from Hite, Utah to Lees Ferry, Arizona. Water surface elevations were obtained from 5-ft contour intervals, and horizontal distances were recorded manually using a map wheel. These data were then joined with the Birdseye (1924) survey of the Colorado Rive in Grand Canyon to produce a continuous river profile from the mouth of Grand Canyon upstream to the top of Glen Canyon. The survey point density for the Birdseye (1924) data for Grand Canyon is three orders of magnitude higher than that for Glen Canyon data (~275 points/km vs. ~0.2 points/km). A two-dimensional linear interpolation algorithm was run on the combined survey data in order to resolve this resolution disparity and provide systematic elevation values every 0.16 river km (0.1 mi). This process produced a total of 4,064 distance-elevation pairs for the entire 655.8 km profile. All river distances were set in reference to Lees Ferry, located between Glen and Grand canyons, in keeping with the original river location system established by the U.S.G.S in the 1920's (Birdseye, 1924). In this manner, river distance locations along the profile are negative and positive for Glen and Grand canyons, respectively.

Hydraulic-Driving Forces

The distribution of stream power along the length of the Colorado River's profile reveals areas where erosive energy is focused, allowing one to spatially correlate erosive potential to erosive resistance. Unit stream power values were generated every 0.16 km (0.1 mi) along the profile according to Equation (2) using values of discharge, slope, and width calculated as described below, and an assumed value of 9.8 kN/m^3 for the specific weight of water.

Discharge, Q, is a quantity empirically shown to increase downstream as the drainage area, and thus tributary water input, increases down river. However, the majority of the Colorado River's discharge originates from mountain sources far upstream, and with the exception of at high-flood stage, it may actually loose significant amounts to evaporation, infiltration, and transpiration as it flows through an arid landscape. The San Juan River in Glen Canyon is the only tributary contributing an annually significant proportion of water to the Colorado River within the study area (Figure 3). Other notable tributaries are the Escalante, Paria, and Little Colorado Rivers; however, these have flashy hydrographs that are controlled mostly by late summer-early fall monsoonal storms, and collectively contribute less than several percent to the total annual discharge of the Colorado River.

A step-wise downstream increase in discharge (Q) was prescribed at the confluence of the San Juan River, based on data of average annual peak discharge at four U.S.G.S. gage stations for the decades prior to the closing of Glen Canyon Dam in 1963. These gages are the Colorado River at Hite, UT (1948-1958), San Juan River at Bluff,

UT (1915-2003), Colorado River at Lees Ferry, AZ (1922-1962), and Colorado River near Grand Canyon, AZ (1922-1962). These data show a 19% increase in the average annual peak discharge of the Colorado River between Hite, UT and Lees Ferry, AZ, due to the input of the San Juan River. This is corroborated by the fact that the San Juan River at Bluff, UT has an average annual peak discharge value that is 20% of the discharge at Lees Ferry, closely matching the difference between the two gages. A discharge, Q, value of 190 m^3/s (6,700 ft^3/s) was used for the study reach segment from Hite, UT to the mouth of the San Juan River and 227 m^3/s (8,000 ft^3/s) was the prescribed discharge for the remaining downstream portion.

The above discharge values were chosen due to mesh with values for channel widths (W), which were measured from a GIS coverage of the river's channel boundary that was originally processed from high-resolution, low-altitude aerial photographs during a discharge of 227 m^3/s (8,000 ft^3/s) (Grand Canyon Monitoring and Research Center, 2003). Channel widths for Glen Canyon were measured from digital images of 1:24,000 scale U.S.G.S. topographical maps, within a GIS. Channel widths in both canyons were defined as the distance between the water edges at the top of the channel and were measured at 0.16 km (0.1 mi) intervals along the profile.

Finally, channel gradients (S) were extracted from the interpolated profile as the local slope through each 0.16 km (0.1 mi) interval. Values were calculated as the elevation change between points up and downstream of the point of interest divided by the distance between those two points (0.32 km or 0.2 mi).

Field Investigations

Field work conducted at each of the 84 sites was focused on quantifying Selby

RMS and fracture density. Repeat measurements ($n \geq 30$) from a Schmidt hammer were

taken at least 20 cm from visible fractures to overcome the weakening effects of

discontinuities (Figure 7). Some very weak rocks, such as the Chinle Formation and

certain sections of the Hermit Shale, had intact-rock strengths below the Schmidt

hammer's minimum tolerance and could not be quantified. Selby (1980) rock-mass

strength (RMS) scores were calculated for each site, which includes seven variables: 1)

intact-rock strength, 2) weathering, 3) "joint" spacing, 4) orientation, 5) continuity, 6)

width, and 7) groundwater outflow. Each variable was ranked into one of five rating

classifications according to Selby (1993).

Data collected on fractures included representative strike and dips, continuity,

discontinuity width, and groundwater outflow were also observed. Discontinuity

spacings at the outcrop-scale (10 cm to 100 m) were recorded with high-resolution digital

photographs from multiple dimensions into and across the outcrop. A free-distribution

software, NIH Image (NIH, 2004), was used for image analysis. In-lab image analysis

made it possible to record a large number of data with reduced time in the field. For a

given sample site, one to four images were analyzed in order to generate average bed-

thicknesses (sedimentary rocks) and discontinuity spacings. Discontinuity spacings were

recorded as the distance between observable discontinuities (≥ 1 mm) along multiple

user-defined scan lines oriented normal and parallel to major fracture/joint sets (Figure

8).

This study makes no genetic distinction regarding discontinuities and will use the terms "fracture," "discontinuity," and "joint" synonymously in referring to planes of separation or failure (Goodman, 1989; Selby, 1993). Observations of the size, angularity, and comminution of rock material delivered by hillslopes at sampling sites were also noted in order to help explore the relation of jointing and hardness to the durability and caliber of regolith.

Statistical Analysis

A variety of statistical tests and summary statistics were conducted in order to compare and contrast hydraulic-driving and bedrock-resisting forces at multiple spatial scales. Throughout all tests, an alpha (α) of 0.05 was used, and data were not normal or randomly sampled due to physical inaccessibility of sites, *a priori* sampling site selection, and the typical log-normal nature of geologic data (Rock, 1988). Thus, non-parametric Mann-Whitney U-tests were used for inter-canyon and inter-reach comparisons of hydraulic driving and bedrock resisting forces. Moreover, correlations between reach-scale (10 km) averages of slope, width, unit stream power, RMS, intact-rock strength, and fracture spacing were evaluated using the non-parametric Spearman's coefficient of rank correlation.
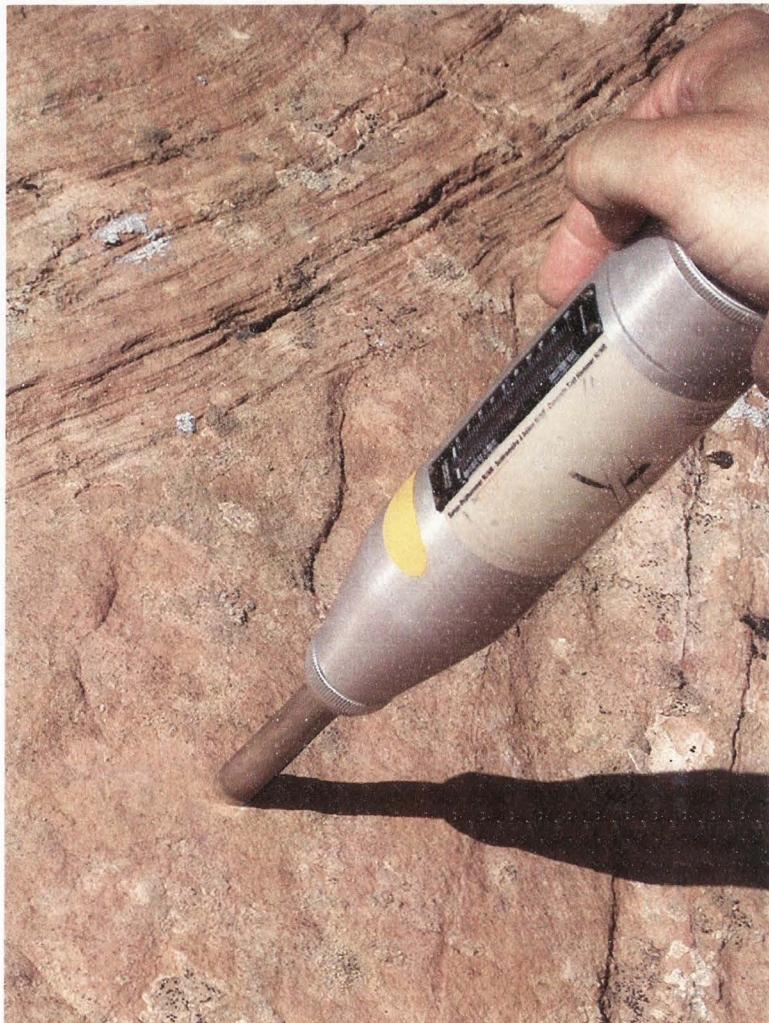
Figure 7. Image showing measurement of intact-rock strength on the Navajo Sandstone using a Schmidt hammer. Intact-rock strength is recorded as the relative rebound distance off the surface of the rock mass, a function of the rock's hardness and compressive strength.
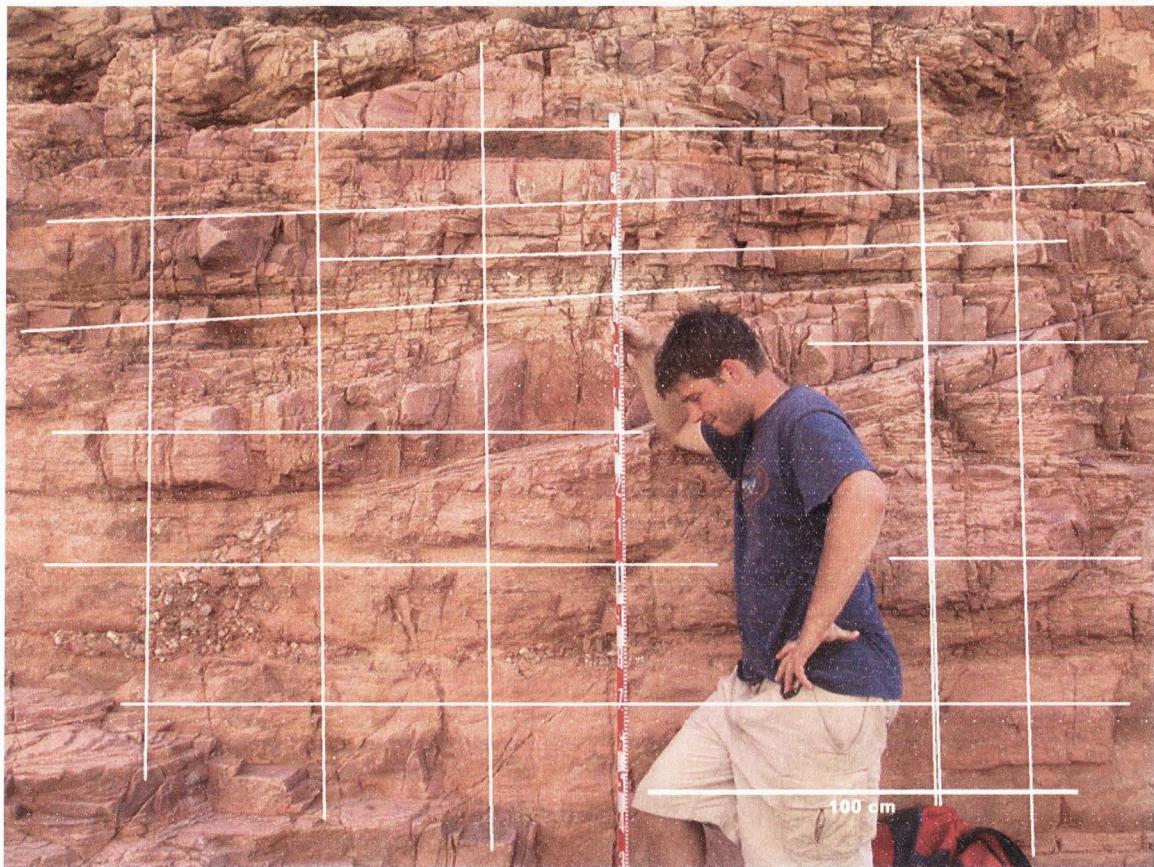
Figure 8. Typical image used in quantification of fracture spacings showing scan lines used for image analysis. Tape measure used for scale in front of the Upper Solomon Member of the Dox Formation, eastern Grand Canyon.

RESULTS

Hydraulic-Driving Forces

Canyon Scale (100 km)

The data generated within this study indicate considerable variability in the hydraulic variables within and between Glen and Grand canyons. The first-order observation is the significant disparity in gradient, width, and unit stream power between the two canyons (Figure 9). The average gradient in Glen Canyon is 0.0004 and the width is 149 m. Grand Canyon has averages of 0.0015 and 74 m for gradient and width, respectively, four times steeper and half as wide as Glen Canyon (Table 2). Mann-Whitney U-test results confirm the statistical difference in gradient and width between the two canyons (Table 2).

Unit-stream-power data inevitably follow similar spatial patterns as the gradient and width data, because of its inclusion of these variables in its calculation. Overall, Glen Canyon can be characterized as having far lower average unit stream power than its downstream counterpart (5 vs. 51 watt/m^2). The prominent change seen in the longitudinal profile and channel width between the two canyons are reflected in the dramatic increase in stream-power values at the beginning of Grand Canyon (Figure 9). Mann-Whitney significance tests for inter-canyon comparisons mimic the individual results for channel gradient and width (Table 2). Higher overall gradient in Grand Canyon is the largest reason for its relatively higher unit-stream-power values. It is

apparent, especially in the running averages (1.6 km or 1 mi moving window), that there is a high degree of intra-canyon variability, particularly for Grand Canyon (Figure 9).

Reach Scale (10 km)

There is variability within both canyons that can be best examined at a smaller, reach scale. Figure 9 illustrates the mean and variance in the reach-averaged values of gradient, width, and unit stream power. Within the overall higher mean gradient of Grand Canyon, values fluctuate from reach to reach by more than a factor of two. Two adjacent reaches, GR6 and GR7, stand out as having particularly high average gradient (Figure 9, Table 3). GR6 (RM 65.4 to 77.2) has an average gradient of 0.0024, and GR7 (RM 77.2 to 117.4) has a slightly lower average of 0.0021. The reach averages may be somewhat misleading since. The break point between these two reaches was made independent of the downstream distribution of hydraulic data, and the significant spike in gradient near the end of GR6, associated with Hance Rapid (RM 77), is positively skewing the average for GR6 (Figure 9). Reach GR4 (RM 36.9 to 58.1) is one of the lowest gradient reaches in Grand Canyon, composed of Cambrian Muav Limestone and Bright Angel Shale, with a gradient average of .0010 (Table 3). It is not surprising that three of the four steepest reaches in Grand Canyon occur within reaches of Precambrian basement (GR7, GR9, and GR13; Table 3). These results are consistent with previously reported averages of gradient in Grand Canyon (e.g., Schmidt and Graf, 1990; Melis, 1997).
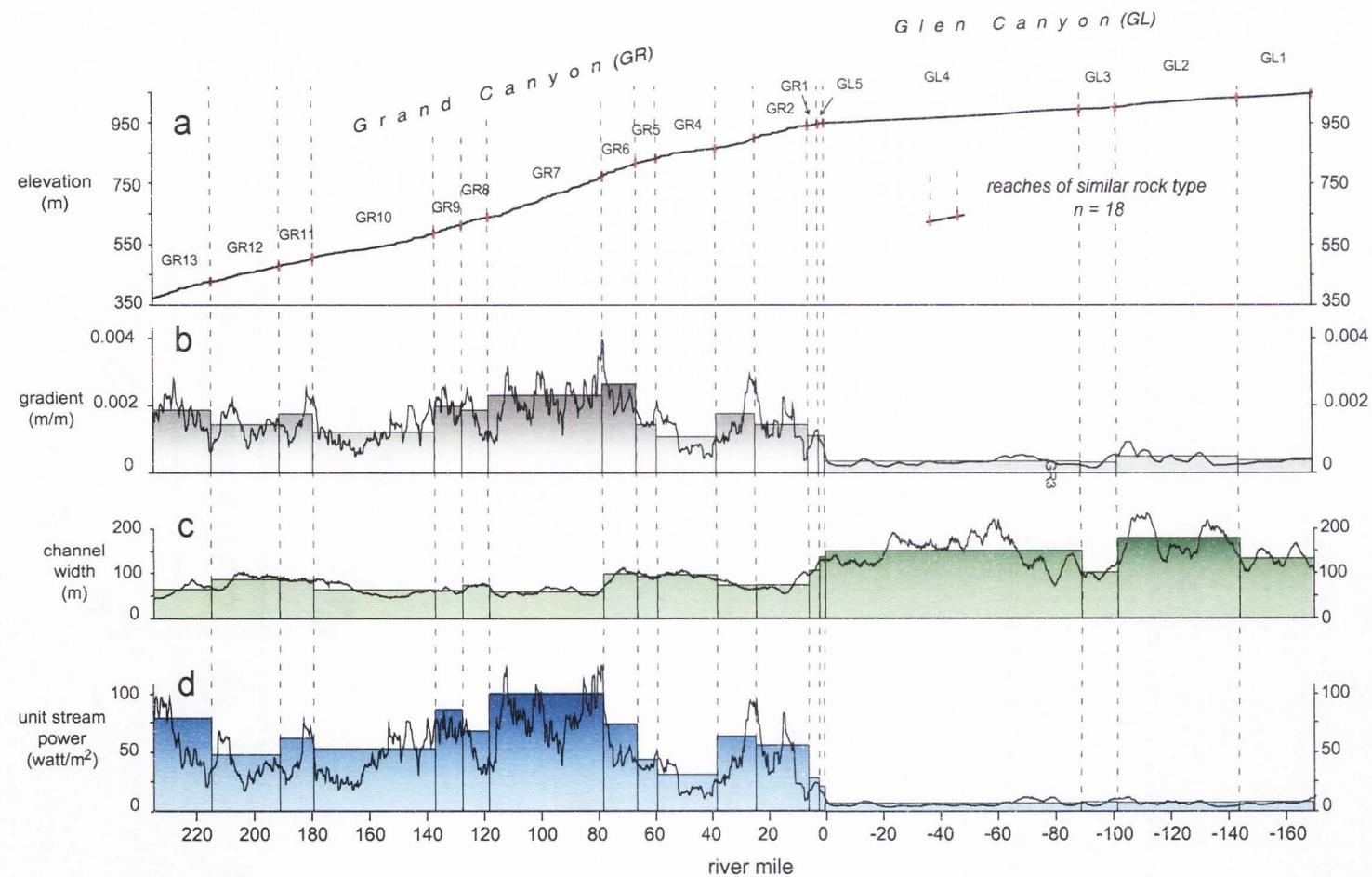
Figure 9. (a) Longitudinal profile of Colorado River in Glen and Grand canyons with study reaches (n = 18) labeled. Below this are reach and moving averages (1 river-mile) of gradient (b), channel width (c), and unit stream power (d). The spatial variability at both the canyon (100 km) and reach (10 km) scale can be seen. River mile 0 represents the location of Lees Ferry, AZ.

TABLE 2. SUMMARY OF CANYON-SCALE HYDRAULIC AND ROCK-STRENGTH DATA

Channel gradient (m/m)			Channel width (m)			Unit stream power (watt/m^2)			Intact rock strength (%rebound)*			Fracture spacing (cm)			Selby RMS[†]		
Avg	SD	n	Avg	SD	n	Avg	SD	n	Avg	SD	n	Avg	SD	n	Avg	SD	n
Glen Canyon																	
0.0004	0.0002	1734	149	58	1734	5	3	1734	41	8	873	75	58	417	70	5	20
Grand Canyon																	
0.0015	0.0018	2329	74	27	2330	51	65	2329	51	12	2797	43	40	3742	73	8	64
Mann-Whitney p-value[§]			<0.001			<0.001			<0.001			<0.001			0.018		

Note: Average (Avg), standard deviation (SD), and number of samples (n) are abbreviated accordingly.

*Intact rock strengths reported as the rebound percent recorded by the Schmidt-hammer instrument.

[†]Selby rock mass strength index (Selby, 1980)

[§]P-values for Mann-Whitney tests of comparison. All variables are significantly different between the two canyons at a confidence of 95%.

Reaches in Glen Canyon show little heterogeneity in gradient. GL5 (RM -1.3 to 0.7) is the outlier within this canyon, having an average gradient of 0.0010 (Table 3) this is two to three times steeper than the other four reaches in Glen Canyon. This is a very short reach, which likely reflects the local effects of a small rapid (Paria Riffle; RM 0.8), rather than the influence of Triassic siltstones and shales of the Moenkopi and Chinle formations near the river. For comparison, GL5's mean gradient ranks within the lower quartile of reach gradients in Grand Canyon (Table 3). The other four reaches in Glen Canyon have mean gradients that are nearly identical (Table 3). This is interesting, considering these reaches have rock types that vary from massive sandstone to shales. Similarities may also be the artifact of the coarseness (5-ft contours of water surface elevation) of the 1:62,500 scale maps.

Three of the four narrowest reaches in Grand Canyon occur in Precambrian basement rocks – the "granite gorges." Reaches GR7 (RM 77.2 to 117.4), GR9 (RM 126.8 to 136.3), and GR13 (RM 214.7 to 234.9) have mean widths of 59, 61, and 64 m, respectively (Table 3). On the other end of the spectrum, GR1 (RM 0.8 to 4.4) and GR4 (RM 36.9 to 58.1) are relatively wide reaches that are dominated mostly by carbonates, having averages of 106 and 96 m, respectively. It is interesting that GR6 (RM 65.4 to 77.1) is unusually wide (98 m), considering that it is also one of the steepest reaches (Table 3); its geology consists of the Precambrian Unkar Group sediments and early Paleozoic shales and limestones of the Muav and Bright Angel formations. Reaches within the Cambrian Tonto Group (Tapeats, Bright Angel, and Muav formations)

comprise four of the six reaches with the greatest channel width (GR4, GR5, GR12, and GR11).

Reaches in Glen Canyon are drastically wider than those in Grand Canyon. GL2 (RM -146.7 to -104) is the widest reach at 177 m, and is almost exclusively surrounded by sandstone (Table 1). The narrowest reach is GL3 (RM -104.1 to -91.3), confined to a slightly narrower channel (101.3 m) by the siltstones and shales of the Moenkopi and Chinle formations; this is interesting, since one might expect shales to be associated with wider channels.

Reach-scale averages of unit stream power have similar variability as gradient and width. Reaches with the highest unit stream power are those that are steep and narrow. The reaches with the highest mean unit stream power are, not surprisingly in Grand Canyon (Figure 9). These include GR7 (RM 77.2 to 117.4), GR9 (RM 126.8 to 136.3), and GR13 (RM 214 to 234.9), with values of 79, 69, and 63 watt/m^2, respectively; all three of these are "granite gorges," floored in basement rocks (Table 3). Mean unit stream powers for reaches in Glen Canyon are nearly indistinguishable, with one exception, GL5, the short segment influenced by local-scale gradient (Figure 9).

The fact that the reach with the highest gradient (GR6; Unkar Group) ranks fourth in stream power, shows it is offset by a proportionately high channel width (Table 3, Figure 9). Gradient alone does not fully capture or is not a good proxy for the erosive and transport energy of this river.

TABLE 3. SUMMARY OF REACH-SCALE HYDRAULIC AND ROCK-STRENGTH DATA

Reach ID	Channel gradient (m/m)			Channel width (m)			Unit stream power (watt/m^2)			Intact rock strength (r-val)*			Fracture spacing (cm)			Selby RMS[†]		
	Avg	SD	n	Avg	SD	n	Avg	SD	n	Avg	SD	n	Avg	SD	n	Avg	SD	n
Glen Canyon																		
GL1	0.0003	0.0001	259	131	44	259	5	3	259	45	7	300	59	59	194	69	6	7
GL2	0.0004	0.0003	426	177	57	426	5	3	426	39	4	250	107	62	101	71	5	5
GL3	0.0003	0.0002	127	101	26	127	5	3	127	ND	ND	ND	ND	ND	ND	ND	ND	ND
GL4	0.0003	0.0001	901	149	58	901	5	3	901	40	9	280	73	38	87	70	5	7
GL5	0.0010	0.0006	21	135	34	21	17	9	21	35	5	43	79	36	35	67	0	1
Grand Canyon																		
GR1	0.0010	0.0009	37	106	32	37	23	22	37	57	5	187	53	34	105	79	4	4
GR2	0.0013	0.0020	186	74	22	186	45	66	186	47	15	590	38	38	780	70	8	14
GR3	0.0016	0.0017	135	73	19	135	51	56	135	55	5	210	91	56	261	74	5	5
GR4	0.0010	0.0011	213	96	27	213	25	30	213	33	10	290	19	17	422	61	8	6
GR5	0.0013	0.0006	72	92	31	72	35	20	72	51	4	50	27	15	94	72	0	1
GR6	0.0024	0.0028	118	98	28	118	59	77	118	55	7	390	50	49	693	73	5	8
GR7	0.0021	0.0023	398	59	15	398	79	88	398	59	6	580	47	27	625	78	2	16
GR8	0.0017	0.0015	90	73	24	90	54	51	90	48	10	100	50	24	38	69	5	2
GR9	0.0018	0.0024	96	61	16	96	69	91	96	ND	ND	ND	ND	ND	ND	ND	ND	ND
GR10	0.0011	0.0015	425	63	20	425	42	57	425	46	8	110	20	22	258	64	3	2
GR11	0.0016	0.0016	118	84	25	118	49	58	118	57	4	80	65	45	68	78	0	2
GR12	0.0013	0.0012	239	86	30	239	38	40	239	50	10	210	37	28	398	72	6	4
GR13	0.0017	0.0017	203	64	21	203	63	64	203	ND	ND	ND	ND	ND	ND	ND	ND	ND

Note: Average (Avg), standard deviation (SD), and number of samples (n) are abbreviated accordingly.

*Intact rock strengths reported as the uncorrected rebound percent recorded by the Schmidt-hammer instrument.

[†]Selby rock mass strength index (Selby, 1980)

Bedrock-Resisting Forces

Canyon Scale (100 km)

There are significant differences between the two canyons in terms of bedrock

resistance as well. Grand Canyon has higher average intact-rock strengths, smaller

fracture spacings, and slightly higher Selby RMS scores (Table 2). Mean intact-rock

strengths in Grand Canyon (51% rebound) are 23% higher than those in Glen Canyon

(41% rebound). Mann-Whitney test results confirm the statistical difference between the

two canyons (Table 2). Grand Canyon exhibits slightly higher variability in intact-rock

strength (1σ values: Glen = 8 and Grand = 12% rebound), most likely due to its larger

number of heterogeneous rock types.

Fractures are spaced an average distance of 75 cm in Glen Canyon and 43 cm in

Grand Canyon. This difference is significant as confirmed by results from Mann-

Whitney tests (Table 2), but it is important to recognize the considerable spread in the

distribution of fracture spacings for both canyons (1σ values: Glen = 58, Grand = 42 cm).

At nearly all study sites, outcrops typically displayed three main fracture sets: 1) parallel

to the outcrop ("release" joints), 2) perpendicular to bedding or foliation, and 3) parallel

to bedding or foliation.

Semi-quantitative, ordinal-scale Selby RMS scores co-vary with intact-rock

strength and fracture-spacing data, since RMS includes these variables amongst others in

its calculation. Glen and Grand canyons have very similar averages of 70 and 73,

respectively (Table 2). Mann-Whitney test results indicate a statistical difference in RMS

between the two canyons, despite the striking closeness of the two averages. The

similarity in RMS averages, despite having significant intact-rock strength and fracture spacing differences, is due to inter-canyon commonality in the other five RMS variables, especially joint orientation and weathering.

The intact-rock strength and Selby RMS data are in agreement; the former indicates that the rocks in Grand Canyon have higher intact-rock strength, while the latter suggests they might be more resistant to erosion. Yet it is important to remember that the Selby RMS method was originally intended and formulated for analyzing hillslope and mass-wasting erosion processes (Selby, 1980). Higher fracture spacings within the relatively soft rocks of Glen Canyon suggest that the fluvial erosion process of hydraulic plucking would be inhibited due to the larger block/clast sizes of potentially entrained bedrock. Thus, with respect to plucking, the wider fracture spacings might actually make Glen Canyon effectively more resistant to erosion and transport. It is also possible that the other main fluvial erosion process, abrasion, would be more effective in the weaker rocks of Glen Canyon, offsetting the slightly larger block sizes.

Reach Scale (10 km)

The Colorado River encounters over a dozen rock types within the 18 study reaches (Table 1, Figures 2, 4, and 5). Results confirm intuition that there are substantial differences in measurable mechanical properties at the reach scale. Figure 10 shows how intact-rock strength, fracture spacing, and Selby RMS variables fluctuate from reach to reach. The Upper Granite Gorge reach of Precambrian igneous and metamorphic rocks (GR7; RM 77.2 to 114.7) has the highest mean intact-rock strength, whereas the consistently lowest averages come from those reaches dominated by shales and poorly

cemented sandstones (Table 3 and Figure 10). High values in the igneous and

metamorphic rocks reflects their higher bulk-rock densities. Goodman (1989) ranks

granite, limestone, schist, and basalt higher than shales and sandstones in his list of bulk

rock densities for various rocks. Two reaches, GR11 and GR1, located in the western

and easternmost parts of Grand Canyon, respectively, also have relatively high intact-

rock strength averages (both = 57% rebound). GR11 is dominated by Pleistocene basalts,

whereas GR1 is primarily composed of dense limestones and sandstones. GL5 and GR4

are the two lowest reaches in terms of average intact-rock strength (GL5 = 35% rebound;

GR4 = 33% rebound), about half that of the Precambrian basement (Table 3). Both are

reaches dominated by shale (Table 1). These shale reaches are nearly half the intact-rock

strength of the Precambrian basement reach (GR7). The rest of the reaches, formed

mostly in sandstone and limestone, have intermediate rock strength, with the limestones

having slightly higher averages (Table 3).

It is well known that bedding influences fracture spacing (e.g., Narr and Suppe,

1991). In general, reaches with large fracture spacing values are associated with thickly

bedded sandstones and limestones. The reach with the largest spacing between fractures

is the GL2 reach in Glen Canyon, dominated by thick sandstone, having a mean of 107

cm (Table 3). GR3, located in eastern Grand Canyon, is another reach with relatively

large fracture spacings (91 cm), composed entirely of the thickly-bedded Redwall

Limestone (Table 3). Fracture spacings are the smallest in reaches containing Cambrian

shales, shaley limestones, and thinly bedded sandstones (e.g., GR4, GR5, and GR10),

where fractures spacing are four to five times smaller. The Precambrian basement reach

(GR7), mechanically distinct for its hardness and strength, has an average fracture spacing that falls within the intermediate range of reach averages (Table 3). Although the crystalline-basement rocks lack sedimentary bedding, some display foliations and metamorphic fabrics behave like mechanical fractures.

Selby RMS scores are likewise sensitive to differences between rock types (Figure 10). Reaches with carbonates, basalts, igneous/metamorphic rocks, and well-cemented sandstones have the highest rock-mass strengths, similar to intact-rock strength results (Table 3). GR1, GR11, GR7, GR3, and GR6 are the top five reaches with respect to Selby RMS, just as they are with intact-rock strength. GR1, composed of carbonates and sandstones of the Kaibab and Toroweap formations is the highest of these, with an average of 79. On the low end of the Selby RMS continuum are reaches GL5, GR10, and GR4, having averages of 67, 64, and 61, respectively (Table 3). All three of these reaches have significant shales (Table 1).

There is a distinct chronological trend in rock strength, particularly for intact-rock strength, in the study area (Table 4). Precambrian igneous, metamorphic, and sedimentary rock units dominate the upper strength rankings. Younger and less compacted or buried Mesozoic sedimentary rocks, such as the Navajo Sandstone, rank near the bottom. This is consistent with theories concerning the effects of age and burial on the porosity of sedimentary rocks, and the fact that crystalline rocks are denser than porous sandstones and shales (Goodman, 1989).
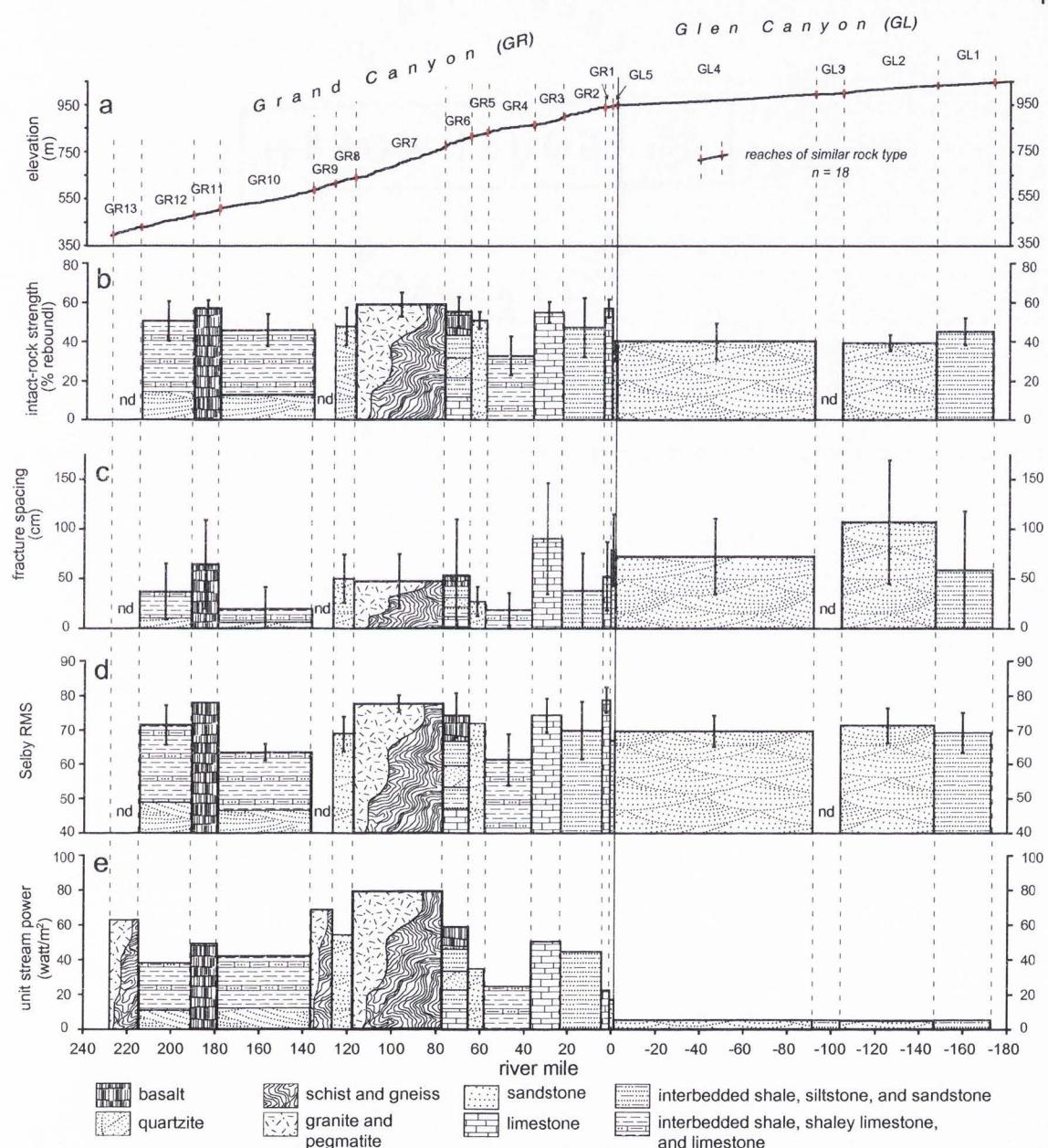
Figure 10. Profile and reach averages of rock-strength properties and unit stream power. Three reaches have no rock-strength data, and are labeled "nd." 1σ error bars are shown for strength data, except for Selby RMS for two reaches having only one sample site.

TABLE 4. RELATION BETWEEN ROCK STRENGTH AND AGE

Rock unit	Age (Period)	Dominant rock type	Intact-rock strength* (% rebound)				Selby RMS[†]			
			Rank	Avg	SD	n	Rank	Avg	SD	n
Bass	Proterozoic	carbonate	1	59.7	4.3	50	2	78.0	0.0	1
Zoroaster	Proterozoic	granite, gneiss, pegmatite	2	59.3	6.2	250	5	77.4	2.6	7
Shinumo	Proterozoic	quartzite	3	59.2	3.4	80	13	75.0	3.0	2
Kaibab	Permian	carbonate	4	58.8	3.5	76	1	80.5	4.5	2
Vishnu	Proterozoic	schist, gneiss	5	58.5	6.0	330	4	77.8	2.4	9
Wescogame	Pennsylvanian	sandstone, siltstone	6	58.0	3.6	100	14	75.0	3.0	2
Dox	Proterozoic	siltstone, shale, sandstone	7	57.1	6.1	150	11	75.3	1.9	3
Pleist. Basalts	Quaternary	basalt	8	57.0	4.1	80	3	78.0	0.0	2
Toroweap	Permian	carbonate	9	55.7	4.8	111	6	77.0	1.0	2
Esplanade	Permian	sandstone	10	55.1	2.9	60	8	76.0	0.0	1
Redwall	Mississippian	carbonate	11	54.9	5.3	210	15	74.4	4.9	5
Coconino	Permian	sandstone	12	54.6	4.5	130	10	75.3	2.5	3
Watahomigi	Pennsylvanian	mudstone, siltstone	13	52.2	5.1	50	9	76.0	0.0	1
Tapeats	Cambrian	sandstone	14	51.7	8.9	200	18	72.0	5.1	4
Cardenas	Proterozoic	basalt	15	49.7	5.2	50	25	61.0	0.0	1
Wingate	Jurassic	sandstone	16	49.0	5.4	110	7	76.3	3.3	3
Organ Rock	Permian	shale, siltstone, sandstone	17	48.8	3.7	100	16	73.0	2.0	2
Manakacha	Pennsylvanian	sandstone, mudstone	18	46.7	11.4	100	12	75.0	3.0	2
Hakatai	Proterozoic	mudstone, sandstone	19	46.2	8.0	60	17	72.0	0.0	1
Muav	Cambrian	carbonate, shale	20	42.7	9.7	320	21	68.7	3.8	6
Chinle	Triassic	shale, siltstone	21	42.0	7.7	143	22	67.0	2.4	4
Moenkopi	Triassic	shale, siltstone	22	41.4	7.2	100	20	69.0	9.0	2
Navajo	Jurassic	sandstone	23	38.0	5.8	250	19	70.8	1.0	5
Kayenta	Jurassic	sandstone	24	37.7	4.9	70	23	65.5	0.5	2
Page	Jurassic	sandstone	25	35.6	4.5	100	24	65.5	4.5	2
Bright Angel	Cambrian	shale	26	35.2	12.8	240	27	58.2	5.8	5
Hermit	Permian	siltstone, shale, mudstone	27	29.2	17.2	150	26	60.2	6.5	5

Note: Average (Avg), standard deviation (SD), and number of samples (n) are abbreviated accordingly.

*Intact-rock strengths reported as the uncorrected rebound percent recorded by the Schmidt-hammer instrument.

[†]Selby rock mass strength index (Selby, 1980).

Correlations Between Hydraulic and Bedrock Data

Several relations between variables, namely those between bedrock-resisting and hydraulic-driving forces, lie at the heart of this study. From a qualitative perspective, reaches high in unit stream power are generally also higher in intact-rock strength and Selby RMS (Figure 10). In other words, reaches with stronger or more resistant rock types have concentrated hydraulic power in the form of steeper and narrower channels. The upper granite gorge (GR7) is a prime example. Here, the Colorado River is narrow and runs at a relatively high gradient as it flows through 65 km of strong Precambrian rocks. There are, however, some exceptions to the positive trend between measures of hydraulic driving forces and bedrock resistance. For example, the difference in unit stream power between Glen and Grand canyons is disproportionately large compared to their difference in intact-rock strength (Figures 9 and 10). Grand Canyon has over nine times greater average unit stream power than Glen Canyon; however, its rocks have only 1.2 times higher intact rock strength. Interestingly, Sklar and Dietrich (2001) also show a nonlinear relation between tensile rock strength and bedrock erodibility. Furthermore, Glen Canyon's reaches, when looked at alone, show no correlation between intact-rock strength and unit stream power (Figure 11).

Despite the scatter in the data, statistical testing confirms the significance in correlation between reach averages of intact-rock strength and unit stream power (Figure 11). The Spearman coefficient of rank correlation is 0.69, significant at the 95% level (Table 5). When viewed individually, gradient (Figure 12) and width (Figure 13) each have a significant correlation to rock strength (Table 5).
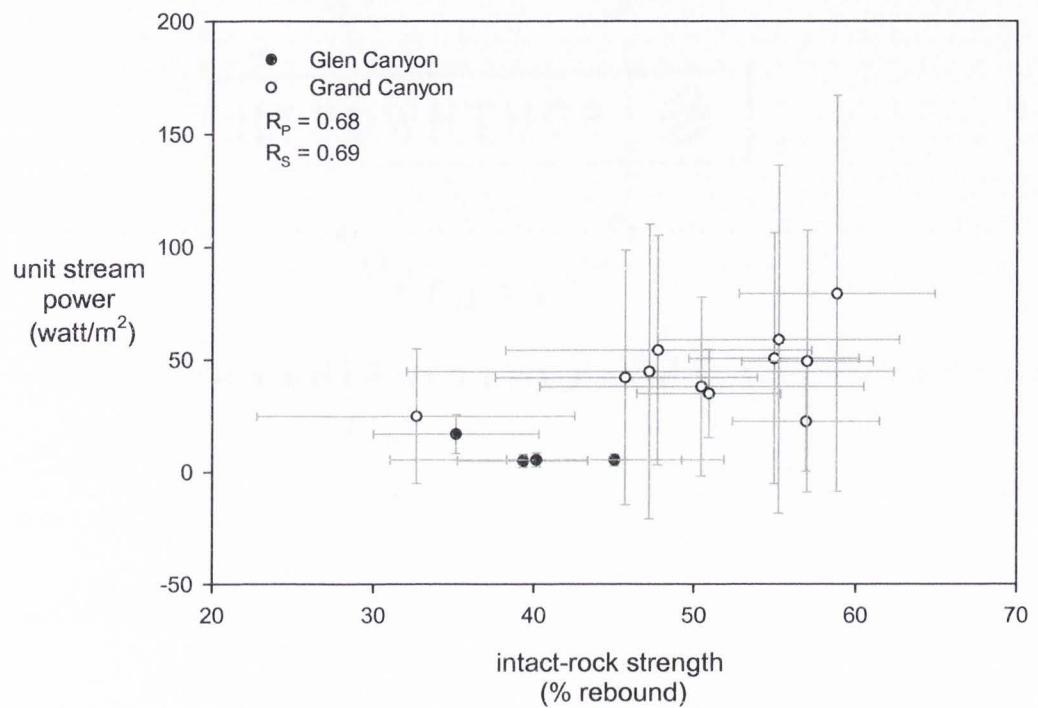
Figure 11. Relation between reach-scale averages of intact-rock strength and unit stream power for 15 reaches within Glen (black-filled circles) and Grand (hollow circles) canyons, including 1σ error bars. Pearson's correlation coefficient (R_p) and the non-parametric Spearman rank-correlation coefficient (R_S) are also included.
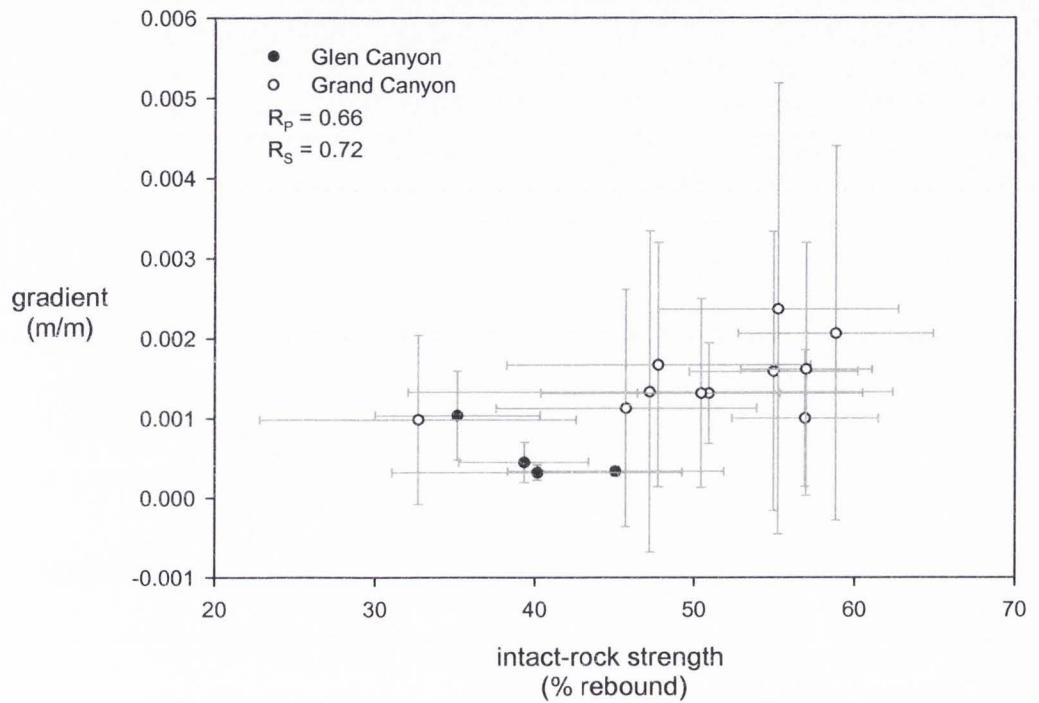
Figure 12. Relation between reach-scale averages of intact-rock strength and channel gradient for 15 reaches within Glen (black-filled circles) and Grand (hollow circles) canyons, including 1σ error bars. Pearson's correlation coefficient (R_p) and the non-parametric Spearman rank-correlation coefficient (R_S) are also included.
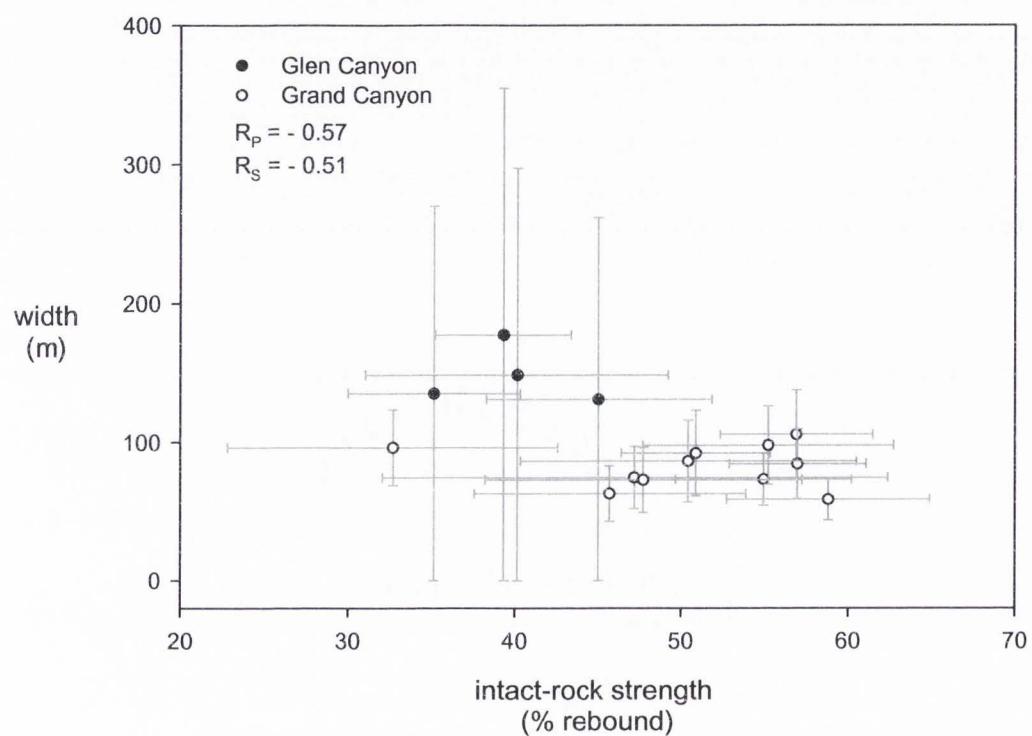
Figure 13. Relation between reach-scale averages of intact-rock strength and channel width for 15 reaches within Glen (black-filled circles) and Grand (hollow circles) canyons, including 1σ error bars. Pearson's correlation coefficient (R_p) and the non-parametric Spearman rank-correlation coefficient (R_S) are also included.
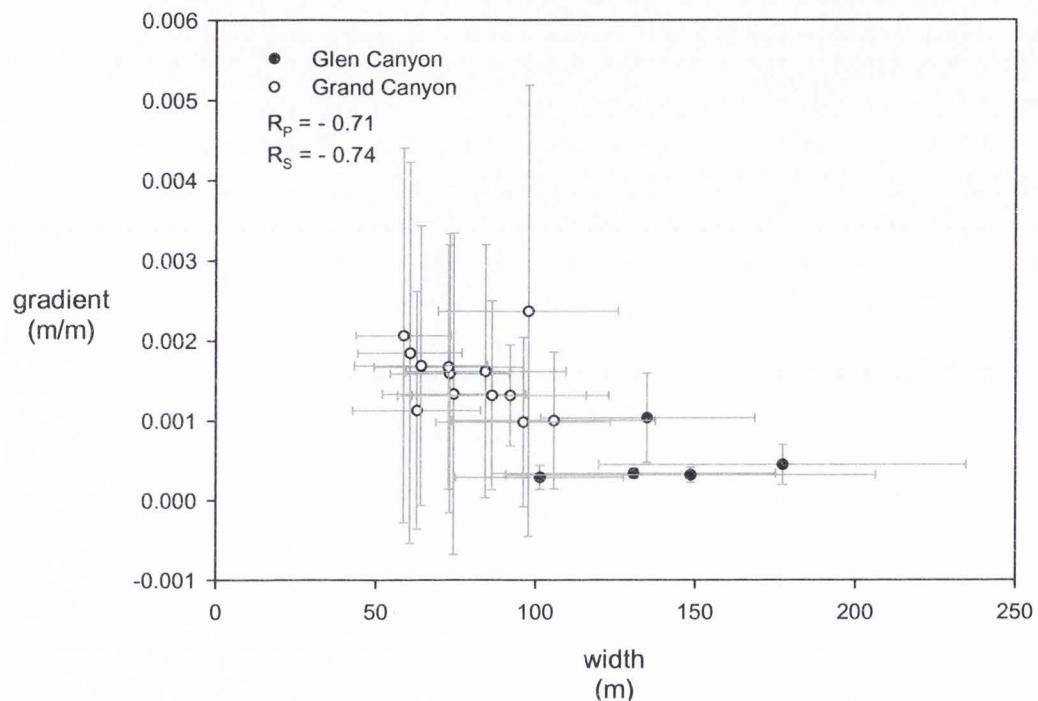
Figure 14. Relation between reach-scale averages of channel width and gradient for 18 reaches within Glen (black-filled circles) and Grand (hollow circles) canyons, including 1σ error bars. Pearson's correlation coefficient (R_p) and the non-parametric Spearman rank-correlation coefficient (R_S) are also included.

Reach-scale averages of fracture spacing do not correlate with any bedrock-strength or hydraulic variable, despite previous thoughts that channel width and depth in Grand Canyon increase within rocks that are more fractured (Dolan et al., 1978; Howard and Dolan, 1981) (Table 5). However, the lack of correlation between fracturing and hydraulic-driving forces does not preclude the notion that fracturing has an influence on weathering and fluvial erosion processes.

Spearman test results show that Selby RMS correlates only to intact-rock strength (Table 5). This is expected; the two have an internal correlation due to the inclusion of the latter into the former. It is noteworthy that RMS does not correlate to any of the hydraulic variables in spite of this internal correlation, and the fact that intact-rock strength correlates to all three. Moreover, RMS values do not correlate with fracture spacing values, which are also incorporated into RMS (Table 5).

As a final exploration of the results, the sedimentary rock-unit subset of the fracture spacing data was used to quantify the relation between fracturing and bed thickness. Over three thousand fracture spacings were binned according to bed-thickness and averaged. Fracture spacings show a strong power-law dependence upon bed thickness, and the Spearman rank correlation coefficient (R_s) for this relation is 0.85 (Figure 15). These results strongly support the conclusions of other studies (e.g., Narr and Suppe, 1991) regarding the dependence of fracture spacing on bed thickness.

TABLE 5. CORRELATIONS BETWEEN BEDROCK-RESISTING AND
HYDRAULIC-DRIVING FORCES

	Intact-rock strength	Fracture spacing	Selby RMS	Channel gradient	Channel width
Fracture spacing	-0.05				
Selby RMS	**0.87**	0.25			
Channel gradient	**0.72**	-0.19	0.44		
Channel width	**-0.51**	0.48	-0.12	**-0.74**	
Unit stream power	**0.69**	-0.3	0.35	**0.95**	**-0.86**

Note: Results from Spearman rank correlation (R_S) of reach-average values of hydraulic-driving forces to bedrock-resisting forces for 15 reaches. Correlations significant at a confidence of 95% (α =0.05) are in bold.
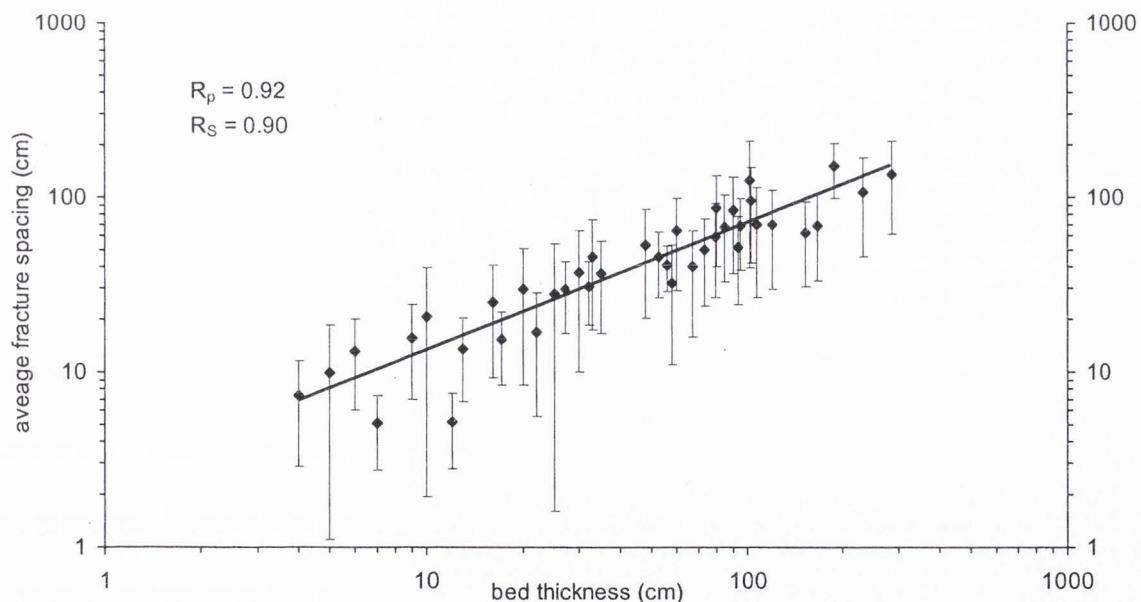
Figure 15. Relation of bed thickness to average fracture spacing. Each data point represents the average fracture spacing for a particular bed thickness, and error bars represent one standard-deviation unit from the mean. Pearson's correlation coefficient (R_p) and the non-parametric Spearman rank-correlation coefficient (R_S) are included.

DISCUSSION

Accurate and Relevant Measures of Bedrock Resistance

Results suggest that the three rock-strength indices used in this study are not created equal, at least as they pertain to fluvial erodibility. Although there is general agreement between the intact-rock strength and Selby RMS data, intact-rock strength, as measured with a Schmidt hammer, avoids critical weaknesses implicit in the Selby RMS. Although this study's primary goal was not the evaluation of rock-strength measurements, there are two reasons for discussing them: 1) any interpretations of the rock-strength results in this study hinge on their accuracy; and 2) studies have and may continue to use the Selby RMS system in fluvial studies for which it was not originally intended.

Selby RMS has become increasingly used in characterizing and correlating bedrock properties to fluvial geomorphology (e.g., Wohl and Merritt, 2001; Snyder et al., 2003). Despite the recent popularity of Selby RMS in fluvial studies, there are several aspects which weaken its relevance to fluvial processes. First of all, the Selby (1980) RMS method was developed to analyze and predict the processes of hillslope erosion and mass wasting using the combined influence of seven subjectively-weighted parameters. Some of the seven Selby RMS parameters, namely intact-rock strength, joint spacing, and weathering relate to fluvial resistance. However, others such as joint orientation (relative to outcrop face, not to the course of the river) or joint width, while directly connected to slope stability and form (e.g., Terzaghi, 1962; Selby, 1993), have no known relation to fluvial erosion. The problem is further complicated by the ranking

scheme, in that the seven Selby RMS parameters are assigned numerical weightings based on an assumed relative contribution to the overall strength of the rock mass (Selby, 1993). For example, intact-rock strength and joint orientation are weighted equally, but recent studies show that rock strength is a much more dominant control than joint orientation on fluvial erosion (Sklar and Dietrich, 2001; Whipple et al., 2000a). An improved-revised RMS ranking might include higher weighting for intact-rock strength and dropping groundwater outflow and joint orientation from the parameters. Further studies, both empirical and physical modeling, are needed in order to quantify the relative roles of each parameter and bring the numerical weightings to a less subjective state.

It is intuitive that the spacing between fractures in a rock mass should affect its erodibility. Exposed rock masses with closely spaced fractures will experience increased physical and chemical weathering and be weaker. Also, fracture spacings would theoretically control the geometry and dimensions of fluvially entrained blocks (Whipple et al., 2000a). Surprisingly, the robust fracture data set collected in this study do not correlate to any of the hydraulic-driving forces, despite previous Grand Canyon studies concluding that local channel widths increase in more fractured rock (Dolan et al., 1978; Howard and Dolan, 1981). It may imply that the Colorado River has eroded more by abrasion rather than by plucking or quarrying of blocks. This is supported by the fact that the Colorado River is historically known for its unusually high concentrations of suspended sediment, necessary tools for abrasion.

There are several reasons to believe that intact-rock strengths via the Schmidt hammer are a reliable and relevant means of relating bedrock strength to fluvial

resistance. Except for a few interesting exceptions, which will be discussed later in more detail, rock units generally considered harder or stronger by most people (e.g., granite or limestone) have a consistently higher Schmidt hammer reading than intuitively weaker rock units (e.g., shale or poorly-cemented sandstones) (Table 4). Secondly, the Schmidt hammer has been repeatedly validated as a reliable method for measuring rock strength by field and laboratory studies (e.g., Day and Goudie, 1977; Poole and Farmer, 1980; Goktan and Ayday; 1993; Katz et al., 2000).

This rebound percentage or intact strength measured by the Schmidt hammer is a direct function of compressive strength, and relates indirectly to density and other measures of strength such as tensile or shear strength (Selby, 1993). Sklar and Dietrich (2001) argue that when relating rock strength to erodibility, tensile strength should be the preferred strength measurement, not compressive strength, since this property relates to breakage by abrasion. Their argument may be valid. However, the most commonly accepted tensile strength tests are conducted on cylindrical-core samples in the laboratory, which is expensive, logistically impossible in some field settings, and less likely to capture heterogeneities within a rock mass. A single measure is unlikely to wholly capture the erosional resistance of a rock mass, especially in light of varying fluvial erosion processes. However, the results of this study confirm that intact-rock strength measured with a Schmidt hammer does serve well enough to relate bedrock resisting and hydraulic driving forces.

What Is the Role of Bedrock on the Colorado River?

We have wrestled since the time of Powell (1869) with how to explain

downstream variations in the geomorphology of the Colorado River, including the role of

river-level bedrock. There has not been a collection of data on bedrock strength,

specifically. The results from this study bring us one step closer to understanding the

connection between the Colorado River and the rock it encounters. However, these

results first need to be placed in the context of prevailing and alternate views on the

longitudinal profile controls of the Colorado River. There are at least two alternative

explanations in addition to rock strength, 1) debris fans and their resultant rapids and 2)

tectonic and drainage integration induced knickzones, with the former being the most-

commonly accepted view.

Debris Fans

There is widespread agreement that the fundamental geomorphic control within

Grand Canyon is debris fans and their resultant rapids (e.g., Webb et al., 1989). There is

little doubt that the frequency and magnitude of debris flows and their accompanying

debris fans control the local (1 km) gradient. The influence of debris fans and debris

flows at larger scales is, however, unclear. Recently, workers have extrapolated the

influence of debris fans and rapids to larger spatial scales in order to explain convexities

which span distances of 10 to 100 km (e.g., Grams and Schmidt, 1999; Webb et al.,

2004). They argue that the late Holocene Colorado River is an alluvial system where

there is a considerable thickness (12 to 70 m; Webb et al., 2004) of alluvial fill overlying

bedrock, and that convexities are the result broad aggradation along the river due to a

relatively higher frequency of debris fan forming events associated with changes in climate (Hanks and Blair, 2003).

The effects of individual rapids are indeed superimposed on the overall reach and canyon averages. These are seen as a highly fluctuating signal of "spikes" in gradient Figure 9). For example, Lava Rapid (RM 179) in western Grand Canyon is such a significant drop that it skews the entire reach-average gradient in the short reach in which it occurs (GR11; Figure 9). The GR6 reach is another example where an intense local spike in gradient (Hance Rapid, RM 77) elevates the reach-average gradient enough that it appears to be higher than the downstream reach (GR7), which is consistently steeper. Individual debris fans and rapids do influence local gradient and channel width as the river responds to local bed coarsening and constriction. Although there are places in Grand Canyon with considerable thicknesses of alluvium (Webb, 2004), it is doubtful they exert an integrated rapid-pool effect over the entire canyon-scale profile.

Tectonic Knickzones

A second possible control on the profile of the Colorado River is tectonic knickzones. Workers have recently raised the possibility that knickzones or steep segments in the long profile (e.g., Marble and Cataract canyons) are transient tectonic features (Wagner and Karlstrom, 2002, Coblentz and Karlstrom, 2003; Karlstrom and Kirby, 2004). This localization of transient knickzones is speculated to be the result of recurrent faulting in western Grand Canyon or left-over features related to the late Neogene drainage integration of the Colorado River (e.g., Wolkowinsky and Granger, 2004).

Coblentz and Karlstrom (2003) showed an increase in topographic roughness near the transition between Grand and Glen canyons and attribute this to late Quaternary incision driven by recently active tectonic structures (e.g., Hurricane-Toroweap faults system). Pederson et al. (2002) argue that this is geometrically impossible given the fact that rates of L. Quaternary incision exceed rates of slip on the Hurrican-Toroweap faults. Faulting in western Grand Canyon would not increase upstream incision rates, but rather, it would dampen incision downstream of the fault (Pederson et al., 2002). Moreover, Coblentz and Karlstrom (2002) concede that differences in topographic roughness may be the persistent expression of spatially varying rock-type and erodibility. After all, it is here that the softer sandstones, siltstones, and shales of the Mesozoic Glen Canyon Group give way to a host of resistant Paleozoic and Precambrian limestones, sandstones, and basement rocks (Figure 10).

Workers speculate that, in addition to faulting in western Grand Canyon, the knickzone located below Lees Ferry could be related to Neogene drainage integration (e.g., Coblentz and Karlstrom, 2003; Wolkowinsky and Granger, 2004). Slightly higher incision rates in eastern Grand Canyon compared to Glen and San Juan canyons leads them to speculate that the knickzone represents a continuing response of incision left over from original drainage integration during the late Miocene (Wolkowinsky and Granger, 2004). However, it is tenuous to distinguish between the effects of tectonics or drainage integration on knickzones because in both cases, knickzone migration is a function of bedrock and can become "hung up" on resistant bedrock (Gardner, 1983).

The spatial relation of rock-strength to gradient, width, and unit stream power

support the argument that the upper Grand Canyon knickzone is a persistent feature

maintaining its form in a state of dynamic equilibrium between driving and resisting

forces.

Bedrock Resistance

The recurring theme in many of the previous studies of the geomorphology of the

Colorado River and similar rivers is that lithology affects canyon or channel width, and

that width, in turn, at least partially sets the fluvial geomorphic template (Howard and

Dolan, 1981; Schmidt and Graf, 1990; Melis, 1997; Grams and Schmidt, 1999). The

results in this study certainly confirm this model. Rocks previously perceived as being

harder are measurably higher in rock strength properties and are thus more confining to

the river, translating to a narrower and steeper river.

There are significant differences in gradient, width, and unit stream power

between Glen and Grand Canyon, as well as between reaches. The results draw out the

fact that this is a "tale of two rivers" in the two neighboring canyons. In Glen Canyon,

the river ran wide and flat and had only a fraction of the transporting and eroding

capacity compared to Grand Canyon, where the data show a seemingly different river

with a four times steeper and half as wide channel (Table 2). It is noteworthy that Grand

Canyon has over nine times higher unit stream power than Glen Canyon (Table 2). The

results also confirm Powell's observation that the river is narrowest and steepest in the

hydraulically powerful Granite Gorge reaches (Figure 9). To point out the extremes, the

Upper Granite Gorge (GR7) is twice as steep, twice as narrow, and the river expends

three times more power on a unit of bed than lower Marble Canyon (GR4) (Table 2). Again, this is all consistent with previously reported observations (e.g., Howard and Dolan, 1981; Schmidt and Graf, 1990; Melis, 1997).

Strong correlations suggest these large-scale differences in hydraulic parameters are physically linked to downstream changes in bedrock strength. The older, well-cemented sandstones, dense limestones, and crystalline basement rocks of Grand Canyon are measurably stronger than the younger and less-compacted sandstones of Glen Canyon (Table 2 and Table 3). The data have a statistically significant correlation between width, gradient, and stream power to reach averages of intact-rock strength (Table 5). These results support the observations of previous workers connecting lithology to the geomorphology of Grand Canyon (e.g., Dolan et al., 1978; Howard and Dolan, 1981; Schmidt and Graf, 1990; Melis, 1997).

Rock-strength and bed material are certainly not mutually exclusive controls. The strong relation between bedrock-resisting and hydraulic-driving forces implies that the long-term, large-scale profile is set by a bedrock template established during episodes of bedrock incision, especially in the context of Pleistocene history of bedrock-river episodes (Anders, 2003). However, rock-strength, weathering, and erodibility properties in bedrock of tributary catchments influence the yield and caliber of sediments transported to the Colorado River. The inherent strength of the coarse material, once delivered to the bed, affects its resistance to comminution and debris fan maintenance (Grams and Schmidt, 1999). In these ways, bedrock acts as an *indirect* control on local gradient.

In summary, there a number of proposed causes for variations in gradient along the Colorado River's longitudinal profile which include rock strength, debris fans, and tectonic knickzones. The debate is partly muddled by confusion regarding time and space scales. Debris fans and rock strength are not mutually exclusive controls; they act over differing time and space scales. There is now stronger support that bedrock may be a *direct* control on the long-term erosion and large-scale profile of the Colorado River. At smaller time and space scales, bedrock is an *indirect* control in its associated role on debris flow initiation and fan material strength. Rock-strength, weathering, and erodibility of bedrock in tributary catchments influences sediment yield, caliber, and inherent resistance of debris fan and bed material.

CONCLUSIONS

1) The Colorado River at the larger scales is steeper, narrower, and exerts significantly more stream power in Grand Canyon than in Glen Canyon. This is matched by the fact that Paleozoic and Precambrian sedimentary, igneous, and metamorphic rocks in Grand Canyon have significantly higher intact-rock strength, fracture spacing, and Selby RMS (1980) than Mesozoic sedimentary rocks in Glen Canyon.

2) Reach-scale averages of intact-rock strength likewise correlate to hydraulic-driving forces. Reaches with relatively higher rock strength are generally narrower, steeper in gradient, and higher in unit stream power.

3) Selby RMS (1980), originally intended for hillslope-stability studies, loses explanatory power when applied to fluvial erosion due to its inclusion of irrelevant variables and non-representative parameter weightings. Revisions of the Selby method, such as increasing the relative weighting of intact-rock strength and eliminated variables such as groundwater outflow and joint orientation, are recommended for its use in fluvial studies.

4) There are now field measurements that support the hypothesis that rock strength corresponds to changes in channel width and gradient along the Colorado River. Strength properties of river-level bedrock hypothetically exert a *direct* control on the large-scale profile of the Colorado River by setting up its first-order template during episodes in the long-term history when it is a bedrock river.

5) The results of this study also support the hypothesis that bedrock in tributary catchments, where debris flows initiate, acts as an *indirect* control on the local-scale profile by influencing sediment yield, caliber, and comminution potential of debris fan and bed material.

REFERENCES

Allison, R.J., Goudie, A.S., and Cox, N.J., 1993, Geotechnical properties of rock masses: Their control on slope form and mechanisms of change along the Napier Range, western Australia: Geomorphology, v. 8, p. 65-80.

Anders, M.D., 2003, Quaternary geology and landscape evolution of eastern Grand Canyon, Arizona [M.S. thesis]: Logan, Utah State University, 147p.

Beus, S.S., 2003a, Temple Butte Formation, *in* Beus, S.S., and Morales, M., eds., Grand Canyon geology: New York, Oxford, p. 107-114.

Beus, S.S., 2003b, Redwall Limestone and Surprise Canyon Formation, *in* Beus, S.S., and Morales, M., eds., Grand Canyon geology: New York, Oxford, p. 115-135.

Bieniawski, Z.T., 1976, Rock mass classifications in rock engineering: Proceedings of symposium on exploration for rock engineering, Balkema, Rotterdam, v. 1, p. 97-106.

Birdseye, C.H., 1924, Plan and profile of Colorado River from Lees Ferry, Arizona to Black Canyon, Arizona-Nevada, and Virgin River, Nevada: U.S. Geological Survey, 21 sheets.

Blakey, R.C., 2003, Supai Group and Hermit Formation, *in* Beus, S.S., and Morales, M., eds., Grand Canyon geology: New York, Oxford, p. 136-162.

Bray, D.I., 1982, Regime equations for gravel-bed rivers, *in* Hey, R.D., Bathurst, J.C. and Thorne, C.R., eds., Gravel bed rivers: Chichester, Wiley, p. 517-542.

Brown, E.H., Babcock, R.S., Clark, M.D., and Livingston, D.E., 1979, Geology of the older Precambrian rocks of the Grand Canyon. Part 1. Petrology and structure of the Vishnu Complex: Precambrian Research, v. 8, p. 219-241.

Brush, L.M., 1961, Drainage basins, channels, and flow characteristics of selected streams in central Pennsylvania: United States Geological Survey Professional Paper 282-F, p. 145-181.

Burke, K.J., Fairley, H.C., Hereford, R., and Thompson, K.S., 2003, Holocene terraces, sand dunes, and debris fans along the Colorado River in Grand Canyon, *in* Beus, S.S., and Morales, M., eds., Grand Canyon geology: New York, Oxford, p. 352-370.

Campbell, I., and Maxson, J.H., 1938, Geological studies of the Archean rocks at the Grand Canyon: Carnegie Institution of Washington Year Book, v. 37, p. 359-364.

Coblentz, D.D., and Karlstrom, K, 2003, A topographic analysis of the Colorado River Drainage: Insights into interaction between topography and incision history: Eos (Transactions, American Geophysical Union 2003), abs. T21C-0474.

Day, M.J., and Goudie, A.S., 1977, Field assessment of rock hardness using the Schimidt Test Hammer: British Geomorphological Research Group Technical Bulletin, v. 18, p. 19-29.

Dolan, R., Howard, A., and Trimble, D., 1978, Structural control of the rapids and pools of the Colorado River in the Grand Canyon: Science, v. 202, p. 629-631.

Faulds, J.E., Schreiber, C., Reynolds, S.J., Gonzales, L.A., and Okaya, D., 1997, Origin and paleogeography of an immense, nonmarine Miocene Salt Deposit in the Basin Range (western USA): Journal of Geology, v. 105, p. 19-36.

Fenton, C.R., Webb, R.H., Pearthree, P.A., Cerling, T.E., and Poreda, R.J., 2001, Displacement rates on the Toroweap and Hurricane faults: Implications for Quaternary downcutting in the Grand Canyon, Arizona: Geology, v. 29, p. 1035-1038.

Ford, T.D. and Dehler, C.M., 2003, Grand Canyon Supergroup: Nankoweap Formation, Chuar Group, and Sixtymile Formation, in Beus, S.S., and Morales, M., eds., Grand Canyon geology: New York, Oxford, p. 53-75.

Gardner, T.W., 1983, Experimental study of knickpoint and longitudinal profile evolution in cohesive, homogenous material: Geological Society of America Bulletin, v. 94, p. 664-672.

Gilbert, G.K., 1877, Report on the Geology of the Henry Mountains: Washington, D.C., Government Printing Office.

Goktan, R.M. and Ayday, C.A., 1993, Suggested improvement to the Schmidt rebound hardness ISRM suggested methods with particular reference to rock machineability: International Journal of Rock Mechanics and Mining Sciences and Geomechanics Abstracts, v. 30, p. 321-322.

Goodman, Richard E., 1989, Introduction to rock mechanics: Second Edition, New York, John Wiley and Sons.

Grams, P.E. and Schmidt, J.C., 1999, Geomorphology of the Green River in the eastern Uinta Mountains, Dinosaur National Monument, Colorado and Utah, *in* A.J. Miller and A. Gupta, eds., Varieties of fluvial form: Chichester, John Wiley & Sons Ltd, p. 81-111.

Grand Canyon Monitoring Research Center, 2003, Profile of the Colorado River in Grand Canyon from Lees Ferry to Diamond Creek, AZ: Products available for download from website, http://www.gcmrc.gov/.

Hack, J.T., 1957, Studies of longitudinal stream profiles in Virginia and Maryland: United States Geological Survey Professional Paper, 294B.

Hancock, G.S., Anderson, R.S., and Whipple, K.X., 1998, Beyond power: Bedrock river incision process and form, *in* Tinkler, K.J. and Wohl, E.E., eds., Rivers over rock, fluvial processes in bedrock channels: Washington, D.C., American Geophysical Union, Monograph 107, p. 35-60

Hanks, T.C., and Blair, J.L., 2003, Differential incision of the Grand Canyon related to Quaternary faulting-Constraints from U-series and Ar/Ar dating: COMMENT: Geology: *Online Forum*, p. e16-e17.

Harden, D.R., 1990, Controlling factors in the distribution and development of incised meanders in the central Colorado Plateau: Geological Society of America Bulletin, v. 102, p. 233-242.

Hendricks, J.D. and Stevenson, G.M., 2003, Grand Canyon Supergroup: Unkar Group, *in* Beus, S.S., and Morales, M., eds., Grand Canyon geology: New York, Oxford, p. 39-52.

Hereford, R., Fairley, H.C., Thompson, K.S., and Blasom, J.R., 1993, Surficial geology, geomorphology, and erosion of archeological sites along the Colorado River, eastern Grand Canyon, Grand Canyon, Grand Canyon National Park, Arizona: U.S. Geological Survey Open-File Report 93-517, 45 p., 4 plates.

Hereford, R., Thompson, K.S., Burke, K.J., and Fairley, H.C., 1996, Tributary debris fans and the late Holocene alluvial chronology of the Colorado River, eastern Grand Canyon, Arizona: Geological Society of America Bulletin, v. 108, p. 3-19.

Hey, R.D., and Thorne, C.R., 1986, Stable channels with mobile gravel beds: Journal of Hydraulic Engineering, v. 112, p 671-689.

Hopkins, R.L. and Thompson, K.L, 2003, Toroweap Formation, *in* Beus, S.S., and Morales, M., eds., Grand Canyon geology: New York, Oxford, p. 196-211.

Howard, A.D., and Dolan, R., 1981, Geomorphology of the Colorado River in the Grand Canyon: Journal of Geology, v. 89, no. 3, p. 259-298.

Howard, A.D., and Kerby, G., 1983, Channel changes in badlands: Geological Society of America Bulletin, v. 94, p. 739-752.

Howard, A.D, Dietrich, W.E., and Seidl, M.A., 1994, Modeling of fluvial erosion on regional to continental scales: Journal of Geophysical Research, v. 99, no. B7, p. 13,971-13,986.

Huntoon, P.W., 2003, Post-Precambrian tectonism in the Grand Canyon Region, *in* Beus, S.S., and Morales, M., eds., Grand Canyon geology: New York, Oxford, p. 222-259.

Ilg, B.R., Karlstrom, D.E., Williams, M.L., and Hawkins, D.P., 1996, Tectonic evolution of Paleoproterozoic rocks in the Grand Canyon: Insights into middle crustal processes: Geological Society of America Bulletin, v. 108, p. 1149-1166.

Karlstrom, K.E., and Kirby, E., 2004, Colorado River system of the southwestern U.S.: Longitudinal Profiles, Differential incision, and a hypothesis for quaternary tectonism at both ends: Geological Society of America Abstracts with Programs, v. 36, no. 5, p. 550.

Karlstrom, K.E., Ilg, B.R., Williams, M.L., Hawkins, D.P., Bowring, S.A., and Seaman, S.J., 2003, Paleoproterozoic rocks of the Granite Gorges, *in* Beus, S.S., and Morales, M., eds., Grand Canyon geology: New York, Oxford, p. 9-38.

Katz, O., Reches, Z., and Roegiers, J.C., 2000, Evaluation of mechanical rock properties using a Schmidt Hammer: International Journal of Rock Mechanics and Mining Sciences, v. 37, p. 723-728.

Kieffer, S.W., 1985, The 1983 hydraulic jump in Crystal Rapid: Implications for river-running and geomorphic evolution in the Grand Canyon: Journal of Geology, v. 93, p. 385-406.

Knighton, A.D., 1976, Stream adjustment in a small Rocky Mountain basin: Arctic and Alpine Research, v. 8, p. 197-212.

Knighton, A.D., 1998, Fluvial Forms and Processes: A new perspective, New York, Oxford University Press.

Knox, J.C., 1976, Concept of the graded stream, in Melhorn, W. and Flemal, R. eds., Theories of landform development, Binghamton: New York, State University of New York, Publications in Geomorphology, p. 169-198.

Lane, E.W., 1955, Design of stable channels: Transactions of the American Society of Civil Engineers, v. 120, p. 1234-1260.

Leopold, L.B., 1969, The rapids and pools-Grand Canyon: U.S. Geological Survey Professional Paper 669-D.

Leopold, L.B., and Bull, W.B., 1979, Base level, aggradation, and grade: Proceedings of the American Philosophical Society, v. 123, no. 3, p. 168-202.

Lucchitta, I., 1979, Late Cenozoic uplift of the southwestern Colorado Plateau and adjacent Colorado River region: Tectonophysics, v. 61, p. 63-95.

Lucchitta, I., 2003, History of the Grand Canyon and of the Colorado River in Arizona , in Beus, S.S., and Morales, M., eds., Grand Canyon geology: New York, Oxford, p. 260-274.

Lucchitta, I., Curtis, G.H., Davis M.E., Davis, S.W, and Turrin, B., 2000, Cyclic aggradation and downcutting, fluvial response to volcanic activity, and calibration of soil-carbonate stages in western Grand Canyon: Quaternary Research, v. 53, p. 23-33.

Lucchitta, I., and Young, R.A., 1986, Structure and geomorphic character of Western Colorado Plateau in the Grand Canyon-Lake Mead Region, in Nations, J.D. Conway, C.M., and Swann, G.A., eds., Geology of Central and Northern Arizona, Geological Society of America, Rocky Mountain Section, Field Trip Guidebook, p. 159-176.

Machette, M.N., and Rosholt, J.N., 1991, Quaternary geology of the Grand Canyon, in Morrison, R.B., ed., The geology of North America, v. K-2, Quaternary nonglacial geology: Conterminous U.S.: Boulder, Geological Society of America, p. 397-401.

Mackin, J.H., 1948, Concept of the graded stream: Geological Society of America Bulletin, v. 59, p. 463-512.

Melis, T. S., 1997, Geomorphology of debris flows and alluvial fans in Grand Canyon National Park and their influences on the Colorado River below Glen Canyon Dam, Arizona [Ph.D. dissert.], Tucson, University of Arizona, 495 p.

Middleton, L.T., and Elliott, D.K., 2003, Tonto Group, in Beus, S.S., and Morales, M., eds., Grand Canyon geology: New York, Oxford, p. 90-106.

Miller, J.R., 1991, The influence of bedrock geology on knickpoint development and channel-bed degradations along downcutting steams in south-central Indian: Journal of Geology, v. 99, p. 591-605.

Moon, B.P., 1984, Refinement of a technique for determining rock mass strength for geomorphological purposes: Earth Surface Processes and Landforms, v. 9, p. 189-193.

Narr, W., and Suppe, J., 1991, Joint spacing in sedimentary rocks: Journal of Structural Geology, v. 13, p. 11037-48.

NIH, 2004, NIH Image: U.S. National Institutes of Health, http://rsb.info.nih.gov/nih-image.

Pazzaglia, F.J., Gardner, T.W., and Merritts, D.J., 1998, Bedrock fluvial incision and longitudinal profile development over geologic time scales determined by fluvial terraces, *in* Tinkler, K.J. and Wohl, E.E., eds., Rivers over rock, fluvial processes in bedrock channels: Washington, D.C., American Geophysical Union, Monograph 107, p. 207-235.

Pederson, J., Karlstrom, K., Sharp, W., and McIntosh, W., 2002, Differential incision of the Grand Canyon related Quaternary faulting-Constraints from U-series and Ar/Ar dating: Geology, v. 30, p. 739-742.

Pederson, J., Karlstrom, K., Sharp, W., and McIntosh, W., 2003, Differential incision of the Grand Canyon related Quaternary faulting-Constraints from U-series and Ar/Ar dating: REPLY: Geology: Online Forum, p. e17.

Poole, R.W., and Farmer, I.W., 1980, Consistency and repeatability of Schmidt Hammer rebound data during field testing: International Journal of Rock Mechanics and Mining Science and Geomechanics Abstracts, v. 17, p. 167-171.

Powell, J.W., 1876, Exploration of the Colorado River of the West: Washington, DC, Smithsonian Institution, 291 p.

Schmidt, E., 1951, A non-destructive concrete test: Concrete, v. 59, no. 8, p. 34-35.

Schmidt, J.C., and Graf, J.B., 1990, Recirculating flow and sedimentation in the Colorado River in Grand Canyon, Arizona, Journal of Geology, v. 98, p. 709-724.

Selby, M.J., 1980, A rock mass strength classification for geomorphic purposes: With tests from Antarctica and New Zealand: Zeitschrift fur Geomorphologie, v. 24, p. 31-51.

Selby, M.J, 1982, Controls on the stability and inclinations of hillslopes formed on hard rock: Earth Surface Processes and Landforms, v. 7, p. 449-467.

Selby, M.J., 1993, Hillslope Materials and Processes: Oxford, U.K., Oxford University Press, 451 p.

Sklar, L.S. and Dietrich, W.E., 1998, River longitudinal profiles and bedrock incision models: Stream power and the influence of sediment supply, *in* Tinkler, K.J. and Wohl, E.E., eds., Rivers over rock, fluvial processes in bedrock channels: Washington, D.C., American Geophysical Union, Monograph 107, p. 237-260.

Sklar L.S. and Dietrich, W.E., 2001, Sediment and rock strength controls on river incision into bedrock: Geology, v. 29, no. 12, p. 1087-1090.

Slingerland, R.L., Willett, S.D., and Hennessey, H.L., 1997, A new fluvial bedrock incision model based on the work-energy principle [abs]: Eos (Transactions, American Geophysical Union), v. 78, p. F299.

Snow, R.S., and Slingerland, R.L., 1987, Mathematical modeling of graded river profiles: Journal of Geology, v. 95, p. 15-33.

Snyder, N.P., Whipple, K.X., Tucker, G.E., and Merritts, D.J., 2003, Channel response to tectonic forcing: field analysis of stream morphology and hydrology in the Mendocino triple junction region, northern California: Geomorphology, v. 53, p. 97-127.

Stock, J.D., and Montgomery, D.R., 1999, Geologic constraints on bedrock river incision using the stream power law, Journal of Geophysical Research, v. 104, B3, p. 4,983-4,993.

Terzaghi, K., 1962, Stability of steep slopes in hard unweathered rock, Geotechnique, v. 12, p. 251-271.

Turner, C.E. , 2003, Toroweap Formation, *in* Beus, S.S., and Morales, M., eds., Grand Canyon geology: New York, Oxford, p. 180-195.

Wagner, S.S., and Karlstrom, K.E., 2002, Neogene profile of the Colorado River: Different reaches and differential incision within a young river system: Geological Society of America Annual Meeting, Denver, CO, Abstract of Paper 144-2.

Walcott, C.D., 1889, A study of a line of displacement in the Grand Canyon of the Colorado in Northern Arizona: Geological Society of America Bulletin, v. 1, p. 49-64.

Webb, R.H., Pringle, P.T., and Rink, G.R., 1989, Debris flows from the tributaries of the Colorado River, Grand Canyon National Park, Arizona: U.S. Geological Survey Professional Paper, 1492, 39 p.

Webb, R.H., Melis, T.S, and Griffiths, P.G., 2003, Debris flows and the Colorado River, *in* Beus, S.S., and Morales, M., eds., Grand Canyon geology: New York, Oxford, p. 371-390.

Webb, R.H., Griffiths, P.G., Fleming, J.B., Callegary, J.B., Fenton, C.R., and Hanks, T.C., 2004, The longitudinal profile of the Colorado River on the Colorado plateau: How deep is alluvium beneath the river: Geological Society of America Annual Meeting, Denver, CO, Abstract of Paper 238-5.

Whipple, K.X., Hancock, G.S., and Anderson, R.S, 2000a, River incision into bedrock: Mechanics and relative efficacy of plucking, abrasion, and cavitation: Geological Society of America Bulletin, v. 112, no. 3, p. 490-503.

Whipple, K.X., Snyder, N.P., and Dollenmayer, K., 2000b, Rates and processes of bedrock incision by the Upper Ukak River since the 1912 Novarupta ash flow in the Valley of Ten Thousand Smokes, Alaska: Geology, v. 28, p. 835-838.

Wohl, E.E., Greenbaum, N., Schick, A.P., and Baker, V.R., 1994, Controls on bedrock channel incision along Nahal Paran, Israel: Earth Surface Processes and Landforms, v. 19, p. 1-13.

Wohl, E.E., and Merritt, D.M., 2001, Bedrock channel morphology: Geological Society of America Bulletin, v. 113, no. 9, p. 1205-1212.

Wolkowinsky, A.J., and Granger, D.E., 2004, Early Pleistocene incision of the San Juan River, Utah, dated with ^{25}Al and ^{10}Be: Geology, v. 32, no. 9, p. 749-752.

Young, R.A., and Brennan, W.J., 1974, Peach Springs tuff, its bearing on structural evolution of the Colorado Plateau and development of Cenozoic drainage in Mohave County, Arizona, Geological Society of American Bulletin, v. 85, p. 83-90.

APPENDICES

Appendix A. Sample Sites

The following appendix contains a map showing the locations of 84 outcrop-scale

study sites used in this study and a table with detailed information for each sample site.
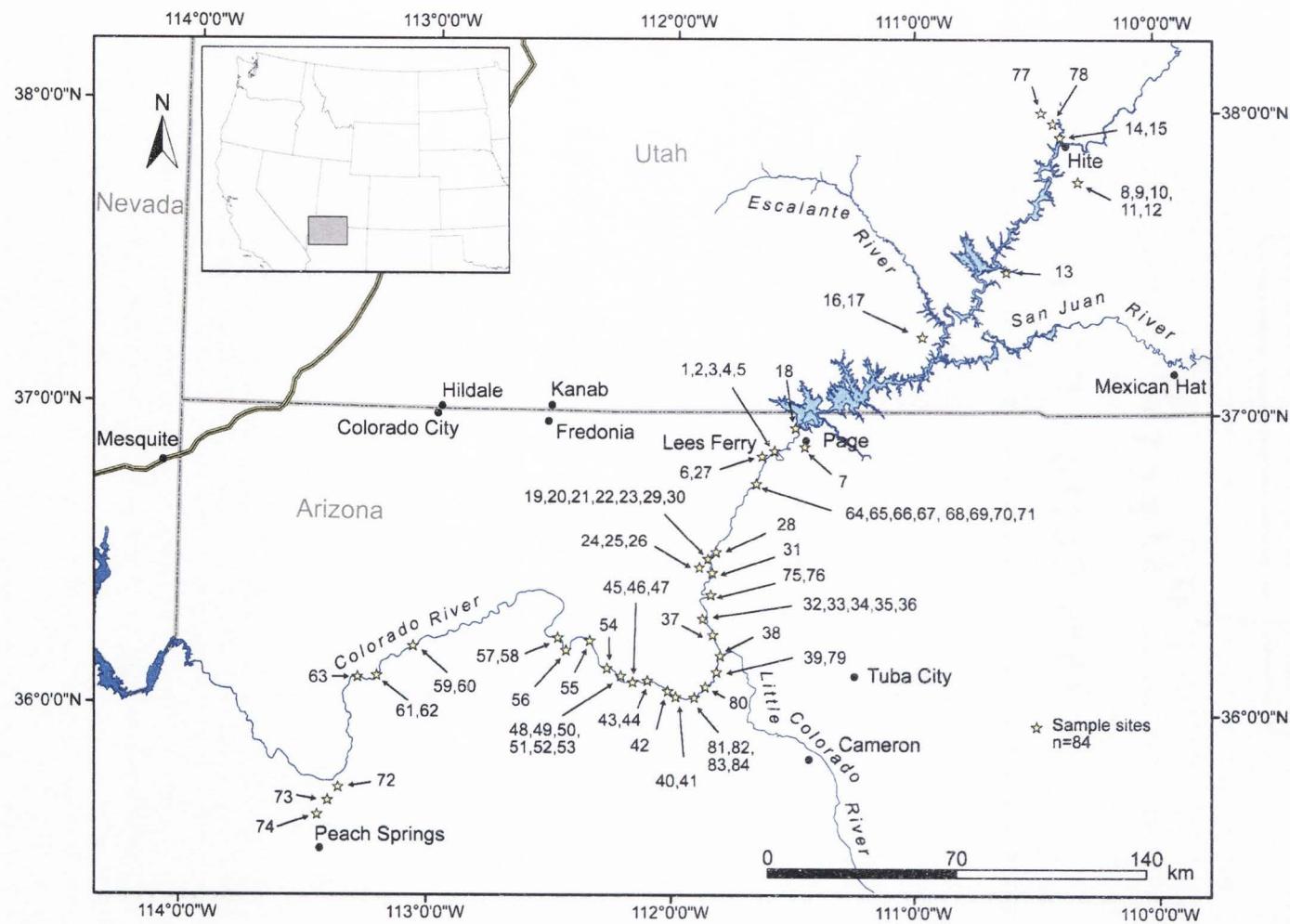
Figure A.1. Map of sample site locations within study area of Glen and Grand canyons. Sample sites are labeled with their respective Site ID (Table 1) and symbolized with stars.

Table A.1. GENERAL SAMPLE SITE INFORMATION

Site ID	X* (m)	Y† (m)	Z§ (m)	Description	Rock unit	Stratigraphic position	Lithology	Sample date	Notes
1	448863	4080341	1414	Vermillion Cliffs; Top of Spencer's trail, near Lee's Ferry, AZ	Navajo Sandstone	upper, several meters from top of unit	sandstone	05/09/03	
2	448696	4080337	1368	Vermillion Cliffs; just down from the top of Spencer's trail, Lee's Ferry, AZ	Navajo Sandstone	middle, 75 to 100 meters from top of unit	sandstone	05/09/03	
3	448591	4080405	1304	Vermillion Cliffs; along Spencer's Trail, near Lees Ferry, AZ	Kayenta Formation	upper, just below contact with Navajo	sandstone	05/09/03	Not 100% certain this is Kayenta. It may still be in the Navajo, very tough to call
4	448467	4080251	1122	Vermillion Cliffs; along Spencer's Trail, Lees Ferry, AZ	Wingate Sandstone	upper Middle	sandstone	05/09/03	Suspect elevation, only 3 satellites on GPS
5	448515	4080097	1104	Vermillion Cliffs; along Spencer's Trail, Lees Ferry, AZ	Wingate Sandstone	middle	sandstone	05/09/03	Suspect elevation, only 3 satellites on GPS
6	447551	4080001	960	Shinarump outcrop near boatramp at Lees Ferry, AZ	Chinle Formation	middle	cong-lomerate	05/10/03	
7	459537	4082835	1341	Manson Mesa, near Page, AZ	Page Sandstone	upper, 20 m below contact with Carmel	sandstone	05/11/03	
8	561177	4179950	1634	Saddle/divide at top of Blue Notch Canyon, east of Hite, UT	Chinle Formation	Trcl: ledgy mbr, limey unit of Chinle	shaley limestone	05/17/03	
9	560409	4180035	1560	3/4 up Blue Notch Canyon, near Hite, UT	Chinle Formation	Trcms: verigated mud, shale & ss unit	shale	05/18/03	more pebbly outcrop of Trcms
10	560409	4180035	1562	3/4 up Blue Notch Canyon, near Hite, UT	Chinle Formation	Trcms: verigated mud, shale & ss unit	shale	05/18/03	less pebbly, more sandy outcrop
11	559494	4179865	1426	1/2 up/down Blue Notch Canyon, UT	Moenkopi Formation	Upper; ledgey f. sandstones interbedded with shales; thicker (1-2m) beds	siltstone	05/18/03	blocky ss portion
12	559494	4179865	1426	1/2 up/down Blue Notch Canyon, UT	Moenkopi Formation	Upper; ledgey f. sandstones interbedded with shales; thinner (.10 - .5 m) beds	shale	05/18/03	thinner bedded sands interbedded with silts
13	533861	4146786	1240	2 mi east of Halls Crossing, Lake Powell, UT	Page Sandstone	mid to upper	sandstone	05/19/03	
14	552898	4194466	1158	Near Hite, UT along hwy 95, just north of Dirty Devil confluence w/ L. Powell	Organ Rock Formation	lower to middle; f. grain sandstone interbedded with silt/shales	siltstone	05/19/03	
15	552091	4193541	1173	Near Hite, UT along hwy 95 at Dirty Devil overlook	Organ Rock Formation	upper; more massive (3-5m) beds	siltstone	05/19/03	Roadcut surface; may be fresher and give elevated R-values, so moved down into non-roadcut "ampitheater"
16	505309	4123391	1348	End of Hole-in-the-rock road, north of Straight Cliffs, UT	Navajo Sandstone	upper	sandstone	05/20/03	
17	505309	4123391	1348	End of Hole-in-the-rock road, north of Straight Cliffs, UT	Navajo Sandstone	upper	sandstone	05/20/03	

Table A.1 SAMPLE SITE INFORMATION continued

Site ID	X* (m)	Y† (m)	Z§ (m)	Description	Rock unit	Stratigraphic position	Lithology	Sample date	Notes
18	457227	4089163	1152	Beach access area near GC dam, down gravel road to parking lost (East side of river/lake)	Navajo Sandstone	middle to upper	sandstone	05/30/03	To get there: Turn off 89 just after crossin gover to east side of dam, go down road to swim access parking lot.
19	423163	4039834	908	At River level at mouth of South Canyon, Marble Canyon, AZ	Redwall Limestone	Lower Middle	limestone	05/31/03	I put stickers on outcrop where I took Scmidt hammer samples; I took photos.
20	423255	4040140	939	Mouth of South Canyon, AZ	Redwall Limestone	Upper Middle	limestone	05/31/03	About 1/3 up Redwall L.S. along trail coming up from beach camps
21	423217	4040198	981	Mouth of South Canyon, AZ	Redwall Limestone	Top, 5m below contact with overlying Supai Gp.	limestone	05/31/03	near top of South Canyon trail leaving beach camp
22	422955	4040041	1000	South Canyon, AZ	Watahomigi Formation	middle	sandstone	06/01/03	above "junky" carbonate unit; this is Watahomigi
23	423029	4040315	1143	South Canyon, AZ	Wescogame Formation	Unknown	sandstone	06/01/03	these huge (3 to 5m) blocks came from the Wescogame
24	419113	4037666		South Canyon, AZ	Wescogame Formation	upper	sandstone	06/01/03	Wescogame Fm.
25	417117	4036460	1465	South Canyon, AZ	Coconino Sandstone	middle	sandstone	06/01/03	
26	417001	4036582		South Canyon, AZ	Kaibab Limestone	lower, near base	limestone	06/01/03	
27	446002	4078696	1606	Paria beach, AZ	Kaibab Limestone	Upper; just below contact with Moenkopi	limestone	09/08/03	
28	424341	4041589	880	1 mi upstream from South Canyon, AZ; River Mile 30.3, river left	Redwall Limestone	Upper	limestone	09/09/03	This site is straddling the Fence Fault-zone
29	423007	4040304		Slopes above South Canyon, AZ	Manakacha Formation	middle	sandstone	09/09/03	Cliff exposure about 1/3 up Manakacha
30	423141	4040302	1062	Slopes above South Canyon, AZ	Manakacha Formation	Upper	siltstone	09/09/03	Upper slope former in Manakacha
31	424733	4036288	1062	Mouth of Nautiloid Canyon, Marble Canyon	Redwall Limestone	Base	limestone	09/10/03	
32	422446	4018179	1062	Mouth of Little Nankoweap Canyon	Bright Angel Shale	middle	shale	09/11/03	Outcrop is on downstream side of debris fan above talus slope
33	421923	4018346	914	Little Nankoweap Canyon	Bright Angel Shale	Top	shale	09/11/03	Stream cut exposure
34	421564	4018278	981	Little Nankoweap Canyon	Muav Limestone	Mid to upper	shaley limestone	09/11/03	coords taken off map(no GPS sats); stream cut outcrop
35	421374	4018384	1000	Little Nankoweap Canyon	Muav Limestone	Top	shaley limestone	09/11/03	Just below where the gradational contact gets really tough to distinguish, between base of undiff. dol/Redwall.
36	421779	4018346	927	Little Nankoweap Canyon	Muav Limestone	lower	shaley limestone	09/11/03	lower block-more resistant unit in Muav, stream cut

Table A.1 SAMPLE SITE INFORMATION continued

Site ID	X* (m)	Y† (m)	Z§ (m)	Description	Rock unit	Stratigraphic position	Lithology	Sample date	Notes
37	425298	4012993	878	Mouth of Kwagunt Canyon	Bright Angel Shale	lower "greenish" f. gr. Unit	shale	09/11/03	
38	428209	4005446	830	LCR Confluence	Tapeats Sandstone	upper	sandstone	09/12/03	ledgy/blocky outcrop above river on river left
39	427011	3999903	869	Palisades?	Dox Formation	upper	well-cemented sandstone	09/12/03	Near Palisades Creek Canyon, across from Chuar Lava Hill
40	410980	3989990		River Mile 80.6	Vishnu Schist		schist	09/13/03	
41	410980	3989990		River Mile 80.6	Zoroaster Granite		granite	09/13/03	
42	408112	3991911	762	River Mile 83	Vishnu Schist		schist	09/13/03	
43	400150	3995242	749	Phantom Ranch	Vishnu Schist		schist	09/14/03	Just below Phantom Ranch on river left
44	400150	3995242	749	Phantom Ranch	Zoroaster Granite		granite	09/14/03	Just below Phantom Ranch on river left
45	397519	3995685	814	River Mile 90.6	Zoroaster Granite		granite	09/14/03	Upper Granite Gorge;River left
46	394839	3995528	735	River Mile 92.6	Zoroaster Granite		gneiss	09/14/03	Upper Granite Gorge;River left
47	392267	3995159	731	River Mile 94	Vishnu Schist		schist	09/14/03	Upper Granite Gorge; River left, just above Hermit
48	390909	3995528	731	River Mile 95.2	Vishnu Schist		gneiss	09/14/03	Upper Granite Gorge; River left, just below Hermit
49	389873	3996453	731	River Mile 95.7	Vishnu Schist		schist	09/14/03	Upper Granite Gorge; River right, just below Hermit
50	390221	3995927	719	River Mile 95.7	Vishnu Schist		schist	09/14/03	Upper Granite Gorge; River left, just below Hermit
51	389747	3996430	713	River Mile 96	Vishnu Schist		gneiss	09/15/03	Upper Granite Gorge; River left
52	389723	3996461	713	River Mile 96	Zoroaster Granite		granite	09/15/03	Upper Granite Gorge; River left
53	389243	3997288	695	Mouth of Topaz/Boucher Canyon, River mile 96.5	Vishnu Schist		schist	09/15/03	Upper Granite Gorge; River left
54	385674	4000414	692	River Mile 100	Zoroaster Granite		granite	09/15/03	Upper Granite Gorge; River left
55	379377	4011026	695	Above Bass Camp on Bass trail, River mile 108	Bass Limestone		limestone	09/15/03	Upper Granite Gorge; River right; near indian ruin above and to east of camp
56	369662	4006647	646	Elves Chasm, River mile 116.5	Zoroaster Granite		granite	09/16/03	Upper Granite Gorge; River left
57	367667	4011682	655	Blacktail Canyon, River mile 120	Tapeats Sandstone	lower	sandstone	09/16/03	Just inside slot canyon, 50yd up from beach;purple to greenish purple coarse sandstone
58	367667	4011682	655	Blacktail Canyon, River mile 120	Tapeats Sandstone	lower	sandstone	09/16/03	Just inside slot canyon, 50yd up from beach area; lighter colored x-bedded unit
59	315693	4008993	536	River Mile 177.7; just upstream from Vulcan's Anvil	Bright Angel Shale		sandstone	09/17/03	Western Grand Canyon; river left
60	313135	4007942	543	Lava Falls Scout Area; river mile 178	Bright Angel Shale		sandstone	09/19/03	Western Grand Canyon; river right

Table A.1 SAMPLE SITE INFORMATION continued

Site ID	X* (m)	Y† (m)	Z§ (m)	Description	Rock unit	Stratigraphic position	Lithology	Sample date	Notes
61	300789	3998094	491	River mile 191.2	Pleistocene Basalts		basalt	09/19/03	Western Grand Canyon; river left
62	300084	3996888	482	River mile 192	Pleistocene Basalts		basalt	09/19/03	Western Grand Canyon; river right; Hamblin's Grey Ledge Basalt
63	293664	3996948	488	River mile 196; near Frogy Fault	Muav Limestone		shaley limestone	09/20/03	Western Grand Canyon river left
64	442515	4068715	1079	Jackass Canyon, AZ	Toroweap Formation	lower middle	sandstone	11/15/03	Half-way down Jackass to river
65	442279	4069237	1009	Jackass Canyon, AZ	Coconino Sandstone	middle	sandstone	11/15/03	Half-way down Jackass to river
66	442181	4069327	991	Jackass Canyon, AZ	Hermit Formation	massive sandstone interbed	siltstone	11/15/03	Two-thirds way down Jackass to river
67	442181	4069327	991	Jackass Canyon, AZ	Hermit Formation	mud/f. gr. Interbed	shale	11/15/03	Two-thirds way down Jackass to river
68	441915	4069551	975	Jackass Canyon, AZ	Hermit Formation	massive sandstone interbed	siltstone	11/15/03	3/4 down Jackass
69	441915	4069551	975	Jackass Canyon, AZ	Hermit Formation	mud/f. gr. Interbed	shale	11/15/03	3/4 down Jackass
70	441628	4069758	963	Mouth of Jackass Canyon, river mile 7.8	Hermit Formation	thin sand/silt interbeds	shale	11/15/03	Mouth of Canyon, just above fan on upstream side of rapid
71	442539	4068813	1036	Jackass Canyon, AZ	Toroweap Formation	upper	sandstone	11/15/03	1/2 way up/down Jackass
72	285966	3957301	576	Diamond Creek, AZ	Tapeats Sandstone	lower	well-cemented sandstone	02/27/04	cutbank on west side of valley within fault-zone
73	282283	3952327	866	Diamond Creek, AZ	Muav Limestone	lower	shaley limestone	02/27/04	cliff former above contact with slope forming Bright Angel below
74	278645	3947138	1033	Diamond Creek, AZ	Muav Limestone	upper	limestone	02/27/04	ephemeral stream channel on west side of diamond creek road
75	425142	4028642	1402	Tatahatso Point, AZ	Coconino Sandstone	middle	sandstone	02/28/04	down along hikers trail at tatahatso point
76	425110	4028596	1372	Tatahatso Point, AZ	Esplanade Sandstone	middle	sandstone	02/28/04	down along hikers trail at tatahatso point
77	542502	4206239	1332	Hwy 95 to Hite, UT	Kayenta Formation	middle	sandstone	04/16/04	along HWY 95 going from Hanksville to Hite, UT
78	544794	4201631	1317	Hog Spring Picnic Area, near Hite, UT	Wingate Sandstone	middle	sandstone	04/16/04	along HWY 95 going from Hanksville to Hite; across road from Hog Springs Picnic Area
79	426818	3999218	832	Palisades, river mile 65.6	Cardenas Formation		basalt	04/22/04	just downstream from mouth of Cardenas Creek, Furnace Flats
80	422199	3993441	834	Cardenas Creek, river mile 71	Dox Formation	middle	siltstone	04/22/04	stream cut in Cardenas Creek, 1/4 mi up from mouth
81	420439	3990354	1013	Escalante Creek	Dox Formation	lower	shaley sandstone	04/23/04	stream cut in north arm of escalante creek, 1/4 mi from mouth
82	418580	3989257	795	just upstream of Papago Creek, river mile 75.6	Shinumo Quartzite	lower	quartzite	04/23/04	2 meters above modern river level; between 75 mile and Papago Creeks

Table A.1 SAMPLE SITE INFORMATION continued

Site ID	X^* (m)	$Y^\dagger$ (m)	$Z^\S$ (m)	Description	Rock unit	Stratigraphic position	Lithology	Sample date	Notes
83	419075	3989742	811	75 Mile Creek	Shinumo Quartzite	middle	quartzite	04/24/04	500 yards into 75 Mile Creek slot canyon
84	416593	3989173	802	just below Hance Rapid, river mile 76.8	Hakatai Shale	lower	shaley sandstone	04/24/04	gully cut on river left just below Hance

Note: Coordinates are in the Universal Transverse Mercator (UTM) coordinate system, Zone 12, North American Datum 1927 (NAD27).
*Easting in meters.
†Northing in meters.
§Elevation in meters.

Appendix B. Intact-Rock Strength Data

The following appendix contains a table of summary statistics on intact-rock

strength, organized by sample site, and the raw data itself.

Summary Statistics

Table B.1. INTACT-ROCK STRENGTH SUMMARY STATISTICS

Site ID	n	Avg	SD	Min	Q1*	Median	Q3†	Max
1	50	32.9	5.9	25	28	31.0	37	47
2	50	45.4	4.6	36	42	45.0	48	56
3	20	33.2	5.7	24	30	32.0	35	50
4	30	52.2	2.6	48	49	53.5	54	56
5	30	54.1	2.9	49	51	55.0	57	58
6	43	35.2	5.2	22	31	35.0	39	48
7	50	33.0	2.4	28	31	33.0	35	39
8	50	48.3	5.6	38	44	48.0	52	60
9	19	41.2	5.1	32	38	40.0	45	51
10	31	41.9	6.5	32	35	41.0	49	53
11	50	46.2	5.1	35	42	47.5	49	58
12	50	36.7	5.8	20	34	36.5	41	48
13	50	38.1	4.6	28	35	38.0	42	47
14	50	48.7	3.6	42	46	49.0	51	56
15	50	48.9	3.8	42	45	49.0	52	55
16	50	39.2	2.6	35	37	40.0	41	45
17	50	35.9	2.2	31	34	36.0	38	41
18	50	36.5	3.4	32	34	35.0	39	44
19	50	58.5	3.3	50	56	58.5	61	65
20	50	56.1	3.3	49	55	56.5	58	62
21	28	58.1	3.7	50	56	58.5	62	64
22	50	52.2	5.1	42	48	53.0	55	60
23	50	57.9	2.7	51	56	58.0	60	62
24	50	58.1	4.4	50	54	58.0	62	65
25	50	57.1	3.7	47	55	58.0	59	64
26	26	57.3	2.8	52	55	57.5	60	62
27	50	59.5	3.7	52	56	59.5	62	68
28	32	48.4	3.9	43	46	47.0	51	60
29	50	54.9	4.7	48	50	54.5	58	64
30	50	38.5	10.2	22	30	38.5	46	60
31	50	52.7	5.0	42	50	52.0	57	63
32	50	28.0	7.6	11	22	29.0	34	45
33	50	30.2	6.4	19	25	30.0	36	42
34	80	37.1	8.7	20	32	35.5	42	60

Table B.1. SUMMARY STATISTICS OF INTACT-ROCK STRENGTH DATA
continued

Site ID	n	Avg	SD	Min	Q1*	Median	Q3†	Max
35	50	38.2	5.6	26	34	39.0	43	48
36	30	40.0	6.4	30	35	38.0	46	52
37	30	16.4	4.4	10	12	15.5	20	24
38	50	50.9	4.5	40	48	50.5	54	60
39	50	63.5	4.3	50	61	63.5	67	72
40	30	63.4	3.8	57	60	64.0	66	70
41	30	59.3	5.6	50	56	58.5	62	70
42	50	61.2	6.1	42	57	60.5	67	71
43	30	54.6	4.8	48	50	54.5	58	64
44	30	51.3	4.6	45	49	50.0	53	65
45	30	56.0	4.0	50	52	55.5	59	63
46	50	63.5	5.9	50	61	64.0	68	73
47	30	60.7	5.8	45	59	61.5	65	69
48	50	60.8	4.6	51	58	60.0	64	70
49	30	51.5	4.5	44	48	51.0	53	64
50	30	56.5	4.3	47	54	56.0	60	64
51	50	56.6	5.4	48	52	56.0	61	70
52	50	60.8	4.6	50	58	60.0	64	69
53	30	59.0	3.9	51	56	59.0	62	65
54	30	58.3	4.8	45	56	58.0	62	70
55	50	59.7	4.3	49	56	60.5	63	68
56	30	62.0	4.2	53	59	63.0	64	69
57	50	39.4	4.6	30	36	39.5	44	48
58	50	56.1	4.4	45	52	56.5	59	64
59	60	41.7	8.2	28	35	41.5	48	58
60	50	50.5	4.7	42	47	50.5	54	60
61	50	57.6	4.3	48	54	58.0	61	66
62	30	56.0	3.6	50	53	56.5	59	63
63	50	35.9	3.7	30	33	35.0	38	50
64	61	55.9	5.3	48	50	55.0	61	65
65	50	54.9	3.7	48	52	54.0	57	63
66	30	39.0	5.2	30	36	38.0	42	52
67	30	12.2	2.6	9	10	11.5	13	20
68	30	56.2	2.6	50	55	56.0	58	61
69	30	13.1	2.7	10	11	12.0	15	20
70	30	25.7	7.3	15	20	25.0	30	42
71	50	55.4	3.9	45	53	55.5	59	62
72	50	60.4	3.0	54	58	60.0	62	68

Table B.1. SUMMARY STATISTICS OF INTACT-ROCK STRENGTH DATA
continued

Site ID	n	Avg	SD	Min	Q1*	Median	Q3†	Max
73	60	48.9	5.3	40	45	49.0	53	60
74	50	56.8	3.9	44	54	57.0	60	64
75	30	49.8	2.7	45	48	49.0	52	55
76	60	55.1	2.9	49	54	55.0	57	62
77	50	39.5	3.1	34	38	39.5	41	48
78	50	43.9	2.6	39	42	44.0	46	49
79	50	49.7	5.2	41	46	48.5	54	61
80	50	54.9	4.0	46	52	55.0	58	63
81	50	52.7	3.6	42	50	52.5	55	61
82	30	60.4	3.9	51	58	61.0	63	68
83	50	58.5	2.7	54	56	58.0	60	65
84	60	46.2	8.0	30	42	46.5	52	60

Note: Intact-rock strength values are reported as the rebound percent recorded
by the Schmidt hammer instrument and organized by sample site.
*First quartile value.
†Third quartile value.

Complete Dataset

Table B.2. INTACT-ROCK STRENGTH DATA

Site ID	Raw*	Ang†	Adj§	Site ID	Raw*	Ang†	Adj§	Site ID	Raw*	Ang†	Adj§	Site ID	Raw*	Ang†	Adj§
1	22	45	25	1	38	45	41	2	48	0	48	4	52	0	52
1	22	45	25	1	39	45	42	2	49	0	49	4	53	0	53
1	22	45	25	1	40	45	43	2	49	0	49	4	53	0	53
1	22	45	25	1	41	45	44	2	50	0	50	4	54	0	54
1	22	45	25	1	42	45	45	2	50	0	50	4	54	0	54
1	23	45	26	1	44	45	47	2	52	0	52	4	54	0	54
1	24	45	27	2	36	0	36	2	52	0	52	4	54	0	54
1	24	45	27	2	38	0	38	2	52	0	52	4	54	0	54
1	24	45	27	2	38	0	38	2	54	0	54	4	54	0	54
1	25	45	28	2	40	0	40	2	54	0	54	4	54	0	54
1	25	45	28	2	40	0	40	2	55	0	55	4	54	0	54
1	25	45	28	2	40	0	40	2	56	0	56	4	54	0	54
1	25	45	28	2	40	0	40	3	24	0	24	4	54	0	54
1	26	45	29	2	40	0	40	3	26	0	26	4	55	0	55
1	26	45	29	2	40	0	40	3	26	0	26	4	55	0	55
1	26	45	29	2	40	0	40	3	30	0	30	4	55	0	55
1	26	45	29	2	42	0	42	3	30	0	30	4	55	0	55
1	26	45	29	2	42	0	42	3	30	0	30	4	56	0	56
1	26	45	29	2	42	0	42	3	31	0	31	4	56	0	56
1	27	45	30	2	42	0	42	3	31	0	31	5	49	0	49
1	27	45	30	2	43	0	43	3	32	0	32	5	50	0	50
1	28	45	31	2	43	0	43	3	32	0	32	5	50	0	50
1	28	45	31	2	44	0	44	3	32	0	32	5	50	0	50
1	28	45	31	2	44	0	44	3	33	0	33	5	50	0	50
1	28	45	31	2	44	0	44	3	33	0	33	5	50	0	50
1	28	45	31	2	44	0	44	3	34	0	34	5	51	0	51
1	30	45	33	2	44	0	44	3	35	0	35	5	51	0	51
1	30	45	33	2	44	0	44	3	35	0	35	5	51	0	51
1	30	45	33	2	44	0	44	3	40	0	40	5	52	0	52
1	31	45	34	2	45	0	45	3	40	0	40	5	53	0	53
1	32	45	35	2	45	0	45	3	40	0	40	5	54	0	54
1	32	45	35	2	45	0	45	3	50	0	50	5	54	0	54
1	32	45	35	2	45	0	45	4	48	0	48	5	54	0	54
1	32	45	35	2	45	0	45	4	48	0	48	5	55	0	55
1	32	45	35	2	45	0	45	4	48	0	48	5	55	0	55
1	32	45	35	2	46	0	46	4	49	0	49	5	55	0	55
1	34	45	37	2	46	0	46	4	49	0	49	5	55	0	55
1	36	45	39	2	46	0	46	4	49	0	49	5	56	0	56
1	36	45	39	2	46	0	46	4	49	0	49	5	56	0	56
1	36	45	39	2	47	0	47	4	49	0	49	5	56	0	56
1	37	45	40	2	48	0	48	4	50	0	50	5	56	0	56
1	38	45	41	2	48	0	48	4	50	0	50	5	57	0	57
1	38	45	41	2	48	0	48	4	51	0	51	5	57	0	57
								4	51	0	51	5	57	0	57
												5	57	0	57

Table B.2. INTACT-ROCK STRENGTH DATA continued

Site ID	Raw*	Ang†	Adj§	Site ID	Raw*	Ang†	Adj§	Site ID	Raw*	Ang†	Adj§	Site ID	Raw*	Ang†	Adj§
5	58	0	58	6	44	0	44	7	32	45	35	8	52	0	52
5	58	0	58	6	48	0	48	7	34	45	37	8	53	0	53
5	58	0	58	7	25	45	28	7	34	45	37	8	55	0	55
5	58	0	58	7	26	45	29	7	34	45	37	8	55	0	55
6	22	0	22	7	26	45	29	7	34	45	37	8	56	0	56
6	25	0	25	7	26	45	29	7	34	45	37	8	56	0	56
6	28	0	28	7	27	45	30	7	36	45	39	8	57	0	57
6	29	0	29	7	27	45	30	8	38	0	38	8	58	0	58
6	29	0	29	7	28	45	31	8	40	0	40	8	58	0	58
6	30	0	30	7	28	45	31	8	40	0	40	8	58	0	58
6	31	0	31	7	28	45	31	8	40	0	40	8	60	0	60
6	31	0	31	7	28	45	31	8	41	0	41	8	60	0	60
6	31	0	31	7	28	45	31	8	42	0	42	9	32	0	32
6	31	0	31	7	28	45	31	8	42	0	42	9	32	0	32
6	31	0	31	7	28	45	31	8	43	0	43	9	36	0	36
6	31	0	31	7	28	45	31	8	43	0	43	9	37	0	37
6	32	0	32	7	28	45	31	8	44	0	44	9	38	0	38
6	32	0	32	7	29	45	32	8	44	0	44	9	39	0	39
6	33	0	33	7	29	45	32	8	44	0	44	9	40	0	40
6	34	0	34	7	29	45	32	8	44	0	44	9	40	0	40
6	34	0	34	7	29	45	32	8	45	0	45	9	40	0	40
6	34	0	34	7	29	45	32	8	45	0	45	9	40	0	40
6	34	0	34	7	30	45	33	8	45	0	45	9	41	0	41
6	34	0	34	7	30	45	33	8	45	0	45	9	42	0	42
6	34	0	34	7	30	45	33	8	45	0	45	9	43	0	43
6	35	0	35	7	30	45	33	8	45	0	45	9	45	0	45
6	35	0	35	7	30	45	33	8	46	0	46	9	45	0	45
6	35	0	35	7	30	45	33	8	46	0	46	9	46	0	46
6	36	0	36	7	30	45	33	8	46	0	46	9	46	0	46
6	36	0	36	7	30	45	33	8	47	0	47	9	50	0	50
6	37	0	37	7	30	45	33	8	47	0	47	9	51	0	51
6	37	0	37	7	30	45	33	8	47	0	47	10	32	0	32
6	38	0	38	7	31	45	34	8	48	0	48	10	32	0	32
6	38	0	38	7	31	45	34	8	48	0	48	10	32	0	32
6	38	0	38	7	31	45	34	8	48	0	48	10	34	0	34
6	39	0	39	7	31	45	34	8	48	0	48	10	34	0	34
6	39	0	39	7	31	45	34	8	48	0	48	10	35	0	35
6	39	0	39	7	31	45	34	8	49	0	49	10	35	0	35
6	40	0	40	7	31	45	34	8	50	0	50	10	35	0	35
6	40	0	40	7	32	45	35	8	50	0	50	10	36	0	36
6	41	0	41	7	32	45	35	8	50	0	50	10	39	0	39
6	41	0	41	7	32	45	35	8	50	0	50	10	40	0	40
6	41	0	41	7	32	45	35	8	50	0	50	10	40	0	40
6	42	0	42	7	32	45	35	8	50	0	50	10	40	0	40
6	43	0	43	7	32	45	35	8	52	0	52	10	40	0	40

Table B.2. INTACT-ROCK STRENGTH DATA continued

Site ID	Raw*	Ang†	Adj§	Site ID	Raw*	Ang†	Adj§	Site ID	Raw*	Ang†	Adj§	Site ID	Raw*	Ang†	Adj§
10	41	0	41	11	48	0	48	12	36	0	36	13	34	45	37
10	41	0	41	11	48	0	48	12	36	0	36	13	34	45	37
10	42	0	42	11	48	0	48	12	37	0	37	13	34	45	37
10	42	0	42	11	49	0	49	12	38	0	38	13	34	45	37
10	43	0	43	11	49	0	49	12	38	0	38	13	35	45	38
10	44	0	44	11	49	0	49	12	38	0	38	13	35	45	38
10	45	0	45	11	49	0	49	12	39	0	39	13	35	45	38
10	46	0	46	11	49	0	49	12	39	0	39	13	35	45	38
10	48	0	48	11	49	0	49	12	40	0	40	13	35	45	38
10	49	0	49	11	49	0	49	12	40	0	40	13	36	45	39
10	49	0	49	11	50	0	50	12	40	0	40	13	36	45	39
10	50	0	50	11	50	0	50	12	40	0	40	13	36	45	39
10	50	0	50	11	50	0	50	12	40	0	40	13	36	45	39
10	50	0	50	11	50	0	50	12	40	0	40	13	37	45	40
10	51	0	51	11	50	0	50	12	41	0	41	13	37	45	40
10	52	0	52	11	51	0	51	12	41	0	41	13	38	45	41
10	53	0	53	11	52	0	52	12	41	0	41	13	38	45	41
11	35	0	35	11	52	0	52	12	41	0	41	13	39	45	42
11	38	0	38	11	53	0	53	12	42	0	42	13	39	45	42
11	38	0	38	11	54	0	54	12	42	0	42	13	39	45	42
11	38	0	38	11	55	0	55	12	42	0	42	13	40	45	43
11	38	0	38	11	58	0	58	12	43	0	43	13	40	45	43
11	40	0	40	12	20	0	20	12	44	0	44	13	40	45	43
11	40	0	40	12	21	0	21	12	44	0	44	13	40	45	43
11	40	0	40	12	25	0	25	12	45	0	45	13	40	45	43
11	40	0	40	12	28	0	28	12	46	0	46	13	40	45	43
11	40	0	40	12	28	0	28	12	48	0	48	13	40	45	43
11	42	0	42	12	30	0	30	13	25	45	28	13	40	45	43
11	42	0	42	12	30	0	30	13	25	45	28	13	41	45	44
11	45	0	45	12	32	0	32	13	26	45	29	13	42	45	45
11	42	0	42	12	32	0	32	13	28	45	31	13	42	45	45
11	45	0	45	12	33	0	33	13	29	45	32	13	42	45	45
11	45	0	45	12	34	0	34	13	29	45	32	13	44	45	47
11	45	0	45	12	34	0	34	13	30	45	33	14	42	0	42
11	45	0	45	12	34	0	34	13	30	45	33	14	42	0	42
11	46	0	46	12	34	0	34	13	31	45	34	14	44	0	44
11	46	0	46	12	35	0	35	13	31	45	34	14	44	0	44
11	46	0	46	12	35	0	35	13	32	45	35	14	44	0	44
11	47	0	47	12	35	0	35	13	32	45	35	14	44	0	44
11	47	0	47	12	35	0	35	13	32	45	35	14	45	0	45
11	48	0	48	12	35	0	35	13	32	45	35	14	45	0	45
11	48	0	48	12	35	0	35	13	32	45	35	14	45	0	45
11	48	0	48	12	36	0	36	13	34	45	37	14	45	0	45
				12	36	0	36	13	34	45	37	14	46	0	46

Table B.2. INTACT-ROCK STRENGTH DATA continued

Site ID	Raw*	Ang†	Adj§	Site ID	Raw*	Ang†	Adj§	Site ID	Raw*	Ang†	Adj§	Site ID	Raw*	Ang†	Adj§
14	46	0	46	15	45	0	45	16	33	45	36	16	41	45	44
14	46	0	46	15	45	0	45	16	33	45	36	16	42	45	45
14	46	0	46	15	45	0	45	16	33	45	36	17	28	90	31
14	46	0	46	15	45	0	45	16	33	45	36	17	29	90	32
14	47	0	47	15	45	0	45	16	33	45	36	17	30	90	33
14	47	0	47	15	45	0	45	16	33	45	36	17	30	90	33
14	48	0	48	15	46	0	46	16	33	45	36	17	30	90	33
14	48	0	48	15	46	0	46	16	34	45	37	17	30	90	33
14	48	0	48	15	46	0	46	16	34	45	37	17	30	90	33
14	48	0	48	15	46	0	46	16	34	45	37	17	30	90	33
14	49	0	49	15	47	0	47	16	34	45	37	17	31	90	34
14	49	0	49	15	48	0	48	16	34	45	37	17	31	90	34
14	49	0	49	15	48	0	48	16	34	45	37	17	31	90	34
14	50	0	50	15	48	0	48	16	35	45	38	17	31	90	34
14	50	0	50	15	48	0	48	16	35	45	38	17	31	90	34
14	50	0	50	15	48	0	48	16	35	45	38	17	31	90	34
14	50	0	50	15	49	0	49	16	35	45	38	17	32	90	35
14	50	0	50	15	49	0	49	16	35	45	38	17	32	90	35
14	50	0	50	15	49	0	49	16	35	45	38	17	32	90	35
14	50	0	50	15	50	0	50	16	35	45	38	17	32	90	35
14	50	0	50	15	50	0	50	16	36	45	39	17	32	90	35
14	51	0	51	15	50	0	50	16	37	45	40	17	32	90	35
14	51	0	51	15	50	0	50	16	37	45	40	17	32	90	35
14	51	0	51	15	51	0	51	16	37	45	40	17	32	90	35
14	51	0	51	15	51	0	51	16	37	45	40	17	32	90	35
14	51	0	51	15	51	0	51	16	37	45	40	17	32	90	35
14	52	0	52	15	51	0	51	16	37	45	40	17	33	90	36
14	52	0	52	15	52	0	52	16	38	45	41	17	33	90	36
14	52	0	52	15	52	0	52	16	38	45	41	17	33	90	36
14	53	0	53	15	52	0	52	16	38	45	41	17	33	90	36
14	54	0	54	15	53	0	53	16	38	45	41	17	34	90	37
14	54	0	54	15	53	0	53	16	38	45	41	17	34	90	37
14	54	0	54	15	53	0	53	16	38	45	41	17	34	90	37
14	54	0	54	15	53	0	53	16	38	45	41	17	34	90	37
14	54	0	54	15	53	0	53	16	38	45	41	17	34	90	37
14	55	0	55	15	54	0	54	16	38	45	41	17	34	90	37
14	56	0	56	15	54	0	54	16	38	45	41	17	34	90	37
15	42	0	42	15	54	0	54	16	38	45	41	17	34	90	37
15	43	0	43	15	55	0	55	16	38	45	41	17	35	90	38
15	44	0	44	15	55	0	55	16	38	45	41	17	35	90	38
15	44	0	44	15	55	0	55	16	39	45	42	17	35	90	38
15	44	0	44	15	55	0	55	16	40	45	43	17	35	90	38
15	44	0	44	16	32	45	35	16	40	45	43	17	35	90	38
15	45	0	45	16	32	45	35	16	41	45	44	17	35	90	38
15	45	0	45	16	32	45	35	16	41	45	44	17	35	90	38

Table B.2. INTACT-ROCK STRENGTH DATA continued

Site ID	Raw*	Ang†	Adj§	Site ID	Raw*	Ang†	Adj§	Site ID	Raw*	Ang†	Adj§	Site ID	Raw*	Ang†	Adj§
17	35	90	38	18	37	45	40	19	60	0	60	20	58	0	58
17	36	90	39	18	38	45	41	19	60	0	60	20	58	0	58
17	36	90	39	18	38	45	41	19	61	0	61	20	58	0	58
17	36	90	39	18	38	45	41	19	61	0	61	20	58	0	58
17	36	90	39	18	38	45	41	19	61	0	61	20	58	0	58
17	37	90	40	18	38	45	41	19	61	0	61	20	58	0	58
17	38	90	41	18	38	45	41	19	62	0	62	20	58	0	58
18	29	45	32	18	38	45	41	19	62	0	62	20	58	0	58
18	30	45	33	18	40	45	43	19	62	0	62	20	58	0	58
18	30	45	33	18	40	45	43	19	62	0	62	20	58	0	58
18	30	45	33	18	40	45	43	19	62	0	62	20	58	0	58
18	30	45	33	18	41	45	44	19	62	0	62	20	59	0	59
18	30	45	33	19	50	0	50	19	63	0	63	20	59	0	59
18	30	45	33	19	52	0	52	19	63	0	63	20	59	0	59
18	30	45	33	19	52	0	52	19	63	0	63	20	60	0	60
18	30	45	33	19	54	0	54	19	64	0	64	20	60	0	60
18	30	45	33	19	54	0	54	19	65	0	65	20	60	0	60
18	31	45	34	19	55	0	55	20	49	0	49	20	60	0	60
18	31	45	34	19	55	0	55	20	50	0	50	20	61	0	61
18	31	45	34	19	55	0	55	20	50	0	50	20	61	0	61
18	31	45	34	19	55	0	55	20	50	0	50	20	61	0	61
18	31	45	34	19	55	0	55	20	50	0	50	20	62	0	62
18	31	45	34	19	55	0	55	20	50	0	50	21	50	0	50
18	31	45	34	19	56	0	56	20	51	0	51	21	52	0	52
18	31	45	34	19	56	0	56	20	52	0	52	21	52	0	52
18	31	45	34	19	56	0	56	20	52	0	52	21	54	0	54
18	31	45	34	19	57	0	57	20	54	0	54	21	54	0	54
18	31	45	34	19	57	0	57	20	54	0	54	21	55	0	55
18	32	45	35	19	57	0	57	20	54	0	54	21	55	0	55
18	32	45	35	19	57	0	57	20	55	0	55	21	56	0	56
18	32	45	35	19	57	0	57	20	55	0	55	21	56	0	56
18	32	45	35	19	58	0	58	20	55	0	55	21	56	0	56
18	32	45	35	19	58	0	58	20	55	0	55	21	56	0	56
18	32	45	35	19	58	0	58	20	55	0	55	21	56	0	56
18	32	45	35	19	58	0	58	20	55	0	55	21	58	0	58
18	33	45	36	19	58	0	58	20	55	0	55	21	58	0	58
18	34	45	37	19	58	0	58	20	55	0	55	21	59	0	59
18	34	45	37	19	59	0	59	20	55	0	55	21	59	0	59
18	34	45	37	19	59	0	59	20	55	0	55	21	60	0	60
18	35	45	38	19	59	0	59	20	56	0	56	21	60	0	60
18	35	45	38	19	59	0	59	20	56	0	56	21	61	0	61
18	35	45	38	19	60	0	60	20	56	0	56	21	61	0	61
18	35	45	38	19	60	0	60	20	57	0	57	21	61	0	61
18	35	45	38	19	60	0	60	20	57	0	57	21	62	0	62
18	36	45	39	19	60	0	60	20	57	0	57	21	62	0	62

Table B.2. INTACT-ROCK STRENGTH DATA continued

Site ID	Raw*	Ang†	Adj§	Site ID	Raw*	Ang†	Adj§	Site ID	Raw*	Ang†	Adj§	Site ID	Raw*	Ang†	Adj§
21	62	0	62	22	58	0	58	23	60	0	60	24	60	0	60
21	62	0	62	22	58	0	58	23	60	0	60	24	61	0	61
21	63	0	63	22	58	0	58	23	60	0	60	24	61	0	61
21	63	0	63	22	58	0	58	23	60	0	60	24	61	0	61
21	64	0	64	22	59	0	59	23	60	0	60	24	61	0	61
22	42	0	42	22	59	0	59	23	60	0	60	24	61	0	61
22	42	0	42	22	60	0	60	23	60	0	60	24	62	0	62
22	44	0	44	22	60	0	60	23	60	0	60	24	62	0	62
22	44	0	44	22	60	0	60	23	61	0	61	24	62	0	62
22	44	0	44	22	60	0	60	23	61	0	61	24	62	0	62
22	45	0	45	23	51	0	51	23	61	0	61	24	62	0	62
22	45	0	45	23	52	0	52	23	61	0	61	24	62	0	62
22	45	0	45	23	52	0	52	23	61	0	61	24	63	0	63
22	46	0	46	23	54	0	54	23	62	0	62	24	63	0	63
22	47	0	47	23	54	0	54	23	62	0	62	24	64	0	64
22	48	0	48	23	55	0	55	24	50	0	50	24	64	0	64
22	48	0	48	23	55	0	55	24	50	0	50	24	65	0	65
22	48	0	48	23	55	0	55	24	51	0	51	24	65	0	65
22	49	0	49	23	55	0	55	24	52	0	52	24	65	0	65
22	49	0	49	23	55	0	55	24	52	0	52	24	65	0	65
22	50	0	50	23	55	0	55	24	52	0	52	25	44	45	47
22	50	0	50	23	56	0	56	24	52	0	52	25	45	45	48
22	50	0	50	23	56	0	56	24	53	0	53	25	48	45	51
22	50	0	50	23	56	0	56	24	53	0	53	25	48	45	51
22	52	0	52	23	57	0	57	24	54	0	54	25	48	45	51
22	52	0	52	23	58	0	58	24	54	0	54	25	49	45	52
22	52	0	52	23	58	0	58	24	54	0	54	25	50	45	53
22	52	0	52	23	58	0	58	24	54	0	54	25	50	45	53
22	53	0	53	23	58	0	58	24	55	0	55	25	50	45	53
22	53	0	53	23	58	0	58	24	55	0	55	25	51	45	54
22	53	0	53	23	58	0	58	24	55	0	55	25	51	45	54
22	54	0	54	23	58	0	58	24	55	0	55	25	51	45	54
22	54	0	54	23	58	0	58	24	56	0	56	25	52	45	55
22	54	0	54	23	59	0	59	24	56	0	56	25	52	45	55
22	54	0	54	23	59	0	59	24	57	0	57	25	52	45	55
22	54	0	54	23	59	0	59	24	57	0	57	25	52	45	55
22	54	0	54	23	59	0	59	24	58	0	58	25	52	45	55
22	55	0	55	23	59	0	59	24	58	0	58	25	54	45	57
22	55	0	55	23	59	0	59	24	58	0	58	25	54	45	57
22	55	0	55	23	59	0	59	24	58	0	58	25	54	45	57
22	55	0	55	23	59	0	59	24	58	0	58	25	54	45	57
22	56	0	56	23	60	0	60	24	59	0	59	25	55	45	58
22	57	0	57	23	60	0	60	24	60	0	60	25	55	45	58
								24	60	0	60	25	55	45	58
								24	60	0	60	25	55	45	58

Table B.2. INTACT-ROCK STRENGTH DATA continued

Site ID	Raw*	Ang†	Adj§	Site ID	Raw*	Ang†	Adj§	Site ID	Raw*	Ang†	Adj§	Site ID	Raw*	Ang†	Adj§
25	55	45	58	26	60	0	60	27	63	0	63	29	48	0	48
25	55	45	58	26	60	0	60	27	63	0	63	29	48	0	48
25	55	45	58	26	61	0	61	27	63	0	63	29	49	0	49
25	56	45	59	26	61	0	61	27	63	0	63	29	50	0	50
25	56	45	59	26	62	0	62	27	64	0	64	29	50	0	50
25	56	45	59	26	62	0	62	27	64	0	64	29	50	0	50
25	56	45	59	27	52	0	52	27	64	0	64	29	50	0	50
25	56	45	59	27	52	0	52	27	64	0	64	29	50	0	50
25	56	45	59	27	54	0	54	27	64	0	64	29	50	0	50
25	56	45	59	27	54	0	54	27	64	0	64	29	50	0	50
25	56	45	59	27	55	0	55	27	67	0	67	29	50	0	50
25	56	45	59	27	55	0	55	27	68	0	68	29	50	0	50
25	56	45	59	27	55	0	55	28	43	0	43	29	51	0	51
25	56	45	59	27	55	0	55	28	45	0	45	29	51	0	51
25	56	45	59	27	55	0	55	28	45	0	45	29	52	0	52
25	57	45	60	27	55	0	55	28	45	0	45	29	52	0	52
25	57	45	60	27	56	0	56	28	45	0	45	29	52	0	52
25	58	45	61	27	56	0	56	28	45	0	45	29	52	0	52
25	58	45	61	27	56	0	56	28	45	0	45	29	52	0	52
25	58	45	61	27	56	0	56	28	45	0	45	29	52	0	52
25	58	45	61	27	57	0	57	28	46	0	46	29	54	0	54
25	59	45	62	27	58	0	58	28	46	0	46	29	54	0	54
25	59	45	62	27	58	0	58	28	46	0	46	29	54	0	54
25	59	45	62	27	58	0	58	28	46	0	46	29	54	0	54
25	60	45	63	27	58	0	58	28	46	0	46	29	55	0	55
25	61	45	64	27	58	0	58	28	46	0	46	29	55	0	55
26	52	0	52	27	59	0	59	28	46	0	46	29	55	0	55
26	54	0	54	27	59	0	59	28	47	0	47	29	56	0	56
26	54	0	54	27	59	0	59	28	47	0	47	29	56	0	56
26	54	0	54	27	59	0	59	28	48	0	48	29	56	0	56
26	54	0	54	27	59	0	59	28	48	0	48	29	56	0	56
26	55	0	55	27	60	0	60	28	48	0	48	29	57	0	57
26	55	0	55	27	60	0	60	28	49	0	49	29	58	0	58
26	56	0	56	27	60	0	60	28	50	0	50	29	58	0	58
26	56	0	56	27	61	0	61	28	50	0	50	29	58	0	58
26	56	0	56	27	61	0	61	28	52	0	52	29	58	0	58
26	56	0	56	27	61	0	61	28	52	0	52	29	58	0	58
26	57	0	57	27	61	0	61	28	53	0	53	29	59	0	59
26	58	0	58	27	61	0	61	28	54	0	54	29	60	0	60
26	58	0	58	27	61	0	61	28	54	0	54	29	60	0	60
26	58	0	58	27	62	0	62	28	54	0	54	29	60	0	60
26	59	0	59	27	62	0	62	28	56	0	56	29	61	0	61
26	59	0	59	27	62	0	62	28	60	0	60	29	62	0	62
26	59	0	59	27	62	0	62	29	48	0	48	29	62	0	62
26	60	0	60	27	62	0	62	29	48	0	48	29	63	0	63

Table B.2. INTACT-ROCK STRENGTH DATA continued

Site ID	Raw[*]	Ang[†]	Adj[§]	Site ID	Raw[*]	Ang[†]	Adj[§]	Site ID	Raw[*]	Ang[†]	Adj[§]	Site ID	Raw[*]	Ang[†]	Adj[§]
29	63	0	63	30	50	0	50	31	57	0	57	32	31	0	31
29	64	0	64	30	52	0	52	31	57	0	57	32	32	0	32
29	64	0	64	30	52	0	52	31	58	0	58	32	32	0	32
30	22	0	22	30	54	0	54	31	58	0	58	32	32	0	32
30	24	0	24	30	55	0	55	31	58	0	58	32	32	0	32
30	24	0	24	30	55	0	55	31	58	0	58	32	34	0	34
30	24	0	24	30	58	0	58	31	58	0	58	32	34	0	34
30	24	0	24	30	60	0	60	31	58	0	58	32	35	0	35
30	25	0	25	31	42	0	42	31	59	0	59	32	35	0	35
30	26	0	26	31	43	0	43	31	59	0	59	32	35	0	35
30	26	0	26	31	43	0	43	31	60	0	60	32	35	0	35
30	26	0	26	31	44	0	44	31	60	0	60	32	35	0	35
30	28	0	28	31	44	0	44	31	63	0	63	32	38	0	38
30	28	0	28	31	44	0	44	32	11	0	11	32	38	0	38
30	30	0	30	31	48	0	48	32	14	0	14	32	39	0	39
30	30	0	30	31	48	0	48	32	14	0	14	32	40	0	40
30	30	0	30	31	49	0	49	32	16	0	16	32	42	0	42
30	31	0	31	31	49	0	49	32	18	0	18	32	45	0	45
30	31	0	31	31	50	0	50	32	19	0	19	33	19	0	19
30	32	0	32	31	50	0	50	32	19	0	19	33	20	0	20
30	32	0	32	31	50	0	50	32	19	0	19	33	20	0	20
30	32	0	32	31	50	0	50	32	19	0	19	33	20	0	20
30	36	0	36	31	50	0	50	32	20	0	20	33	20	0	20
30	36	0	36	31	50	0	50	32	20	0	20	33	21	0	21
30	37	0	37	31	50	0	50	32	21	0	21	33	22	0	22
30	37	0	37	31	50	0	50	32	22	0	22	33	24	0	24
30	38	0	38	31	50	0	50	32	22	0	22	33	24	0	24
30	38	0	38	31	50	0	50	32	24	0	24	33	24	0	24
30	39	0	39	31	51	0	51	32	24	0	24	33	24	0	24
30	40	0	40	31	52	0	52	32	25	0	25	33	25	0	25
30	40	0	40	31	52	0	52	32	26	0	26	33	25	0	25
30	41	0	41	31	52	0	52	32	27	0	27	33	25	0	25
30	41	0	41	31	52	0	52	32	27	0	27	33	26	0	26
30	42	0	42	31	53	0	53	32	27	0	27	33	26	0	26
30	42	0	42	31	54	0	54	32	28	0	28	33	28	0	28
30	42	0	42	31	54	0	54	32	28	0	28	33	28	0	28
30	42	0	42	31	54	0	54	32	29	0	29	33	28	0	28
30	44	0	44	31	55	0	55	32	29	0	29	33	28	0	28
30	45	0	45	31	55	0	55	32	29	0	29	33	28	0	28
30	46	0	46	31	56	0	56	32	29	0	29	33	29	0	29
30	46	0	46	31	56	0	56	32	30	0	30	33	29	0	29
30	46	0	46	31	56	0	56	32	30	0	30	33	30	0	30
30	47	0	47	31	56	0	56	32	30	0	30	33	30	0	30
30	49	0	49	31	56	0	56	32	31	0	31	33	30	0	30
30	50	0	50	31	57	0	57	32	31	0	31	33	31	0	31

Table B.2. INTACT-ROCK STRENGTH DATA continued

Site ID	Raw[*]	Ang[†]	Adj[§]	Site ID	Raw[*]	Ang[†]	Adj[§]	Site ID	Raw[*]	Ang[†]	Adj[§]	Site ID	Raw[*]	Ang[†]	Adj[§]
33	31	0	31	34	30	90	33	34	48	0	48	35	41	0	41
33	31	0	31	34	30	90	33	34	48	0	48	35	41	0	41
33	32	0	32	34	31	90	34	34	48	0	48	35	41	0	41
33	32	0	32	34	31	90	34	34	49	0	49	35	42	0	42
33	32	0	32	34	31	90	34	34	50	0	50	35	42	0	42
33	34	0	34	34	32	0	32	34	50	0	50	35	43	0	43
33	34	0	34	34	32	0	32	34	50	0	50	35	43	0	43
33	34	0	34	34	32	0	32	34	51	0	51	35	44	0	44
33	34	0	34	34	32	0	32	34	52	0	52	35	44	0	44
33	34	0	34	34	32	90	35	34	54	0	54	35	44	0	44
33	36	0	36	34	32	90	35	34	55	0	55	35	44	0	44
33	36	0	36	34	32	90	35	34	58	0	58	35	45	0	45
33	36	0	36	34	33	0	33	34	60	0	60	35	45	0	45
33	37	0	37	34	33	90	36	35	26	0	26	35	46	0	46
33	38	0	38	34	33	90	36	35	28	0	28	35	46	0	46
33	38	0	38	34	34	0	34	35	30	0	30	35	48	0	48
33	40	0	40	34	34	0	34	35	30	0	30	35	48	0	48
33	40	0	40	34	34	0	34	35	30	0	30	35	48	0	48
33	40	0	40	34	34	90	37	35	31	0	31	36	30	0	30
33	40	0	40	34	35	0	35	35	32	0	32	36	30	0	30
33	41	0	41	34	35	0	35	35	32	0	32	36	33	0	33
33	42	0	42	34	35	90	38	35	32	0	32	36	34	0	34
34	20	0	20	34	36	0	36	35	32	0	32	36	34	0	34
34	20	0	20	34	36	0	36	35	32	0	32	36	34	0	34
34	20	90	23	34	36	0	36	35	33	0	33	36	35	0	35
34	22	90	25	34	36	90	39	35	34	0	34	36	35	0	35
34	23	90	26	34	37	90	40	35	34	0	34	36	35	0	35
34	24	0	24	34	38	0	38	35	34	0	34	36	35	0	35
34	25	0	25	34	38	90	41	35	35	0	35	36	36	0	36
34	25	90	28	34	38	90	41	35	35	0	35	36	36	0	36
34	26	0	26	34	39	0	39	35	35	0	35	36	37	0	37
34	26	0	26	34	39	0	39	35	36	0	36	36	37	0	37
34	26	90	29	34	40	0	40	35	36	0	36	36	38	0	38
34	28	0	28	34	40	0	40	35	37	0	37	36	38	0	38
34	28	0	28	34	40	0	40	35	38	0	38	36	38	0	38
34	28	90	31	34	40	0	40	35	38	0	38	36	40	0	40
34	28	90	31	34	40	90	43	35	38	0	38	36	40	0	40
34	28	90	31	34	40	90	43	35	39	0	39	36	44	0	44
34	29	90	32	34	41	0	41	35	39	0	39	36	45	0	45
34	30	0	30	34	41	0	41	35	39	0	39	36	46	0	46
34	30	0	30	34	41	90	44	35	40	0	40	36	46	0	46
34	30	0	30	34	41	90	44	35	40	0	40	36	46	0	46
34	30	0	30	34	44	0	44	35	40	0	40	36	46	0	46
34	30	0	30	34	44	0	44	35	40	0	40	36	47	0	47
34	30	90	33	34	48	0	48	35	41	0	41	36	48	0	48
												36	49	0	49

Table B.2. INTACT-ROCK STRENGTH DATA continued

Site ID	Raw*	Ang†	Adj§	Site ID	Raw*	Ang†	Adj§	Site ID	Raw*	Ang†	Adj§	Site ID	Raw*	Ang†	Adj§
36	50	0	50	38	48	0	48	39	60	0	60	40	58	0	58
36	51	0	51	38	48	0	48	39	60	0	60	40	58	0	58
36	52	0	52	38	48	0	48	39	60	0	60	40	60	0	60
37	10	0	10	38	49	0	49	39	60	0	60	40	60	0	60
37	11	0	11	38	49	0	49	39	60	0	60	40	60	0	60
37	11	0	11	38	49	0	49	39	61	0	61	40	60	0	60
37	11	0	11	38	49	0	49	39	61	0	61	40	60	0	60
37	11	0	11	38	50	0	50	39	62	0	62	40	61	0	61
37	11	0	11	38	50	0	50	39	62	0	62	40	61	0	61·
37	12	0	12	38	50	0	50	39	62	0	62	40	61	0	61
37	12	0	12	38	50	0	50	39	62	0	62	40	62	0	62
37	13	0	13	38	50	0	50	39	63	0	63	40	63	0	63
37	13	0	13	38	50	0	50	39	63	0	63	40	64	0	64
37	13	0	13	38	51	0	51	39	63	0	63	40	64	0	64
37	13	0	13	38	52	0	52	39	63	0	63	40	64	0	64
37	14	0	14	38	52	0	52	39	63	0	63	40	65	0	65
37	15	0	15	38	52	0	52	39	63	0	63	40	65	0	65
37	15	0	15	38	52	0	52	39	63	0	63	40	65	0	65
37	16	0	16	38	53	0	53	39	64	0	64	40	65	0	65
37	18	0	18	38	53	0	53	39	64	0	64	40	65	0	65
37	19	0	19	38	53	0	53	39	64	0	64	40	66	0	66
37	19	0	19	38	53	0	53	39	64	0	64	40	67	0	67
37	19	0	19	38	53	0	53	39	65	0	65	40	67	0	67
37	20	0	20	38	54	0	54	39	65	0	65	40	68	0	68
37	20	0	20	38	54	0	54	39	65	0	65	40	68	0	68
37	20	0	20	38	54	0	54	39	66	0	66	40	70	0	70
37	21	0	21	38	54	0	54	39	66	0	66	40	70	0	70
37	21	0	21	38	54	0	54	39	66	0	66	40	70	0	70
37	21	0	21	38	55	0	55	39	66	0	66	41	50	0	50
37	22	0	22	38	55	0	55	39	67	0	67	41	50	0	50
37	22	0	22	38	55	0	55	39	67	0	67	41	50	0	50
37	24	0	24	38	56	0	56	39	67	0	67	41	54	0	54
37	24	0	24	38	57	0	57	39	67	0	67	41	54	0	54
38	40	0	40	38	57	0	57	39	67	0	67	41	54	0	54
38	43	0	43	38	58	0	58	39	67	0	67	41	55	0	55
38	45	0	45	38	58	0	58	39	67	0	67	41	56	0	56
38	45	0	45	38	60	0	60	39	68	0	68	41	56	0	56
38	45	0	45	38	60	0	60	39	69	0	69	41	56	0	56
38	45	0	45	39	50	0	50	39	69	0	69	41	56	0	56
38	45	0	45	39	54	0	54	39	69	0	69	41	56	0	56
38	46	0	46	39	57	0	57	39	70	0	70	41	57	0	57
38	46	0	46	39	57	0	57	39	71	0	71	41	57	0	57
38	46	0	46	39	58	0	58	39	72	0	72	41	58	0	58
38	47	0	47	39	59	0	59	40	57	0	57	41	58	0	58
38	47	0	47	39	59	0	59	40	58	0	58	41	60	0	60

Table B.2. INTACT-ROCK STRENGTH DATA continued

Site ID	Raw[*]	Ang[†]	Adj[§]	Site ID	Raw[*]	Ang[†]	Adj[§]	Site ID	Raw[*]	Ang[†]	Adj[§]	Site ID	Raw[*]	Ang[†]	Adj[§]
41	60	0	60	42	64	0	64	43	63	0	63	45	54	0	54
41	60	0	60	42	64	0	64	43	64	0	64	45	55	0	55
41	61	0	61	42	65	0	65	43	64	0	64	45	55	0	55
41	62	0	62	42	66	0	66	44	45	0	45	45	56	0	56
41	62	0	62	42	67	0	67	44	46	0	46	45	56	0	56
41	62	0	62	42	67	0	67	44	46	0	46	45	57	0	57
41	63	0	63	42	67	0	67	44	46	0	46	45	58	0	58
41	64	0	64	42	67	0	67	44	48	0	48	45	58	0	58
41	67	0	67	42	67	0	67	44	48	0	48	45	58	0	58
41	68	0	68	42	68	0	68	44	48	0	48	45	59	0	59
41	69	0	69	42	68	0	68	44	49	0	49	45	59	0	59
41	70	0	70	42	68	0	68	44	49	0	49	45	60	0	60
41	70	0	70	42	68	0	68	44	49	0	49	45	60	0	60
42	42	0	42	42	68	0	68	44	49	0	49	45	61	0	61
42	50	0	50	42	69	0	69	44	50	0	50	45	61	0	61
42	50	0	50	42	70	0	70	44	50	0	50	45	63	0	63
42	52	0	52	42	71	0	71	44	50	0	50	45	63	0	63
42	53	0	53	42	71	0	71	44	50	0	50	45	63	0	63
42	55	0	55	43	48	0	48	44	50	0	50	46	50	0	50
42	55	0	55	43	48	0	48	44	50	0	50	46	50	0	50
42	55	0	55	43	50	0	50	44	51	0	51	46	50	0	50
42	56	0	56	43	50	0	50	44	51	0	51	46	50	0	50
42	56	0	56	43	50	0	50	44	51	0	51	46	52	0	52
42	56	0	56	43	50	0	50	44	51	0	51	46	56	0	56
42	57	0	57	43	50	0	50	44	53	0	53	46	58	0	58
42	57	0	57	43	50	0	50	44	53	0	53	46	60	0	60
42	57	0	57	43	50	0	50	44	54	0	54	46	60	0	60
42	58	0	58	43	50	0	50	44	54	0	54	46	60	0	60
42	58	0	58	43	50	0	50	44	54	0	54	46	61	0	61
42	60	0	60	43	51	0	51	44	57	0	57	46	61	0	61
42	60	0	60	43	52	0	52	44	58	0	58	46	61	0	61
42	60	0	60	43	53	0	53	44	64	0	64	46	61	0	61
42	60	0	60	43	54	0	54	44	65	0	65	46	61	0	61
42	60	0	60	43	55	0	55	45	50	0	50	46	61	0	61
42	60	0	60	43	55	0	55	45	50	0	50	46	61	0	61
42	60	0	60	43	56	0	56	45	51	0	51	46	62	0	62
42	60	0	60	43	56	0	56	45	51	0	51	46	62	0	62
42	60	0	60	43	56	0	56	45	51	0	51	46	62	0	62
42	61	0	61	43	57	0	57	45	52	0	52	46	62	0	62
42	61	0	61	43	58	0	58	45	52	0	52	46	62	0	62
42	62	0	62	43	58	0	58	45	52	0	52	46	63	0	63
42	62	0	62	43	59	0	59	45	52	0	52	46	63	0	63
42	63	0	63	43	60	0	60	45	54	0	54	46	64	0	64
42	63	0	63	43	60	0	60	45	54	0	54	46	64	0	64
42	64	0	64	43	60	0	60	45	54	0	54	46	64	0	64

Table B.2. INTACT-ROCK STRENGTH DATA continued

Site ID	Raw*	Ang†	Adj§	Site ID	Raw*	Ang†	Adj§	Site ID	Raw*	Ang†	Adj§	Site ID	Raw*	Ang†	Adj§
46	64	0	64	47	65	0	65	48	64	0	64	50	50	0	50
46	64	0	64	47	65	0	65	48	64	0	64	50	52	0	52
46	65	0	65	47	66	0	66	48	65	0	65	50	52	0	52
46	65	0	65	47	66	0	66	48	65	0	65	50	54	0	54
46	65	0	65	47	67	0	67	48	66	0	66	50	54	0	54
46	67	0	67	47	68	0	68	48	66	0	66	50	54	0	54
46	67	0	67	47	69	0	69	48	67	0	67	50	54	0	54
46	67	0	67	47	69	0	69	48	68	0	68	50	54	0	54
46	67	0	67	48	51	0	51	48	68	0	68	50	55	0	55
46	68	0	68	48	52	0	52	48	68	0	68	50	55	0	55
46	68	0	68	48	52	0	52	48	69	0	69	50	55	0	55
46	69	0	69	48	54	0	54	48	69	0	69	50	56	0	56
46	69	0	69	48	55	0	55	48	70	0	70	50	56	0	56
46	69	0	69	48	55	0	55	49	44	0	44	50	56	0	56
46	69	0	69	48	55	0	55	49	46	0	46	50	58	0	58
46	70	0	70	48	57	0	57	49	46	0	46	50	58	0	58
46	70	0	70	48	58	0	58	49	46	0	46	50	58	0	58
46	71	0	71	48	58	0	58	49	48	0	48	50	58	0	58
46	71	0	71	48	58	0	58	49	48	0	48	50	60	0	60
46	71	0	71	48	58	0	58	49	48	0	48	50	60	0	60
46	72	0	72	48	58	0	58	49	48	0	48	50	60	0	60
46	72	0	72	48	58	0	58	49	48	0	48	50	60	0	60
46	73	0	73	48	58	0	58	49	49	0	49	50	60	0	60
47	45	0	45	48	58	0	58	49	49	0	49	50	61	0	61
47	48	0	48	48	58	0	58	49	50	0	50	50	62	0	62
47	50	0	50	48	59	0	59	49	50	0	50	50	62	0	62
47	51	0	51	48	59	0	59	49	50	0	50	50	63	0	63
47	57	0	57	48	59	0	59	49	51	0	51	50	64	0	64
47	58	0	58	48	60	0	60	49	51	0	51	51	48	0	48
47	58	0	58	48	60	0	60	49	52	0	52	51	50	0	50
47	59	0	59	48	60	0	60	49	52	0	52	51	50	0	50
47	60	0	60	48	60	0	60	49	52	0	52	51	50	0	50
47	60	0	60	48	60	0	60	49	52	0	52	51	50	0	50
47	60	0	60	48	60	0	60	49	53	0	53	51	50	0	50
47	61	0	61	48	60	0	60	49	53	0	53	51	50	0	50
47	61	0	61	48	61	0	61	49	53	0	53	51	51	0	51
47	61	0	61	48	62	0	62	49	54	0	54	51	51	0	51
47	61	0	61	48	62	0	62	49	54	0	54	51	52	0	52
47	62	0	62	48	62	0	62	49	57	0	57	51	52	0	52
47	62	0	62	48	62	0	62	49	57	0	57	51	52	0	52
47	62	0	62	48	62	0	62	49	58	0	58	51	52	0	52
47	62	0	62	48	62	0	62	49	62	0	62	51	52	0	52
47	62	0	62	48	63	0	63	49	64	0	64	51	53	0	53
47	64	0	64	48	63	0	63	50	47	0	47	51	54	0	54

Table B.2. INTACT-ROCK STRENGTH DATA continued

Site ID	Raw*	Ang†	Adj§	Site ID	Raw*	Ang†	Adj§	Site ID	Raw*	Ang†	Adj§	Site ID	Raw*	Ang†	Adj§
51	54	0	54	52	58	0	58	53	56	0	56	54	62	0	62
51	54	0	54	52	58	0	58	53	56	0	56	54	62	0	62
51	54	0	54	52	58	0	58	53	56	0	56	54	62	0	62
51	54	0	54	52	58	0	58	53	56	0	56	54	64	0	64
51	55	0	55	52	59	0	59	53	58	0	58	54	65	0	65
51	55	0	55	52	60	0	60	53	58	0	58	54	65	0	65
51	55	0	55	52	60	0	60	53	59	0	59	54	65	0	65
51	56	0	56	52	60	0	60	53	59	0	59	54	70	0	70
51	56	0	56	52	60	0	60	53	59	0	59	55	49	0	49
51	56	0	56	52	60	0	60	53	60	0	60	55	50	0	50
51	56	0	56	52	60	0	60	53	60	0	60	55	52	0	52
51	57	0	57	52	60	0	60	53	61	0	61	55	54	0	54
51	57	0	57	52	60	0	60	53	61	0	61	55	54	0	54
51	58	0	58	52	60	0	60	53	62	0	62	55	55	0	55
51	58	0	58	52	60	0	60	53	62	0	62	55	55	0	55
51	59	0	59	52	61	0	61	53	62	0	62	55	55	0	55
51	60	0	60	52	61	0	61	53	63	0	63	55	56	0	56
51	60	0	60	52	62	0	62	53	63	0	63	55	56	0	56
51	60	0	60	52	62	0	62	53	63	0	63	55	56	0	56
51	60	0	60	52	63	0	63	53	64	0	64	55	56	0	56
51	61	0	61	52	63	0	63	53	64	0	64	55	56	0	56
51	61	0	61	52	63	0	63	53	65	0	65	55	56	0	56
51	61	0	61	52	64	0	64	53	65	0	65	55	56	0	56
51	61	0	61	52	64	0	64	54	45	0	45	55	57	0	57
51	61	0	61	52	64	0	64	54	52	0	52	55	58	0	58
51	62	0	62	52	64	0	64	54	54	0	54	55	58	0	58
51	62	0	62	52	64	0	64	54	54	0	54	55	59	0	59
51	63	0	63	52	65	0	65	54	55	0	55	55	59	0	59
51	64	0	64	52	65	0	65	54	55	0	55	55	59	0	59
51	67	0	67	52	66	0	66	54	55	0	55	55	59	0	59
51	68	0	68	52	66	0	66	54	56	0	56	55	60	0	60
51	68	0	68	52	67	0	67	54	56	0	56	55	60	0	60
51	70	0	70	52	67	0	67	54	56	0	56	55	60	0	60
52	50	0	50	52	68	0	68	54	56	0	56	55	61	0	61
52	51	0	51	52	68	0	68	54	56	0	56	55	61	0	61
52	52	0	52	52	68	0	68	54	57	0	57	55	61	0	61
52	54	0	54	52	68	0	68	54	57	0	57	55	61	0	61
52	54	0	54	52	69	0	69	54	58	0	58	55	62	0	62
52	54	0	54	53	51	0	51	54	58	0	58	55	62	0	62
52	54	0	54	53	51	0	51	54	58	0	58	55	62	0	62
52	58	0	58	53	54	0	54	54	58	0	58	55	62	0	62
52	58	0	58	53	55	0	55	54	58	0	58	55	62	0	62
52	58	0	58	53	55	0	55	54	58	0	58	55	62	0	62
52	58	0	58	53	56	0	56	54	61	0	61	55	63	0	63
52	58	0	58	53	56	0	56	54	62	0	62	55	63	0	63

Table B.2. INTACT-ROCK STRENGTH DATA continued

Site ID	Raw[*]	Ang[†]	Adj[§]	Site ID	Raw[*]	Ang[†]	Adj[§]	Site ID	Raw[*]	Ang[†]	Adj[§]	Site ID	Raw[*]	Ang[†]	Adj[§]
55	63	0	63	57	32	0	32	57	46	0	46	58	61	0	61
55	63	0	63	57	32	0	32	57	48	0	48	58	62	0	62
55	64	0	64	57	32	0	32	57	48	0	48	58	62	0	62
55	64	0	64	57	32	0	32	58	45	0	45	58	62	0	62
55	64	0	64	57	32	0	32	58	48	0	48	58	63	0	63
55	64	0	64	57	34	0	34	58	50	0	50	58	63	0	63
55	64	0	64	57	34	0	34	58	50	0	50	58	64	0	64
55	64	0	64	57	34	0	34	58	50	0	50	58	64	0	64
55	64	0	64	57	35	0	35	58	50	0	50	59	28	0	28
55	65	0	65	57	36	0	36	58	52	0	52	59	28	0	28
55	66	0	66	57	36	0	36	58	52	0	52	59	30	0	30
55	67	0	67	57	37	0	37	58	52	0	52	59	30	0	30
55	68	0	68	57	38	0	38	58	52	0	52	59	30	0	30
56	53	0	53	57	38	0	38	58	52	0	52	59	31	0	31
56	56	0	56	57	38	0	38	58	52	0	52	59	32	0	32
56	56	0	56	57	38	0	38	58	52	0	52	59	32	0	32
56	56	0	56	57	38	0	38	58	52	0	52	59	32	0	32
56	56	0	56	57	38	0	38	58	54	0	54	59	32	0	32
56	58	0	58	57	38	0	38	58	54	0	54	59	33	0	33
56	59	0	59	57	38	0	38	58	54	0	54	59	33	0	33
56	59	0	59	57	38	0	38	58	55	0	55	59	34	0	34
56	59	0	59	57	38	0	38	58	55	0	55	59	35	0	35
56	60	0	60	57	39	0	39	58	55	0	55	59	35	0	35
56	60	0	60	57	40	0	40	58	55	0	55	59	35	0	35
56	60	0	60	57	40	0	40	58	55	0	55	59	35	0	35
56	61	0	61	57	40	0	40	58	55	0	55	59	35	0	35
56	61	0	61	57	40	0	40	58	55	0	55	59	36	0	36
56	63	0	63	57	41	0	41	58	56	0	56	59	37	0	37
56	63	0	63	57	42	0	42	58	56	0	56	59	37	0	37
56	63	0	63	57	42	0	42	58	57	0	57	59	37	0	37
56	64	0	64	57	42	0	42	58	57	0	57	59	37	0	37
56	64	0	64	57	42	0	42	58	57	0	57	59	38	0	38
56	64	0	64	57	42	0	42	58	58	0	58	59	39	0	39
56	64	0	64	57	42	0	42	58	58	0	58	59	40	0	40
56	64	0	64	57	43	0	43	58	58	0	58	59	40	0	40
56	64	0	64	57	44	0	44	58	58	0	58	59	40	0	40
56	66	0	66	57	44	0	44	58	58	0	58	59	41	0	41
56	67	0	67	57	44	0	44	58	58	0	58	59	41	0	41
56	67	0	67	57	44	0	44	58	58	0	58	59	42	0	42
56	67	0	67	57	44	0	44	58	59	0	59	59	42	0	42
56	68	0	68	57	44	0	44	58	59	0	59	59	43	0	43
56	68	0	68	57	44	0	44	58	60	0	60	59	44	0	44
56	69	0	69	57	45	0	45	58	60	0	60	59	44	0	44
57	30	0	30	57	45	0	45	58	60	0	60	59	44	0	44
57	32	0	32	57	45	0	45	58	60	0	60	59	44	0	44

Table B.2. INTACT-ROCK STRENGTH DATA continued

Site ID	Raw[*]	Ang[†]	Adj[§]	Site ID	Raw[*]	Ang[†]	Adj[§]	Site ID	Raw[*]	Ang[†]	Adj[§]	Site ID	Raw[*]	Ang[†]	Adj[§]
59	45	0	45	60	50	0	50	61	56	0	56	62	54	0	54
59	45	0	45	60	50	0	50	61	56	0	56	62	54	0	54
59	45	0	45	60	50	0	50	61	56	0	56	62	56	0	56
59	45	0	45	60	51	0	51	61	57	0	57	62	57	0	57
59	45	0	45	60	51	0	51	61	58	0	58	62	57	0	57
59	46	0	46	60	51	0	51	61	58	0	58	62	57	0	57
59	46	0	46	60	52	0	52	61	58	0	58	62	57	0	57
59	47	0	47	60	52	0	52	61	58	0	58	62	58	0	58
59	48	0	48	60	52	0	52	61	58	0	58	62	58	0	58
59	48	0	48	60	52	0	52	61	58	0	58	62	58	0	58
59	48	0	48	60	53	0	53	61	58	0	58	62	59	0	59
59	49	0	49	60	53	0	53	61	58	0	58	62	59	0	59
59	50	0	50	60	53	0	53	61	59	0	59	62	59	0	59
59	52	0	52	60	54	0	54	61	59	0	59	62	60	0	60
59	53	0	53	60	54	0	54	61	60	0	60	62	60	0	60
59	54	0	54	60	54	0	54	61	60	0	60	62	62	0	62
59	54	0	54	60	54	0	54	61	60	0	60	62	62	0	62
59	55	0	55	60	55	0	55	61	60	0	60	62	63	0	63
59	55	0	55	60	55	0	55	61	60	0	60	63	30	0	30
59	56	0	56	60	56	0	56	61	60	0	60	63	30	0	30
59	57	0	57	60	56	0	56	61	60	0	60	63	32	0	32
59	57	0	57	60	56	0	56	61	61	0	61	63	32	0	32
59	58	0	58	60	57	0	57	61	61	0	61	63	32	0	32
60	42	0	42	60	58	0	58	61	62	0	62	63	32	0	32
60	42	0	42	60	58	0	58	61	62	0	62	63	32	0	32
60	43	0	43	60	58	0	58	61	62	0	62	63	32	0	32
60	44	0	44	60	58	0	58	61	62	0	62	63	32	0	32
60	44	0	44	60	60	0	60	61	62	0	62	63	33	0	33
60	44	0	44	61	48	0	48	61	63	0	63	63	33	0	33
60	44	0	44	61	50	0	50	61	63	0	63	63	33	0	33
60	44	0	44	61	50	0	50	61	64	0	64	63	33	0	33
60	45	0	45	61	52	0	52	61	64	0	64	63	34	0	34
60	46	0	46	61	52	0	52	61	65	0	65	63	34	0	34
60	46	0	46	61	52	0	52	61	66	0	66	63	34	0	34
60	46	0	46	61	52	0	52	62	50	0	50	63	34	0	34
60	47	0	47	61	52	0	52	62	50	0	50	63	34	0	34
60	48	0	48	61	53	0	53	62	52	0	52	63	34	0	34
60	48	0	48	61	53	0	53	62	52	0	52	63	35	0	35
60	48	0	48	61	54	0	54	62	52	0	52	63	35	0	35
60	48	0	48	61	54	0	54	62	52	0	52	63	35	0	35
60	48	0	48	61	54	0	54	62	53	0	53	63	35	0	35
60	49	0	49	61	54	0	54	62	54	0	54	63	35	0	35
60	50	0	50	61	56	0	56	62	54	0	54	63	35	0	35
60	50	0	50	61	56	0	56	62	54	0	54	63	35	0	35

Table B.2. INTACT-ROCK STRENGTH DATA continued

Site ID	Raw*	Ang†	Adj§	Site ID	Raw*	Ang†	Adj§	Site ID	Raw*	Ang†	Adj§	Site ID	Raw*	Ang†	Adj§
63	35	0	35	64	54	0	54	65	51	0	51	66	30	0	30
63	36	0	36	64	54	0	54	65	51	0	51	66	31	0	31
63	36	0	36	64	54	0	54	65	51	0	51	66	32	0	32
63	36	0	36	64	54	0	54	65	52	0	52	66	35	0	35
63	37	0	37	64	54	0	54	65	52	0	52	66	35	0	35
63	37	0	37	64	55	0	55	65	52	0	52	66	36	0	36
63	38	0	38	64	55	0	55	65	52	0	52	66	36	0	36
63	38	0	38	64	55	0	55	65	52	0	52	66	36	0	36
63	38	0	38	64	55	0	55	65	52	0	52	66	37	0	37
63	38	0	38	64	55	0	55	65	53	0	53	66	37	0	37
63	38	0	38	64	56	0	56	65	53	0	53	66	37	0	37
63	38	0	38	64	56	0	56	65	53	0	53	66	37	0	37
63	38	0	38	64	57	0	57	65	53	0	53	66	38	0	38
63	38	0	38	64	58	0	58	65	53	0	53	66	38	0	38
63	38	0	38	64	58	0	58	65	54	0	54	66	38	0	38
63	39	0	39	64	58	0	58	65	54	0	54	66	40	0	40
63	39	0	39	64	58	0	58	65	54	0	54	66	40	0	40
63	39	0	39	64	59	0	59	65	54	0	54	66	40	0	40
63	40	0	40	64	60	0	60	65	54	0	54	66	40	0	40
63	41	0	41	64	60	0	60	65	54	0	54	66	40	0	40
63	42	0	42	64	60	0	60	65	54	0	54	66	41	0	41
63	45	0	45	64	60	0	60	65	55	0	55	66	42	0	42
63	50	0	50	64	60	0	60	65	55	0	55	66	42	0	42
64	48	0	48	64	61	0	61	65	55	0	55	66	44	0	44
64	48	0	48	64	61	0	61	65	55	0	55	66	44	0	44
64	48	0	48	64	61	0	61	65	55	0	55	66	45	0	45
64	48	0	48	64	61	0	61	65	56	0	56	66	48	0	48
64	48	0	48	64	61	0	61	65	56	0	56	66	48	0	48
64	49	0	49	64	62	0	62	65	56	0	56	66	52	0	52
64	49	0	49	64	62	0	62	65	57	0	57	67	9	0	9
64	50	0	50	64	63	0	63	65	57	0	57	67	10	0	10
64	50	0	50	64	63	0	63	65	57	0	57	67	10	0	10
64	50	0	50	64	63	0	63	65	58	0	58	67	10	0	10
64	50	0	50	64	63	0	63	65	58	0	58	67	10	0	10
64	50	0	50	64	63	0	63	65	58	0	58	67	10	0	10
64	50	0	50	64	64	0	64	65	60	0	60	67	10	0	10
64	50	0	50	64	65	0	65	65	60	0	60	67	10	0	10
64	50	0	50	64	65	0	65	65	60	0	60	67	10	0	10
64	50	0	50	64	65	0	65	65	60	0	60	67	10	0	10
64	51	0	51	65	48	0	48	65	60	0	60	67	11	0	11
64	51	0	51	65	50	0	50	65	61	0	61	67	11	0	11
64	52	0	52	65	50	0	50	65	62	0	62	67	11	0	11
64	54	0	54	65	50	0	50	65	63	0	63	67	11	0	11
64	54	0	54	65	50	0	50	65	63	0	63	67	11	0	11
64	54	0	54	65	51	0	51	66	30	0	30	67	12	0	12

Table B.2. INTACT-ROCK STRENGTH DATA continued

Site ID	Raw*	Ang†	Adj§	Site ID	Raw*	Ang†	Adj§	Site ID	Raw*	Ang†	Adj§	Site ID	Raw*	Ang†	Adj§
67	12	0	12	69	10	0	10	70	28	0	28	71	58	0	58
67	12	0	12	69	10	0	10	70	28	0	28	71	58	0	58
67	12	0	12	69	10	0	10	70	28	0	28	71	58	0	58
67	12	0	12	69	11	0	11	70	28	0	28	71	58	0	58
67	12	0	12	69	11	0	11	70	28	0	28	71	58	0	58
67	13	0	13	69	11	0	11	70	30	0	30	71	58	0	58
67	13	0	13	69	11	0	11	70	30	0	30	71	59	0	59
67	13	0	13	69	11	0	11	70	30	0	30	71	59	0	59
67	14	0	14	69	11	0	11	70	30	0	30	71	59	0	59
67	15	0	15	69	12	0	12	70	32	0	32	71	59	0	59
67	15	0	15	69	12	0	12	70	35	0	35	71	59	0	59
67	18	0	18	69	12	0	12	70	40	0	40	71	59	0	59
67	18	0	18	69	12	0	12	70	40	0	40	71	60	0	60
67	20	0	20	69	12	0	12	70	42	0	42	71	60	0	60
68	50	0	50	69	12	0	12	71	45	0	45	71	60	0	60
68	50	0	50	69	13	0	13	71	48	0	48	71	61	0	61
68	52	0	52	69	13	0	13	71	48	0	48	71	61	0	61
68	54	0	54	69	14	0	14	71	48	0	48	71	61	0	61
68	54	0	54	69	14	0	14	71	50	0	50	71	62	0	62
68	55	0	55	69	14	0	14	71	50	0	50	72	54	0	54
68	55	0	55	69	15	0	15	71	50	0	50	72	55	0	55
68	55	0	55	69	15	0	15	71	50	0	50	72	56	0	56
68	55	0	55	69	15	0	15	71	52	0	52	72	56	0	56
68	55	0	55	69	15	0	15	71	52	0	52	72	57	0	57
68	55	0	55	69	15	0	15	71	52	0	52	72	57	0	57
68	55	0	55	69	15	0	15	71	53	0	53	72	58	0	58
68	56	0	56	69	18	0	18	71	53	0	53	72	58	0	58
68	56	0	56	69	20	0	20	71	54	0	54	72	58	0	58
68	56	0	56	69	20	0	20	71	54	0	54	72	58	0	58
68	56	0	56	70	15	0	15	71	54	0	54	72	58	0	58
68	57	0	57	70	15	0	15	71	54	0	54	72	58	0	58
68	57	0	57	70	15	0	15	71	54	0	54	72	58	0	58
68	57	0	57	70	16	0	16	71	55	0	55	72	58	0	58
68	58	0	58	70	18	0	18	71	55	0	55	72	59	0	59
68	58	0	58	70	18	0	18	71	55	0	55	72	59	0	59
68	58	0	58	70	20	0	20	71	55	0	55	72	59	0	59
68	58	0	58	70	20	0	20	71	55	0	55	72	59	0	59
68	59	0	59	70	20	0	20	71	55	0	55	72	59	0	59
68	59	0	59	70	22	0	22	71	55	0	55	72	59	0	59
68	59	0	59	70	22	0	22	71	56	0	56	72	59	0	59
68	60	0	60	70	22	0	22	71	56	0	56	72	60	0	60
68	60	0	60	70	24	0	24	71	56	0	56	72	60	0	60
68	61	0	61	70	24	0	24	71	56	0	56	72	60	0	60
69	10	0	10	70	25	0	25	71	57	0	57	72	60	0	60
				70	25	0	25	71	57	0	57	72	60	0	60

Table B.2. INTACT-ROCK STRENGTH DATA continued

Site ID	Raw*	Ang†	Adj§	Site ID	Raw*	Ang†	Adj§	Site ID	Raw*	Ang†	Adj§	Site ID	Raw*	Ang†	Adj§
72	60	0	60	73	47	0	47	74	52	0	52	75	46	0	46
72	60	0	60	73	47	0	47	74	53	0	53	75	46	0	46
72	60	0	60	73	48	0	48	74	54	0	54	75	47	0	47
72	61	0	61	73	48	0	48	74	54	0	54	75	47	0	47
72	61	0	61	73	48	0	48	74	54	0	54	75	48	0	48
72	62	0	62	73	48	0	48	74	54	0	54	75	48	0	48
72	62	0	62	73	48	0	48	74	54	0	54	75	48	0	48
72	62	0	62	73	48	0	48	74	54	0	54	75	48	0	48
72	62	0	62	73	48	0	48	74	55	0	55	75	48	0	48
72	62	0	62	73	50	0	50	74	55	0	55	75	49	0	49
72	62	0	62	73	50	0	50	74	55	0	55	75	49	0	49
72	62	0	62	73	50	0	50	74	55	0	55	75	49	0	49
72	63	0	63	73	50	0	50	74	56	0	56	75	49	0	49
72	63	0	63	73	50	0	50	74	56	0	56	75	49	0	49
72	63	0	63	73	50	0	50	74	56	0	56	75	49	0	49
72	63	0	63	73	50	0	50	74	57	0	57	75	50	0	50
72	63	0	63	73	51	0	51	74	57	0	57	75	50	0	50
72	64	0	64	73	51	0	51	74	57	0	57	75	50	0	50
72	64	0	64	73	52	0	52	74	57	0	57	75	50	0	50
72	65	0	65	73	52	0	52	74	57	0	57	75	50	0	50
72	65	0	65	73	52	0	52	74	58	0	58	75	51	0	51
72	65	0	65	73	52	0	52	74	58	0	58	75	52	0	52
72	67	0	67	73	52	0	52	74	58	0	58	75	52	0	52
72	68	0	68	73	52	0	52	74	58	0	58	75	52	0	52
73	40	0	40	73	53	0	53	74	58	0	58	75	54	0	54
73	40	0	40	73	54	0	54	74	58	0	58	75	54	0	54
73	40	0	40	73	54	0	54	74	59	0	59	75	54	0	54
73	40	0	40	73	54	0	54	74	59	0	59	75	55	0	55
73	41	0	41	73	54	0	54	74	59	0	59	75	55	0	55
73	41	0	41	73	54	0	54	74	60	0	60	76	49	0	49
73	41	0	41	73	54	0	54	74	60	0	60	76	50	0	50
73	42	0	42	73	55	0	55	74	60	0	60	76	50	0	50
73	42	0	42	73	55	0	55	74	60	0	60	76	50	0	50
73	42	0	42	73	56	0	56	74	60	0	60	76	50	0	50
73	42	0	42	73	57	0	57	74	60	0	60	76	50	0	50
73	44	0	44	73	58	0	58	74	60	0	60	76	50	0	50
73	44	0	44	73	58	0	58	74	61	0	61	76	51	0	51
73	45	0	45	73	60	0	60	74	61	0	61	76	52	0	52
73	45	0	45	73	60	0	60	74	61	0	61	76	52	0	52
73	45	0	45	74	44	0	44	74	61	0	61	76	52	0	52
73	45	0	45	74	48	0	48	74	62	0	62	76	52	0	52
73	46	0	46	74	52	0	52	74	62	0	62	76	53	0	53
73	46	0	46	74	52	0	52	74	63	0	63	76	54	0	54
73	46	0	46	74	52	0	52	74	64	0	64	76	54	0	54
73	47	0	47	74	52	0	52	75	45	0	45	76	54	0	54

Table B.2. INTACT-ROCK STRENGTH DATA continued

Site ID	Raw[*]	Ang[†]	Adj[§]	Site ID	Raw[*]	Ang[†]	Adj[§]	Site ID	Raw[*]	Ang[†]	Adj[§]	Site ID	Raw[*]	Ang[†]	Adj[§]
76	54	0	54	77	34	0	34	77	44	0	44	78	46	0	46
76	54	0	54	77	35	0	35	77	44	0	44	78	47	0	47
76	54	0	54	77	35	0	35	77	46	0	46	78	47	0	47
76	54	0	54	77	35	0	35	77	48	0	48	78	47	0	47
76	54	0	54	77	36	0	36	78	39	0	39	78	47	0	47
76	54	0	54	77	36	0	36	78	40	0	40	78	48	0	48
76	54	0	54	77	36	0	36	78	40	0	40	78	48	0	48
76	54	0	54	77	36	0	36	78	40	0	40	78	48	0	48
76	54	0	54	77	36	0	36	78	40	0	40	78	49	0	49
76	55	0	55	77	36	0	36	78	40	0	40	79	41	0	41
76	55	0	55	77	37	0	37	78	41	0	41	79	41	0	41
76	55	0	55	77	38	0	38	78	41	0	41	79	41	0	41
76	55	0	55	77	38	0	38	78	41	0	41	79	41	0	41
76	55	0	55	77	38	0	38	78	41	0	41	79	42	0	42
76	55	0	55	77	38	0	38	78	41	0	41	79	45	0	45
76	56	0	56	77	38	0	38	78	42	0	42	79	45	0	45
76	56	0	56	77	38	0	38	78	42	0	42	79	45	0	45
76	56	0	56	77	38	0	38	78	42	0	42	79	46	0	46
76	56	0	56	77	39	0	39	78	42	0	42	79	46	0	46
76	56	0	56	77	39	0	39	78	42	0	42	79	46	0	46
76	56	0	56	77	39	0	39	78	42	0	42	79	46	0	46
76	56	0	56	77	39	0	39	78	42	0	42	79	46	0	46
76	56	0	56	77	39	0	39	78	43	0	43	79	46	0	46
76	56	0	56	77	39	0	39	78	43	0	43	79	46	0	46
76	56	0	56	77	40	0	40	78	43	0	43	79	46	0	46
76	56	0	56	77	40	0	40	78	44	0	44	79	47	0	47
76	57	0	57	77	40	0	40	78	44	0	44	79	47	0	47
76	57	0	57	77	40	0	40	78	44	0	44	79	47	0	47
76	57	0	57	77	40	0	40	78	44	0	44	79	47	0	47
76	57	0	57	77	40	0	40	78	44	0	44	79	47	0	47
76	58	0	58	77	40	0	40	78	45	0	45	79	48	0	48
76	58	0	58	77	40	0	40	78	45	0	45	79	48	0	48
76	58	0	58	77	40	0	40	78	45	0	45	79	48	0	48
76	58	0	58	77	41	0	41	78	45	0	45	79	48	0	48
76	58	0	58	77	41	0	41	78	45	0	45	79	49	0	49
76	58	0	58	77	41	0	41	78	45	0	45	79	49	0	49
76	58	0	58	77	41	0	41	78	45	0	45	79	49	0	49
76	59	0	59	77	42	0	42	78	45	0	45	79	50	0	50
76	59	0	59	77	42	0	42	78	45	0	45	79	50	0	50
76	59	0	59	77	42	0	42	78	46	0	46	79	50	0	50
76	60	0	60	77	42	0	42	78	46	0	46	79	51	0	51
76	60	0	60	77	42	0	42	78	46	0	46	79	51	0	51
76	60	0	60	77	43	0	43	78	46	0	46	79	51	0	51
76	62	0	62	77	44	0	44	78	46	0	46	79	51	0	51
77	34	0	34	77	44	0	44	78	46	0	46	79	52	0	52

Table B.2. INTACT-ROCK STRENGTH DATA continued

Site ID	Raw*	Ang†	Adj§	Site ID	Raw*	Ang†	Adj§	Site ID	Raw*	Ang†	Adj§	Site ID	Raw*	Ang†	Adj§
79	53	0	53	80	56	0	56	81	53	0	53	82	63	0	63
79	54	0	54	80	56	0	56	81	54	0	54	82	63	0	63
79	54	0	54	80	57	0	57	81	54	0	54	82	64	0	64
79	54	0	54	80	58	0	58	81	54	0	54	82	64	0	64
79	55	0	55	80	58	0	58	81	54	0	54	82	64	0	64
79	56	0	56	80	58	0	58	81	54	0	54	82	64	0	64
79	56	0	56	80	58	0	58	81	54	0	54	82	65	0	65
79	58	0	58	80	58	0	58	81	55	0	55	82	67	0	67
79	58	0	58	80	58	0	58	81	55	0	55	82	68	0	68
79	58	0	58	80	59	0	59	81	55	0	55	83	54	0	54
79	58	0	58	80	59	0	59	81	55	0	55	83	54	0	54
79	59	0	59	80	60	0	60	81	55	0	55	83	55	0	55
79	60	0	60	80	60	0	60	81	56	0	56	83	55	0	55
79	61	0	61	80	60	0	60	81	56	0	56	83	55	0	55
80	46	0	46	80	60	0	60	81	56	0	56	83	55	0	55
80	47	0	47	80	61	0	61	81	56	0	56	83	55	0	55
80	48	0	48	80	61	0	61	81	56	0	56	83	55	0	55
80	48	0	48	80	61	0	61	81	56	0	56	83	55	0	55
80	49	0	49	80	63	0	63	81	56	0	56	83	55	0	55
80	50	0	50	81	42	0	42	81	56	0	56	83	56	0	56
80	50	0	50	81	45	0	45	81	58	0	58	83	56	0	56
80	50	0	50	81	46	0	46	81	59	0	59	83	56	0	56
80	51	0	51	81	49	0	49	81	60	0	60	83	56	0	56
80	51	0	51	81	49	0	49	81	61	0	61	83	57	0	57
80	51	0	51	81	49	0	49	82	51	0	51	83	57	0	57
80	51	0	51	81	50	0	50	82	52	0	52	83	58	0	58
80	52	0	52	81	50	0	50	82	55	0	55	83	58	0	58
80	53	0	53	81	50	0	50	82	56	0	56	83	58	0	58
80	53	0	53	81	50	0	50	82	56	0	56	83	58	0	58
80	53	0	53	81	50	0	50	82	57	0	57	83	58	0	58
80	54	0	54	81	50	0	50	82	58	0	58	83	58	0	58
80	54	0	54	81	50	0	50	82	58	0	58	83	58	0	58
80	54	0	54	81	50	0	50	82	58	0	58	83	58	0	58
80	54	0	54	81	50	0	50	82	58	0	58	83	58	0	58
80	54	0	54	81	50	0	50	82	59	0	59	83	58	0	58
80	55	0	55	81	51	0	51	82	60	0	60	83	58	0	58
80	55	0	55	81	51	0	51	82	60	0	60	83	59	0	59
80	55	0	55	81	51	0	51	82	61	0	61	83	59	0	59
80	55	0	55	81	51	0	51	82	61	0	61	83	59	0	59
80	55	0	55	81	52	0	52	82	61	0	61	83	59	0	59
80	55	0	55	81	52	0	52	82	61	0	61	83	60	0	60
80	55	0	55	81	52	0	52	82	62	0	62	83	60	0	60
80	55	0	55	81	52	0	52	82	62	0	62	83	60	0	60
80	56	0	56	81	52	0	52	82	62	0	62	83	60	0	60
80	56	0	56	81	53	0	53	82	62	0	62	83	60	0	60

Table B.2. INTACT-ROCK STRENGTH DATA continued

Site ID	Raw*	Ang†	Adj§	Site ID	Raw*	Ang†	Adj§	Site ID	Raw*	Ang†	Adj§	Site ID	Raw*	Ang†	Adj§
83	60	0	60	84	32	0	32	84	45	0	45	84	51	0	51
83	60	0	60	84	34	0	34	84	45	0	45	84	52	0	52
83	61	0	61	84	35	0	35	84	46	0	46	84	52	0	52
83	61	0	61	84	35	0	35	84	46	0	46	84	52	0	52
83	61	0	61	84	36	0	36	84	46	0	46	84	52	0	52
83	61	0	61	84	40	0	40	84	46	0	46	84	54	0	54
83	61	0	61	84	40	0	40	84	47	0	47	84	55	0	55
83	62	0	62	84	41	0	41	84	47	0	47	84	55	0	55
83	62	0	62	84	42	0	42	84	48	0	48	84	56	0	56
83	63	0	63	84	42	0	42	84	48	0	48	84	56	0	56
83	63	0	63	84	42	0	42	84	48	0	48	84	56	0	56
83	63	0	63	84	42	0	42	84	48	0	48	84	56	0	56
83	64	0	64	84	42	0	42	84	50	0	50	84	58	0	58
83	65	0	65	84	42	0	42	84	50	0	50	84	58	0	58
84	30	0	30	84	43	0	43	84	50	0	50	84	58	0	58
84	30	0	30	84	44	0	44	84	50	0	50	84	59	0	59
84	30	0	30	84	44	0	44	84	50	0	50	84	60	0	60
84	32	0	32	84	44	0	44	84	51	0	51				
84	32	0	32	84	45	0	45	84	51	0	51				

Note: Intact-rock strength values are reported as the rebound percent recorded by the Schmidt hammer instrument and organized by sample site. Data are ordered down and across for each page.

*Raw intact-rock strength (% rebound).

†Inclination angle of Schmidt hammer (degrees above horizontal).

§Intact-rock strength (% rebound) adjusted for inclination of Schmidt hammer instrument (Selby, 1993).

Appendix C. Fracture Spacing Data

The following appendix contains a table of summary statistics on fracture spacing, organized by sample site, and the raw data itself.

Summary Statistics

Table C.1. FRACTURE SPACING SUMMARY STATISTICS

Site ID	n	Mean	SD	Min	Q1*	Median	Q3†	Max
1	1	188	0	188	188	188	188	188
2	11	73	30	18	71	74	89	134
3	13	77	55	18	31	56	123	185
4	25	63	32	12	39	53	82	139
5	23	79	39	24	58	76	103	210
6	35	79	36	48	56	67	81	210
7	14	66	10	50	63	66	70	80
8	19	60	22	15	42	58	81	86
9§		20		5				30
10	42	45	19	15	29	42	59	92
11	26	124	85	9	59	121	167	320
12	52	12	6	3	7	10	13	31
13§		150		100				200
14	36	46	19	18	30	47	57	114
15	19	152	53	30	116	164	191	238
16	26	93	12	73	84	90	100	124
17§		75		100				50
18§		350		200				400
19	88	95	53	22	55	81	122	243
20	27	74	28	20	55	67	94	128
21§		75		100				50
22	57	53	33	17	27	45	66	159
23§		15		10				20
24	37	79	38	15	50	72	104	170
25§		75		100				50
26§		325		100				400
27	32	76	43	22	40	70	97	168
28	36	44	22	10	27	41	59	91
29	61	80	46	18	42	69	107	206
30	24	58	30	10	35	63	76	109
31	110	107	61	21	59	97	146	347
32	89	26	21	4	13	18	29	103
33	77	15	7	6	9	13	18	40
34	65	11	6	3	6	9	14	34
35	56	16	9	3	10	14	20	40

Table C.1. FRACTURE SPACING SUMMARY STATISTICS continued

Site ID	n	Mean	SD	Min	Q1*	Median	Q3†	Max
36	56	40	22	9	23	39	50	102
37	79	8	5	3	5	8	11	23
38	94	27	15	4	16	28	35	73
39	65	15	7	4	9	15	19	37
40	24	55	19	27	41	50	66	97
41	12	35	15	20	26	30	42	74
42	36	61	25	24	39	60	77	130
43	31	45	21	6	29	44	63	103
44	40	41	17	9	27	41	51	77
45	36	65	31	13	46	58	82	139
46	43	74	40	16	45	60	108	185
47§		50		25				75
48	49	37	17	9	26	34	49	78
49§		15		5				20
50	42	52	24	16	37	47	70	132
51	101	36	19	5	21	34	50	104
52	50	46	18	16	31	45	60	95
53	58	40	22	9	22	34	50	101
54	35	22	13	7	13	20	26	81
55	31	51	27	11	30	50	69	126
56	68	60	33	10	39	52	75	170
57§		15		5				20
58	38	50	24	10	32	51	66	115
59	146	27	25	2	10	18	32	135
60	112	11	10	2	4	7	14	53
61	44	79	49	19	41	57	106	220
62	24	38	14	20	27	33	50	75
63	120	32	21	6	16	25	43	126
64	24	53	21	13	31	58	71	85
65	117	72	31	13	52	68	90	145
66	39	31	14	10	20	31	42	64
67	74	5	2	1	3	5	7	12
68	32	40	12	22	31	39	50	63
69	77	5	2	2	3	5	6	13
70	171	9	7	1	3	7	14	36
71	49	38	22	11	22	32	46	141
72	101	59	34	9	35	49	71	154
73	120	19	14	2	8	14	28	60

Table C.1. FRACTURE SPACING SUMMARY STATISTICS continued

Site ID	n	Mean	SD	Min	Q1*	Median	Q3[†]	Max
74	57	47	23	8	27	41	68	95
75	66	36	24	7	20	29	39	124
76	25	69	36	25	42	50	91	158
77	30	76	48	16	34	61	110	198
78	45	136	74	37	78	129	162	339
79	71	20	10	5	13	18	24	46
80	100	87	47	16	48	78	118	192
81	119	84	48	12	48	73	117	213
82	136	28	16	6	14	24	38	84
83	53	84	87	13	28	48	110	439
84	118	31	28	5	13	21	39	142

Note : Most of the fracture spacing data were measured from digital images calibrated to scale. Field estimates of fracture spacing were used for sites with no available images.

*First quartile value.

[†]Third quartile value.

[§]Study sites having no digital images; field estimates were made for the mean, min, and max spacing of fractures.

<u>Complete Dataset</u>

Table C.2. FRACTURE SPACING DATA

Site ID	FS*	BT†	Site ID	FS*	BT†	Site ID	FS*	BT†	Site ID	FS*	BT†
1	188	ND	4	36	152	6	81	ND	7	80	ND
2	74	ND	4	45	152	6	83	ND	7	80	ND
2	134	ND	4	46	152	6	106	ND	8	42	120
2	18	ND	4	49	152	6	108	ND	8	42	120
2	22	ND	4	50	152	6	113	ND	8	58	120
2	71	ND	4	53	152	6	51	ND	8	74	120
2	71	ND	4	74	152	6	52	ND	8	78	120
2	73	ND	4	101	152	6	54	ND	8	80	120
2	80	ND	4	102	152	6	54	ND	8	81	120
2	85	ND	4	106	152	6	55	ND	8	81	120
2	89	ND	5	38	79	6	55	ND	8	85	120
2	89	ND	5	49	79	6	56	ND	8	86	120
3	18	ND	5	58	79	6	57	ND	8	86	120
3	21	ND	5	66	79	6	58	ND	8	15	120
3	28	ND	5	74	79	6	60	ND	8	24	120
3	35	ND	5	76	79	6	62	ND	8	25	120
3	49	ND	5	77	79	6	63	ND	8	47	120
3	51	ND	5	77	79	6	63	ND	8	52	120
3	56	ND	5	80	79	6	64	ND	8	53	120
3	66	ND	5	84	79	6	65	ND	8	56	120
3	79	ND	5	103	79	6	67	ND	8	77	120
3	95	ND	5	105	79	6	71	ND	10	23	53
3	150	ND	5	112	79	6	48	ND	10	27	53
3	169	ND	5	114	79	6	55	ND	10	28	53
3	185	ND	5	210	79	6	95	ND	10	34	53
4	12	152	5	24	79	6	121	ND	10	35	53
4	33	152	5	26	79	6	201	ND	10	36	53
4	42	152	5	27	79	6	210	ND	10	38	53
4	45	152	5	68	79	7	50	ND	10	40	53
4	60	152	5	70	79	7	52	ND	10	43	53
4	70	152	5	76	79	7	53	ND	10	45	53
4	76	152	5	102	79	7	63	ND	10	51	53
4	79	152	5	111	79	7	63	ND	10	52	53
4	80	152	6	74	ND	7	64	ND	10	53	53
4	84	152	6	75	ND	7	65	ND	10	55	53
4	113	152	6	76	ND	7	66	ND	10	55	53
4	139	152	6	77	ND	7	69	ND	10	55	53
4	19	152	6	77	ND	7	69	ND	10	55	53
4	20	152	6	79	ND	7	70	ND	10	59	53
4	30	152	6	80	ND	7	79	ND	10	59	53

Table C.2. FRACTURE SPACING DATA continued

Site ID	FS*	BT†	Site ID	FS*	BT†	Site ID	FS*	BT†	Site ID	FS*	BT†
10	17	53	11	118	102	12	23	10	14	24	79
10	21	53	11	134	102	12	25	10	14	26	79
10	23	53	11	140	102	12	27	10	14	26	79
10	25	53	11	142	102	12	27	10	14	30	79
10	25	53	11	155	102	12	31	10	14	40	79
10	27	53	11	167	102	12	5	10	14	43	79
10	29	53	11	168	102	12	5	10	14	53	79
10	30	53	12	3	10	12	5	10	14	57	79
10	37	53	12	5	10	12	5	10	14	58	79
10	37	53	12	5	10	12	8	10	14	62	79
10	41	53	12	6	10	12	8	10	14	62	79
10	42	53	12	6	10	12	9	10	15	90	187
10	61	53	12	6	10	12	9	10	15	97	187
10	61	53	12	6	10	12	10	10	15	116	187
10	63	53	12	7	10	12	11	10	15	119	187
10	69	53	12	7	10	12	15	10	15	132	187
10	73	53	12	7	10	12	20	10	15	164	187
10	90	53	12	8	10	14	23	79	15	170	187
10	92	53	12	8	10	14	28	79	15	173	187
10	15	53	12	9	10	14	30	79	15	187	187
10	42	53	12	9	10	14	30	79	15	191	187
10	63	53	12	9	10	14	31	79	15	203	187
10	73	53	12	9	10	14	32	79	15	30	187
11	24	102	12	9	10	14	33	79	15	79	187
11	51	102	12	9	10	14	38	79	15	127	187
11	59	102	12	10	10	14	45	79	15	155	187
11	96	102	12	10	10	14	47	79	15	166	187
11	116	102	12	11	10	14	47	79	15	221	187
11	125	102	12	11	10	14	48	79	15	222	187
11	139	102	12	11	10	14	48	79	15	238	187
11	169	102	12	11	10	14	49	79	16	73	ND
11	254	102	12	12	10	14	51	79	16	82	ND
11	268	102	12	12	10	14	52	79	16	85	ND
11	297	102	12	12	10	14	56	79	16	86	ND
11	320	102	12	13	10	14	60	79	16	92	ND
11	9	102	12	13	10	14	64	79	16	97	ND
11	11	102	12	14	10	14	67	79	16	97	ND
11	15	102	12	14	10	14	75	79	16	100	ND
11	38	102	12	16	10	14	80	79	16	108	ND
11	59	102	12	17	10	14	114	79	16	111	ND
11	80	102	12	18	10	14	18	79	16	116	ND
11	80	102	12	20	10	14	24	79	16	77	ND

Table C.2. FRACTURE SPACING DATA continued

Site ID	FS*	BT†	Site ID	FS*	BT†	Site ID	FS*	BT†	Site ID	FS*	BT†
16	81	ND	19	53	103	19	26	103	20	67	85
16	82	ND	19	60	103	19	27	103	20	86	85
16	83	ND	19	71	103	19	43	103	20	98	85
16	84	ND	19	71	103	19	48	103	22	22	48
16	85	ND	19	72	103	19	51	103	22	23	48
16	86	ND	19	73	103	19	54	103	22	24	48
16	87	ND	19	73	103	19	63	103	22	25	48
16	89	ND	19	81	103	19	66	103	22	30	48
16	94	ND	19	108	103	19	69	103	22	36	48
16	97	ND	19	122	103	19	71	103	22	42	48
16	99	ND	19	123	103	19	84	103	22	45	48
16	101	ND	19	129	103	19	92	103	22	45	48
16	102	ND	19	154	103	19	93	103	22	46	48
16	124	ND	19	161	103	19	94	103	22	46	48
19	41	103	19	171	103	19	99	103	22	52	48
19	44	103	19	178	103	19	103	103	22	53	48
19	52	103	19	191	103	19	159	103	22	53	48
19	63	103	19	197	103	19	176	103	22	54	48
19	65	103	19	201	103	20	54	85	22	54	48
19	69	103	19	243	103	20	76	85	22	55	48
19	73	103	19	22	103	20	77	85	22	57	48
19	78	103	19	43	103	20	78	85	22	59	48
19	80	103	19	44	103	20	84	85	22	62	48
19	95	103	19	45	103	20	92	85	22	69	48
19	97	103	19	51	103	20	94	85	22	82	48
19	98	103	19	56	103	20	103	85	22	87	48
19	120	103	19	58	103	20	111	85	22	88	48
19	122	103	19	66	103	20	123	85	22	93	48
19	132	103	19	71	103	20	125	85	22	98	48
19	142	103	19	80	103	20	128	85	22	101	48
19	156	103	19	80	103	20	20	85	22	110	48
19	181	103	19	81	103	20	23	85	22	110	48
19	192	103	19	82	103	20	40	85	22	113	48
19	195	103	19	82	103	20	53	85	22	126	48
19	207	103	19	83	103	20	55	85	22	132	48
19	237	103	19	85	103	20	55	85	22	159	48
19	31	103	19	89	103	20	55	85	22	17	48
19	35	103	19	89	103	20	57	85	22	18	48
19	38	103	19	117	103	20	57	85	22	19	48
19	38	103	19	121	103	20	60	85	22	20	48
19	41	103	19	161	103	20	65	85	22	23	48
19	48	103	19	23	103	20	66	85	22	23	48

Table C.2. FRACTURE SPACING DATA continued

Site ID	FS*	BT†	Site ID	FS*	BT†	Site ID	FS*	BT†	Site ID	FS*	BT†
22	24	48	24	36	60	27	99	85	29	47	107
22	24	48	24	42	60	27	105	85	29	50	107
22	25	48	24	50	60	27	168	85	29	71	107
22	26	48	24	54	60	28	10	ND	29	73	107
22	27	48	24	56	60	28	11	ND	29	77	107
22	28	48	24	59	60	28	12	ND	29	89	107
22	30	48	24	61	60	28	18	ND	29	101	107
22	30	48	24	62	60	28	22	ND	29	154	107
22	33	48	24	63	60	28	27	ND	29	174	107
22	33	48	24	65	60	28	27	ND	29	180	107
22	34	48	24	68	60	28	28	ND	29	200	107
22	36	48	24	86	60	28	33	ND	29	206	107
22	39	48	24	93	60	28	36	ND	29	54	107
22	40	48	27	28	85	28	36	ND	29	55	107
22	50	48	27	35	85	28	39	ND	29	59	107
22	52	48	27	35	85	28	39	ND	29	66	107
22	64	48	27	40	85	28	43	ND	29	98	107
22	69	48	27	41	85	28	43	ND	29	102	107
24	83	60	27	43	85	28	47	ND	29	108	107
24	85	60	27	45	85	28	55	ND	29	133	107
24	86	60	27	57	85	28	59	ND	29	158	107
24	113	60	27	138	85	28	60	ND	29	18	107
24	114	60	27	153	85	28	62	ND	29	28	107
24	148	60	27	161	85	28	71	ND	29	31	107
24	148	60	27	166	85	28	72	ND	29	32	107
24	159	60	27	22	85	28	81	ND	29	33	107
24	170	60	27	26	85	28	82	ND	29	37	107
24	48	60	27	26	85	28	16	ND	29	39	107
24	72	60	27	30	85	28	17	ND	29	39	107
24	73	60	27	42	85	28	25	ND	29	40	107
24	83	60	27	45	85	28	38	ND	29	42	107
24	27	60	27	51	85	28	40	ND	29	42	107
24	39	60	27	61	85	28	41	ND	29	42	107
24	49	60	27	78	85	28	42	ND	29	49	107
24	92	60	27	82	85	28	45	ND	29	49	107
24	99	60	27	86	85	28	54	ND	29	50	107
24	108	60	27	88	85	28	66	ND	29	52	107
24	118	60	27	93	85	28	83	ND	29	55	107
24	125	60	27	96	85	28	91	ND	29	70	107
24	15	60	27	92	85	29	24	107	29	72	107
24	23	60	27	95	85	29	29	107	29	92	107
24	34	60	27	98	85	29	41	107	29	102	107

Table C.2. FRACTURE SPACING DATA continued

Site ID	FS*	BT†	Site ID	FS*	BT†	Site ID	FS*	BT†	Site ID	FS*	BT†
29	113	107	31	64	231	31	69	231	31	80	231
29	117	107	31	67	231	31	72	231	31	80	231
29	42	107	31	69	231	31	77	231	31	97	231
29	47	107	31	74	231	31	88	231	31	100	231
29	60	107	31	83	231	31	97	231	31	101	231
29	61	107	31	90	231	31	99	231	31	107	231
29	69	107	31	90	231	31	103	231	31	110	231
29	70	107	31	104	231	31	115	231	31	144	231
29	73	107	31	104	231	31	118	231	31	42	231
29	83	107	31	120	231	31	118	231	31	51	231
29	106	107	31	126	231	31	121	231	31	53	231
29	108	107	31	140	231	31	122	231	31	54	231
29	124	107	31	142	231	31	125	231	31	61	231
29	139	107	31	144	231	31	130	231	31	68	231
29	140	107	31	148	231	31	143	231	31	83	231
29	154	107	31	174	231	31	145	231	31	117	231
30	10	73	31	179	231	31	146	231	31	126	231
30	19	73	31	179	231	31	147	231	31	134	231
30	33	73	31	189	231	31	159	231	31	149	231
30	36	73	31	191	231	31	163	231	31	154	231
30	39	73	31	196	231	31	170	231	31	156	231
30	50	73	31	210	231	31	185	231	31	158	231
30	75	73	31	216	231	31	210	231	31	182	231
30	84	73	31	217	231	31	211	231	31	199	231
30	99	73	31	220	231	31	238	231	32	11	10
30	101	73	31	244	231	31	28	231	32	13	10
30	102	73	31	347	231	31	35	231	32	14	10
30	109	73	31	21	231	31	35	231	32	14	10
30	13	73	31	24	231	31	35	231	32	14	10
30	17	73	31	26	231	31	40	231	32	15	10
30	18	73	31	27	231	31	43	231	32	16	10
30	42	73	31	30	231	31	43	231	32	17	10
30	46	73	31	32	231	31	47	231	32	17	10
30	61	73	31	36	231	31	55	231	32	18	10
30	66	73	31	36	231	31	58	231	32	18	10
30	68	73	31	36	231	31	60	231	32	18	10
30	68	73	31	43	231	31	65	231	32	18	10
30	70	73	31	48	231	31	71	231	32	18	10
30	75	73	31	59	231	31	73	231	32	18	10
30	77	73	31	62	231	31	74	231	32	19	10
31	57	231	31	63	231	31	75	231	32	19	10
31	59	231	31	63	231	31	76	231	32	20	10

Table C.2. FRACTURE SPACING DATA continued

Site ID	FS*	BT†	Site ID	FS*	BT†	Site ID	FS*	BT†	Site ID	FS*	BT†
32	20	10	32	11	10	33	10	6	33	9	6
32	20	10	32	11	10	33	10	6	33	10	6
32	20	10	32	11	10	33	11	6	33	10	6
32	21	10	32	11	10	33	11	6	33	10	6
32	22	10	32	11	10	33	11	6	33	11	6
32	22	10	32	11	10	33	12	6	33	11	6
32	24	10	32	11	10	33	12	6	33	11	6
32	24	10	32	11	10	33	12	6	33	12	6
32	24	10	32	13	10	33	12	6	33	13	6
32	25	10	32	13	10	33	13	6	33	14	6
32	25	10	32	13	10	33	14	6	33	16	6
32	26	10	32	14	10	33	14	6	33	16	6
32	27	10	32	15	10	33	14	6	33	18	6
32	31	10	32	16	10	33	15	6	33	18	6
32	32	10	32	17	10	33	15	6	33	20	6
32	33	10	32	17	10	33	15	6	33	22	6
32	34	10	32	17	10	33	16	6	33	25	6
32	36	10	32	17	10	33	16	6	33	26	6
32	41	10	32	18	10	33	16	6	33	29	6
32	43	10	32	18	10	33	17	6	33	30	6
32	46	10	32	20	10	33	17	6	33	32	6
32	46	10	32	20	10	33	17	6	33	32	6
32	53	10	32	20	10	33	18	6	34	4	6
32	59	10	32	22	10	33	19	6	34	4	6
32	64	10	32	25	10	33	19	6	34	5	6
32	66	10	32	25	10	33	19	6	34	5	6
32	72	10	32	30	10	33	20	6	34	5	6
32	83	10	32	34	10	33	20	6	34	6	6
32	89	10	32	52	10	33	20	6	34	6	6
32	94	10	33	6	6	33	20	6	34	6	6
32	101	10	33	7	6	33	21	6	34	7	6
32	103	10	33	7	6	33	24	6	34	8	6
32	4	10	33	7	6	33	29	6	34	8	6
32	5	10	33	7	6	33	40	6	34	8	6
32	6	10	33	7	6	33	6	6	34	9	6
32	9	10	33	9	6	33	7	6	34	9	6
32	9	10	33	9	6	33	7	6	34	9	6
32	10	10	33	9	6	33	7	6	34	9	6
32	11	10	33	9	6	33	8	6	34	9	6
32	11	10	33	9	6	33	8	6	34	10	6
32	11	10	33	10	6	33	8	6	34	11	6
32	11	10	33	10	6	33	9	6	34	11	6

Table C.2. FRACTURE SPACING DATA continued

Site ID	FS*	BT†	Site ID	FS*	BT†	Site ID	FS*	BT†	Site ID	FS*	BT†
34	11	6	34	17	6	35	8	9	36	66	35
34	12	6	34	18	6	35	9	9	36	66	35
34	12	6	34	18	6	35	10	9	36	67	35
34	13	6	35	7	9	35	11	9	36	98	35
34	13	6	35	8	9	35	11	9	36	102	35
34	14	6	35	9	9	35	12	9	36	13	35
34	16	6	35	9	9	35	13	9	36	13	35
34	16	6	35	10	9	35	14	9	36	16	35
34	17	6	35	10	9	35	14	9	36	16	35
34	19	6	35	10	9	35	17	9	36	17	35
34	19	6	35	11	9	35	17	9	36	17	35
34	20	6	35	11	9	35	23	9	36	18	35
34	27	6	35	12	9	35	23	9	36	20	35
34	32	6	35	12	9	35	24	9	36	23	35
34	34	6	35	12	9	35	25	9	36	23	35
34	3	6	35	13	9	35	29	9	36	27	35
34	3	6	35	14	9	35	40	9	36	27	35
34	3	6	35	14	9	36	9	35	36	36	35
34	5	6	35	14	9	36	15	35	36	39	35
34	5	6	35	15	9	36	15	35	36	39	35
34	5	6	35	15	9	36	18	35	36	40	35
34	5	6	35	16	9	36	22	35	36	41	35
34	5	6	35	16	9	36	22	35	36	41	35
34	6	6	35	17	9	36	25	35	36	44	35
34	6	6	35	17	9	36	29	35	36	46	35
34	7	6	35	18	9	36	29	35	36	46	35
34	7	6	35	20	9	36	29	35	36	48	35
34	8	6	35	20	9	36	29	35	36	54	35
34	9	6	35	21	9	36	35	35	36	54	35
34	9	6	35	26	9	36	35	35	36	90	35
34	9	6	35	30	9	36	37	35	36	100	35
34	10	6	35	31	9	36	40	35	37	5	4
34	10	6	35	31	9	36	43	35	37	5	4
34	11	6	35	34	9	36	46	35	37	5	4
34	11	6	35	38	9	36	46	35	37	5	4
34	11	6	35	3	9	36	47	35	37	5	4
34	12	6	35	4	9	36	48	35	37	6	4
34	13	6	35	5	9	36	51	35	37	6	4
34	14	6	35	5	9	36	53	35	37	6	4
34	15	6	35	5	9	36	54	35	37	6	4
34	16	6	35	6	9	36	56	35	37	7	4
34	16	6	35	6	9	36	62	35	37	7	4

Table C.2. FRACTURE SPACING DATA continued

Site ID	FS*	BT†	Site ID	FS*	BT†	Site ID	FS*	BT†	Site ID	FS*	BT†
37	7	4	37	3	4	38	38	16	38	16	27
37	7	4	37	3	4	38	39	16	38	16	27
37	8	4	37	4	4	38	44	16	38	17	27
37	8	4	37	4	4	38	52	16	38	21	27
37	8	4	37	4	4	38	58	16	38	21	27
37	9	4	37	4	4	38	67	16	38	21	27
37	9	4	37	4	4	38	73	16	38	24	27
37	9	4	37	4	4	38	4	16	38	27	27
37	9	4	37	5	4	38	5	16	38	27	27
37	9	4	37	6	4	38	6	16	38	29	27
37	9	4	37	6	4	38	7	16	38	29	27
37	9	4	37	6	4	38	8	16	38	29	27
37	9	4	37	7	4	38	8	16	38	29	27
37	9	4	37	7	4	38	8	16	38	30	27
37	10	4	37	7	4	38	9	16	38	32	27
37	10	4	37	7	4	38	10	16	38	32	27
37	10	4	37	7	4	38	10	16	38	32	27
37	11	4	37	8	4	38	12	16	38	32	27
37	12	4	37	8	4	38	14	16	38	32	27
37	12	4	37	8	4	38	15	16	38	33	27
37	12	4	37	8	4	38	15	16	38	33	27
37	12	4	37	9	4	38	17	16	38	35	27
37	12	4	37	9	4	38	21	16	38	35	27
37	13	4	37	11	4	38	22	16	38	35	27
37	14	4	37	14	4	38	22	16	38	36	27
37	14	4	37	19	4	38	23	16	38	37	27
37	16	4	38	8	16	38	30	16	38	37	27
37	16	4	38	15	16	38	30	16	38	38	27
37	17	4	38	17	16	38	33	16	38	39	27
37	17	4	38	18	16	38	34	16	38	40	27
37	17	4	38	19	16	38	35	16	38	41	27
37	18	4	38	19	16	38	38	16	38	46	27
37	19	4	38	20	16	38	40	16	38	52	27
37	23	4	38	22	16	38	6	27	38	56	27
37	3	4	38	25	16	38	11	27	38	62	27
37	3	4	38	26	16	38	13	27	38	64	27
37	3	4	38	28	16	38	14	27	39	6	17
37	3	4	38	28	16	38	14	27	39	6	17
37	3	4	38	28	16	38	15	27	39	6	17
37	3	4	38	33	16	38	16	27	39	8	17
37	3	4	38	34	16	38	16	27	39	9	17
37	3	4	38	38	16	38	16	27	39	9	17

Table C.2. FRACTURE SPACING DATA continued

Site ID	FS*	BT†	Site ID	FS*	BT†	Site ID	FS*	BT†	Site ID	FS*	BT†
39	10	17	39	13	17	41	23	ND	42	77	ND
39	10	17	39	13	17	41	25	ND	42	81	ND
39	12	17	39	13	17	41	27	ND	42	89	ND
39	15	17	39	14	17	41	28	ND	42	95	ND
39	16	17	39	14	17	41	29	ND	42	110	ND
39	16	17	39	14	17	41	31	ND	43	6	ND
39	16	17	39	16	17	41	32	ND	43	11	ND
39	17	17	39	16	17	41	40	ND	43	22	ND
39	17	17	39	16	17	41	45	ND	43	22	ND
39	17	17	39	16	17	41	51	ND	43	25	ND
39	18	17	39	17	17	41	74	ND	43	25	ND
39	18	17	39	17	17	42	25	ND	43	29	ND
39	19	17	39	18	17	42	28	ND	43	31	ND
39	19	17	39	19	17	42	30	ND	43	35	ND
39	20	17	39	19	17	42	32	ND	43	41	ND
39	21	17	39	23	17	42	32	ND	43	47	ND
39	21	17	39	27	17	42	35	ND	43	48	ND
39	24	17	40	32	ND	42	37	ND	43	63	ND
39	24	17	40	35	ND	42	49	ND	43	64	ND
39	26	17	40	40	ND	42	54	ND	43	67	ND
39	27	17	40	46	ND	42	59	ND	43	28	ND
39	29	17	40	48	ND	42	61	ND	43	29	ND
39	29	17	40	52	ND	42	63	ND	43	36	ND
39	31	17	40	58	ND	42	63	ND	43	39	ND
39	37	17	40	63	ND	42	72	ND	43	40	ND
39	4	17	40	70	ND	42	78	ND	43	44	ND
39	5	17	40	87	ND	42	86	ND	43	44	ND
39	8	17	40	97	ND	42	110	ND	43	56	ND
39	8	17	40	27	ND	42	130	ND	43	58	ND
39	8	17	40	28	ND	42	24	ND	43	60	ND
39	8	17	40	40	ND	42	34	ND	43	61	ND
39	8	17	40	42	ND	42	42	ND	43	66	ND
39	9	17	40	45	ND	42	49	ND	43	68	ND
39	9	17	40	46	ND	42	53	ND	43	70	ND
39	9	17	40	47	ND	42	55	ND	43	71	ND
39	9	17	40	52	ND	42	56	ND	43	103	ND
39	10	17	40	53	ND	42	60	ND	44	15	ND
39	11	17	40	53	ND	42	61	ND	44	17	ND
39	12	17	40	83	ND	42	61	ND	44	21	ND
39	12	17	40	83	ND	42	69	ND	44	21	ND
39	13	17	40	83	ND	42	74	ND	44	23	ND
39	13	17	41	20	ND	42	76	ND	44	28	ND

Table C.2. FRACTURE SPACING DATA continued

Site ID	FS*	BT†	Site ID	FS*	BT†	Site ID	FS*	BT†	Site ID	FS*	BT†
44	29	ND	45	46	ND	46	55	ND	48	36	ND
44	29	ND	45	46	ND	46	56	ND	48	36	ND
44	42	ND	45	47	ND	46	60	ND	48	36	ND
44	43	ND	45	48	ND	46	60	ND	48	38	ND
44	48	ND	45	48	ND	46	61	ND	48	39	ND
44	50	ND	45	49	ND	46	76	ND	48	41	ND
44	51	ND	45	49	ND	46	81	ND	48	47	ND
44	55	ND	45	52	ND	46	81	ND	48	53	ND
44	55	ND	45	53	ND	46	111	ND	48	58	ND
44	57	ND	45	54	ND	46	113	ND	48	59	ND
44	65	ND	45	61	ND	46	141	ND	48	68	ND
44	67	ND	45	63	ND	46	26	ND	48	22	ND
44	72	ND	45	63	ND	46	41	ND	48	22	ND
44	77	ND	45	64	ND	46	49	ND	48	24	ND
44	9	ND	45	75	ND	46	51	ND	48	26	ND
44	16	ND	45	75	ND	46	67	ND	48	27	ND
44	24	ND	45	79	ND	46	67	ND	48	29	ND
44	25	ND	45	80	ND	46	74	ND	48	33	ND
44	27	ND	45	81	ND	46	84	ND	48	52	ND
44	29	ND	45	83	ND	46	84	ND	48	54	ND
44	32	ND	45	84	ND	46	99	ND	48	64	ND
44	32	ND	45	86	ND	46	108	ND	48	68	ND
44	35	ND	45	93	ND	46	120	ND	48	78	ND
44	39	ND	45	99	ND	46	131	ND	48	15	ND
44	39	ND	45	117	ND	46	131	ND	48	17	ND
44	40	ND	45	126	ND	46	134	ND	48	30	ND
44	45	ND	45	128	ND	46	138	ND	48	30	ND
44	46	ND	45	139	ND	46	147	ND	48	32	ND
44	48	ND	46	16	ND	46	185	ND	48	33	ND
44	48	ND	46	23	ND	48	9	ND	48	34	ND
44	50	ND	46	27	ND	48	10	ND	48	35	ND
44	51	ND	46	30	ND	48	12	ND	48	40	ND
44	56	ND	46	31	ND	48	19	ND	48	42	ND
44	72	ND	46	35	ND	48	20	ND	48	59	ND
45	13	ND	46	39	ND	48	25	ND	48	72	ND
45	18	ND	46	39	ND	48	28	ND	48	74	ND
45	20	ND	46	45	ND	48	28	ND	50	22	ND
45	26	ND	46	48	ND	48	31	ND	50	27	ND
45	27	ND	46	50	ND	48	33	ND	50	27	ND
45	40	ND	46	50	ND	48	33	ND	50	29	ND
45	44	ND	46	55	ND	48	34	ND	50	33	ND
45	45	ND	46	55	ND	48	34	ND	50	35	ND

Table C.2. FRACTURE SPACING DATA continued

Site ID	FS*	BT†	Site ID	FS*	BT†	Site ID	FS*	BT†	Site ID	FS*	BT†
50	40	ND	51	23	ND	51	17	ND	51	44	ND
50	42	ND	51	26	ND	51	18	ND	51	44	ND
50	43	ND	51	26	ND	51	20	ND	51	47	ND
50	44	ND	51	27	ND	51	23	ND	51	50	ND
50	47	ND	51	27	ND	51	25	ND	51	51	ND
50	47	ND	51	28	ND	51	26	ND	51	59	ND
50	48	ND	51	32	ND	51	27	ND	51	63	ND
50	50	ND	51	34	ND	51	28	ND	51	64	ND
50	56	ND	51	34	ND	51	29	ND	51	70	ND
50	63	ND	51	36	ND	51	29	ND	51	99	ND
50	66	ND	51	37	ND	51	34	ND	51	104	ND
50	70	ND	51	38	ND	51	37	ND	52	16	ND
50	71	ND	51	41	ND	51	39	ND	52	17	ND
50	77	ND	51	43	ND	51	49	ND	52	18	ND
50	78	ND	51	45	ND	51	50	ND	52	20	ND
50	82	ND	51	5	ND	51	50	ND	52	21	ND
50	16	ND	51	13	ND	51	50	ND	52	25	ND
50	17	ND	51	15	ND	51	52	ND	52	29	ND
50	22	ND	51	19	ND	51	52	ND	52	29	ND
50	28	ND	51	20	ND	51	53	ND	52	29	ND
50	37	ND	51	23	ND	51	53	ND	52	31	ND
50	39	ND	51	23	ND	51	53	ND	52	33	ND
50	39	ND	51	27	ND	51	55	ND	52	36	ND
50	43	ND	51	28	ND	51	60	ND	52	36	ND
50	43	ND	51	30	ND	51	67	ND	52	42	ND
50	43	ND	51	36	ND	51	70	ND	52	44	ND
50	47	ND	51	39	ND	51	86	ND	52	45	ND
50	57	ND	51	41	ND	51	17	ND	52	53	ND
50	59	ND	51	46	ND	51	18	ND	52	53	ND
50	69	ND	51	53	ND	51	19	ND	52	57	ND
50	73	ND	51	55	ND	51	19	ND	52	57	ND
50	78	ND	51	56	ND	51	21	ND	52	58	ND
50	80	ND	51	63	ND	51	22	ND	52	59	ND
50	88	ND	51	63	ND	51	22	ND	52	60	ND
50	93	ND	51	66	ND	51	26	ND	52	62	ND
50	132	ND	51	9	ND	51	27	ND	52	63	ND
51	9	ND	51	11	ND	51	29	ND	52	65	ND
51	12	ND	51	14	ND	51	34	ND	52	66	ND
51	13	ND	51	15	ND	51	35	ND	52	70	ND
51	14	ND	51	15	ND	51	36	ND	52	81	ND
51	16	ND	51	17	ND	51	37	ND	52	20	ND
51	21	ND	51	17	ND	51	44	ND	52	27	ND

Table C.2. FRACTURE SPACING DATA continued

Site ID	FS*	BT†	Site ID	FS*	BT†	Site ID	FS*	BT†	Site ID	FS*	BT†
52	27	ND	53	47	ND	54	18	ND	55	17	93
52	32	ND	53	47	ND	54	18	ND	55	17	93
52	34	ND	53	49	ND	54	20	ND	55	21	93
52	37	ND	53	51	ND	54	21	ND	55	26	93
52	39	ND	53	60	ND	54	21	ND	55	30	93
52	40	ND	53	63	ND	54	22	ND	55	32	93
52	42	ND	53	63	ND	54	24	ND	55	42	93
52	44	ND	53	65	ND	54	25	ND	55	42	93
52	50	ND	53	71	ND	54	25	ND	55	44	93
52	55	ND	53	90	ND	54	26	ND	55	50	93
52	55	ND	53	9	ND	54	27	ND	55	51	93
52	57	ND	53	11	ND	54	31	ND	55	54	93
52	59	ND	53	22	ND	54	33	ND	55	56	93
52	61	ND	53	22	ND	54	39	ND	55	71	93
52	62	ND	53	22	ND	54	7	ND	55	73	93
52	63	ND	53	22	ND	54	9	ND	55	87	93
52	73	ND	53	22	ND	54	9	ND	55	126	93
52	75	ND	53	23	ND	54	12	ND	56	10	ND
52	95	ND	53	25	ND	54	14	ND	56	20	ND
53	10	ND	53	28	ND	54	18	ND	56	22	ND
53	11	ND	53	32	ND	54	18	ND	56	24	ND
53	14	ND	53	33	ND	54	20	ND	56	25	ND
53	17	ND	53	33	ND	54	24	ND	56	25	ND
53	19	ND	53	35	ND	54	26	ND	56	27	ND
53	20	ND	53	46	ND	54	29	ND	56	30	ND
53	21	ND	53	50	ND	54	31	ND	56	32	ND
53	22	ND	53	50	ND	54	45	ND	56	35	ND
53	24	ND	53	50	ND	54	81	ND	56	39	ND
53	25	ND	53	52	ND	55	29	93	56	43	ND
53	26	ND	53	71	ND	55	35	93	56	44	ND
53	28	ND	53	78	ND	55	42	93	56	45	ND
53	31	ND	53	85	ND	55	42	93	56	46	ND
53	33	ND	53	87	ND	55	58	93	56	47	ND
53	34	ND	53	101	ND	55	59	93	56	47	ND
53	35	ND	54	9	ND	55	62	93	56	49	ND
53	38	ND	54	10	ND	55	63	93	56	50	ND
53	40	ND	54	11	ND	55	69	93	56	54	ND
53	41	ND	54	13	ND	55	75	93	56	55	ND
53	43	ND	54	13	ND	55	80	93	56	60	ND
53	44	ND	54	15	ND	55	111	93	56	65	ND
53	44	ND	54	16	ND	55	11	93	56	71	ND
53	45	ND				55	13	93	56	72	ND

Table C.2. FRACTURE SPACING DATA continued

Site ID	FS*	BT[†]	Site ID	FS*	BT[†]	Site ID	FS*	BT[†]	Site ID	FS*	BT[†]
56	73	ND	56	170	ND	59	28	33	59	24	33
56	74	ND	58	19	60	59	29	33	59	27	33
56	77	ND	58	20	60	59	31	33	59	34	33
56	77	ND	58	24	60	59	32	33	59	35	33
56	78	ND	58	25	60	59	34	33	59	36	33
56	79	ND	58	34	60	59	43	33	59	38	33
56	88	ND	58	38	60	59	45	33	59	40	33
56	90	ND	58	39	60	59	49	33	59	45	33
56	44	ND	58	43	60	59	51	33	59	46	33
56	45	ND	58	46	60	59	51	33	59	48	33
56	52	ND	58	50	60	59	65	33	59	57	33
56	70	ND	58	55	60	59	66	33	59	57	33
56	75	ND	58	57	60	59	69	33	59	65	33
56	87	ND	58	59	60	59	73	33	59	65	33
56	92	ND	58	59	60	59	76	33	59	66	33
56	102	ND	58	66	60	59	79	33	59	76	33
56	103	ND	58	66	60	59	82	33	59	80	33
56	108	ND	58	68	60	59	85	33	59	81	33
56	116	ND	58	73	60	59	87	33	59	4	5
56	17	ND	58	76	60	59	87	33	59	5	5
56	18	ND	58	78	60	59	112	33	59	6	5
56	20	ND	58	78	60	59	116	33	59	6	5
56	25	ND	58	111	60	59	135	33	59	7	5
56	28	ND	58	10	60	59	11	33	59	8	5
56	37	ND	58	12	60	59	12	33	59	9	5
56	39	ND	58	18	60	59	14	33	59	9	5
56	41	ND	58	19	60	59	14	33	59	9	5
56	45	ND	58	21	60	59	16	33	59	9	5
56	47	ND	58	32	60	59	17	33	59	9	5
56	50	ND	58	45	60	59	17	33	59	10	5
56	50	ND	58	45	60	59	18	33	59	10	5
56	51	ND	58	47	60	59	18	33	59	13	5
56	55	ND	58	52	60	59	18	33	59	16	5
56	57	ND	58	52	60	59	20	33	59	16	5
56	58	ND	58	54	60	59	21	33	59	16	5
56	61	ND	58	56	60	59	21	33	59	17	5
56	65	ND	58	68	60	59	21	33	59	17	5
56	70	ND	58	76	60	59	21	33	59	17	5
56	73	ND	58	115	60	59	22	33	59	17	5
56	124	ND	59	20	33	59	24	33	59	18	5
56	156	ND	59	26	33	59	24	33	59	18	5
56	162	ND	59	27	33	59	24	33	59	18	5

Table C.2. FRACTURE SPACING DATA continued

Site ID	FS*	BT†	Site ID	FS*	BT†	Site ID	FS*	BT†	Site ID	FS*	BT†
59	19	5	59	10	5	60	10	4	60	12	22
59	19	5	59	10	5	60	11	4	60	13	22
59	20	5	59	10	5	60	11	4	60	14	22
59	20	5	59	10	5	60	12	4	60	14	22
59	20	5	59	11	5	60	13	4	60	14	22
59	21	5	59	11	5	60	13	4	60	15	22
59	22	5	59	11	5	60	15	4	60	15	22
59	22	5	59	12	5	60	16	4	60	16	22
59	23	5	59	12	5	60	17	4	60	16	22
59	26	5	59	13	5	60	2	4	60	17	22
59	27	5	59	13	5	60	2	4	60	18	22
59	27	5	59	13	5	60	2	4	60	19	22
59	29	5	59	14	5	60	3	4	60	21	22
59	29	5	59	15	5	60	3	4	60	23	22
59	30	5	59	15	5	60	3	4	60	24	22
59	31	5	59	17	5	60	3	4	60	26	22
59	33	5	59	18	5	60	3	4	60	26	22
59	2	5	60	3	4	60	3	4	60	27	22
59	2	5	60	4	4	60	3	4	60	27	22
59	2	5	60	4	4	60	3	4	60	31	22
59	3	5	60	4	4	60	3	4	60	33	22
59	3	5	60	4	4	60	3	4	60	38	22
59	3	5	60	4	4	60	3	4	60	43	22
59	3	5	60	4	4	60	3	4	60	49	22
59	4	5	60	4	4	60	3	4	60	53	22
59	4	5	60	4	4	60	3	4	60	4	22
59	4	5	60	4	4	60	4	4	60	5	22
59	4	5	60	4	4	60	4	4	60	5	22
59	4	5	60	5	4	60	4	4	60	6	22
59	4	5	60	5	4	60	4	4	60	7	22
59	4	5	60	5	4	60	4	4	60	7	22
59	5	5	60	5	4	60	4	4	60	7	22
59	5	5	60	6	4	60	4	4	60	8	22
59	5	5	60	7	4	60	5	4	60	8	22
59	5	5	60	7	4	60	5	4	60	8	22
59	5	5	60	7	4	60	5	4	60	8	22
59	6	5	60	8	4	60	5	4	60	9	22
59	6	5	60	9	4	60	5	4	60	9	22
59	6	5	60	9	4	60	5	4	60	10	22
59	7	5	60	9	4	60	6	22	60	10	22
59	7	5	60	10	4	60	6	22	60	12	22
59	9	5	60	10	4	60	10	22	60	13	22

Table C.2. FRACTURE SPACING DATA continued

Site ID	FS*	BT†	Site ID	FS*	BT†	Site ID	FS*	BT†	Site ID	FS*	BT†
60	15	22	61	107	ND	63	32	58	63	18	58
60	16	22	61	108	ND	63	33	58	63	19	58
60	19	22	61	111	ND	63	34	58	63	20	58
61	21	ND	61	156	ND	63	35	58	63	22	58
61	27	ND	61	220	ND	63	39	58	63	24	58
61	35	ND	62	23	ND	63	40	58	63	25	58
61	41	ND.	62	24	ND	63	42	58	63	27	58
61	43	ND	62	24	ND	63	43	58	63	31	58
61	49	ND	62	27	ND	63	44	58	63	34	58
61	58	ND	62	28	ND	63	46	58	63	34	58
61	61	ND	62	30	ND	63	48	58	63	35	58
61	70	ND	62	42	ND	63	50	58	63	36	58
61	88	ND	62	45	ND	63	54	58	63	39	58
61	94	ND	62	50	ND	63	59	58	63	41	58
61	96	ND	62	50	ND	63	63	58	63	43	58
61	97	ND	62	53	ND	63	6	58	63	46	58
61	99	ND	62	57	ND	63	10	58	63	49	58
61	112	ND	62	75	ND	63	11	58	63	50	58
61	141	ND	62	20	ND	63	11	58	63	54	58
61	168	ND	62	23	ND	63	11	58	63	57	58
61	19	ND	62	27	ND	63	12	58	63	59	58
61	34	ND	62	30	ND	63	12	58	63	61	58
61	41	ND	62	30	ND	63	14	58	63	64	58
61	41	ND	62	31	ND	63	15	58	63	71	58
61	50	ND	62	35	ND	63	15	58	63	72	58
61	54	ND	62	43	ND	63	16	58	63	73	58
61	55	ND	62	46	ND	63	16	58	63	89	58
61	56	ND	62	53	ND	63	18	58	63	126	58
61	78	ND	62	53	ND	63	21	58	63	9	58
61	78	ND	63	13	58	63	22	58	63	9	58
61	156	ND	63	17	58	63	24	58	63	9	58
61	179	ND	63	18	58	63	25	58	63	9	58
61	183	ND	63	18	58	63	33	58	63	9	58
61	22	ND	63	19	58	63	36	58	63	9	58
61	37	ND	63	20	58	63	37	58	63	10	58
61	37	ND	63	21	58	63	43	58	63	11	58
61	38	ND	63	22	58	63	45	58	63	11	58
61	43	ND	63	22	58	63	59	58	63	12	58
61	52	ND	63	25	58	63	74	58	63	12	58
61	52	ND	63	26	58	63	10	58	63	13	58
61	57	ND	63	31	58	63	15	58	63	14	58
61	106	ND	63	32	58	63	16	58	63	15	58

Table C.2. FRACTURE SPACING DATA continued

Site ID	FS*	BT†	Site ID	FS*	BT†	Site ID	FS*	BT†	Site ID	FS*	BT†
63	15	58	64	67	95	65	83	95	65	17	95
63	15	58	64	72	95	65	85	95	65	23	95
63	17	58	64	75	95	65	91	95	65	25	95
63	17	58	64	76	95	65	91	95	65	25	95
63	20	58	64	79	95	65	92	95	65	27	95
63	21	58	65	13	95	65	104	95	65	28	95
63	21	58	65	29	95	65	109	95	65	31	95
63	22	58	65	35	95	65	116	95	65	34	95
63	23	58	65	36	95	65	120	95	65	36	95
63	24	58	65	50	95	65	19	95	65	37	95
63	26	58	65	51	95	65	20	95	65	38	95
63	27	58	65	54	95	65	27	95	65	38	95
63	28	58	65	55	95	65	39	95	65	47	95
63	31	58	65	57	95	65	44	95	65	47	95
63	34	58	65	58	95	65	53	95	65	51	95
63	35	58	65	59	95	65	55	95	65	51	95
63	35	58	65	61	95	65	56	95	65	52	95
63	39	58	65	71	95	65	58	95	65	55	95
63	52	58	65	76	95	65	60	95	65	57	95
63	64	58	65	79	95	65	62	95	65	60	95
63	64	58	65	79	95	65	63	95	65	62	95
63	73	58	65	88	95	65	66	95	65	62	95
63	97	58	65	89	95	65	67	95	65	62	95
64	13	95	65	104	95	65	68	95	65	66	95
64	18	95	65	104	95	65	68	95	65	69	95
64	22	95	65	110	95	65	68	95	65	71	95
64	29	95	65	119	95	65	68	95	65	72	95
64	29	95	65	125	95	65	70	95	65	78	95
64	38	95	65	125	95	65	72	95	65	104	95
64	51	95	65	142	95	65	73	95	65	105	95
64	64	95	65	20	95	65	75	95	65	106	95
64	65	95	65	39	95	65	77	95	65	107	95
64	67	95	65	60	95	65	78	95	65	117	95
64	70	95	65	62	95	65	78	95	65	117	95
64	74	95	65	62	95	65	79	95	65	120	95
64	85	95	65	65	95	65	82	95	65	122	95
64	25	95	65	66	95	65	86	95	65	130	95
64	33	95	65	69	95	65	88	95	65	134	95
64	47	95	65	73	95	65	110	95	65	137	95
64	53	95	65	78	95	65	120	95	66	24	35
64	56	95	65	79	95	65	135	95	66	24	35
64	60	95	65	80	95	65	145	95	66	27	35
									66	32	35

Table C.2. FRACTURE SPACING DATA continued

Site ID	FS*	BT†	Site ID	FS*	BT†	Site ID	FS*	BT†	Site ID	FS*	BT†
66	33	35	67	3	12	67	4	12	68	43	56
66	34	35	67	3	12	67	4	12	68	44	56
66	36	35	67	3	12	67	4	12	68	47	56
66	36	35	67	3	12	67	5	12	68	48	56
66	39	35	67	3	12	67	5	12	68	34	56
66	39	35	67	3	12	67	5	12	68	48	56
66	42	35	67	3	12	67	5	12	68	49	56
66	47	35	67	3	12	67	5	12	68	50	56
66	47	35	67	4	12	67	5	12	68	52	56
66	49	35	67	4	12	67	6	12	68	54	56
66	49	35	67	4	12	67	6	12	68	56	56
66	53	35	67	4	12	67	6	12	68	57	56
66	64	35	67	4	12	67	6	12	68	59	56
66	10	35	67	4	12	67	6	12	68	62	56
66	11	35	67	4	12	67	6	12	68	63	56
66	11	35	67	4	12	67	6	12	69	2	7
66	11	35	67	5	12	67	7	12	69	2	7
66	12	35	67	5	12	67	7	12	69	2	7
66	12	35	67	5	12	67	7	12	69	2	7
66	13	35	67	5	12	67	7	12	69	3	7
66	16	35	67	5	12	67	8	12	69	3	7
66	17	35	67	5	12	67	8	12	69	3	7
66	20	35	67	6	12	67	9	12	69	4	7
66	22	35	67	6	12	67	11	12	69	4	7
66	24	35	67	7	12	67	11	12	69	4	7
66	25	35	67	7	12	68	22	56	69	4	7
66	27	35	67	7	12	68	22	56	69	5	7
66	28	35	67	7	12	68	24	56	69	5	7
66	28	35	67	8	12	68	27	56	69	5	7
66	31	35	67	9	12	68	28	56	69	5	7
66	32	35	67	9	12	68	29	56	69	6	7
66	32	35	67	9	12	68	30	56	69	6	7
66	44	35	67	9	12	68	31	56	69	6	7
66	50	35	67	10	12	68	31	56	69	6	7
66	52	35	67	12	12	68	31	56	69	6	7
67	1	12	67	2	12	68	31	56	69	6	7
67	2	12	67	2	12	68	32	56	69	6	7
67	2	12	67	3	12	68	34	56	69	6	7
67	2	12	67	3	12	68	38	56	69	6	7
67	2	12	67	3	12	68	39	56	69	7	7
67	2	12	67	4	12	68	40	56	69	7	7
67	2	12	67	4	12	68	40	56	69	8	7

Table C.2. FRACTURE SPACING DATA continued

Site ID	FS*	BT†	Site ID	FS*	BT†	Site ID	FS*	BT†	Site ID	FS*	BT†
69	8	7	69	5	7	70	18	13	70	8	13
69	8	7	69	5	7	70	18	13	70	8	13
69	9	7	69	5	7	70	19	13	70	8	13
69	9	7	69	5	7	70	19	13	70	8	13
69	9	7	69	6	7	70	20	13	70	9	13
69	10	7	69	6	7	70	21	13	70	9	13
69	10	7	69	8	7	70	21	13	70	10	13
69	12	7	69	8	7	70	22	13	70	10	13
69	13	7	70	6	13	70	22	13	70	10	13
69	2	7	70	7	13	70	22	13	70	10	13
69	2	7	70	7	13	70	22	13	70	11	13
69	2	7	70	8	13	70	23	13	70	11	13
69	2	7	70	9	13	70	24	13	70	11	13
69	3	7	70	9	13	70	24	13	70	12	13
69	3	7	70	10	13	70	25	13	70	12	13
69	3	7	70	10	13	70	25	13	70	12	13
69	3	7	70	10	13	70	25	13	70	12	13
69	3	7	70	11	13	70	28	13	70	13	13
69	3	7	70	11	13	70	35	13	70	13	13
69	3	7	70	11	13	70	36	13	70	13	13
69	3	7	70	11	13	70	4	13	70	14	13
69	3	7	70	12	13	70	5	13	70	15	13
69	3	7	70	12	13	70	5	13	70	15	13
69	3	7	70	13	13	70	5	13	70	15	13
69	3	7	70	13	13	70	5	13	70	18	13
69	3	7	70	13	13	70	5	13	70	19	13
69	4	7	70	14	13	70	6	13	70	22	13
69	4	7	70	15	13	70	6	13	70	1	5
69	4	7	70	15	13	70	6	13	70	2	5
69	4	7	70	15	13	70	6	13	70	2	5
69	4	7	70	15	13	70	7	13	70	2	5
69	4	7	70	15	13	70	7	13	70	2	5
69	4	7	70	16	13	70	7	13	70	2	5
69	5	7	70	16	13	70	7	13	70	2	5
69	5	7	70	16	13	70	7	13	70	3	5
69	5	7	70	17	13	70	7	13	70	3	5
69	5	7	70	17	13	70	8	13	70	3	5
69	5	7	70	17	13	70	8	13	70	3	5
69	5	7	70	17	13	70	8	13	70	3	5
69	5	7	70	17	13	70	8	13	70	3	5
69	5	7	70	18	13	70	8	13	70	3	5
69	5	7	70	18	13	70	8	13	70	3	5

Table C.2. FRACTURE SPACING DATA continued

Site ID	FS*	BT†	Site ID	FS*	BT†	Site ID	FS*	BT†	Site ID	FS*	BT†
70	3	5	70	4	5	71	14	ND	72	60	107
70	3	5	70	4	5	71	17	ND	72	67	107
70	3	5	70	4	5	71	18	ND	72	70	107
70	3	5	70	4	5	71	19	ND	72	71	107
70	3	5	70	4	5	71	20	ND	72	80	107
70	4	5	70	4	5	71	20	ND	72	83	107
70	4	5	70	4	5	71	20	ND	72	9	107
70	4	5	70	4	5	71	32	ND	72	11	107
70	4	5	70	4	5	71	33	ND	72	12	107
70	4	5	70	5	5	71	36	ND	72	17	107
70	5	5	70	5	5	71	38	ND	72	29	107
70	5	5	71	31	67	71	43	ND	72	30	107
70	5	5	71	40	67	71	43	ND	72	31	107
70	5	5	71	41	67	71	47	ND	72	32	107
70	5	5	71	42	67	71	49	ND	72	54	107
70	5	5	71	54	67	71	53	ND	72	60	107
70	6	5	71	57	67	71	53	ND	72	63	107
70	1	5	71	60	67	71	76	ND	72	65	107
70	2	5	71	63	67	72	13	107	72	66	107
70	2	5	71	67	67	72	18	107	72	66	107
70	2	5	71	70	67	72	19	107	72	67	107
70	2	5	71	141	67	72	20	107	72	69	107
70	3	5	71	11	67	72	22	107	72	71	107
70	3	5	71	15	67	72	25	107	72	75	107
70	3	5	71	15	67	72	33	107	72	77	107
70	3	5	71	21	67	72	33	107	72	85	107
70	3	5	71	23	67	72	33	107	72	85	107
70	3	5	71	24	67	72	34	107	72	86	107
70	3	5	71	25	67	72	35	107	72	93	107
70	3	5	71	25	67	72	37	107	72	120	107
70	3	5	71	27	67	72	38	107	72	134	107
70	3	5	71	28	67	72	38	107	72	139	107
70	3	5	71	29	67	72	40	107	72	139	107
70	3	5	71	29	67	72	41	107	72	141	107
70	3	5	71	30	67	72	42	107	72	144	107
70	3	5	71	31	67	72	43	107	72	147	107
70	3	5	71	31	67	72	43	107	72	154	107
70	3	5	71	39	67	72	43	107	72	13	85
70	3	5	71	44	67	72	44	107	72	15	85
70	3	5	71	44	67	72	46	107	72	31	85
70	3	5	71	46	67	72	49	107	72	32	85
70	4	5	71	13	ND	72	53	107	72	33	85

Table C.2. FRACTURE SPACING DATA continued

Site ID	FS*	BT†	Site ID	FS*	BT†	Site ID	FS*	BT†	Site ID	FS*	BT†
72	33	85	73	38	32	73	12	5	73	6	5
72	36	85	73	38	32	73	13	5	73	6	5
72	36	85	73	38	32	73	14	5	73	6	5
72	36	85	73	39	32	73	14	5	73	7	5
72	40	85	73	40	32	73	15	5	73	7	5
72	40	85	73	40	32	73	15	5	73	7	5
72	41	85	73	42	32	73	16	5	73	7	5
72	43	85	73	43	32	73	16	5	73	7	5
72	43	85	73	45	32	73	16	5	73	8	5
72	46	85	73	48	32	73	18	5	73	8	5
72	47	85	73	50	32	73	18	5	73	8	5
72	49	85	73	60	32	73	19	5	73	8	5
72	51	85	73	13	32	73	20	5	73	8	5
72	52	85	73	13	32	73	22	5	73	8	5
72	56	85	73	13	32	73	26	5	73	8	5
72	57	85	73	14	32	73	27	5	73	8	5
72	60	85	73	14	32	73	30	5	73	8	5
72	62	85	73	16	32	73	34	5	73	9	5
72	62	85	73	16	32	73	35	5	73	10	5
72	40	85	73	16	32	73	35	5	73	10	5
72	40	85	73	19	32	73	36	5	73	11	5
72	44	85	73	21	32	73	42	5	73	11	5
72	46	85	73	21	32	73	44	5	73	11	5
72	55	85	73	22	32	73	50	5	73	12	5
72	62	85	73	22	32	73	2	5	73	12	5
72	64	85	73	22	32	73	3	5	73	12	5
72	67	85	73	23	32	73	3	5	73	13	5
72	79	85	73	25	32	73	3	5	73	13	5
72	87	85	73	35	32	73	3	5	73	20	5
72	101	85	73	37	32	73	3	5	74	19	73
72	105	85	73	42	32	73	3	5	74	19	73
72	110	85	73	46	32	73	3	5	74	21	73
72	118	85	73	47	32	73	3	5	74	21	73
72	118	85	73	5	5	73	4	5	74	23	73
72	126	85	73	8	5	73	4	5	74	25	73
73	24	32	73	9	5	73	4	5	74	28	73
73	28	32	73	10	5	73	4	5	74	29	73
73	28	32	73	11	5	73	4	5	74	30	73
73	29	32	73	11	5	73	5	5	74	32	73
73	32	32	73	11	5	73	5	5	74	33	73
73	35	32	73	11	5	73	5	5	74	36	73
73	35	32	73	12	5	73	5	5	74	36	73

Table C.2. FRACTURE SPACING DATA continued

Site ID	FS*	BT†	Site ID	FS*	BT†	Site ID	FS*	BT†	Site ID	FS*	BT†
74	46	73	74	89	73	75	38	ND	76	41	166
74	49	73	74	95	73	75	43	ND	76	43	166
74	49	73	75	28	30	75	44	ND	76	47	166
74	52	73	75	35	30	75	47	ND	76	48	166
74	55	73	75	69	30	75	66	ND	76	50	166
74	56	73	75	80	30	75	124	ND	76	84	166
74	58	73	75	81	30	75	12	ND	76	92	166
74	60	73	75	84	30	75	14	ND	76	156	166
74	62	73	75	90	30	75	17	ND	76	158	166
74	66	73	75	98	30	75	18	ND	77	53	120
74	70	73	75	113	30	75	20	ND	77	56	120
74	71	73	75	7	30	75	20	ND	77	68	120
74	71	73	75	11	30	75	23	ND	77	74	120
74	72	73	75	14	30	75	26	ND	77	106	120
74	74	73	75	14	30	75	26	ND	77	109	120
74	78	73	75	17	30	75	28	ND	77	110	120
74	79	73	75	17	30	75	29	ND	77	132	120
74	83	73	75	17	30	75	32	ND	77	153	120
74	8	73	75	18	30	75	32	ND	77	157	120
74	10	73	75	18	30	75	34	ND	77	198	120
74	17	73	75	19	30	75	35	ND	77	16	120
74	17	73	75	20	30	75	36	ND	77	18	120
74	19	73	75	23	30	75	39	ND	77	23	120
74	21	73	75	24	30	75	40	ND	77	23	120
74	21	73	75	25	30	75	45	ND	77	25	120
74	24	73	75	25	30	75	52	ND	77	29	120
74	32	73	75	27	30	76	25	166	77	33	120
74	32	73	75	27	30	76	37	166	77	34	120
74	32	73	75	28	30	76	44	166	77	35	120
74	35	73	75	29	30	76	47	166	77	44	120
74	36	73	75	29	30	76	47	166	77	45	120
74	38	73	75	30	30	76	64	166	77	55	120
74	40	73	75	32	30	76	79	166	77	57	120
74	41	73	75	34	30	76	79	166	77	65	120
74	45	73	75	34	30	76	80	166	77	99	120
74	51	73	75	34	30	76	90	166	77	103	120
74	57	73	75	46	30	76	94	166	77	120	120
74	61	73	75	21	ND	76	109	166	77	122	120
74	80	73	75	24	ND	76	112	166	77	124	120
74	81	73	75	27	ND	76	30	166	78	50	285
74	82	73	75	31	ND	76	35	166	78	70	285
74	87	73	75	34	ND	76	37	166	78	81	285

Table C.2. FRACTURE SPACING DATA continued

Site ID	FS*	BT†	Site ID	FS*	BT†	Site ID	FS*	BT†	Site ID	FS*	BT†
78	93	285	79	5	ND	79	14	ND	80	56	80
78	107	285	79	7	ND	79	14	ND	80	68	80
78	108	285	79	7	ND	79	14	ND	80	76	80
78	113	285	79	8	ND	79	14	ND	80	76	80
78	124	285	79	9	ND	79	17	ND	80	76	80
78	130	285	79	9	ND	79	17	ND	80	78	80
78	137	285	79	10	ND	79	18	ND	80	78	80
78	149	285	79	13	ND	79	19	ND	80	81	80
78	149	285	79	13	ND	79	19	ND	80	81	80
78	154	285	79	14	ND	79	21	ND	80	82	80
78	155	285	79	15	ND	79	21	ND	80	83	80
78	156	285	79	15	ND	79	21	ND	80	89	80
78	166	285	79	15	ND	79	22	ND	80	93	80
78	167	285	79	16	ND	79	22	ND	80	95	80
78	169	285	79	17	ND	79	22	ND	80	98	80
78	172	285	79	17	ND	79	23	ND	80	100	80
78	199	285	79	18	ND	79	23	ND	80	112	80
78	240	285	79	18	ND	79	24	ND	80	116	80
78	254	285	79	19	ND	79	26	ND	80	116	80
78	295	285	79	20	ND	79	27	ND	80	120	80
78	37	285	79	21	ND	79	27	ND	80	127	80
78	41	285	79	21	ND	79	28	ND	80	131	80
78	42	285	79	21	ND	79	28	ND	80	145	80
78	44	285	79	21	ND	79	32	ND	80	145	80
78	52	285	79	23	ND	79	33	ND	80	146	80
78	53	285	79	26	ND	79	37	ND	80	150	80
78	60	285	79	30	ND	79	37	ND	80	151	80
78	67	285	79	35	ND	79	44	ND	80	156	80
78	75	285	79	37	ND	79	45	ND	80	156	80
78	82	285	79	41	ND	80	34	80	80	158	80
78	84	285	79	46	ND	80	38	80	80	159	80
78	112	285	79	8	ND	80	42	80	80	160	80
78	116	285	79	8	ND	80	64	80	80	161	80
78	118	285	79	8	ND	80	66	80	80	161	80
78	129	285	79	9	ND	80	67	80	80	180	80
78	146	285	79	10	ND	80	72	80	80	183	80
78	156	285	79	10	ND	80	73	80	80	183	80
78	157	285	79	10	ND	80	77	80	80	190	80
78	158	285	79	11	ND	80	91	80	80	192	80
78	291	285	79	12	ND	80	92	80	80	19	80
78	314	285	79	12	ND	80	97	80	80	25	80
78	339	285	79	13	ND	80	52	80	80	31	80

Table C.2. FRACTURE SPACING DATA continued

Site ID	FS*	BT†	Site ID	FS*	BT†	Site ID	FS*	BT†	Site ID	FS*	BT†
80	31	80	80	145	80	81	49	90	81	70	90
80	16	80	80	154	80	81	50	90	81	71	90
80	18	80	80	154	80	81	53	90	81	80	90
80	19	80	81	45	90	81	53	90	81	81	90
80	20	80	81	48	90	81	54	90	81	82	90
80	25	80	81	53	90	81	55	90	81	87	90
80	32	80	81	59	90	81	59	90	81	123	90
80	56	80	81	62	90	81	61	90	81	159	90
80	59	80	81	79	90	81	61	90	81	172	90
80	59	80	81	85	90	81	64	90	81	173	90
80	63	80	81	86	90	81	68	90	81	181	90
80	31	80	81	89	90	81	69	90	81	182	90
80	33	80	81	94	90	81	69	90	81	12	90
80	33	80	81	98	90	81	70	90	81	15	90
80	37	80	81	105	90	81	73	90	81	24	90
80	39	80	81	105	90	81	78	90	81	29	90
80	39	80	81	107	90	81	82	90	81	30	90
80	40	80	81	109	90	81	86	90	81	30	90
80	40	80	81	110	90	81	87	90	81	31	90
80	40	80	81	110	90	81	88	90	81	32	90
80	41	80	81	116	90	81	88	90	81	33	90
80	48	80	81	116	90	81	94	90	81	37	90
80	48	80	81	118	90	81	100	90	81	39	90
80	48	80	81	121	90	81	117	90	81	40	90
80	54	80	81	132	90	81	121	90	81	42	90
80	54	80	81	137	90	81	129	90	81	47	90
80	60	80	81	145	90	81	138	90	81	48	90
80	67	80	81	148	90	81	153	90	81	49	90
80	69	80	81	150	90	81	13	90	81	49	90
80	73	80	81	154	90	81	15	90	81	57	90
80	75	80	81	156	90	81	27	90	81	63	90
80	79	80	81	159	90	81	27	90	81	65	90
80	81	80	81	170	90	81	31	90	81	74	90
80	83	80	81	171	90	81	36	90	81	79	90
80	89	80	81	172	90	81	36	90	81	80	90
80	93	80	81	178	90	81	36	90	81	124	90
80	96	80	81	200	90	81	37	90	81	129	90
80	100	80	81	213	90	81	46	90	81	150	90
80	112	80	81	12	90	81	48	90	82	9	20
80	114	80	81	36	90	81	55	90	82	12	20
80	123	80	81	41	90	81	59	90	82	13	20
80	131	80	81	46	90	81	63	90	82	14	20

Table C.2. FRACTURE SPACING DATA continued

Site ID	FS*	BT†	Site ID	FS*	BT†	Site ID	FS*	BT†	Site ID	FS*	BT†
82	15	20	82	10	20	82	33	20	82	47	20
82	18	20	82	10	20	82	34	20	82	47	20
82	18	20	82	10	20	82	36	20	82	47	20
82	19	20	82	10	20	82	36	20	82	50	20
82	19	20	82	11	20	82	36	20	82	52	20
82	20	20	82	12	20	82	37	20	82	58	20
82	21	20	82	13	20	82	38	20	83	13	ND
82	22	20	82	13	20	82	39	20	83	13	ND
82	22	20	82	14	20	82	41	20	83	18	ND
82	23	20	82	14	20	82	43	20	83	21	ND
82	23	20	82	15	20	82	44	20	83	22	ND
82	26	20	82	16	20	82	46	20	83	23	ND
82	26	20	82	18	20	82	48	20	83	25	ND
82	29	20	82	18	20	82	52	20	83	25	ND
82	29	20	82	18	20	82	57	20	83	26	ND
82	30	20	82	19	20	82	62	20	83	30	ND
82	30	20	82	19	20	82	64	20	83	31	ND
82	33	20	82	21	20	82	65	20	83	32	ND
82	36	20	82	22	20	82	77	20	83	33	ND
82	36	20	82	23	20	82	8	20	83	38	ND
82	40	20	82	32	20	82	9	20	83	39	ND
82	41	20	82	45	20	82	10	20	83	44	ND
82	44	20	82	8	20	82	11	20	83	44	ND
82	44	20	82	12	20	82	11	20	83	48	ND
82	44	20	82	12	20	82	11	20	83	50	ND
82	44	20	82	17	20	82	12	20	83	62	ND
82	47	20	82	17	20	82	13	20	83	70	ND
82	48	20	82	18	20	82	15	20	83	71	ND
82	50	20	82	18	20	82	16	20	83	93	ND
82	50	20	82	19	20	82	17	20	83	99	ND
82	56	20	82	21	20	82	18	20	83	106	ND
82	60	20	82	22	20	82	23	20	83	114	ND
82	84	20	82	25	20	82	24	20	83	123	ND
82	6	20	82	25	20	82	25	20	83	127	ND
82	7	20	82	26	20	82	25	20	83	131	ND
82	7	20	82	27	20	82	25	20	83	134	ND
82	7	20	82	28	20	82	30	20	83	137	ND
82	8	20	82	30	20	82	33	20	83	140	ND
82	8	20	82	31	20	82	34	20	83	164	ND
82	8	20	82	31	20	82	35	20	83	14	ND
82	9	20	82	31	20	82	36	20	83	19	ND
82	9	20	82	33	20	82	46	20	83	27	ND

Table C.2. FRACTURE SPACING DATA continued

Site ID	FS*	BT[†]	Site ID	FS*	BT[†]	Site ID	FS*	BT[†]	Site ID	FS*	BT[†]
83	27	ND	84	64	20	84	47	20	84	6	25
83	31	ND	84	80	20	84	48	20	84	7	25
83	32	ND	84	83	20	84	8	25	84	7	25
83	38	ND	84	99	20	84	9	25	84	8	25
83	41	ND	84	117	20	84	9	25	84	9	25
83	46	ND	84	118	20	84	10	25	84	10	25
83	52	ND	84	142	20	84	14	25	84	10	25
83	56	ND	84	5	20	84	14	25	84	10	25
83	66	ND	84	9	20	84	20	25	84	11	25
83	77	ND	84	9	20	84	20	25	84	11	25
83	89	ND	84	9	20	84	21	25	84	12	25
83	107	ND	84	11	20	84	22	25	84	12	25
83	229	ND	84	11	20	84	23	25	84	13	25
83	236	ND	84	11	20	84	25	25	84	14	25
83	327	ND	84	11	20	84	26	25	84	14	25
83	332	ND	84	11	20	84	27	25	84	14	25
83	439	ND	84	11	20	84	27	25	84	15	25
84	9	20	84	12	20	84	28	25	84	15	25
84	13	20	84	14	20	84	29	25	84	16	25
84	13	20	84	14	20	84	34	25	84	16	25
84	16	20	84	15	20	84	40	25	84	16	25
84	19	20	84	15	20	84	40	25	84	17	25
84	27	20	84	16	20	84	42	25	84	17	25
84	30	20	84	19	20	84	42	25	84	18	25
84	31	20	84	19	20	84	43	25	84	19	25
84	34	20	84	21	20	84	49	25	84	20	25
84	39	20	84	21	20	84	49	25	84	20	25
84	39	20	84	22	20	84	71	25	84	22	25
84	44	20	84	27	20	84	96	25	84	22	25
84	44	20	84	28	20	84	100	25	84	23	25
84	44	20	84	29	20	84	103	25	84	26	25
84	50	20	84	29	20	84	119	25	84	39	25
84	53	20	84	30	20	84	119	25	84	39	25
84	56	20	84	33	20	84	5	25			

Note: This table contains fracture spacings measured from digital images calibrated to scale.
The symbol "ND" indicates no data for records in the bed thickness field for either non-sedimentary
rocks or outcrops where bed thicknesses were not obtained.

*Fracture spacing (cm) normal to major joint/fracture sets or foliations.

[†]Bed thickness (cm) of sedimentary rocks.

Appendix D. Selby Rock-Mass Strength (RMS) Data

The following appendix contains rock-strength characteristics associated with Selby RMS, organized according to the sample site it was collected at. These data include rankings of intact-rock strength, fracture spacing, fracture orientation, fracture continuity, fracture width, weathering, groundwater outflow, and the overall Selby RMS score or index.

Table D.1. SELBY ROCK-MASS STRENGTH (RMS) DATA

Site ID	Intact-rock strength[*]	Fractures				Weathering[††]	Ground water[§§]	RMS score[##]
		Spacing[†]	Orientation[§]	Continuity[#]	Width[**]			
1	5	28	14	5	5	7	6	70
2	14	21	14	5	5	7	6	72
3	5	21	14	5	5	9	6	65
4	14	21	14	5	5	9	6	74
5	14	21	14	5	5	9	6	74
6	10	21	14	5	4	7	6	67
7	5	21	14	5	5	7	5	62
8	14	21	14	5	4	5	6	69
9	14	15	14	5	4	5	6	63
10	14	21	14	5	4	5	6	69
11	14	28	14	5	4	7	6	78
12	10	15	14	5	5	5	6	60
13	10	28	14	5	5	5	5	72
14	14	21	14	5	5	9	5	73
15	14	28	14	5	5	5	5	76
16	10	21	14	5	5	9	6	70
17	10	21	14	5	5	9	6	70
18	5	30	14	5	5	7	6	72
19	18	21	14	5	5	7	6	76
20	18	21	14	5	5	7	4	74
21	18	21	14	5	5	7	5	75
22	18	21	14	5	5	7	6	76
23	18	15	14	5	5	9	6	72
24	18	21	14	5	5	9	6	78
25	18	21	14	5	5	7	6	76
26	18	30	14	5	5	7	6	85
27	20	21	14	5	5	7	5	77
28	14	21	14	5	5	7	5	71
29	18	21	14	5	5	9	6	78
30	14	21	14	5	5	7	6	72
31	18	28	14	5	5	7	6	83
32	5	15	14	5	5	5	5	54
33	5	21	14	5	5	5	6	61
34	10	21	14	5	5	7	5	67
35	10	21	14	5	5	7	6	68
36	14	21	14	5	5	7	5	71
37	5	15	14	5	5	5	5	54
38	18	15	14	5	5	9	6	72

Table C.2. SELBY ROCK-MASS STRENGTH (RMS) DATA continued

Site ID	Intact-rock strength[*]	Fractures				Weathering[††]	Ground water[§§]	RMS score[##]
		Spacing[†]	Orientation[§]	Continuity[#]	Width**			
39	20	15	14	5	5	9	6	74
40	20	21	14	5	5	9	6	80
41	18	21	14	5	5	9	6	78
42	20	21	14	5	5	9	6	80
43	18	21	14	5	5	9	5	77
44	18	21	14	5	5	9	5	77
45	18	21	14	5	5	9	6	78
46	20	21	14	5	5	7	6	78
47	20	21	14	5	5	7	6	78
48	20	21	14	5	5	9	6	80
49	18	15	14	5	5	9	6	72
50	18	21	14	5	5	9	6	78
51	18	21	14	5	5	9	6	78
52	20	21	14	5	5	9	6	80
53	18	21	14	5	5	9	6	78
54	18	15	14	5	5	9	6	72
55	20	21	14	5	5	7	6	78
56	20	21	14	5	5	9	6	80
57	14	15	14	5	5	7	5	65
58	18	21	14	5	5	7	5	75
59	14	15	14	5	5	5	4	62
60	18	15	14	5	5	5	5	67
61	18	21	14	5	5	9	6	78
62	18	21	14	5	5	9	6	78
63	10	21	14	5	5	7	6	68
64	18	21	14	5	5	9	6	78
65	18	21	14	5	5	9	6	78
66	10	21	14	5	5	5	6	66
67	5	15	14	5	5	5	6	55
68	14	21	14	5	5	5	6	70
69	5	15	14	5	5	5	6	55
70	5	15	14	5	5	5	6	55
71	18	21	14	5	5	7	6	76
72	18	21	14	5	5	9	6	78
73	14	15	14	5	5	5	6	64
74	18	21	14	5	5	7	6	76
75	14	21	14	5	5	7	6	72
76	18	21	14	5	5	7	6	76
77	10	21	14	5	5	5	6	66
78	14	28	14	5	5	9	6	81
79	14	15	14	5	5	5	5	63

Table C.2. SELBY ROCK-MASS STRENGTH (RMS) DATA continued

Site ID	Intact-rock strength[*]	Fractures				Weathering[††]	Ground water[§§]	RMS score[##]
		Spacing[†]	Orientation[§]	Continuity[#]	Width**			
80	18	21	14	5	5	9	6	78
81	18	21	14	5	5	7	5	75
82	18	15	14	5	5	9	6	72
83	18	21	14	5	5	9	6	78
84	14	21	14	5	5	7	6	72

Note: Individual Selby RMS parameter values are unitless rankings according to Selby (1993).

*Intact-rock strength (% rebound) from Schmidt hammer: 100-60 (20), 60-50 (18), 50-40 (14), 40-35 (10), and 35-10 (5).

[†]Fracture spacing: >300cm (30), 300-100cm (28), 100-30cm (21), 30-5cm (15), and <5cm (8).

[§]Fracture orientation: very favorable (20), favorable (18), fair (14), unfavorable (9), and very unfavorable (5).

[#]Fracture continuity: none (7), few (6), continuous with no infill (5), continous with thin infill (4), and continous with thick infill (1).

**Fracture width: <0.01cm (7), 0.01-0.1cm (6), 0.1-0.5cm (5), 0.5-2cm (4), and >2cm (2).

[††]Weathering: unweathered (10), slightly (9), moderately (7), highly (5), and completely (3).

[§§]Groundwater outflow: none (6), trace (5), slight (4), moderate (3), and great (1).

[##]RMS score calculated as the sum of the ranks of the 7 parameters.

Appendix E. Hydraulic Data

The following appendix contains the hydraulic data measured and generated every 0.1 river miles. These data include water surface elevation, channel gradient, width, and unit stream power, organized by river mile.

Table E.1. HYRAULIC DATA

RM*	$Z^\dagger$	$S^\S$	$w^\#$	Ω^{**}	RM*	$Z^\dagger$	$S^\S$	$w^\#$	Ω^{**}	RM*	$Z^\dagger$	$S^\S$	$w^\#$	Ω^{**}
-172.6	1048.3	0.0004	40	20	-166.7	1044.3	0.0004	180	4	-160.8	1040.8	0.0003	132	4
-172.5	1048.2	0.0004	42	19	-166.6	1044.2	0.0004	193	4	-160.7	1040.8	0.0003	157	4
-172.4	1048.1	0.0004	41	19	-166.5	1044.1	0.0004	167	5	-160.6	1040.7	0.0003	175	3
-172.3	1048.1	0.0004	47	17	-166.4	1044.1	0.0004	157	5	-160.5	1040.7	0.0003	77	8
-172.2	1048.0	0.0004	64	12	-166.3	1044.0	0.0004	173	5	-160.4	1040.6	0.0003	54	11
-172.1	1047.9	0.0004	51	15	-166.2	1043.9	0.0004	190	4	-160.3	1040.6	0.0003	60	10
-172.0	1047.9	0.0004	61	13	-166.1	1043.9	0.0004	196	4	-160.2	1040.5	0.0003	65	9
-171.9	1047.8	0.0004	103	8	-166.0	1043.8	0.0004	222	4	-160.1	1040.5	0.0003	74	8
-171.8	1047.7	0.0004	103	8	-165.9	1043.7	0.0004	221	4	-160.0	1040.4	0.0003	101	6
-171.7	1047.6	0.0004	91	9	-165.8	1043.7	0.0004	210	4	-159.9	1040.4	0.0003	78	7
-171.6	1047.6	0.0004	106	7	-165.7	1043.6	0.0004	214	4	-159.8	1040.3	0.0003	71	8
-171.5	1047.5	0.0004	166	5	-165.6	1043.5	0.0004	225	3	-159.7	1040.3	0.0003	76	8
-171.4	1047.4	0.0004	63	12	-165.5	1043.5	0.0004	172	5	-159.6	1040.2	0.0003	104	6
-171.3	1047.4	0.0004	108	7	-165.4	1043.4	0.0004	121	6	-159.5	1040.2	0.0003	143	4
-171.2	1047.3	0.0004	134	6	-165.3	1043.3	0.0004	231	3	-159.4	1040.1	0.0003	130	4
-171.1	1047.2	0.0004	133	6	-165.2	1043.3	0.0004	179	4	-159.3	1040.1	0.0003	125	5
-171.0	1047.2	0.0004	119	7	-165.1	1043.2	0.0004	143	5	-159.2	1040.0	0.0003	127	5
-170.9	1047.1	0.0004	111	7	-165.0	1043.1	0.0004	139	6	-159.1	1040.0	0.0003	87	7
-170.8	1047.0	0.0004	166	5	-164.9	1043.1	0.0004	165	5	-159.0	1039.9	0.0003	143	4
-170.7	1047.0	0.0004	178	4	-164.8	1043.0	0.0004	167	5	-158.9	1039.9	0.0003	144	4
-170.6	1046.9	0.0004	176	4	-164.7	1042.9	0.0004	165	5	-158.8	1039.8	0.0003	125	5
-170.5	1046.8	0.0004	166	5	-164.6	1042.9	0.0004	149	5	-158.7	1039.8	0.0003	114	5
-170.4	1046.8	0.0004	100	8	-164.5	1042.8	0.0004	157	5	-158.6	1039.7	0.0003	117	5
-170.3	1046.7	0.0004	106	7	-164.4	1042.7	0.0004	178	4	-158.5	1039.7	0.0003	180	3
-170.2	1046.6	0.0004	161	5	-164.3	1042.7	0.0004	233	3	-158.4	1039.6	0.0003	282	2
-170.1	1046.6	0.0004	178	4	-164.2	1042.6	0.0004	158	5	-158.3	1039.6	0.0003	214	3
-170.0	1046.5	0.0004	208	4	-164.1	1042.5	0.0004	73	11	-158.2	1039.5	0.0003	280	2
-169.9	1046.4	0.0004	221	4	-164.0	1042.5	0.0004	101	7	-158.1	1039.5	0.0003	142	4
-169.8	1046.4	0.0004	143	5	-163.9	1042.4	0.0003	122	5	-158.0	1039.4	0.0003	118	5
-169.7	1046.3	0.0004	103	8	-163.8	1042.4	0.0003	126	5	-157.9	1039.4	0.0003	99	6
-169.6	1046.2	0.0004	81	10	-163.7	1042.3	0.0003	153	4	-157.8	1039.3	0.0003	77	8
-169.5	1046.2	0.0004	112	7	-163.6	1042.3	0.0003	158	4	-157.7	1039.3	0.0003	87	7
-169.4	1046.1	0.0004	95	8	-163.5	1042.2	0.0003	154	4	-157.6	1039.2	0.0003	123	5
-169.3	1046.0	0.0004	110	7	-163.4	1042.2	0.0003	130	4	-157.5	1039.2	0.0003	137	4
-169.2	1046.0	0.0004	96	8	-163.3	1042.1	0.0003	79	7	-157.4	1039.1	0.0003	122	5
-169.1	1045.9	0.0004	80	10	-163.2	1042.0	0.0003	77	8	-157.3	1039.1	0.0003	93	6
-169.0	1045.8	0.0004	60	13	-163.1	1042.0	0.0003	87	7	-157.2	1039.0	0.0003	113	5
-168.9	1045.8	0.0004	97	8	-163.0	1041.9	0.0003	110	5	-157.1	1039.0	0.0003	146	4
-168.8	1045.7	0.0004	118	7	-162.9	1041.9	0.0003	139	4	-157.0	1038.9	0.0003	126	5
-168.7	1045.6	0.0004	176	4	-162.8	1041.8	0.0003	156	4	-156.9	1038.9	0.0003	97	6
-168.6	1045.6	0.0004	174	4	-162.7	1041.8	0.0003	95	6	-156.8	1038.8	0.0003	113	5
-168.5	1045.5	0.0004	134	6	-162.6	1041.7	0.0003	95	6	-156.7	1038.8	0.0003	120	5
-168.4	1045.4	0.0004	123	6	-162.5	1041.7	0.0003	159	4	-156.6	1038.7	0.0003	82	7
-168.3	1045.4	0.0004	87	9	-162.4	1041.6	0.0003	175	3	-156.5	1038.7	0.0003	81	7
-168.2	1045.3	0.0004	77	10	-162.3	1041.6	0.0003	104	6	-156.4	1038.6	0.0003	113	5
-168.1	1045.2	0.0004	106	7	-162.2	1041.5	0.0003	103	6	-156.3	1038.6	0.0003	155	4
-168.0	1045.2	0.0004	143	5	-162.1	1041.5	0.0003	103	6	-156.2	1038.5	0.0003	165	4
-167.9	1045.1	0.0004	142	6	-162.0	1041.4	0.0003	185	3	-156.1	1038.5	0.0003	122	5
-167.8	1045.0	0.0004	168	5	-161.9	1041.4	0.0003	104	6	-156.0	1038.4	0.0003	132	4
-167.7	1045.0	0.0004	172	5	-161.8	1041.3	0.0003	110	5	-155.9	1038.4	0.0003	224	3
-167.6	1044.9	0.0004	157	5	-161.7	1041.3	0.0003	177	3	-155.8	1038.3	0.0003	174	3
-167.5	1044.8	0.0004	186	4	-161.6	1041.2	0.0003	167	3	-155.7	1038.3	0.0003	154	4
-167.4	1044.8	0.0004	183	4	-161.5	1041.2	0.0003	129	4	-155.6	1038.2	0.0003	137	4
-167.3	1044.7	0.0004	154	5	-161.4	1041.1	0.0003	129	5	-155.5	1038.2	0.0003	122	5
-167.2	1044.6	0.0004	72	11	-161.3	1041.1	0.0003	92	6	-155.4	1038.1	0.0003	133	4
-167.1	1044.6	0.0004	132	6	-161.2	1041.0	0.0003	121	5	-155.3	1038.1	0.0003	117	5
-167.0	1044.5	0.0004	178	4	-161.1	1041.0	0.0003	95	6	-155.2	1038.0	0.0003	134	4
-166.9	1044.4	0.0004	160	5	-161.0	1040.9	0.0003	106	5	-155.1	1038.0	0.0003	162	4
-166.8	1044.3	0.0004	144	5	-160.9	1040.9	0.0003	124	5	-155.0	1037.9	0.0003	183	3

Table E.1. HYDRAULIC DATA continued

RM*	$Z^\dagger$	$S^\S$	$w^\#$	Ω^{**}	RM*	$Z^\dagger$	$S^\S$	$w^\#$	Ω^{**}	RM*	$Z^\dagger$	$S^\S$	$w^\#$	Ω^{**}
-154.9	1037.9	0.0003	185	3	-149.0	1035.2	0.0003	97	5	-143.1	1032.8	0.0002	149	3
-154.8	1037.8	0.0003	196	3	-148.9	1035.1	0.0003	109	4	-143.0	1032.7	0.0002	155	3
-154.7	1037.8	0.0003	161	4	-148.8	1035.1	0.0003	107	5	-142.9	1032.7	0.0002	152	3
-154.6	1037.7	0.0003	169	3	-148.7	1035.0	0.0003	97	5	-142.8	1032.6	0.0002	167	3
-154.5	1037.7	0.0003	177	3	-148.6	1035.0	0.0003	102	5	-142.7	1032.6	0.0002	185	2
-154.4	1037.6	0.0003	206	3	-148.5	1035.0	0.0003	118	4	-142.6	1032.6	0.0002	200	2
-154.3	1037.6	0.0003	269	2	-148.4	1034.9	0.0003	97	5	-142.5	1032.5	0.0002	235	2
-154.2	1037.5	0.0003	217	3	-148.3	1034.9	0.0003	71	7	-142.4	1032.5	0.0002	239	2
-154.1	1037.5	0.0003	139	4	-148.2	1034.8	0.0003	71	7	-142.3	1032.4	0.0002	247	2
-154.0	1037.4	0.0003	127	5	-148.1	1034.8	0.0003	68	7	-142.2	1032.4	0.0002	258	2
-153.9	1037.4	0.0003	108	5	-148.0	1034.7	0.0003	69	7	-142.1	1032.4	0.0002	230	2
-153.8	1037.3	0.0003	108	5	-147.9	1034.7	0.0003	82	6	-142.0	1032.3	0.0002	157	3
-153.7	1037.3	0.0003	193	3	-147.8	1034.7	0.0003	87	6	-141.9	1032.3	0.0002	132	3
-153.6	1037.2	0.0003	173	3	-147.7	1034.6	0.0003	146	3	-141.8	1032.3	0.0002	142	3
-153.5	1037.2	0.0003	173	3	-147.6	1034.6	0.0003	166	3	-141.7	1032.2	0.0002	169	3
-153.4	1037.1	0.0003	166	3	-147.5	1034.5	0.0003	121	4	-141.6	1032.2	0.0002	179	2
-153.3	1037.1	0.0003	168	3	-147.4	1034.5	0.0003	100	5	-141.5	1032.1	0.0002	175	3
-153.2	1037.0	0.0003	155	4	-147.3	1034.5	0.0003	110	4	-141.4	1032.1	0.0002	168	3
-153.1	1037.0	0.0003	121	5	-147.2	1034.4	0.0003	117	4	-141.3	1032.1	0.0002	132	3
-153.0	1036.9	0.0003	119	5	-147.1	1034.4	0.0003	110	4	-141.2	1032.0	0.0002	135	3
-152.9	1036.9	0.0003	111	5	-147.0	1034.3	0.0003	110	4	-141.1	1032.0	0.0002	188	2
-152.8	1036.8	0.0003	114	5	-146.9	1034.3	0.0003	113	4	-141.0	1032.0	0.0002	215	2
-152.7	1036.8	0.0003	124	5	-146.8	1034.2	0.0003	151	3	-140.9	1031.9	0.0002	237	2
-152.6	1036.7	0.0003	153	4	-146.7	1034.2	0.0003	175	3	-140.8	1031.9	0.0002	222	2
-152.5	1036.7	0.0003	148	4	-146.6	1034.2	0.0003	148	3	-140.7	1031.8	0.0002	221	2
-152.4	1036.6	0.0003	139	4	-146.5	1034.1	0.0003	145	3	-140.6	1031.8	0.0002	218	2
-152.3	1036.6	0.0003	135	4	-146.4	1034.1	0.0003	99	5	-140.5	1031.8	0.0002	151	3
-152.2	1036.5	0.0003	119	5	-146.3	1034.0	0.0003	107	4	-140.4	1031.7	0.0002	119	4
-152.1	1036.5	0.0003	120	5	-146.2	1034.0	0.0003	87	6	-140.3	1031.7	0.0002	142	3
-152.0	1036.4	0.0003	132	4	-146.1	1034.0	0.0003	122	4	-140.2	1031.7	0.0002	201	2
-151.9	1036.4	0.0003	152	4	-146.0	1033.9	0.0003	130	4	-140.1	1031.6	0.0002	236	2
-151.8	1036.3	0.0003	186	3	-145.9	1033.9	0.0003	159	3	-140.0	1031.6	0.0002	267	2
-151.7	1036.3	0.0003	200	2	-145.8	1033.8	0.0003	143	3	-139.9	1031.5	0.0002	285	1
-151.6	1036.2	0.0003	115	4	-145.7	1033.8	0.0003	156	3	-139.8	1031.5	0.0002	266	2
-151.5	1036.2	0.0003	85	6	-145.6	1033.7	0.0003	178	3	-139.7	1031.5	0.0002	98	4
-151.4	1036.2	0.0003	92	5	-145.5	1033.7	0.0003	214	2	-139.6	1031.4	0.0002	135	3
-151.3	1036.1	0.0003	93	5	-145.4	1033.7	0.0003	172	3	-139.5	1031.4	0.0002	119	4
-151.2	1036.1	0.0003	149	3	-145.3	1033.6	0.0003	147	3	-139.4	1031.4	0.0002	124	3
-151.1	1036.0	0.0003	174	3	-145.2	1033.6	0.0003	155	3	-139.3	1031.3	0.0002	169	2
-151.0	1036.0	0.0003	166	3	-145.1	1033.5	0.0003	185	3	-139.2	1031.3	0.0002	214	2
-150.9	1036.0	0.0003	133	4	-145.0	1033.5	0.0003	198	2	-139.1	1031.3	0.0002	244	2
-150.8	1035.9	0.0003	111	4	-144.9	1033.5	0.0003	171	3	-139.0	1031.2	0.0002	259	2
-150.7	1035.9	0.0003	77	6	-144.8	1033.4	0.0003	175	3	-138.9	1031.2	0.0002	282	1
-150.6	1035.8	0.0003	94	5	-144.7	1033.4	0.0003	185	3	-138.8	1031.1	0.0002	235	2
-150.5	1035.8	0.0003	131	4	-144.6	1033.3	0.0003	150	3	-138.7	1031.1	0.0002	223	2
-150.4	1035.7	0.0003	134	4	-144.5	1033.3	0.0003	148	3	-138.6	1031.1	0.0002	203	2
-150.3	1035.7	0.0003	143	3	-144.4	1033.2	0.0002	130	3	-138.5	1031.0	0.0002	186	2
-150.2	1035.7	0.0003	55	9	-144.3	1033.2	0.0002	133	3	-138.4	1031.0	0.0002	201	2
-150.1	1035.6	0.0003	61	8	-144.2	1033.2	0.0002	112	4	-138.3	1031.0	0.0002	200	2
-150.0	1035.6	0.0003	56	9	-144.1	1033.1	0.0002	100	4	-138.2	1030.9	0.0002	200	2
-149.9	1035.5	0.0003	72	7	-144.0	1033.1	0.0002	114	4	-138.1	1030.9	0.0002	224	2
-149.8	1035.5	0.0003	80	6	-143.9	1033.1	0.0002	133	3	-138.0	1030.9	0.0002	210	2
-149.7	1035.5	0.0003	75	6	-143.8	1033.0	0.0002	129	3	-137.9	1030.8	0.0002	216	2
-149.6	1035.4	0.0003	93	5	-143.7	1033.0	0.0002	127	3	-137.8	1030.8	0.0002	233	2
-149.5	1035.4	0.0003	101	5	-143.6	1032.9	0.0002	170	3	-137.7	1030.7	0.0002	264	2
-149.4	1035.3	0.0003	121	4	-143.5	1032.9	0.0002	183	2	-137.6	1030.7	0.0002	186	2
-149.3	1035.3	0.0003	137	4	-143.4	1032.9	0.0002	178	2	-137.5	1030.7	0.0002	172	2
-149.2	1035.2	0.0003	150	3	-143.3	1032.8	0.0002	134	3	-137.4	1030.6	0.0002	161	3
-149.1	1035.2	0.0003	124	4	-143.2	1032.8	0.0002	147	3	-137.3	1030.6	0.0002	155	3

Table E.1. HYDRAULIC DATA continued

RM*	$Z^\dagger$	$S^\S$	$w^\#$	Ω^{**}	RM*	$Z^\dagger$	$S^\S$	$w^\#$	Ω^{**}	RM*	$Z^\dagger$	$S^\S$	$w^\#$	Ω^{**}
-137.2	1030.6	0.0002	159	3	-131.3	1025.7	0.0006	45	23	-125.4	1022.6	0.0004	112	6
-137.1	1030.5	0.0002	213	2	-131.2	1025.6	0.0004	71	10	-125.3	1022.6	0.0004	121	6
-137.0	1030.5	0.0002	245	2	-131.1	1025.6	0.0003	71	8	-125.2	1022.5	0.0004	115	6
-136.9	1030.5	0.0002	270	2	-131.0	1025.5	0.0003	93	6	-125.1	1022.4	0.0004	123	6
-136.8	1030.4	0.0002	219	2	-130.9	1025.5	0.0003	134	4	-125.0	1022.4	0.0004	113	6
-136.7	1030.4	0.0002	224	2	-130.8	1025.4	0.0003	100	5	-124.9	1022.3	0.0004	102	7
-136.6	1030.3	0.0002	207	2	-130.7	1025.4	0.0003	110	5	-124.8	1022.2	0.0004	126	6
-136.5	1030.3	0.0002	220	2	-130.6	1025.3	0.0003	131	4	-124.7	1022.2	0.0004	139	5
-136.4	1030.3	0.0002	184	2	-130.5	1025.3	0.0003	127	4	-124.6	1022.1	0.0004	135	5
-136.3	1030.2	0.0003	172	3	-130.4	1025.3	0.0003	98	6	-124.5	1022.1	0.0004	124	6
-136.2	1030.2	0.0005	156	5	-130.3	1025.2	0.0003	129	4	-124.4	1022.0	0.0004	119	6
-136.1	1030.1	0.0005	153	6	-130.2	1025.2	0.0003	115	5	-124.3	1021.9	0.0004	147	5
-136.0	1030.0	0.0005	162	6	-130.1	1025.1	0.0003	119	5	-124.2	1021.9	0.0004	171	4
-135.9	1029.9	0.0005	195	5	-130.0	1025.1	0.0003	122	4	-124.1	1021.8	0.0004	197	4
-135.8	1029.8	0.0005	186	5	-129.9	1025.0	0.0003	133	4	-124.0	1021.7	0.0004	229	3
-135.7	1029.8	0.0005	204	5	-129.8	1025.0	0.0003	142	4	-123.9	1021.7	0.0004	229	3
-135.6	1029.7	0.0005	193	5	-129.7	1024.9	0.0003	150	4	-123.8	1021.6	0.0004	212	3
-135.5	1029.6	0.0005	184	5	-129.6	1024.9	0.0003	147	4	-123.7	1021.6	0.0004	227	3
-135.4	1029.5	0.0005	195	5	-129.5	1024.8	0.0003	167	3	-123.6	1021.5	0.0004	204	4
-135.3	1029.4	0.0005	197	5	-129.4	1024.8	0.0003	194	3	-123.5	1021.4	0.0004	221	3
-135.2	1029.4	0.0005	209	5	-129.3	1024.7	0.0003	190	3	-123.4	1021.4	0.0004	184	4
-135.1	1029.3	0.0005	196	5	-129.2	1024.7	0.0003	214	3	-123.3	1021.3	0.0004	130	6
-135.0	1029.2	0.0005	175	5	-129.1	1024.6	0.0003	193	3	-123.2	1021.3	0.0004	167	4
-134.9	1029.1	0.0005	163	6	-129.0	1024.6	0.0003	178	3	-123.1	1021.2	0.0004	176	4
-134.8	1029.0	0.0005	185	5	-128.9	1024.5	0.0003	122	4	-123.0	1021.1	0.0004	229	4
-134.7	1028.9	0.0005	204	5	-128.8	1024.5	0.0003	121	4	-122.9	1021.0	0.0007	273	5
-134.6	1028.9	0.0005	207	5	-128.7	1024.5	0.0003	134	4	-122.8	1020.9	0.0009	281	6
-134.5	1028.8	0.0005	219	4	-128.6	1024.4	0.0003	150	4	-122.7	1020.8	0.0009	188	9
-134.4	1028.7	0.0005	233	4	-128.5	1024.4	0.0003	179	3	-122.6	1020.6	0.0009	137	12
-134.3	1028.6	0.0006	281	4	-128.4	1024.3	0.0003	129	4	-122.5	1020.5	0.0009	180	9
-134.2	1028.5	0.0006	359	3	-128.3	1024.3	0.0003	95	6	-122.4	1020.3	0.0009	142	11
-134.1	1028.4	0.0006	266	4	-128.2	1024.2	0.0003	97	6	-122.3	1020.2	0.0009	126	13
-134.0	1028.3	0.0006	245	4	-128.1	1024.2	0.0003	144	4	-122.2	1020.1	0.0009	128	13
-133.9	1028.2	0.0006	189	6	-128.0	1024.1	0.0003	167	4	-122.1	1019.9	0.0009	145	11
-133.8	1028.2	0.0006	334	3	-127.9	1024.1	0.0004	181	4	-122.0	1019.8	0.0009	178	9
-133.7	1028.1	0.0006	409	3	-127.8	1024.0	0.0004	144	5	-121.9	1019.7	0.0008	219	7
-133.6	1028.0	0.0006	326	3	-127.7	1023.9	0.0004	135	5	-121.8	1019.5	0.0005	191	5
-133.5	1027.9	0.0006	293	4	-127.6	1023.9	0.0004	127	5	-121.7	1019.5	0.0003	136	4
-133.4	1027.8	0.0006	233	5	-127.5	1023.8	0.0004	107	6	-121.6	1019.4	0.0003	87	6
-133.3	1027.7	0.0006	157	7	-127.4	1023.8	0.0004	94	7	-121.5	1019.4	0.0003	90	6
-133.2	1027.6	0.0006	124	9	-127.3	1023.7	0.0004	119	6	-121.4	1019.4	0.0003	99	6
-133.1	1027.5	0.0006	159	7	-127.2	1023.7	0.0004	196	3	-121.3	1019.3	0.0003	102	5
-133.0	1027.4	0.0006	179	6	-127.1	1023.6	0.0004	233	3	-121.2	1019.3	0.0003	105	5
-132.9	1027.3	0.0006	169	6	-127.0	1023.5	0.0004	245	3	-121.1	1019.2	0.0003	106	5
-132.8	1027.2	0.0006	148	7	-126.9	1023.5	0.0004	272	2	-121.0	1019.2	0.0003	88	6
-132.7	1027.2	0.0006	126	9	-126.8	1023.4	0.0004	200	3	-120.9	1019.1	0.0003	105	5
-132.6	1027.0	0.0006	140	9	-126.7	1023.4	0.0004	188	4	-120.8	1019.1	0.0003	106	5
-132.5	1026.9	0.0006	145	8	-126.6	1023.3	0.0004	212	3	-120.7	1019.0	0.0003	120	5
-132.4	1026.8	0.0006	142	8	-126.5	1023.3	0.0004	170	4	-120.6	1019.0	0.0003	143	4
-132.3	1026.7	0.0006	170	7	-126.4	1023.2	0.0004	119	6	-120.5	1018.9	0.0003	207	3
-132.2	1026.6	0.0006	192	6	-126.3	1023.1	0.0004	60	11	-120.4	1018.9	0.0003	227	2
-132.1	1026.5	0.0006	206	6	-126.2	1023.1	0.0004	136	5	-120.3	1018.8	0.0003	153	4
-132.0	1026.4	0.0006	196	6	-126.1	1023.0	0.0004	198	3	-120.2	1018.8	0.0003	92	6
-131.9	1026.3	0.0006	172	7	-126.0	1023.0	0.0004	123	5	-120.1	1018.7	0.0003	65	8
-131.8	1026.2	0.0006	154	8	-125.9	1022.9	0.0004	94	7	-120.0	1018.7	0.0003	84	7
-131.7	1026.1	0.0006	162	7	-125.8	1022.8	0.0004	120	6	-119.9	1018.6	0.0003	88	6
-131.6	1026.0	0.0006	167	7	-125.7	1022.8	0.0004	95	7	-119.8	1018.6	0.0003	86	6
-131.5	1025.9	0.0006	190	6	-125.6	1022.7	0.0004	87	8	-119.7	1018.5	0.0003	102	5
-131.4	1025.8	0.0006	144	8	-125.5	1022.7	0.0004	174	4	-119.6	1018.5	0.0003	102	5

Table E.1. HYDRAULIC DATA continued

RM*	Z†	S§	w#	Ω**	RM*	Z†	S§	w#	Ω**	RM*	Z†	S§	w#	Ω**
-119.5	1018.5	0.0003	81	7	-113.6	1013.5	0.0008	291	5	-107.7	1007.0	0.0013	210	12
-119.4	1018.4	0.0003	75	7	-113.5	1013.4	0.0005	268	3	-107.6	1006.8	0.0013	221	11
-119.3	1018.4	0.0003	105	5	-113.4	1013.3	0.0005	207	4	-107.5	1006.6	0.0013	271	9
-119.2	1018.3	0.0003	124	4	-113.3	1013.2	0.0005	224	4	-107.4	1006.4	0.0013	275	9
-119.1	1018.3	0.0003	106	5	-113.2	1013.2	0.0005	174	5	-107.3	1006.1	0.0013	272	9
-119.0	1018.2	0.0003	101	5	-113.1	1013.1	0.0005	216	4	-107.2	1005.9	0.0011	244	8
-118.9	1018.2	0.0003	116	5	-113.0	1013.0	0.0005	218	4	-107.1	1005.8	0.0006	187	6
-118.8	1018.1	0.0003	131	4	-112.9	1013.0	0.0005	201	4	-107.0	1005.7	0.0005	201	4
-118.7	1018.1	0.0003	142	4	-112.8	1012.9	0.0005	203	4	-106.9	1005.6	0.0005	172	5
-118.6	1018.0	0.0003	140	4	-112.7	1012.8	0.0005	198	4	-106.8	1005.6	0.0005	186	5
-118.5	1018.0	0.0004	153	4	-112.6	1012.7	0.0005	218	4	-106.7	1005.5	0.0005	169	5
-118.4	1017.9	0.0004	157	4	-112.5	1012.7	0.0005	217	4	-106.6	1005.4	0.0005	177	5
-118.3	1017.9	0.0004	168	4	-112.4	1012.6	0.0005	220	4	-106.5	1005.4	0.0005	139	6
-118.2	1017.8	0.0004	186	4	-112.3	1012.5	0.0005	243	4	-106.4	1005.3	0.0005	78	11
-118.1	1017.7	0.0004	234	3	-112.2	1012.4	0.0005	261	3	-106.3	1005.2	0.0005	76	11
-118.0	1017.7	0.0004	146	5	-112.1	1012.4	0.0005	314	3	-106.2	1005.1	0.0005	53	16
-117.9	1017.6	0.0004	174	4	-112.0	1012.3	0.0005	218	4	-106.1	1005.1	0.0005	46	19
-117.8	1017.6	0.0004	191	3	-111.9	1012.2	0.0005	200	4	-106.0	1005.0	0.0005	73	12
-117.7	1017.5	0.0004	169	4	-111.8	1012.1	0.0005	188	5	-105.9	1004.9	0.0005	106	8
-117.6	1017.5	0.0004	169	4	-111.7	1012.1	0.0005	195	4	-105.8	1004.8	0.0005	127	7
-117.5	1017.4	0.0004	141	5	-111.6	1012.0	0.0005	200	4	-105.7	1004.8	0.0005	136	6
-117.4	1017.3	0.0004	153	4	-111.5	1011.9	0.0005	193	4	-105.6	1004.7	0.0005	137	6
-117.3	1017.3	0.0004	147	5	-111.4	1011.8	0.0005	194	4	-105.5	1004.6	0.0005	156	5
-117.2	1017.2	0.0004	110	6	-111.3	1011.8	0.0005	212	4	-105.4	1004.5	0.0005	160	5
-117.1	1017.2	0.0004	112	6	-111.2	1011.7	0.0005	251	3	-105.3	1004.5	0.0005	186	5
-117.0	1017.1	0.0004	138	5	-111.1	1011.6	0.0005	193	4	-105.2	1004.4	0.0005	172	5
-116.9	1017.0	0.0004	178	4	-111.0	1011.5	0.0005	184	5	-105.1	1004.3	0.0005	143	7
-116.8	1017.0	0.0004	172	4	-110.9	1011.5	0.0005	189	5	-105.0	1004.2	0.0006	136	8
-116.7	1016.9	0.0004	186	4	-110.8	1011.4	0.0005	270	3	-104.9	1004.1	0.0006	124	8
-116.6	1016.9	0.0004	225	3	-110.7	1011.3	0.0005	245	3	-104.8	1004.0	0.0006	118	9
-116.5	1016.8	0.0004	214	3	-110.6	1011.3	0.0005	196	4	-104.7	1004.0	0.0006	123	9
-116.4	1016.8	0.0004	208	3	-110.5	1011.2	0.0005	213	4	-104.6	1003.9	0.0006	94	11
-116.3	1016.7	0.0004	219	3	-110.4	1011.1	0.0005	256	3	-104.5	1003.8	0.0006	136	8
-116.2	1016.6	0.0004	247	3	-110.3	1011.0	0.0005	241	4	-104.4	1003.7	0.0006	126	8
-116.1	1016.6	0.0004	262	3	-110.2	1011.0	0.0005	250	3	-104.3	1003.6	0.0006	111	9
-116.0	1016.5	0.0004	293	3	-110.1	1010.9	0.0005	237	4	-104.2	1003.5	0.0006	106	10
-115.9	1016.4	0.0006	341	3	-110.0	1010.8	0.0005	220	4	-104.1	1003.4	0.0006	108	10
-115.8	1016.3	0.0006	349	3	-109.9	1010.7	0.0005	210	4	-104.0	1003.3	0.0006	113	9
-115.7	1016.2	0.0006	312	4	-109.8	1010.7	0.0005	261	3	-103.9	1003.2	0.0006	116	9
-115.6	1016.1	0.0006	235	5	-109.7	1010.6	0.0005	240	4	-103.8	1003.1	0.0006	103	10
-115.5	1016.0	0.0006	201	6	-109.6	1010.5	0.0005	274	3	-103.7	1003.0	0.0006	119	9
-115.4	1015.9	0.0006	146	8	-109.5	1010.4	0.0007	275	5	-103.6	1003.0	0.0006	131	8
-115.3	1015.8	0.0006	165	7	-109.4	1010.3	0.0012	272	8	-103.5	1002.9	0.0006	131	8
-115.2	1015.7	0.0006	195	6	-109.3	1010.1	0.0013	234	11	-103.4	1002.8	0.0005	141	7
-115.1	1015.6	0.0006	211	6	-109.2	1009.8	0.0013	235	11	-103.3	1002.7	0.0005	155	6
-115.0	1015.5	0.0006	223	5	-109.1	1009.6	0.0013	235	11	-103.2	1002.6	0.0005	146	6
-114.9	1015.4	0.0006	243	5	-109.0	1009.4	0.0013	229	11	-103.1	1002.5	0.0005	127	7
-114.8	1015.3	0.0006	178	7	-108.9	1009.2	0.0013	241	10	-103.0	1002.4	0.0005	166	6
-114.7	1015.2	0.0006	202	6	-108.8	1009.0	0.0013	257	9	-102.9	1002.4	0.0005	130	7
-114.6	1015.1	0.0006	210	6	-108.7	1008.8	0.0011	241	9	-102.8	1002.3	0.0005	130	7
-114.5	1015.0	0.0008	217	7	-108.6	1008.6	0.0011	231	9	-102.7	1002.2	0.0005	94	10
-114.4	1014.8	0.0010	209	9	-108.5	1008.4	0.0011	148	13	-102.6	1002.1	0.0005	72	13
-114.3	1014.7	0.0011	225	9	-108.4	1008.3	0.0011	136	14	-102.5	1002.0	0.0005	95	10
-114.2	1014.5	0.0011	242	8	-108.3	1008.1	0.0011	175	11	-102.4	1002.0	0.0005	80	12
-114.1	1014.3	0.0011	249	8	-108.2	1007.9	0.0011	173	11	-102.3	1001.9	0.0005	76	12
-114.0	1014.2	0.0011	251	8	-108.1	1007.8	0.0011	207	9	-102.2	1001.8	0.0005	107	9
-113.9	1014.0	0.0011	283	7	-108.0	1007.6	0.0011	159	12	-102.1	1001.7	0.0005	137	7
-113.8	1013.8	0.0011	272	7	-107.9	1007.4	0.0011	143	15	-102.0	1001.6	0.0005	118	8
-113.7	1013.7	0.0011	275	7	-107.8	1007.2	0.0013	184	13	-101.9	1001.5	0.0005	142	7

Table E.1. HYDRAULIC DATA continued

RM*	Z†	S§	w#	Ω**	RM*	Z†	S§	w#	Ω**	RM*	Z†	S§	w#	Ω**
-101.8	1001.5	0.0005	158	6	-95.9	998.9	0.0002	105	3	-90.0	997.0	0.0002	149	3
-101.7	1001.4	0.0005	127	7	-95.8	998.9	0.0002	92	3	-89.9	996.9	0.0002	150	3
-101.6	1001.3	0.0005	108	8	-95.7	998.9	0.0002	92	3	-89.8	996.9	0.0002	164	3
-101.5	1001.2	0.0004	94	9	-95.6	998.8	0.0002	90	3	-89.7	996.8	0.0002	157	3
-101.4	1001.2	0.0004	95	8	-95.5	998.8	0.0002	86	3	-89.6	996.8	0.0002	145	3
-101.3	1001.1	0.0004	121	6	-95.4	998.8	0.0002	86	3	-89.5	996.8	0.0002	148	3
-101.2	1001.0	0.0004	122	6	-95.3	998.8	0.0002	90	3	-89.4	996.7	0.0003	150	3
-101.1	1001.0	0.0004	100	8	-95.2	998.7	0.0002	99	3	-89.3	996.7	0.0003	120	4
-101.0	1000.9	0.0004	121	6	-95.1	998.7	0.0002	89	3	-89.2	996.6	0.0003	112	4
-100.9	1000.8	0.0004	64	12	-95.0	998.7	0.0002	107	3	-89.1	996.6	0.0003	143	3
-100.8	1000.8	0.0004	67	12	-94.9	998.7	0.0002	129	2	-89.0	996.5	0.0003	114	4
-100.7	1000.7	0.0004	87	9	-94.8	998.6	0.0002	108	3	-88.9	996.5	0.0003	80	6
-100.6	1000.6	0.0004	110	7	-94.7	998.6	0.0002	117	2	-88.8	996.5	0.0003	139	4
-100.5	1000.6	0.0004	117	7	-94.6	998.6	0.0002	132	2	-88.7	996.4	0.0003	149	3
-100.4	1000.5	0.0004	122	6	-94.5	998.6	0.0002	152	2	-88.6	996.4	0.0003	138	4
-100.3	1000.4	0.0004	108	7	-94.4	998.5	0.0002	117	2	-88.5	996.3	0.0003	153	3
-100.2	1000.4	0.0004	105	7	-94.3	998.5	0.0002	116	2	-88.4	996.3	0.0003	145	3
-100.1	1000.3	0.0004	122	6	-94.2	998.5	0.0002	104	3	-88.3	996.3	0.0003	156	3
-100.0	1000.2	0.0004	146	5	-94.1	998.5	0.0002	102	3	-88.2	996.2	0.0003	138	4
-99.9	1000.1	0.0004	116	7	-94.0	998.4	0.0002	100	3	-88.1	996.2	0.0003	114	4
-99.8	1000.1	0.0004	96	8	-93.9	998.4	0.0002	113	3	-88.0	996.1	0.0003	161	3
-99.7	1000.0	0.0004	127	6	-93.8	998.4	0.0002	65	4	-87.9	996.1	0.0003	181	3
-99.6	999.9	0.0004	118	7	-93.7	998.4	0.0002	74	4	-87.8	996.0	0.0003	155	3
-99.5	999.9	0.0004	141	6	-93.6	998.3	0.0002	125	2	-87.7	996.0	0.0003	147	3
-99.4	999.8	0.0004	129	6	-93.5	998.3	0.0002	146	2	-87.6	996.0	0.0003	142	3
-99.3	999.7	0.0003	106	5	-93.4	998.3	0.0002	162	2	-87.5	995.9	0.0003	158	3
-99.2	999.7	0.0002	74	4	-93.3	998.3	0.0002	157	2	-87.4	995.9	0.0003	159	3
-99.1	999.7	0.0002	84	3	-93.2	998.2	0.0002	128	3	-87.3	995.8	0.0003	159	3
-99.0	999.7	0.0002	98	3	-93.1	998.2	0.0002	102	4	-87.2	995.8	0.0003	190	3
-98.9	999.6	0.0002	125	2	-93.0	998.2	0.0002	101	5	-87.1	995.7	0.0003	154	3
-98.8	999.6	0.0002	117	2	-92.9	998.1	0.0002	92	5	-87.0	995.7	0.0003	104	5
-98.7	999.6	0.0002	92	3	-92.8	998.1	0.0002	53	9	-86.9	995.7	0.0003	140	3
-98.6	999.6	0.0002	86	3	-92.7	998.0	0.0002	43	11	-86.8	995.6	0.0003	143	3
-98.5	999.5	0.0002	121	2	-92.6	998.0	0.0002	53	9	-86.7	995.6	0.0003	110	4
-98.4	999.5	0.0002	86	3	-92.5	998.0	0.0002	61	8	-86.6	995.5	0.0003	121	4
-98.3	999.5	0.0002	73	4	-92.4	997.9	0.0002	82	6	-86.5	995.5	0.0003	105	5
-98.2	999.5	0.0002	73	4	-92.3	997.9	0.0002	88	5	-86.4	995.5	0.0003	118	4
-98.1	999.4	0.0002	78	4	-92.2	997.8	0.0002	88	5	-86.3	995.4	0.0003	134	4
-98.0	999.4	0.0002	58	5	-92.1	997.8	0.0002	58	8	-86.2	995.4	0.0003	156	3
-97.9	999.4	0.0002	88	3	-92.0	997.8	0.0002	90	5	-86.1	995.3	0.0003	163	3
-97.8	999.4	0.0002	91	3	-91.9	997.7	0.0002	100	5	-86.0	995.3	0.0003	173	3
-97.7	999.3	0.0002	75	4	-91.8	997.7	0.0002	101	5	-85.9	995.2	0.0003	165	3
-97.6	999.3	0.0002	94	3	-91.7	997.6	0.0002	122	4	-85.8	995.2	0.0003	141	3
-97.5	999.3	0.0002	92	3	-91.6	997.6	0.0002	96	5	-85.7	995.2	0.0003	109	4
-97.4	999.3	0.0002	84	3	-91.5	997.6	0.0002	82	6	-85.6	995.1	0.0002	108	4
-97.3	999.2	0.0002	63	5	-91.4	997.5	0.0002	78	6	-85.5	995.1	0.0002	123	4
-97.2	999.2	0.0002	72	4	-91.3	997.5	0.0002	84	6	-85.4	995.0	0.0002	129	4
-97.1	999.2	0.0002	64	4	-91.2	997.4	0.0002	100	5	-85.3	995.0	0.0002	146	3
-97.0	999.2	0.0002	74	4	-91.1	997.4	0.0002	95	5	-85.2	995.0	0.0002	143	3
-96.9	999.1	0.0002	82	3	-91.0	997.4	0.0002	68	7	-85.1	994.9	0.0002	142	3
-96.8	999.1	0.0002	85	3	-90.9	997.3	0.0002	38	12	-85.0	994.9	0.0002	137	3
-96.7	999.1	0.0002	83	3	-90.8	997.3	0.0002	71	7	-84.9	994.8	0.0002	103	5
-96.6	999.1	0.0002	65	4	-90.7	997.2	0.0002	48	10	-84.8	994.8	0.0002	88	5
-96.5	999.0	0.0002	58	5	-90.6	997.2	0.0002	46	10	-84.7	994.8	0.0002	72	6
-96.4	999.0	0.0002	54	5	-90.5	997.2	0.0002	79	6	-84.6	994.7	0.0002	118	4
-96.3	999.0	0.0002	65	4	-90.4	997.1	0.0002	96	5	-84.5	994.7	0.0002	138	3
-96.2	999.0	0.0002	69	4	-90.3	997.1	0.0002	111	4	-84.4	994.6	0.0002	136	3
-96.1	998.9	0.0002	89	3	-90.2	997.0	0.0002	129	4	-84.3	994.6	0.0002	140	3
-96.0	998.9	0.0002	102	3	-90.1	997.0	0.0002	127	4	-84.2	994.6	0.0002	135	3

Table E.1. HYDRAULIC DATA continued

RM*	$Z^\dagger$	$S^\S$	$w^\#$	Ω^{**}	RM*	$Z^\dagger$	$S^\S$	$w^\#$	Ω^{**}	RM*	$Z^\dagger$	$S^\S$	$w^\#$	Ω^{**}
-84.1	994.5	0.0002	137	3	-78.2	991.4	0.0004	57	14	-72.3	987.1	0.0005	47	22
-84.0	994.5	0.0002	121	4	-78.1	991.3	0.0004	63	13	-72.2	987.0	0.0005	83	12
-83.9	994.4	0.0002	91	5	-78.0	991.3	0.0004	55	14	-72.1	987.0	0.0005	151	7
-83.8	994.4	0.0002	99	5	-77.9	991.2	0.0004	125	6	-72.0	986.9	0.0005	57	18
-83.7	994.4	0.0002	93	5	-77.8	991.2	0.0004	130	6	-71.9	986.8	0.0005	57	18
-83.6	994.3	0.0002	74	6	-77.7	991.1	0.0004	109	7	-71.8	986.7	0.0005	58	18
-83.5	994.3	0.0002	67	7	-77.6	991.0	0.0004	103	8	-71.7	986.7	0.0005	146	7
-83.4	994.2	0.0002	79	6	-77.5	991.0	0.0004	134	6	-71.6	986.6	0.0005	195	5
-83.3	994.2	0.0002	60	8	-77.4	990.9	0.0004	183	4	-71.5	986.5	0.0005	159	6
-83.2	994.2	0.0002	81	6	-77.3	990.9	0.0004	166	5	-71.4	986.4	0.0005	93	11
-83.1	994.1	0.0002	106	4	-77.2	990.8	0.0004	118	7	-71.3	986.4	0.0005	91	11
-83.0	994.1	0.0002	95	5	-77.1	990.8	0.0004	107	7	-71.2	986.3	0.0005	112	9
-82.9	994.0	0.0002	70	7	-77.0	990.7	0.0004	103	8	-71.1	986.2	0.0005	118	9
-82.8	994.0	0.0002	76	6	-76.9	990.6	0.0004	102	8	-71.0	986.1	0.0005	141	7
-82.7	994.0	0.0002	78	6	-76.8	990.6	0.0004	95	10	-70.9	986.1	0.0005	179	6
-82.6	993.9	0.0002	92	5	-76.7	990.5	0.0005	92	11	-70.8	986.0	0.0006	79	17
-82.5	993.9	0.0002	103	4	-76.6	990.4	0.0005	149	7	-70.7	985.9	0.0006	65	22
-82.4	993.8	0.0002	100	5	-76.5	990.4	0.0005	164	6	-70.6	985.8	0.0006	88	16
-82.3	993.8	0.0002	79	6	-76.4	990.3	0.0005	229	4	-70.5	985.7	0.0006	102	14
-82.2	993.8	0.0002	51	9	-76.3	990.2	0.0005	193	5	-70.4	985.6	0.0006	163	9
-82.1	993.7	0.0002	40	12	-76.2	990.1	0.0005	180	6	-70.3	985.5	0.0006	170	8
-82.0	993.7	0.0003	41	12	-76.1	990.1	0.0005	206	5	-70.2	985.4	0.0006	200	7
-81.9	993.6	0.0003	39	16	-76.0	990.0	0.0005	172	6	-70.1	985.3	0.0006	150	9
-81.8	993.6	0.0004	52	14	-75.9	989.9	0.0005	165	6	-70.0	985.2	0.0006	178	8
-81.7	993.5	0.0004	58	12	-75.8	989.8	0.0005	101	10	-69.9	985.1	0.0006	85	17
-81.6	993.4	0.0004	67	11	-75.7	989.8	0.0005	121	8	-69.8	985.0	0.0006	92	15
-81.5	993.4	0.0004	64	11	-75.6	989.7	0.0005	65	16	-69.7	984.9	0.0006	110	13
-81.4	993.3	0.0004	51	14	-75.5	989.6	0.0005	35	29	-69.6	984.7	0.0006	119	12
-81.3	993.3	0.0004	87	8	-75.4	989.5	0.0005	80	13	-69.5	984.6	0.0006	100	14
-81.2	993.2	0.0004	93	8	-75.3	989.5	0.0005	94	11	-69.4	984.5	0.0006	153	8
-81.1	993.1	0.0004	87	8	-75.2	989.4	0.0005	146	7	-69.3	984.5	0.0005	148	7
-81.0	993.1	0.0004	81	9	-75.1	989.3	0.0005	188	5	-69.2	984.4	0.0004	66	14
-80.9	993.0	0.0004	92	8	-75.0	989.2	0.0005	205	5	-69.1	984.3	0.0004	78	12
-80.8	992.9	0.0004	79	9	-74.9	989.2	0.0005	183	6	-69.0	984.3	0.0004	84	11
-80.7	992.9	0.0004	60	12	-74.8	989.1	0.0005	207	5	-68.9	984.2	0.0004	158	6
-80.6	992.8	0.0004	68	11	-74.7	989.0	0.0005	112	10	-68.8	984.1	0.0004	203	5
-80.5	992.8	0.0004	35	21	-74.6	988.9	0.0005	116	10	-68.7	984.1	0.0004	178	5
-80.4	992.7	0.0004	45	16	-74.5	988.9	0.0005	147	8	-68.6	984.0	0.0004	187	5
-80.3	992.6	0.0004	64	11	-74.4	988.8	0.0005	125	9	-68.5	983.9	0.0004	231	4
-80.2	992.6	0.0004	65	11	-74.3	988.7	0.0005	81	14	-68.4	983.9	0.0004	229	4
-80.1	992.5	0.0004	69	10	-74.2	988.6	0.0005	54	21	-68.3	983.8	0.0004	207	5
-80.0	992.4	0.0004	79	9	-74.1	988.5	0.0005	67	17	-68.2	983.7	0.0004	164	6
-79.9	992.4	0.0004	71	10	-74.0	988.4	0.0005	95	12	-68.1	983.7	0.0004	140	7
-79.8	992.3	0.0004	61	12	-73.9	988.4	0.0005	143	8	-68.0	983.6	0.0004	100	9
-79.7	992.3	0.0004	101	7	-73.8	988.3	0.0005	137	8	-67.9	983.5	0.0004	68	14
-79.6	992.2	0.0004	123	6	-73.7	988.2	0.0005	102	11	-67.8	983.4	0.0004	100	9
-79.5	992.1	0.0004	136	5	-73.6	988.1	0.0005	105	11	-67.7	983.4	0.0004	147	6
-79.4	992.1	0.0004	120	6	-73.5	988.0	0.0005	71	16	-67.6	983.3	0.0004	213	4
-79.3	992.0	0.0004	100	7	-73.4	988.0	0.0005	93	12	-67.5	983.2	0.0004	254	4
-79.2	992.0	0.0004	123	5	-73.3	987.9	0.0005	112	10	-67.4	983.2	0.0004	258	4
-79.1	991.9	0.0004	117	6	-73.2	987.8	0.0005	101	11	-67.3	983.1	0.0004	234	4
-79.0	991.8	0.0004	103	6	-73.1	987.7	0.0005	105	11	-67.2	983.0	0.0004	193	5
-78.9	991.8	0.0004	125	5	-73.0	987.6	0.0005	123	9	-67.1	983.0	0.0004	110	9
-78.8	991.7	0.0004	150	4	-72.9	987.5	0.0005	121	9	-67.0	982.9	0.0005	138	7
-78.7	991.7	0.0004	121	5	-72.8	987.5	0.0005	137	7	-66.9	982.8	0.0005	165	6
-78.6	991.6	0.0004	154	4	-72.7	987.4	0.0005	152	7	-66.8	982.8	0.0005	138	7
-78.5	991.6	0.0004	197	4	-72.6	987.3	0.0005	152	7	-66.7	982.7	0.0005	153	7
-78.4	991.5	0.0004	203	4	-72.5	987.3	0.0005	103	10	-66.6	982.6	0.0005	120	9
-78.3	991.4	0.0004	138	6	-72.4	987.2	0.0005	118	9	-66.5	982.5	0.0005	201	5

Table E.1. HYDRAULIC DATA continued

RM*	Z†	S§	w#	Ω**	RM*	Z†	S§	w#	Ω**	RM*	Z†	S§	w#	Ω**
-66.4	982.5	0.0005	241	4	-60.5	978.3	0.0003	202	4	-54.6	975.2	0.0003	149	5
-66.3	982.4	0.0005	257	4	-60.4	978.2	0.0003	294	3	-54.5	975.2	0.0003	141	5
-66.2	982.3	0.0005	191	5	-60.3	978.2	0.0003	330	2	-54.4	975.1	0.0003	147	5
-66.1	982.2	0.0005	174	6	-60.2	978.1	0.0003	326	2	-54.3	975.1	0.0003	158	5
-66.0	982.2	0.0005	152	7	-60.1	978.1	0.0003	259	3	-54.2	975.0	0.0003	181	4
-65.9	982.1	0.0005	159	6	-60.0	978.0	0.0003	145	5	-54.1	975.0	0.0003	213	3
-65.8	982.0	0.0005	152	7	-59.9	978.0	0.0003	132	6	-54.0	974.9	0.0003	236	3
-65.7	981.9	0.0005	210	5	-59.8	977.9	0.0003	122	6	-53.9	974.8	0.0003	257	3
-65.6	981.9	0.0005	231	4	-59.7	977.9	0.0003	113	7	-53.8	974.8	0.0003	222	3
-65.5	981.8	0.0005	196	5	-59.6	977.8	0.0003	158	5	-53.7	974.7	0.0003	219	3
-65.4	981.7	0.0005	147	7	-59.5	977.7	0.0003	126	6	-53.6	974.7	0.0003	246	3
-65.3	981.6	0.0005	114	9	-59.4	977.7	0.0003	129	6	-53.5	974.6	0.0003	206	4
-65.2	981.6	0.0005	87	12	-59.3	977.6	0.0003	199	4	-53.4	974.6	0.0003	178	4
-65.1	981.5	0.0005	142	8	-59.2	977.6	0.0003	255	3	-53.3	974.5	0.0003	220	3
-65.0	981.4	0.0005	190	6	-59.1	977.5	0.0003	298	2	-53.2	974.5	0.0003	284	3
-64.9	981.3	0.0006	256	5	-59.0	977.5	0.0003	274	3	-53.1	974.4	0.0003	271	3
-64.8	981.2	0.0006	187	7	-58.9	977.4	0.0003	282	3	-53.0	974.4	0.0003	307	2
-64.7	981.1	0.0006	184	7	-58.8	977.4	0.0003	274	3	-52.9	974.3	0.0003	291	3
-64.6	981.1	0.0006	171	7	-58.7	977.3	0.0003	268	3	-52.8	974.3	0.0003	261	3
-64.5	981.0	0.0006	83	15	-58.6	977.3	0.0003	254	3	-52.7	974.2	0.0003	201	4
-64.4	980.9	0.0006	80	16	-58.5	977.2	0.0003	218	3	-52.6	974.1	0.0003	149	5
-64.3	980.8	0.0006	146	9	-58.4	977.2	0.0003	107	7	-52.5	974.1	0.0003	188	4
-64.2	980.7	0.0006	134	9	-58.3	977.1	0.0003	123	6	-52.4	974.0	0.0003	217	3
-64.1	980.6	0.0006	192	7	-58.2	977.1	0.0003	142	5	-52.3	974.0	0.0003	228	3
-64.0	980.5	0.0006	278	5	-58.1	977.0	0.0003	126	6	-52.2	973.9	0.0003	210	4
-63.9	980.4	0.0006	348	4	-58.0	976.9	0.0003	114	7	-52.1	973.9	0.0003	224	3
-63.8	980.3	0.0006	384	3	-57.9	976.9	0.0003	158	5	-52.0	973.8	0.0003	230	3
-63.7	980.2	0.0006	263	5	-57.8	976.8	0.0003	162	4	-51.9	973.8	0.0003	176	4
-63.6	980.1	0.0006	173	7	-57.7	976.8	0.0003	178	4	-51.8	973.7	0.0003	138	5
-63.5	980.0	0.0006	117	11	-57.6	976.7	0.0003	153	5	-51.7	973.7	0.0003	177	4
-63.4	980.0	0.0005	137	8	-57.5	976.7	0.0003	174	4	-51.6	973.6	0.0003	150	5
-63.3	979.9	0.0004	117	7	-57.4	976.6	0.0003	207	3	-51.5	973.6	0.0003	72	10
-63.2	979.8	0.0004	136	6	-57.3	976.6	0.0003	208	3	-51.4	973.5	0.0003	85	8
-63.1	979.8	0.0004	260	3	-57.2	976.5	0.0003	275	3	-51.3	973.5	0.0003	109	6
-63.0	979.7	0.0004	240	3	-57.1	976.5	0.0003	290	2	-51.2	973.4	0.0003	142	5
-62.9	979.7	0.0004	159	5	-57.0	976.4	0.0003	286	2	-51.1	973.4	0.0003	173	4
-62.8	979.6	0.0004	87	9	-56.9	976.4	0.0003	238	3	-51.0	973.3	0.0003	230	3
-62.7	979.5	0.0004	141	6	-56.8	976.3	0.0003	210	3	-50.9	973.3	0.0003	242	3
-62.6	979.5	0.0004	157	5	-56.7	976.3	0.0003	167	4	-50.8	973.2	0.0003	243	3
-62.5	979.4	0.0004	154	5	-56.6	976.2	0.0003	193	4	-50.7	973.2	0.0003	193	4
-62.4	979.4	0.0004	146	5	-56.5	976.2	0.0003	174	4	-50.6	973.1	0.0003	130	5
-62.3	979.3	0.0004	120	7	-56.4	976.1	0.0003	129	5	-50.5	973.1	0.0003	93	7
-62.2	979.3	0.0004	113	7	-56.3	976.1	0.0003	108	6	-50.4	973.0	0.0003	118	6
-62.1	979.2	0.0004	176	5	-56.2	976.0	0.0003	134	5	-50.3	973.0	0.0003	92	8
-62.0	979.1	0.0004	223	4	-56.1	976.0	0.0003	150	5	-50.2	972.9	0.0003	79	9
-61.9	979.1	0.0004	298	3	-56.0	975.9	0.0003	100	7	-50.1	972.9	0.0003	58	12
-61.8	979.0	0.0004	272	3	-55.9	975.9	0.0003	133	5	-50.0	972.8	0.0003	107	6
-61.7	979.0	0.0004	203	4	-55.8	975.8	0.0003	211	3	-49.9	972.8	0.0003	165	4
-61.6	978.9	0.0004	218	4	-55.7	975.8	0.0003	177	4	-49.8	972.7	0.0003	170	4
-61.5	978.9	0.0004	213	4	-55.6	975.7	0.0003	151	5	-49.7	972.7	0.0003	195	4
-61.4	978.8	0.0004	198	4	-55.5	975.7	0.0003	92	8	-49.6	972.6	0.0003	179	4
-61.3	978.7	0.0004	207	4	-55.4	975.6	0.0003	83	8	-49.5	972.6	0.0003	162	4
-61.2	978.7	0.0004	258	3	-55.3	975.6	0.0003	138	5	-49.4	972.5	0.0003	137	5
-61.1	978.6	0.0004	304	3	-55.2	975.5	0.0003	190	4	-49.3	972.5	0.0003	139	5
-61.0	978.6	0.0004	363	2	-55.1	975.5	0.0003	179	4	-49.2	972.4	0.0003	116	6
-60.9	978.5	0.0004	335	2	-55.0	975.4	0.0003	180	4	-49.1	972.4	0.0003	87	8
-60.8	978.4	0.0004	325	2	-54.9	975.4	0.0003	160	4	-49.0	972.3	0.0003	139	5
-60.7	978.4	0.0003	154	5	-54.8	975.3	0.0003	164	4	-48.9	972.3	0.0003	185	3
-60.6	978.3	0.0003	129	6	-54.7	975.3	0.0003	150	5	-48.8	972.2	0.0003	264	2

Table E.1. HYDRAULIC DATA continued

RM*	$Z^\dagger$	$S^\S$	$w^\#$	Ω^{**}	RM*	$Z^\dagger$	$S^\S$	$w^\#$	Ω^{**}	RM*	$Z^\dagger$	$S^\S$	$w^\#$	Ω^{**}
-48.7	972.2	0.0003	289	2	-42.8	969.5	0.0003	67	10	-36.9	966.4	0.0004	196	4
-48.6	972.1	0.0003	215	3	-42.7	969.4	0.0003	142	5	-36.8	966.3	0.0004	241	4
-48.5	972.1	0.0003	139	4	-42.6	969.4	0.0003	178	4	-36.7	966.2	0.0003	168	5
-48.4	972.1	0.0003	107	6	-42.5	969.3	0.0003	208	3	-36.6	966.2	0.0003	237	3
-48.3	972.0	0.0003	121	5	-42.4	969.3	0.0003	162	4	-36.5	966.2	0.0002	233	2
-48.2	972.0	0.0003	107	6	-42.3	969.2	0.0003	92	7	-36.4	966.1	0.0002	190	3
-48.1	971.9	0.0003	93	7	-42.2	969.2	0.0003	128	5	-36.3	966.1	0.0002	150	4
-48.0	971.9	0.0003	90	7	-42.1	969.2	0.0003	244	3	-36.2	966.0	0.0002	168	3
-47.9	971.8	0.0003	150	4	-42.0	969.1	0.0003	287	2	-36.1	966.0	0.0002	116	5
-47.8	971.8	0.0003	199	3	-41.9	969.1	0.0003	48	13	-36.0	966.0	0.0002	98	5
-47.7	971.7	0.0003	239	3	-41.8	969.0	0.0003	113	6	-35.9	965.9	0.0002	124	4
-47.6	971.7	0.0003	269	2	-41.7	969.0	0.0003	81	8	-35.8	965.9	0.0002	111	5
-47.5	971.7	0.0003	230	3	-41.6	968.9	0.0003	137	5	-35.7	965.9	0.0002	150	3
-47.4	971.6	0.0003	169	4	-41.5	968.9	0.0003	164	4	-35.6	965.8	0.0002	191	3
-47.3	971.6	0.0003	110	6	-41.4	968.8	0.0003	153	4	-35.5	965.8	0.0002	162	3
-47.2	971.5	0.0003	77	8	-41.3	968.8	0.0003	156	4	-35.4	965.7	0.0002	82	6
-47.1	971.5	0.0003	106	6	-41.2	968.7	0.0003	181	4	-35.3	965.7	0.0002	98	5
-47.0	971.4	0.0003	198	3	-41.1	968.7	0.0003	200	3	-35.2	965.7	0.0002	149	4
-46.9	971.4	0.0003	251	2	-41.0	968.6	0.0003	213	3	-35.1	965.6	0.0002	197	3
-46.8	971.3	0.0003	292	2	-40.9	968.6	0.0003	155	4	-35.0	965.6	0.0002	173	3
-46.7	971.3	0.0003	297	2	-40.8	968.5	0.0003	109	6	-34.9	965.5	0.0002	117	4
-46.6	971.2	0.0003	267	2	-40.7	968.5	0.0003	101	6	-34.8	965.5	0.0002	146	4
-46.5	971.2	0.0003	257	2	-40.6	968.4	0.0003	85	8	-34.7	965.5	0.0002	137	4
-46.4	971.2	0.0003	238	3	-40.5	968.4	0.0003	116	6	-34.6	965.4	0.0002	89	6
-46.3	971.1	0.0003	185	3	-40.4	968.3	0.0003	153	4	-34.5	965.4	0.0002	113	5
-46.2	971.1	0.0003	117	5	-40.3	968.3	0.0003	173	4	-34.4	965.4	0.0002	122	4
-46.1	971.0	0.0003	145	4	-40.2	968.3	0.0003	217	3	-34.3	965.3	0.0002	152	3
-46.0	971.0	0.0003	144	4	-40.1	968.2	0.0003	254	3	-34.2	965.3	0.0002	178	3
-45.9	970.9	0.0003	163	4	-40.0	968.2	0.0003	204	3	-34.1	965.2	0.0002	212	2
-45.8	970.9	0.0003	179	3	-39.9	968.1	0.0003	204	3	-34.0	965.2	0.0002	211	2
-45.7	970.8	0.0003	148	4	-39.8	968.1	0.0003	168	4	-33.9	965.2	0.0002	218	2
-45.6	970.8	0.0003	98	6	-39.7	968.0	0.0003	180	4	-33.8	965.1	0.0002	155	3
-45.5	970.8	0.0003	112	6	-39.6	968.0	0.0003	152	4	-33.7	965.1	0.0002	146	4
-45.4	970.7	0.0003	137	5	-39.5	967.9	0.0003	113	6	-33.6	965.1	0.0002	98	5
-45.3	970.7	0.0003	87	8	-39.4	967.9	0.0003	136	5	-33.5	965.0	0.0002	111	5
-45.2	970.6	0.0003	222	3	-39.3	967.8	0.0003	162	4	-33.4	965.0	0.0002	149	4
-45.1	970.6	0.0003	251	3	-39.2	967.8	0.0003	152	4	-33.3	964.9	0.0002	176	3
-45.0	970.5	0.0003	186	4	-39.1	967.7	0.0003	135	6	-33.2	964.9	0.0002	177	3
-44.9	970.5	0.0003	202	3	-39.0	967.7	0.0004	92	9	-33.1	964.9	0.0002	118	4
-44.8	970.4	0.0003	123	5	-38.9	967.6	0.0004	90	10	-33.0	964.8	0.0002	131	4
-44.7	970.4	0.0003	121	5	-38.8	967.5	0.0004	84	10	-32.9	964.8	0.0002	177	3
-44.6	970.3	0.0003	153	4	-38.7	967.5	0.0004	96	9	-32.8	964.7	0.0002	246	2
-44.5	970.3	0.0003	157	4	-38.6	967.4	0.0004	163	5	-32.7	964.7	0.0002	301	2
-44.4	970.2	0.0003	196	3	-38.5	967.4	0.0004	226	4	-32.6	964.7	0.0002	333	2
-44.3	970.2	0.0003	191	3	-38.4	967.3	0.0004	291	3	-32.5	964.6	0.0002	267	2
-44.2	970.1	0.0003	99	7	-38.3	967.2	0.0004	310	3	-32.4	964.6	0.0002	189	3
-44.1	970.1	0.0003	147	4	-38.2	967.2	0.0004	227	4	-32.3	964.5	0.0002	201	3
-44.0	970.0	0.0003	244	3	-38.1	967.1	0.0004	206	4	-32.2	964.5	0.0002	69	8
-43.9	970.0	0.0003	271	2	-38.0	967.0	0.0004	68	13	-32.1	964.5	0.0002	112	5
-43.8	970.0	0.0003	196	3	-37.9	967.0	0.0004	101	8	-32.0	964.4	0.0002	98	6
-43.7	969.9	0.0003	210	3	-37.8	966.9	0.0004	168	5	-31.9	964.4	0.0002	124	4
-43.6	969.9	0.0003	70	9	-37.7	966.9	0.0004	174	5	-31.8	964.3	0.0002	238	2
-43.5	969.8	0.0003	131	5	-37.6	966.8	0.0004	159	5	-31.7	964.3	0.0002	176	3
-43.4	969.8	0.0003	151	4	-37.5	966.7	0.0004	124	7	-31.6	964.3	0.0002	132	4
-43.3	969.7	0.0003	94	7	-37.4	966.7	0.0004	154	6	-31.5	964.2	0.0002	98	6
-43.2	969.7	0.0003	90	7	-37.3	966.6	0.0004	142	6	-31.4	964.2	0.0002	67	8
-43.1	969.6	0.0003	185	4	-37.2	966.6	0.0004	166	5	-31.3	964.1	0.0002	93	6
-43.0	969.6	0.0003	206	3	-37.1	966.5	0.0004	203	4	-31.2	964.1	0.0002	123	5
-42.9	969.5	0.0003	71	9	-37.0	966.4	0.0004	316	3	-31.1	964.1	0.0002	162	3

Table E.1. HYDRAULIC DATA continued

RM*	$Z^{\dagger}$	$S^{\S}$	$w^{\#}$	Ω^{**}	RM*	$Z^{\dagger}$	$S^{\S}$	$w^{\#}$	Ω^{**}	RM*	$Z^{\dagger}$	$S^{\S}$	$w^{\#}$	Ω^{**}
-31.0	964.0	0.0002	220	3	-25.1	961.4	0.0002	280	2	-19.2	959.3	0.0003	126	5
-30.9	964.0	0.0002	213	3	-25.0	961.3	0.0002	234	2	-19.1	959.3	0.0003	132	4
-30.8	963.9	0.0002	196	3	-24.9	961.3	0.0002	172	2	-19.0	959.3	0.0003	128	5
-30.7	963.9	0.0002	177	3	-24.8	961.3	0.0002	128	3	-18.9	959.2	0.0003	139	4
-30.6	963.9	0.0002	168	3	-24.7	961.2	0.0002	171	2	-18.8	959.2	0.0003	141	4
-30.5	963.8	0.0002	171	3	-24.6	961.2	0.0002	173	2	-18.7	959.1	0.0003	127	5
-30.4	963.8	0.0002	82	7	-24.5	961.2	0.0002	253	2	-18.6	959.1	0.0003	115	5
-30.3	963.7	0.0002	101	5	-24.4	961.2	0.0002	268	2	-18.5	959.1	0.0003	108	5
-30.2	963.7	0.0002	155	4	-24.3	961.1	0.0002	215	2	-18.4	959.0	0.0003	86	7
-30.1	963.7	0.0002	186	3	-24.2	961.1	0.0002	195	2	-18.3	959.0	0.0003	74	8
-30.0	963.6	0.0002	222	2	-24.1	961.1	0.0002	180	2	-18.2	958.9	0.0003	85	7
-29.9	963.6	0.0002	240	2	-24.0	961.0	0.0002	196	2	-18.1	958.9	0.0003	126	5
-29.8	963.5	0.0002	217	3	-23.9	961.0	0.0002	208	2	-18.0	958.8	0.0003	119	5
-29.7	963.5	0.0002	191	3	-23.8	961.0	0.0002	225	2	-17.9	958.8	0.0003	87	7
-29.6	963.5	0.0002	210	3	-23.7	960.9	0.0002	224	2	-17.8	958.8	0.0003	89	7
-29.5	963.4	0.0002	211	3	-23.6	960.9	0.0002	195	2	-17.7	958.7	0.0003	91	6
-29.4	963.4	0.0002	126	4	-23.5	960.9	0.0002	149	3	-17.6	958.7	0.0003	97	6
-29.3	963.3	0.0002	140	4	-23.4	960.8	0.0002	174	2	-17.5	958.6	0.0003	83	8
-29.2	963.3	0.0002	205	3	-23.3	960.8	0.0002	160	3	-17.4	958.6	0.0004	79	11
-29.1	963.3	0.0002	151	4	-23.2	960.8	0.0002	164	3	-17.3	958.5	0.0005	97	11
-29.0	963.2	0.0002	209	3	-23.1	960.8	0.0002	174	2	-17.2	958.4	0.0005	95	11
-28.9	963.2	0.0003	212	3	-23.0	960.7	0.0002	161	3	-17.1	958.4	0.0005	134	8
-28.8	963.1	0.0003	171	4	-22.9	960.7	0.0002	152	3	-17.0	958.3	0.0005	125	8
-28.7	963.1	0.0003	171	4	-22.8	960.7	0.0002	132	3	-16.9	958.2	0.0005	136	7
-28.6	963.0	0.0003	88	8	-22.7	960.6	0.0002	101	4	-16.8	958.1	0.0005	133	8
-28.5	963.0	0.0003	130	6	-22.6	960.6	0.0002	120	4	-16.7	958.1	0.0005	159	6
-28.4	962.9	0.0003	199	4	-22.5	960.6	0.0002	120	4	-16.6	958.0	0.0005	119	9
-28.3	962.9	0.0003	281	3	-22.4	960.5	0.0002	138	3	-16.5	957.9	0.0005	130	8
-28.2	962.8	0.0003	257	3	-22.3	960.5	0.0002	163	3	-16.4	957.8	0.0005	143	7
-28.1	962.8	0.0003	159	5	-22.2	960.5	0.0002	121	4	-16.3	957.8	0.0005	165	6
-28.0	962.7	0.0003	88	8	-22.1	960.4	0.0002	83	5	-16.2	957.7	0.0005	126	8
-27.9	962.7	0.0003	102	7	-22.0	960.4	0.0002	94	5	-16.1	957.6	0.0005	84	12
-27.8	962.6	0.0003	171	4	-21.9	960.4	0.0002	91	5	-16.0	957.5	0.0005	78	13
-27.7	962.6	0.0003	200	4	-21.8	960.4	0.0002	112	4	-15.9	957.5	0.0005	100	10
-27.6	962.5	0.0003	209	4	-21.7	960.3	0.0002	105	4	-15.8	957.4	0.0005	155	7
-27.5	962.4	0.0003	167	4	-21.6	960.3	0.0002	98	4	-15.7	957.3	0.0005	201	5
-27.4	962.4	0.0003	162	5	-21.5	960.3	0.0002	88	5	-15.6	957.3	0.0005	220	5
-27.3	962.3	0.0003	149	5	-21.4	960.2	0.0002	153	3	-15.5	957.2	0.0005	162	6
-27.2	962.3	0.0003	135	6	-21.3	960.2	0.0002	178	2	-15.4	957.1	0.0004	121	8
-27.1	962.2	0.0003	118	6	-21.2	960.2	0.0002	159	3	-15.3	957.0	0.0004	130	7
-27.0	962.2	0.0003	179	4	-21.1	960.1	0.0002	157	3	-15.2	957.0	0.0004	86	10
-26.9	962.1	0.0003	190	4	-21.0	960.1	0.0002	155	3	-15.1	956.9	0.0004	97	9
-26.8	962.1	0.0003	197	4	-20.9	960.1	0.0003	157	4	-15.0	956.8	0.0004	132	7
-26.7	962.0	0.0003	155	5	-20.8	960.0	0.0003	128	5	-14.9	956.8	0.0004	141	6
-26.6	962.0	0.0003	155	5	-20.7	960.0	0.0003	116	5	-14.8	956.7	0.0004	123	7
-26.5	961.9	0.0003	173	4	-20.6	959.9	0.0003	119	5	-14.7	956.7	0.0004	90	10
-26.4	961.9	0.0003	191	4	-20.5	959.9	0.0003	128	5	-14.6	956.6	0.0004	98	9
-26.3	961.8	0.0003	198	4	-20.4	959.9	0.0003	132	4	-14.5	956.5	0.0004	155	6
-26.2	961.7	0.0003	193	4	-20.3	959.8	0.0003	183	3	-14.4	956.5	0.0004	111	8
-26.1	961.7	0.0003	179	4	-20.2	959.8	0.0003	183	3	-14.3	956.4	0.0004	95	9
-26.0	961.6	0.0003	124	5	-20.1	959.7	0.0003	180	3	-14.2	956.4	0.0004	100	9
-25.9	961.6	0.0002	111	4	-20.0	959.7	0.0003	131	4	-14.1	956.3	0.0004	110	8
-25.8	961.6	0.0002	99	4	-19.9	959.6	0.0003	119	5	-14.0	956.2	0.0004	116	7
-25.7	961.5	0.0002	157	3	-19.8	959.6	0.0003	149	4	-13.9	956.2	0.0004	138	6
-25.6	961.5	0.0002	256	2	-19.7	959.6	0.0003	136	4	-13.8	956.1	0.0004	132	6
-25.5	961.5	0.0002	258	2	-19.6	959.5	0.0003	90	6	-13.7	956.0	0.0004	127	7
-25.4	961.5	0.0002	240	2	-19.5	959.5	0.0003	54	11	-13.6	956.0	0.0004	115	7
-25.3	961.4	0.0002	257	2	-19.4	959.4	0.0003	138	4	-13.5	955.9	0.0004	144	6
-25.2	961.4	0.0002	255	2	-19.3	959.4	0.0003	162	4	-13.4	955.9	0.0004	150	6

Table E.1. HYDRAULIC DATA continued

RM*	$Z^\dagger$	$S^\S$	$w^\#$	Ω^{**}	RM*	$Z^\dagger$	$S^\S$	$w^\#$	Ω^{**}	RM*	$Z^\dagger$	$S^\S$	$w^\#$	Ω^{**}
-13.3	955.8	0.0004	166	5	-7.4	953.7	0.0002	81	6	-1.5	951.3	0.0003	130	5
-13.2	955.7	0.0004	138	6	-7.3	953.7	0.0002	65	7	-1.4	951.2	0.0003	123	6
-13.1	955.7	0.0004	95	9	-7.2	953.6	0.0002	96	5	-1.3	951.2	0.0003	82	8
-13.0	955.6	0.0004	85	10	-7.1	953.6	0.0002	96	5	-1.2	951.1	0.0003	94	7
-12.9	955.5	0.0003	94	7	-7.0	953.6	0.0002	101	5	-1.1	951.1	0.0003	114	6
-12.8	955.5	0.0002	99	5	-6.9	953.5	0.0002	134	4	-1.0	951.0	0.0003	120	6
-12.7	955.5	0.0002	120	4	-6.8	953.5	0.0002	136	4	-0.9	951.0	0.0006	113	11
-12.6	955.4	0.0002	107	4	-6.7	953.5	0.0002	139	3	-0.8	950.8	0.0008	101	18
-12.5	955.4	0.0002	149	3	-6.6	953.4	0.0002	93	5	-0.7	950.7	0.0008	114	16
-12.4	955.4	0.0002	94	5	-6.5	953.4	0.0002	92	5	-0.6	950.6	0.0008	98	19
-12.3	955.3	0.0002	60	8	-6.4	953.4	0.0002	114	4	-0.5	950.4	0.0008	168	11
-12.2	955.3	0.0002	55	8	-6.3	953.3	0.0002	92	5	-0.4	950.3	0.0008	165	11
-12.1	955.3	0.0002	74	6	-6.2	953.3	0.0002	165	3	-0.3	950.2	0.0008	141	13
-12.0	955.2	0.0002	142	3	-6.1	953.3	0.0002	158	3	-0.2	950.0	0.0008	159	12
-11.9	955.2	0.0002	141	3	-6.0	953.2	0.0002	143	3	-0.1	949.9	0.0008	163	12
-11.8	955.2	0.0002	134	3	-5.9	953.2	0.0002	172	3	0.0	949.8	0.0021	116	40
-11.7	955.1	0.0002	87	5	-5.8	953.1	0.0002	167	3	0.1	949.2	0.0024	185	29
-11.6	955.1	0.0002	119	4	-5.7	953.1	0.0002	162	3	0.2	949.0	0.0015	216	15
-11.5	955.1	0.0002	82	6	-5.6	953.1	0.0002	133	4	0.3	948.8	0.0015	168	19
-11.4	955.0	0.0002	129	4	-5.5	953.0	0.0002	115	4	0.4	948.5	0.0015	142	23
-11.3	955.0	0.0002	116	4	-5.4	953.0	0.0002	121	4	0.5	948.3	0.0015	112	29
-11.2	955.0	0.0002	188	2	-5.3	953.0	0.0002	128	4	0.6	948.1	0.0015	115	28
-11.1	954.9	0.0002	139	3	-5.2	952.9	0.0002	154	3	0.7	947.8	0.0014	149	21
-11.0	954.9	0.0002	158	3	-5.1	952.9	0.0002	125	4	0.8	947.6	0.0014	167	19
-10.9	954.9	0.0002	127	4	-5.0	952.9	0.0002	108	4	0.9	947.4	0.0014	126	25
-10.8	954.8	0.0002	96	5	-4.9	952.8	0.0002	125	4	1.0	947.1	0.0014	68	46
-10.7	954.8	0.0002	121	4	-4.8	952.8	0.0002	110	4	1.1	946.9	0.0014	74	42
-10.6	954.8	0.0002	140	3	-4.7	952.8	0.0002	130	4	1.2	946.7	0.0014	141	22
-10.5	954.7	0.0002	168	3	-4.6	952.7	0.0002	140	3	1.3	946.5	0.0013	186	16
-10.4	954.7	0.0002	109	4	-4.5	952.7	0.0002	141	3	1.4	946.3	0.0010	193	11
-10.3	954.7	0.0002	100	5	-4.4	952.7	0.0002	146	3	1.5	946.1	0.0008	129	13
-10.2	954.6	0.0002	103	4	-4.3	952.6	0.0002	163	3	1.6	946.0	0.0008	137	12
-10.1	954.6	0.0002	127	4	-4.2	952.6	0.0002	191	3	1.7	945.9	0.0008	98	17
-10.0	954.6	0.0002	215	2	-4.1	952.6	0.0002	206	2	1.8	945.8	0.0008	116	15
-9.9	954.5	0.0002	154	3	-4.0	952.5	0.0002	124	4	1.9	945.7	0.0008	133	13
-9.8	954.5	0.0002	192	2	-3.9	952.5	0.0003	157	4	2.0	945.5	0.0008	96	18
-9.7	954.5	0.0002	262	2	-3.8	952.4	0.0003	167	4	2.1	945.4	0.0008	105	16
-9.6	954.4	0.0002	188	2	-3.7	952.4	0.0003	126	6	2.2	945.3	0.0008	125	14
-9.5	954.4	0.0002	164	3	-3.6	952.3	0.0003	129	5	2.3	945.2	0.0008	130	13
-9.4	954.4	0.0002	102	4	-3.5	952.3	0.0003	116	6	2.4	945.0	0.0008	84	20
-9.3	954.3	0.0002	107	4	-3.4	952.2	0.0003	124	6	2.5	944.9	0.0008	112	15
-9.2	954.3	0.0002	102	5	-3.3	952.2	0.0003	137	5	2.6	944.8	0.0025	105	54
-9.1	954.3	0.0002	93	5	-3.2	952.1	0.0003	174	4	2.7	944.1	0.0050	82	134
-9.0	954.2	0.0002	122	4	-3.1	952.1	0.0003	178	4	2.8	943.2	0.0031	108	64
-8.9	954.2	0.0002	145	3	-3.0	952.0	0.0003	147	5	2.9	943.1	0.0005	124	10
-8.8	954.2	0.0002	93	5	-2.9	952.0	0.0003	137	5	3.0	943.0	0.0005	104	12
-8.7	954.1	0.0002	94	5	-2.8	951.9	0.0003	114	6	3.1	942.9	0.0005	106	11
-8.6	954.1	0.0002	116	4	-2.7	951.9	0.0003	96	7	3.2	942.8	0.0005	57	21
-8.5	954.1	0.0002	131	4	-2.6	951.8	0.0003	105	7	3.3	942.8	0.0005	83	15
-8.4	954.1	0.0002	140	3	-2.5	951.8	0.0003	108	6	3.4	942.7	0.0005	52	24
-8.3	954.0	0.0002	134	4	-2.4	951.7	0.0003	111	6	3.5	942.6	0.0005	91	13
-8.2	954.0	0.0002	85	6	-2.3	951.7	0.0003	116	6	3.6	942.5	0.0005	85	14
-8.1	953.9	0.0002	78	6	-2.2	951.6	0.0003	140	5	3.7	942.4	0.0005	74	16
-8.0	953.9	0.0002	82	6	-2.1	951.6	0.0003	127	5	3.8	942.3	0.0005	86	14
-7.9	953.9	0.0002	80	6	-2.0	951.5	0.0003	141	5	3.9	942.2	0.0005	116	10
-7.8	953.8	0.0002	63	8	-1.9	951.5	0.0003	157	4	4.0	942.1	0.0005	64	19
-7.7	953.8	0.0002	155	3	-1.8	951.4	0.0003	101	7	4.1	942.0	0.0005	97	12
-7.6	953.8	0.0002	128	4	-1.7	951.4	0.0003	75	9	4.2	942.0	0.0005	87	14
-7.5	953.7	0.0002	116	4	-1.6	951.3	0.0003	108	6	4.3	941.9	0.0005	81	15

Table E.1. HYDRAULIC DATA continued

RM*	$Z^\dagger$	$S^\S$	$w^\#$	Ω^{**}	RM*	$Z^\dagger$	$S^\S$	$w^\#$	Ω^{**}	RM*	$Z^\dagger$	$S^\S$	$w^\#$	Ω^{**}
4.4	941.8	0.0005	88	14	10.3	934.0	0.0003	62	10	16.2	918.9	0.0004	83	9
4.5	941.7	0.0005	119	10	10.4	934.0	0.0003	64	9	16.3	918.9	0.0004	75	10
4.6	941.6	0.0004	118	8	10.5	933.9	0.0003	83	7	16.4	918.8	0.0007	71	22
4.7	941.6	0.0003	97	7	10.6	933.9	0.0003	63	10	16.5	918.6	0.0013	77	36
4.8	941.5	0.0003	120	6	10.7	933.9	0.0003	70	9	16.6	918.4	0.0015	53	62
4.9	941.5	0.0003	99	7	10.8	933.8	0.0003	63	10	16.7	918.2	0.0015	92	36
5.0	941.4	0.0003	115	6	10.9	933.8	0.0003	68	9	16.8	917.9	0.0015	89	37
5.1	941.4	0.0003	110	6	11.0	933.7	0.0003	66	9	16.9	917.7	0.0040	84	107
5.2	941.3	0.0003	120	6	11.1	933.7	0.0049	70	156	17.0	916.6	0.0093	84	246
5.3	941.3	0.0003	127	6	11.2	932.2	0.0095	81	261	17.1	914.7	0.0064	91	157
5.4	941.2	0.0003	108	7	11.3	930.6	0.0096	72	297	17.2	914.6	0.0009	61	33
5.5	941.2	0.0003	96	7	11.4	929.1	0.0068	41	367	17.3	914.4	0.0009	82	24
5.6	941.1	0.0003	93	8	11.5	928.4	0.0030	49	135	17.4	914.3	0.0009	69	29
5.7	941.1	0.0003	110	6	11.6	928.1	0.0021	89	52	17.5	914.1	0.0009	65	31
5.8	941.0	0.0003	95	7	11.7	927.8	0.0021	66	70	17.6	914.0	0.0009	66	30
5.9	940.9	0.0003	77	9	11.8	927.4	0.0021	42	111	17.7	913.8	0.0009	39	51
6.0	940.9	0.0003	146	5	11.9	927.1	0.0021	52	88	17.8	913.7	0.0009	51	39
6.1	940.8	0.0003	95	7	12.0	926.8	0.0021	57	81	17.9	913.5	0.0009	57	35
6.2	940.8	0.0003	87	8	12.1	926.4	0.0021	60	77	18.0	913.4	0.0009	57	35
6.3	940.7	0.0003	86	8	12.2	926.1	0.0021	84	55	18.1	913.3	0.0009	74	27
6.4	940.7	0.0003	106	7	12.3	925.8	0.0021	39	119	18.2	913.1	0.0009	58	34
6.5	940.6	0.0003	88	8	12.4	925.4	0.0021	55	84	18.3	913.0	0.0007	66	23
6.6	940.6	0.0003	86	8	12.5	925.1	0.0018	68	59	18.4	912.9	0.0005	109	9
6.7	940.5	0.0003	92	8	12.6	924.8	0.0012	49	54	18.5	912.8	0.0004	71	14
6.8	940.5	0.0003	90	8	12.7	924.7	0.0008	42	44	18.6	912.7	0.0004	73	14
6.9	940.4	0.0003	85	8	12.8	924.6	0.0008	44	43	18.7	912.7	0.0004	57	17
7.0	940.4	0.0003	78	9	12.9	924.4	0.0008	49	38	18.8	912.6	0.0004	52	19
7.1	940.3	0.0003	97	7	13.0	924.3	0.0008	46	40	18.9	912.5	0.0004	78	13
7.2	940.3	0.0003	114	6	13.1	924.2	0.0008	51	37	19.0	912.5	0.0004	59	17
7.3	940.2	0.0003	89	8	13.2	924.0	0.0008	60	31	19.1	912.4	0.0004	46	21
7.4	940.2	0.0003	84	8	13.3	923.9	0.0008	49	38	19.2	912.3	0.0004	66	13
7.5	940.1	0.0003	114	6	13.4	923.8	0.0008	42	45	19.3	912.3	0.0002	68	6
7.6	940.1	0.0002	135	4	13.5	923.6	0.0008	42	45	19.4	912.3	0.0001	107	1
7.7	940.1	0.0002	118	4	13.6	923.5	0.0008	53	33	19.5	912.3	0.0001	53	2
7.8	940.0	0.0065	123	119	13.7	923.4	0.0007	51	30	19.6	912.2	0.0001	84	2
7.9	937.9	0.0115	108	237	13.8	923.3	0.0006	46	30	19.7	912.2	0.0001	79	2
8.0	936.3	0.0056	98	127	13.9	923.2	0.0006	38	37	19.8	912.2	0.0001	73	2
8.1	936.1	0.0010	89	26	14.0	923.1	0.0006	49	28	19.9	912.2	0.0001	77	2
8.2	936.0	0.0010	129	18	14.1	923.0	0.0006	49	28	20.0	912.2	0.0001	62	2
8.3	935.8	0.0010	94	25	14.2	922.9	0.0006	52	26	20.1	912.2	0.0001	76	2
8.4	935.6	0.0010	109	21	14.3	922.8	0.0023	63	82	20.2	912.2	0.0001	54	2
8.5	935.5	0.0010	77	30	14.4	922.1	0.0065	63	230	20.3	912.2	0.0001	70	2
8.6	935.3	0.0010	100	23	14.5	920.7	0.0071	58	276	20.4	912.2	0.0001	66	2
8.7	935.1	0.0010	71	32	14.6	919.8	0.0028	58	108	20.5	912.2	0.0022	83	60
8.8	935.0	0.0010	85	27	14.7	919.8	0.0004	74	11	20.6	911.5	0.0077	76	227
8.9	934.8	0.0010	93	25	14.8	919.7	0.0004	52	15	20.7	909.7	0.0092	69	296
9.0	934.6	0.0008	108	15	14.9	919.6	0.0004	53	15	20.8	908.5	0.0042	35	267
9.1	934.6	0.0004	100	10	15.0	919.6	0.0004	34	23	20.9	908.3	0.0011	70	35
9.2	934.5	0.0003	88	8	15.1	919.5	0.0004	60	13	21.0	908.1	0.0011	57	42
9.3	934.5	0.0003	69	8	15.2	919.5	0.0004	67	12	21.1	908.0	0.0011	86	29
9.4	934.4	0.0003	76	8	15.3	919.4	0.0004	57	14	21.2	907.8	0.0021	59	79
9.5	934.4	0.0003	88	7	15.4	919.4	0.0004	76	10	21.3	907.3	0.0030	76	87
9.6	934.3	0.0003	89	6	15.5	919.3	0.0004	91	9	21.4	906.8	0.0030	51	129
9.7	934.3	0.0003	83	7	15.6	919.3	0.0004	76	10	21.5	906.3	0.0030	75	88
9.8	934.2	0.0003	85	7	15.7	919.2	0.0004	60	13	21.6	905.9	0.0030	56	118
9.9	934.2	0.0003	67	9	15.8	919.1	0.0004	56	14	21.7	905.4	0.0030	39	171
10.0	934.2	0.0003	84	7	15.9	919.1	0.0004	48	16	21.8	904.9	0.0023	71	71
10.1	934.1	0.0003	66	9	16.0	919.0	0.0004	65	12	21.9	904.7	0.0008	61	29
10.2	934.1	0.0003	60	10	16.1	919.0	0.0004	83	9	22.0	904.7	0.0000	117	1

Table E.1. HYDRAULIC DATA continued

RM*	Z†	S§	w#	Ω**	RM*	Z†	S§	w#	Ω**	RM*	Z†	S§	w#	Ω**
22.1	904.6	0.0000	49	2	28.0	883.6	0.0006	83	16	33.9	872.0	0.0001	101	2
22.2	904.6	0.0000	98	1	28.1	883.5	0.0006	62	22	34.0	872.0	0.0001	77	3
22.3	904.6	0.0000	78	1	28.2	883.4	0.0014	54	58	34.1	872.0	0.0001	79	3
22.4	904.6	0.0000	52	1	28.3	883.0	0.0029	86	73	34.2	872.0	0.0001	82	2
22.5	904.6	0.0016	65	53	28.4	882.5	0.0019	78	53	34.3	872.0	0.0001	86	2
22.6	904.1	0.0031	62	110	28.5	882.4	0.0003	51	11	34.4	871.9	0.0001	81	2
22.7	903.6	0.0031	50	138	28.6	882.4	0.0003	97	6	34.5	871.9	0.0001	58	3
22.8	903.1	0.0031	55	125	28.7	882.3	0.0003	92	6	34.6	871.9	0.0016	105	34
22.9	902.6	0.0031	78	88	28.8	882.3	0.0003	77	8	34.7	871.4	0.0029	80	81
23.0	902.2	0.0031	56	123	28.9	882.3	0.0003	70	8	34.8	871.0	0.0014	104	30
23.1	901.7	0.0031	68	101	29.0	882.2	0.0003	78	7	34.9	871.0	0.0002	96	4
23.2	901.2	0.0038	75	113	29.1	882.2	0.0017	70	54	35.0	870.9	0.0002	27	12
23.3	900.4	0.0052	71	162	29.2	881.7	0.0058	71	181	35.1	870.9	0.0016	128	28
23.4	899.5	0.0043	79	121	29.3	880.3	0.0045	60	167	35.2	870.4	0.0006	117	10
23.5	899.1	0.0016	42	85	29.4	880.2	0.0006	50	27	35.6	870.5	0.0009	70	28
23.6	899.0	0.0005	73	16	29.5	880.1	0.0006	85	16	35.7	869.7	0.0025	72	77
23.7	898.9	0.0005	60	20	29.6	880.0	0.0006	83	16	35.8	869.7	0.0002	76	7
23.8	898.8	0.0005	64	19	29.7	879.9	0.0006	92	15	35.9	869.6	0.0002	92	6
23.9	898.7	0.0005	56	21	29.8	879.8	0.0006	48	28	36.0	869.6	0.0031	107	64
24.0	898.6	0.0006	64	22	29.9	879.7	0.0006	73	18	36.1	868.6	0.0074	78	210
24.1	898.5	0.0045	44	229	30.0	879.6	0.0006	74	18	36.2	867.2	0.0045	72	138
24.2	897.2	0.0044	50	197	30.1	879.5	0.0021	78	60	36.3	867.2	0.0001	51	6
24.3	897.1	0.0005	71	16	30.2	879.0	0.0039	72	121	36.4	867.2	0.0001	102	3
24.4	897.0	0.0050	72	153	30.3	878.3	0.0026	63	93	36.5	867.1	0.0001	85	4
24.5	895.5	0.0083	93	200	30.4	878.1	0.0009	45	46	36.6	867.1	0.0001	79	4
24.6	894.3	0.0041	84	109	30.5	878.0	0.0009	97	21	36.7	867.1	0.0001	81	4
24.7	894.2	0.0010	39	57	30.6	877.8	0.0009	76	27	36.8	867.1	0.0001	78	4
24.8	894.0	0.0010	62	36	30.7	877.7	0.0009	79	26	36.9	867.1	0.0001	79	4
24.9	893.8	0.0056	97	128	30.8	877.5	0.0009	64	32	37.0	867.0	0.0003	78	10
25.0	892.2	0.0065	62	232	30.9	877.4	0.0009	68	30	37.1	866.9	0.0006	94	13
25.1	891.8	0.0032	44	164	31.0	877.2	0.0009	52	40	37.2	866.8	0.0006	96	13
25.2	891.2	0.0031	83	83	31.1	877.1	0.0007	80	19	37.3	866.8	0.0006	91	14
25.3	890.8	0.0015	82	41	31.2	877.0	0.0004	66	12	37.4	866.7	0.0006	78	16
25.4	890.7	0.0016	39	92	31.3	877.0	0.0002	53	10	37.5	866.6	0.0006	78	16
25.5	890.2	0.0046	59	175	31.4	876.9	0.0002	84	6	37.6	866.5	0.0006	94	13
25.6	889.2	0.0044	68	145	31.5	876.9	0.0008	73	24	37.7	866.4	0.0006	75	17
25.7	888.8	0.0024	57	92	31.6	876.7	0.0033	79	92	37.8	866.3	0.0006	95	13
25.8	888.4	0.0045	99	102	31.7	875.8	0.0040	78	113	37.9	866.2	0.0006	100	13
25.9	887.4	0.0036	73	110	31.8	875.4	0.0024	35	152	38.0	866.1	0.0006	103	12
26.0	887.3	0.0004	33	28	31.9	875.1	0.0020	103	43	38.1	866.0	0.0006	110	12
26.1	887.2	0.0004	54	17	32.0	874.7	0.0020	113	39	38.2	865.9	0.0006	101	13
26.2	887.2	0.0004	70	13	32.1	874.4	0.0020	100	45	38.3	865.8	0.0006	83	15
26.3	887.1	0.0004	65	14	32.2	874.1	0.0016	119	30	38.4	865.7	0.0006	79	16
26.4	887.0	0.0004	46	20	32.3	873.9	0.0011	93	25	38.5	865.7	0.0006	83	17
26.5	887.0	0.0004	83	11	32.4	873.8	0.0010	86	25	38.6	865.5	0.0009	80	24
26.6	886.9	0.0030	75	90	32.5	873.6	0.0010	75	29	38.7	865.4	0.0010	61	35
26.7	886.0	0.0066	96	154	32.6	873.4	0.0010	86	25	38.8	865.2	0.0010	73	30
26.8	884.8	0.0041	60	152	32.7	873.3	0.0010	75	29	38.9	865.1	0.0010	82	27
26.9	884.7	0.0006	42	32	32.8	873.1	0.0010	57	38	39.0	864.9	0.0010	103	21
27.0	884.6	0.0006	60	22	32.9	873.0	0.0010	65	33	39.1	864.8	0.0010	77	28
27.1	884.5	0.0006	50	27	33.0	872.8	0.0009	77	26	39.2	864.6	0.0010	81	27
27.2	884.4	0.0006	42	32	33.1	872.7	0.0008	75	25	39.3	864.4	0.0007	86	18
27.3	884.3	0.0006	62	22	33.2	872.6	0.0008	108	17	39.4	864.4	0.0003	121	6
27.4	884.2	0.0006	59	23	33.3	872.4	0.0008	78	24	39.5	864.3	0.0002	74	7
27.5	884.1	0.0006	59	23	33.4	872.3	0.0008	72	26	39.6	864.3	0.0002	87	6
27.6	884.0	0.0006	56	24	33.5	872.2	0.0007	92	18	39.7	864.3	0.0002	81	6
27.7	883.9	0.0006	73	19	33.6	872.1	0.0004	88	9	39.8	864.2	0.0002	89	6
27.8	883.8	0.0006	75	18	33.7	872.0	0.0001	70	3	39.9	864.2	0.0002	95	5
27.9	883.7	0.0006	52	26	33.8	872.0	0.0001	62	3	40.0	864.2	0.0002	96	5

Table E.1. HYDRAULIC DATA continued

RM*	Z†	S§	w#	Ω**	RM*	Z†	S§	w#	Ω**	RM*	Z†	S§	w#	Ω**
40.1	864.1	0.0002	85	6	46.0	857.2	0.0003	90	8	51.9	852.0	0.0010	104	21
40.2	864.1	0.0002	62	8	46.1	857.2	0.0003	56	13	52.0	851.8	0.0010	137	17
40.3	864.1	0.0002	104	5	46.2	857.1	0.0003	85	8	52.1	851.7	0.0024	106	50
40.4	864.0	0.0002	99	5	46.3	857.1	0.0003	73	10	52.2	851.1	0.0039	52	165
40.5	864.0	0.0002	99	5	46.4	857.0	0.0003	99	7	52.3	850.4	0.0040	160	56
40.6	864.0	0.0002	96	5	46.5	857.0	0.0003	86	7	52.4	849.8	0.0040	46	195
40.7	863.9	0.0002	91	5	46.6	856.9	0.0002	86	4	52.5	849.1	0.0040	54	167
40.8	863.9	0.0002	103	5	46.7	856.9	0.0001	99	2	52.6	848.5	0.0040	65	138
40.9	863.8	0.0008	79	22	46.8	856.9	0.0001	97	2	52.7	847.8	0.0038	86	99
41.0	863.6	0.0015	103	33	46.9	856.9	0.0001	93	2	52.8	847.3	0.0030	111	59
41.1	863.4	0.0011	71	36	47.0	856.9	0.0001	92	2	52.9	846.9	0.0023	140	37
41.2	863.3	0.0006	43	33	47.1	856.9	0.0003	89	8	53.0	846.5	0.0023	60	87
41.3	863.2	0.0006	102	14	47.2	856.8	0.0007	125	13	53.1	846.1	0.0023	63	83
41.4	863.0	0.0006	133	11	47.3	856.6	0.0008	74	25	53.2	845.7	0.0023	87	60
41.5	862.9	0.0006	129	11	47.4	856.5	0.0008	50	35	53.3	845.4	0.0023	128	41
41.6	862.8	0.0006	93	15	47.5	856.4	0.0008	63	27	53.4	845.0	0.0032	118	61
41.7	862.7	0.0006	89	16	47.6	856.3	0.0008	173	10	53.5	844.3	0.0035	89	88
41.8	862.6	0.0006	121	11	47.7	856.1	0.0008	120	14	53.6	843.9	0.0017	200	19
41.9	862.5	0.0005	104	10	47.8	856.0	0.0008	73	23	53.7	843.8	0.0004	156	5
42.0	862.5	0.0004	77	12	47.9	855.9	0.0008	101	17	53.8	843.7	0.0004	108	8
42.1	862.4	0.0004	85	10	48.0	855.8	0.0008	102	16	53.9	843.7	0.0004	66	13
42.2	862.4	0.0004	83	11	48.1	855.6	0.0008	142	12	54.0	843.6	0.0004	103	8
42.3	862.3	0.0004	79	11	48.2	855.5	0.0008	96	18	54.1	843.5	0.0004	47	18
42.4	862.2	0.0004	91	10	48.3	855.4	0.0008	120	14	54.2	843.5	0.0004	54	16
42.5	862.2	0.0004	103	9	48.4	855.3	0.0008	88	19	54.3	843.4	0.0004	102	8
42.6	862.1	0.0004	104	8	48.5	855.2	0.0008	112	15	54.4	843.4	0.0004	124	7
42.7	862.0	0.0004	100	9	48.6	855.0	0.0010	112	20	54.5	843.3	0.0004	60	14
42.8	862.0	0.0004	107	8	48.7	854.8	0.0012	99	27	54.6	843.2	0.0004	86	10
42.9	861.9	0.0004	102	9	48.8	854.6	0.0012	99	27	54.7	843.2	0.0004	86	10
43.0	861.8	0.0004	105	8	48.9	854.5	0.0012	124	22	54.8	843.1	0.0004	87	10
43.1	861.8	0.0004	111	8	49.0	854.3	0.0012	86	31	54.9	843.1	0.0004	90	9
43.2	861.7	0.0004	95	9	49.1	854.1	0.0012	120	22	55.0	843.0	0.0004	102	8
43.3	861.7	0.0004	77	11	49.2	853.9	0.0012	121	22	55.1	842.9	0.0004	136	6
43.4	861.6	0.0004	87	10	49.3	853.7	0.0012	105	25	55.2	842.9	0.0003	139	5
43.5	861.5	0.0004	65	14	49.4	853.5	0.0013	133	22	55.3	842.8	0.0002	62	8
43.6	861.5	0.0012	84	32	49.5	853.3	0.0014	127	24	55.4	842.8	0.0002	113	4
43.7	861.1	0.0044	153	64	49.6	853.0	0.0014	71	42	55.5	842.8	0.0002	159	3
43.8	860.0	0.0040	116	77	49.7	852.8	0.0008	144	12	55.6	842.7	0.0002	109	4
43.9	859.9	0.0012	85	32	49.8	852.8	0.0002	119	4	55.7	842.7	0.0002	105	4
44.0	859.7	0.0012	44	62	49.9	852.8	0.0002	84	5	55.8	842.7	0.0005	83	14
44.1	859.5	0.0012	150	18	50.0	852.7	0.0002	195	2	55.9	842.5	0.0026	69	82
44.2	859.3	0.0012	87	32	50.1	852.7	0.0002	63	7	56.0	841.9	0.0042	132	71
44.3	859.1	0.0012	53	52	50.2	852.7	0.0002	70	6	56.1	841.2	0.0037	167	49
44.4	858.9	0.0012	47	58	50.3	852.6	0.0002	123	4	56.2	840.7	0.0025	114	49
44.5	858.7	0.0010	110	21	50.4	852.6	0.0002	112	4	56.3	840.4	0.0020	87	51
44.6	858.5	0.0005	80	14	50.5	852.6	0.0002	86	5	56.4	840.0	0.0020	58	76
44.7	858.5	0.0002	124	3	50.6	852.5	0.0002	92	5	56.5	839.7	0.0020	69	63
44.8	858.5	0.0002	54	7	50.7	852.5	0.0002	102	4	56.6	839.4	0.0020	78	56
44.9	858.4	0.0002	112	3	50.8	852.5	0.0002	82	5	56.7	839.1	0.0032	101	69
45.0	858.4	0.0002	108	4	50.9	852.4	0.0002	97	5	56.8	838.4	0.0063	119	118
45.1	858.4	0.0002	55	7	51.0	852.4	0.0002	78	6	56.9	837.1	0.0049	87	125
45.2	858.4	0.0002	124	3	51.1	852.4	0.0002	77	6	57.0	836.8	0.0017	76	49
45.3	858.3	0.0007	91	17	51.2	852.3	0.0002	105	4	57.1	836.5	0.0018	78	52
45.4	858.1	0.0013	114	25	51.3	852.3	0.0002	86	5	57.2	836.2	0.0019	90	47
45.5	857.9	0.0012	92	30	51.4	852.3	0.0002	157	3	57.3	835.9	0.0019	59	71
45.6	857.7	0.0012	96	27	51.5	852.3	0.0002	99	4	57.4	835.6	0.0019	76	55
45.7	857.6	0.0012	101	25	51.6	852.2	0.0002	97	5	57.5	835.3	0.0019	186	23
45.8	857.4	0.0008	95	19	51.7	852.2	0.0002	84	5	57.6	835.0	0.0019	83	50
45.9	857.3	0.0004	82	11	51.8	852.2	0.0006	107	12	57.7	834.7	0.0019	127	33

Table E.1. HYDRAULIC DATA continued

RM*	Z†	S§	w#	Ω**	RM*	Z†	S§	w#	Ω**	RM*	Z†	S§	w#	Ω**
57.8	834.4	0.0019	120	35	63.7	821.2	0.0013	55	54	69.6	801.9	0.0026	101	58
57.9	834.1	0.0019	54	77	63.8	820.9	0.0013	139	21	69.7	801.4	0.0021	178	26
58.0	833.8	0.0018	134	30	63.9	820.7	0.0013	109	27	69.8	801.2	0.0014	90	34
58.1	833.5	0.0017	69	55	64.0	820.5	0.0013	69	43	69.9	801.0	0.0012	71	37
58.2	833.2	0.0017	68	55	64.1	820.3	0.0013	69	43	70.0	800.8	0.0012	83	31
58.3	833.0	0.0017	56	66	64.2	820.1	0.0013	149	20	70.1	800.6	0.0012	150	17
58.4	832.7	0.0017	111	34	64.3	819.9	0.0013	82	36	70.2	800.4	0.0012	118	22
58.5	832.4	0.0017	64	58	64.4	819.7	0.0013	120	24	70.3	800.2	0.0012	74	37
58.6	832.2	0.0017	60	62	64.5	819.5	0.0013	104	28	70.4	800.0	0.0013	72	40
58.7	831.9	0.0015	120	28	64.6	819.2	0.0013	57	51	70.5	799.8	0.0013	93	31
58.8	831.7	0.0010	92	23	64.7	819.0	0.0013	152	19	70.6	799.6	0.0013	128	23
58.9	831.6	0.0006	100	12	64.8	818.8	0.0013	125	23	70.7	799.4	0.0013	119	24
59.0	831.5	0.0006	73	17	64.9	818.6	0.0012	70	36	70.8	799.2	0.0013	143	20
59.1	831.4	0.0006	65	19	65.0	818.5	0.0008	117	15	70.9	799.0	0.0013	99	30
59.2	831.3	0.0006	116	11	65.1	818.4	0.0006	69	18	71.0	798.8	0.0012	93	28
59.3	831.2	0.0006	95	13	65.2	818.3	0.0006	65	19	71.1	798.6	0.0010	102	21
59.4	831.1	0.0006	84	15	65.3	818.2	0.0006	95	13	71.2	798.5	0.0009	108	18
59.5	831.1	0.0013	66	43	65.4	818.1	0.0021	91	51	71.3	798.3	0.0009	118	16
59.6	830.7	0.0025	76	73	65.5	817.5	0.0060	126	106	71.4	798.2	0.0009	135	14
59.7	830.3	0.0030	91	73	65.6	816.2	0.0062	154	90	71.5	798.0	0.0009	74	26
59.8	829.8	0.0027	104	57	65.7	815.5	0.0030	72	93	71.6	797.9	0.0009	91	21
59.9	829.4	0.0020	82	54	65.8	815.2	0.0018	102	40	71.7	797.8	0.0009	138	14
60.0	829.1	0.0015	101	32	65.9	814.9	0.0018	95	43	71.8	797.6	0.0009	147	13
60.1	828.9	0.0013	63	47	66.0	814.6	0.0019	53	80	71.9	797.5	0.0009	181	11
60.2	828.7	0.0013	149	20	66.1	814.3	0.0020	107	42	72.0	797.3	0.0009	89	22
60.3	828.5	0.0013	98	30	66.2	814.0	0.0020	108	42	72.1	797.2	0.0009	110	18
60.4	828.3	0.0013	98	30	66.3	813.7	0.0020	134	34	72.2	797.0	0.0010	154	14
60.5	828.1	0.0013	61	49	66.4	813.3	0.0020	131	34	72.3	796.9	0.0026	144	40
60.6	827.8	0.0012	92	29	66.5	813.0	0.0020	114	40	72.4	796.2	0.0086	81	234
60.7	827.7	0.0008	51	36	66.6	812.7	0.0020	72	63	72.5	794.1	0.0129	99	289
60.8	827.6	0.0005	112	9	66.7	812.4	0.0020	70	64	72.6	792.1	0.0114	133	191
60.9	827.5	0.0004	89	9	66.8	812.0	0.0020	157	29	72.7	790.5	0.0055	94	130
61.0	827.5	0.0004	110	7	66.9	811.7	0.0020	131	34	72.8	790.3	0.0011	152	16
61.1	827.4	0.0004	65	12	67.0	811.4	0.0020	69	65	72.9	790.1	0.0011	61	39
61.2	827.4	0.0004	77	10	67.1	811.1	0.0020	68	66	73.0	789.9	0.0011	81	29
61.3	827.3	0.0015	90	38	67.2	810.7	0.0020	81	56	73.1	789.8	0.0011	102	23
61.4	826.9	0.0028	75	83	67.3	810.4	0.0020	75	60	73.2	789.6	0.0011	89	27
61.5	826.4	0.0028	102	62	67.4	810.1	0.0020	99	45	73.3	789.4	0.0011	77	31
61.6	825.9	0.0028	65	98	67.5	809.8	0.0020	81	55	73.4	789.2	0.0008	105	17
61.7	825.5	0.0028	177	36	67.6	809.4	0.0019	68	61	73.5	789.2	0.0005	83	14
61.8	825.0	0.0024	76	71	67.7	809.1	0.0012	51	53	73.6	789.1	0.0005	91	12
61.9	824.7	0.0015	71	47	67.8	809.0	0.0007	88	17	73.7	789.0	0.0005	119	9
62.0	824.5	0.0010	96	23	67.9	808.9	0.0007	94	16	73.8	788.9	0.0005	61	18
62.1	824.4	0.0010	69	32	68.0	808.8	0.0007	125	12	73.9	788.8	0.0005	72	15
62.2	824.2	0.0010	79	28	68.1	808.7	0.0007	100	15	74.0	788.8	0.0005	114	10
62.3	824.1	0.0010	123	18	68.2	808.6	0.0007	143	11	74.1	788.7	0.0005	58	19
62.4	823.9	0.0011	83	30	68.3	808.5	0.0007	149	10	74.2	788.6	0.0005	66	17
62.5	823.7	0.0013	78	37	68.4	808.4	0.0019	121	35	74.3	788.5	0.0005	75	15
62.6	823.5	0.0013	66	45	68.5	807.9	0.0039	125	69	74.4	788.4	0.0005	72	15
62.7	823.3	0.0013	112	26	68.6	807.1	0.0046	111	93	74.5	788.4	0.0005	61	18
62.8	823.1	0.0013	54	54	68.7	806.4	0.0046	70	147	74.6	788.3	0.0005	97	11
62.9	822.9	0.0013	122	24	68.8	805.6	0.0046	111	93	74.7	788.2	0.0005	80	14
63.0	822.6	0.0013	61	49	68.9	804.9	0.0038	99	85	74.8	788.1	0.0006	95	13
63.1	822.4	0.0013	178	17	69.0	804.4	0.0028	106	58	74.9	788.0	0.0007	83	18
63.2	822.2	0.0013	62	48	69.1	804.0	0.0026	133	44	75.0	787.9	0.0007	83	20
63.3	822.0	0.0013	85	35	69.2	803.6	0.0026	127	46	75.1	787.8	0.0007	90	18
63.4	821.8	0.0013	56	52	69.3	803.1	0.0026	77	76	75.2	787.7	0.0033	89	83
63.5	821.6	0.0013	171	17	69.4	802.7	0.0026	67	88	75.3	786.7	0.0111	100	247
63.6	821.4	0.0013	151	20	69.5	802.3	0.0026	95	62	75.4	784.1	0.0124	80	346

Table E.1. HYDRAULIC DATA continued

RM*	Z†	S§	w#	Ω**	RM*	Z†	S§	w#	Ω**	RM*	Z†	S§	w#	Ω**
75.5	782.7	0.0048	95	113	81.4	758.6	0.0003	59	12	87.3	738.8	0.0005	65	18
75.6	782.5	0.0012	61	43	81.5	758.6	0.0061	45	300	87.4	738.7	0.0005	50	24
75.7	782.3	0.0012	119	22	81.6	756.7	0.0119	57	465	87.5	738.6	0.0019	100	43
75.8	782.2	0.0012	62	42	81.7	754.8	0.0098	52	422	87.6	738.0	0.0035	75	103
75.9	782.0	0.0009	77	25	81.8	753.5	0.0047	59	177	87.7	737.5	0.0036	51	155
76.0	781.9	0.0004	75	12	81.9	753.2	0.0016	48	76	87.8	736.9	0.0036	77	103
76.1	781.8	0.0003	66	8	82.0	753.0	0.0016	51	71	87.9	736.3	0.0043	87	110
76.2	781.8	0.0003	101	6	82.1	752.7	0.0016	58	61	88.0	735.5	0.0050	96	115
76.3	781.8	0.0003	69	8	82.2	752.5	0.0016	50	71	88.1	734.7	0.0050	87	127
76.4	781.7	0.0003	97	6	82.3	752.2	0.0016	29	122	88.2	733.9	0.0050	50	220
76.5	781.7	0.0053	51	231	82.4	752.0	0.0016	50	71	88.3	733.1	0.0047	65	160
76.6	780.0	0.0117	56	465	82.5	751.7	0.0015	42	81	88.4	732.4	0.0034	99	77
76.7	777.9	0.0130	95	305	82.6	751.5	0.0011	48	54	88.5	732.0	0.0025	58	96
76.8	775.8	0.0108	72	335	82.7	751.3	0.0009	46	41	88.6	731.6	0.0025	75	74
76.9	774.5	0.0070	84	184	82.8	751.2	0.0009	57	33	88.7	731.2	0.0025	111	50
77.0	773.6	0.0037	76	109	82.9	751.1	0.0009	53	36	88.8	730.8	0.0028	66	95
77.1	773.2	0.0015	84	40	83.0	750.9	0.0009	34	56	88.9	730.3	0.0055	77	158
77.2	773.1	0.0009	122	16	83.1	750.8	0.0009	65	29	89.0	729.1	0.0078	67	259
77.3	773.0	0.0009	66	30	83.2	750.6	0.0009	51	37	89.1	727.8	0.0078	105	166
77.4	772.8	0.0009	69	29	83.3	750.5	0.0008	72	26	89.2	726.5	0.0052	84	139
77.5	772.7	0.0014	93	35	83.4	750.4	0.0009	64	30	89.3	726.1	0.0016	73	47
77.6	772.4	0.0022	72	68	83.5	750.2	0.0068	59	257	89.4	726.0	0.0004	73	14
77.7	772.0	0.0024	52	102	83.6	748.2	0.0069	82	188	89.5	726.0	0.0004	63	16
77.8	771.6	0.0021	45	105	83.7	748.0	0.0011	41	57	89.6	725.9	0.0004	80	12
77.9	771.3	0.0015	38	86	83.8	747.8	0.0011	30	78	89.7	725.8	0.0004	51	20
78.0	771.1	0.0017	64	60	83.9	747.7	0.0016	49	71	89.8	725.7	0.0004	58	17
78.1	770.7	0.0025	69	81	84.0	747.3	0.0022	41	116	89.9	725.7	-0.0012	56	-47
78.2	770.3	0.0027	68	88	84.1	747.0	0.0022	61	80	90.3	726.7	0.0009	40	51
78.3	769.9	0.0027	60	99	84.2	746.6	0.0022	66	73	90.4	724.9	0.0077	64	270
78.4	769.4	0.0041	46	197	84.3	746.3	0.0019	54	80	90.5	724.2	0.0026	53	107
78.5	768.5	0.0090	57	351	84.4	746.0	0.0013	52	58	90.6	724.1	0.0005	71	16
78.6	766.5	0.0125	56	497	84.5	745.8	0.0010	51	43	90.7	724.0	0.0005	67	17
78.7	764.5	0.0099	63	346	84.6	745.7	0.0058	61	210	90.8	723.9	0.0006	87	16
78.8	763.4	0.0038	61	138	84.7	744.0	0.0075	41	407	90.9	723.8	0.0008	41	44
78.9	763.3	0.0003	65	10	84.8	743.3	0.0029	76	85	91.0	723.7	0.0009	64	31
79.0	763.3	0.0003	51	13	84.9	743.1	0.0017	70	55	91.1	723.5	0.0009	51	39
79.1	763.2	0.0009	60	32	85.0	742.7	0.0022	41	116	91.2	723.4	0.0009	52	38
79.2	763.0	0.0016	56	62	85.1	742.4	0.0022	62	77	91.3	723.3	0.0009	60	33
79.3	762.7	0.0017	59	63	85.2	742.0	0.0022	56	86	91.4	723.1	0.0009	44	45
79.4	762.4	0.0017	57	65	85.3	741.7	0.0022	52	93	91.5	723.0	0.0009	50	40
79.5	762.2	0.0025	51	108	85.4	741.3	0.0015	38	91	91.6	722.8	0.0011	60	40
79.6	761.7	0.0033	44	165	85.5	741.2	0.0009	57	36	91.7	722.6	0.0016	50	71
79.7	761.1	0.0026	59	98	85.6	741.0	0.0009	53	38	91.8	722.3	0.0018	60	66
79.8	760.8	0.0014	45	68	85.7	740.9	0.0009	56	36	91.9	722.0	0.0010	71	31
79.9	760.7	0.0008	55	33	85.8	740.7	0.0009	42	48	92.0	722.0	0.0004	48	17
80.0	760.6	0.0007	54	31	85.9	740.6	0.0009	42	47	92.1	721.9	0.0004	63	13
80.1	760.4	0.0007	43	37	86.0	740.4	0.0009	40	49	92.2	721.9	0.0004	58	14
80.2	760.3	0.0007	68	23	86.1	740.3	0.0009	49	41	92.3	721.8	0.0004	65	13
80.3	760.2	0.0007	28	58	86.2	740.2	0.0009	35	58	92.4	721.8	0.0008	73	25
80.4	760.1	0.0008	42	44	86.3	740.0	0.0011	40	58	92.5	721.5	0.0017	67	55
80.5	759.9	0.0010	45	49	86.4	739.8	0.0012	61	43	92.6	721.2	0.0019	93	47
80.6	759.8	0.0010	46	50	86.5	739.6	0.0012	53	50	92.7	720.9	0.0010	51	44
80.7	759.6	0.0010	47	49	86.6	739.4	0.0011	57	42	92.8	720.9	0.0002	58	7
80.8	759.4	0.0010	61	37	86.7	739.3	0.0008	73	23	92.9	720.9	0.0002	101	4
80.9	759.3	0.0010	37	62	86.8	739.2	0.0005	51	23	93.0	720.8	0.0002	52	7
81.0	759.1	0.0010	51	42	86.9	739.1	0.0005	47	26	93.1	720.8	0.0002	65	6
81.1	759.0	0.0009	46	44	87.0	739.0	0.0005	62	20	93.2	720.8	0.0015	64	53
81.2	758.8	0.0009	69	29	87.1	738.9	0.0005	35	34	93.3	720.3	0.0055	87	140
81.3	758.7	0.0006	58	22	87.2	738.8	0.0005	75	16	93.4	719.0	0.0081	68	266

Table E.1. HYDRAULIC DATA continued

RM*	$Z^\dagger$	$S^\S$	$w^\#$	Ω^{**}	RM*	$Z^\dagger$	$S^\S$	$w^\#$	Ω^{**}	RM*	$Z^\dagger$	$S^\S$	$w^\#$	Ω^{**}
93.5	717.7	0.0081	75	240	99.4	695.3	0.0032	56	129	105.3	676.7	0.0008	70	25
93.6	716.4	0.0067	73	203	99.5	694.4	0.0053	59	200	105.4	676.5	0.0008	65	28
93.7	715.6	0.0030	70	94	99.6	693.6	0.0054	60	201	105.5	676.4	0.0008	49	37
93.8	715.4	0.0007	82	18	99.7	692.6	0.0047	80	131	105.6	676.3	0.0008	36	50
93.9	715.3	0.0007	60	24	99.8	692.1	0.0026	61	96	105.7	676.2	0.0008	53	34
94.0	715.2	0.0007	66	22	99.9	691.8	0.0016	72	50	105.8	676.0	0.0017	55	69
94.1	715.1	0.0007	34	43	100.0	691.5	0.0016	84	43	105.9	675.6	0.0054	51	234
94.2	715.0	0.0007	40	37	100.1	691.3	0.0016	40	91	106.0	674.3	0.0082	50	363
94.3	714.9	0.0007	54	27	100.2	691.0	0.0016	44	81	106.1	673.0	0.0057	42	297
94.4	714.8	0.0007	66	22	100.3	690.8	0.0016	48	75	106.2	672.5	0.0023	51	101
94.5	714.7	0.0007	72	20	100.4	690.5	0.0026	56	103	106.3	672.2	0.0011	55	45
94.6	714.6	0.0007	76	19	100.5	689.9	0.0029	46	143	106.4	672.1	0.0007	78	20
94.7	714.5	0.0018	62	64	100.6	689.6	0.0018	60	66	106.5	672.0	0.0007	66	23
94.8	714.0	0.0065	68	210	100.7	689.4	0.0012	57	46	106.6	671.9	0.0007	40	37
94.9	712.4	0.0100	92	244	100.8	689.2	0.0012	46	57	106.7	671.8	0.0007	42	36
95.0	710.8	0.0079	84	209	100.9	689.0	0.0012	48	55	106.8	671.7	0.0007	51	29
95.1	709.9	0.0031	72	96	101.0	688.8	0.0019	53	79	106.9	671.6	0.0007	37	41
95.2	709.8	0.0004	67	14	101.1	688.4	0.0039	36	240	107.0	671.5	0.0008	46	38
95.3	709.7	0.0004	70	13	101.2	687.5	0.0052	54	213	107.1	671.3	0.0011	51	48
95.4	709.7	0.0004	68	14	101.3	686.7	0.0035	55	143	107.2	671.1	0.0013	55	52
95.5	709.6	0.0004	33	28	101.4	686.4	0.0012	43	63	107.3	670.9	0.0013	61	47
95.6	709.5	0.0004	58	16	101.5	686.3	0.0005	83	14	107.4	670.7	0.0013	46	64
95.7	709.5	0.0004	61	15	101.6	686.2	0.0005	64	18	107.5	670.5	0.0014	48	64
95.8	709.4	0.0004	55	17	101.7	686.1	0.0005	44	26	107.6	670.2	0.0014	71	44
95.9	709.3	0.0004	58	16	101.8	686.1	0.0008	46	36	107.7	670.0	0.0014	55	57
96.0	709.3	0.0004	75	13	101.9	685.9	0.0021	53	90	107.8	669.8	0.0014	44	71
96.1	709.2	0.0004	88	11	102.0	685.4	0.0024	43	126	107.9	669.6	0.0013	64	44
96.2	709.1	0.0004	73	13	102.1	685.1	0.0009	46	42	108.0	669.4	0.0009	70	28
96.3	709.1	0.0004	49	19	102.2	685.1	0.0002	50	7	108.1	669.3	0.0006	49	28
96.4	709.0	0.0004	99	9	102.3	685.1	0.0002	43	9	108.2	669.2	0.0006	66	20
96.5	708.9	0.0026	77	76	102.4	685.0	0.0002	63	6	108.3	669.1	0.0006	58	22
96.6	708.1	0.0071	61	259	102.5	685.0	0.0002	45	8	108.4	669.0	0.0006	71	18
96.7	706.6	0.0092	59	350	102.6	685.0	0.0047	48	215	108.5	668.9	0.0023	48	107
96.8	705.2	0.0047	60	177	102.7	683.5	0.0049	64	170	108.6	668.3	0.0056	58	215
96.9	705.1	0.0003	76	9	102.8	683.4	0.0006	54	25	108.7	667.1	0.0059	59	221
97.0	705.1	0.0003	68	9	102.9	683.3	0.0006	57	24	108.8	666.4	0.0027	60	98
97.1	705.0	0.0003	70	9	103.0	683.2	0.0006	43	32	108.9	666.2	0.0010	45	49
97.2	705.0	0.0003	62	10	103.1	683.1	0.0006	60	23	109.0	666.0	0.0019	47	90
97.3	704.9	0.0003	65	10	103.2	683.0	0.0006	86	16	109.1	665.6	0.0024	66	82
97.4	704.9	0.0003	57	11	103.3	682.9	0.0006	64	22	109.2	665.3	0.0036	67	119
97.5	704.8	0.0003	83	8	103.4	682.8	0.0006	86	17	109.3	664.5	0.0066	72	203
97.6	704.8	0.0005	60	18	103.5	682.7	0.0007	54	27	109.4	663.1	0.0082	65	281
97.7	704.7	0.0007	80	21	103.6	682.6	0.0007	56	26	109.5	661.8	0.0057	70	182
97.8	704.5	0.0008	71	25	103.7	682.5	0.0010	53	42	109.6	661.3	0.0026	60	97
97.9	704.4	0.0008	71	25	103.8	682.3	0.0034	53	142	109.7	661.0	0.0039	75	117
98.0	704.3	0.0008	71	25	103.9	681.4	0.0030	46	147	109.8	660.0	0.0044	72	134
98.1	704.2	0.0009	59	36	104.0	681.3	0.0007	44	35	109.9	659.6	0.0017	55	68
98.2	704.0	0.0061	61	225	104.1	681.2	0.0014	42	74	110.0	659.5	0.0005	92	12
98.3	702.2	0.0112	79	315	104.2	680.9	0.0011	54	46	110.1	659.4	0.0005	72	15
98.4	700.4	0.0101	102	220	104.3	680.8	0.0002	56	7	110.2	659.3	0.0013	74	39
98.5	698.9	0.0048	92	116	104.4	680.8	0.0001	56	5	110.3	659.0	0.0040	61	145
98.6	698.9	0.0005	102	11	104.5	680.8	0.0001	56	5	110.4	658.0	0.0033	48	152
98.7	698.8	0.0005	82	14	104.6	680.8	0.0054	52	233	110.5	657.9	0.0007	59	26
98.8	698.7	0.0005	44	26	104.7	679.0	0.0077	59	288	110.6	657.8	0.0009	58	36
98.9	698.6	0.0005	53	22	104.8	678.3	0.0030	42	156	110.7	657.6	0.0018	50	79
99.0	698.5	0.0005	92	12	104.9	678.1	0.0032	45	157	110.8	657.3	0.0024	48	113
99.1	698.4	0.0046	62	163	105.0	677.3	0.0036	57	142	110.9	656.9	0.0055	52	237
99.2	697.1	0.0094	53	396	105.1	676.9	0.0015	52	62	111.0	655.5	0.0052	53	218
99.3	695.4	0.0056	63	195	105.2	676.8	0.0007	53	31	111.1	655.2	0.0016	43	83

Table E.1. HYDRAULIC DATA continued

RM*	$Z^\dagger$	$S^\S$	$w^\#$	Ω^{**}	RM*	$Z^\dagger$	$S^\S$	$w^\#$	Ω^{**}	RM*	$Z^\dagger$	$S^\S$	$w^\#$	Ω^{**}
111.2	655.0	0.0013	37	81	117.3	641.3	0.0008	61	31	123.5	628.7	0.0033	136	53
111.3	654.7	0.0013	50	59	117.4	641.1	0.0008	60	29	123.6	628.3	0.0019	50	85
111.4	654.5	0.0011	38	66	117.5	641.0	0.0008	47	37	123.7	628.1	0.0013	62	45
111.5	654.4	0.0005	55	21	117.6	640.9	0.0008	36	49	123.8	627.9	0.0012	89	29
111.6	654.4	0.0001	40	7	117.7	640.8	0.0008	50	35	123.9	627.7	0.0011	127	20
111.7	654.3	0.0001	66	4	117.8	640.6	0.0008	61	29	124.0	627.6	0.0011	52	49
111.8	654.3	0.0001	45	6	117.9	640.5	0.0008	120	14	124.1	627.4	0.0011	55	45
111.9	654.3	0.0012	46	60	118.0	640.4	0.0008	65	27	124.2	627.2	0.0011	83	30
112.0	653.9	0.0017	51	76	118.1	640.3	0.0008	57	31	124.3	627.0	0.0031	106	66
112.1	653.8	0.0071	40	390	118.2	640.1	0.0008	54	32	124.4	626.2	0.0032	102	70
112.2	651.7	0.0129	53	545	118.3	640.0	0.0008	102	17	124.5	626.0	0.0008	61	30
112.3	649.6	0.0072	42	382	118.4	639.9	0.0008	69	25	124.6	625.9	0.0003	66	11
112.4	649.3	0.0015	52	66	118.5	639.8	0.0008	79	22	124.7	625.9	0.0010	80	27
112.5	649.1	0.0015	54	64	118.6	639.6	0.0020	80	54	124.8	625.6	0.0033	58	126
112.6	648.9	0.0016	53	67	118.7	639.1	0.0023	57	88	124.9	624.8	0.0050	71	157
112.7	648.6	0.0019	85	49	118.8	638.9	0.0010	113	19	125.0	624.0	0.0050	50	223
112.8	648.2	0.0021	48	98	118.9	638.8	0.0005	88	14	125.1	623.2	0.0050	91	123
112.9	647.9	0.0021	54	86	119.0	638.7	0.0005	117	10	125.2	622.4	0.0050	73	154
113.0	647.6	0.0021	53	88	119.1	638.6	0.0005	91	13	125.3	621.6	0.0034	73	104
113.1	647.2	0.0021	75	64	119.2	638.5	0.0005	68	17	125.4	621.3	0.0012	51	51
113.2	646.9	0.0021	38	127	119.3	638.5	0.0005	61	20	125.5	621.2	0.0005	43	25
113.3	646.5	0.0011	35	72	119.4	638.4	0.0005	120	10	125.6	621.1	0.0005	56	20
113.4	646.5	0.0001	47	5	119.5	638.3	0.0005	103	12	125.7	621.1	0.0007	49	31
113.5	646.5	0.0001	46	3	119.6	638.2	0.0006	66	20	125.8	620.9	0.0022	47	106
113.6	646.5	0.0001	37	4	119.7	638.1	0.0006	110	13	125.9	620.3	0.0022	65	74
113.7	646.5	0.0001	58	3	119.8	638.0	0.0006	85	17	126.0	620.2	0.0008	52	33
113.8	646.5	0.0001	53	3	119.9	637.9	0.0023	94	55	126.1	620.1	0.0008	65	26
113.9	646.5	0.0001	44	4	120.0	637.2	0.0062	82	167	126.2	620.0	0.0019	62	67
114.0	646.5	0.0001	44	4	120.1	635.9	0.0043	47	204	126.3	619.5	0.0037	88	94
114.1	646.4	0.0001	35	4	120.2	635.8	0.0004	60	14	126.4	618.8	0.0038	58	143
114.2	646.4	0.0001	42	4	120.3	635.8	0.0004	46	18	126.5	618.3	0.0030	81	84
114.3	646.4	0.0001	35	4	120.4	635.7	0.0004	91	9	126.6	617.8	0.0031	73	94
114.4	646.4	0.0001	48	3	120.5	635.7	0.0004	88	9	126.7	617.3	0.0036	55	148
114.5	646.4	0.0001	36	4	120.6	635.6	0.0004	67	12	126.8	616.6	0.0037	85	98
114.6	646.4	0.0001	57	3	120.7	635.6	0.0004	39	21	126.9	616.1	0.0019	76	56
114.7	646.4	0.0001	62	3	120.8	635.5	0.0004	156	5	127.0	616.0	0.0005	55	19
114.8	646.4	0.0001	40	4	120.9	635.4	-0.0001	43	-5	127.1	615.9	0.0005	54	20
114.9	646.3	0.0004	51	19	121.3	635.6	-0.0001	58	-4	127.2	615.9	0.0004	70	13
115.0	646.2	0.0024	47	110	121.4	635.5	0.0004	45	18	127.3	615.8	0.0003	73	9
115.1	645.6	0.0029	40	161	121.5	635.4	0.0020	58	78	127.4	615.8	0.0003	66	9
115.2	645.3	0.0019	49	88	121.6	634.9	0.0040	63	141	127.5	615.7	0.0005	44	24
115.3	645.0	0.0019	62	69	121.7	634.2	0.0025	68	81	127.6	615.6	0.0011	79	31
115.4	644.7	0.0019	60	71	121.8	634.1	0.0007	57	26	127.7	615.4	0.0015	46	71
115.5	644.4	0.0019	51	84	121.9	634.0	0.0007	57	26	127.8	615.1	0.0015	65	50
115.6	644.0	0.0019	53	81	122.0	633.8	0.0007	66	22	127.9	614.9	0.0012	34	81
115.7	643.7	0.0005	41	25	122.1	633.7	0.0007	72	21	128.0	614.7	0.0006	59	23
116.0	643.7	0.0001	75	3	122.2	633.6	0.0007	57	26	128.1	614.7	0.0002	42	11
116.1	643.7	0.0005	45	23	122.3	633.5	0.0007	88	17	128.2	614.7	0.0002	67	7
116.2	643.6	0.0005	69	15	122.4	633.4	0.0007	54	27	128.3	614.6	0.0002	27	17
116.3	643.5	0.0005	66	16	122.5	633.3	0.0007	72	21	128.4	614.6	0.0025	34	164
116.4	643.4	0.0005	85	12	122.6	633.2	0.0007	70	23	128.5	613.8	0.0068	51	299
116.5	643.4	0.0018	60	68	122.7	633.1	0.0051	56	200	128.6	612.4	0.0044	48	206
116.6	642.9	0.0032	84	84	122.8	631.6	0.0068	97	156	128.7	612.4	0.0001	62	5
116.7	642.3	0.0027	58	103	122.9	630.9	0.0030	69	98	128.8	612.4	0.0001	63	5
116.8	642.0	0.0015	59	58	123.0	630.6	0.0019	110	38	128.9	612.3	0.0001	61	5
116.9	641.8	0.0009	63	32	123.1	630.3	0.0019	73	57	129.0	612.3	0.0046	55	186
117.0	641.7	0.0009	49	41	123.2	630.0	0.0019	98	43	129.1	610.9	0.0053	65	183
117.1	641.6	0.0009	69	29	123.3	629.7	0.0019	65	65	129.2	610.6	0.0009	43	48
117.2	641.4	0.0009	58	34	123.4	629.4	0.0030	55	119	129.3	610.6	0.0003	47	16

Table E.1. HYDRAULIC DATA continued

RM*	Z†	S§	w#	Ω**	RM*	Z†	S§	w#	Ω**	RM*	Z†	S§	w#	Ω**
129.4	610.5	0.0003	41	18	135.3	590.8	0.0002	67	6	141.2	575.4	0.0005	53	21
129.5	610.4	0.0003	50	15	135.4	590.7	0.0002	50	8	141.3	575.3	0.0004	44	21
129.6	610.4	0.0003	43	17	135.5	590.7	0.0002	46	9	141.4	575.2	0.0004	89	11
129.7	610.3	0.0003	59	13	135.6	590.7	0.0002	54	8	141.5	575.2	0.0004	63	15
129.8	610.3	0.0003	57	13	135.7	590.6	0.0002	27	15	141.6	575.1	0.0004	63	15
129.9	610.2	0.0003	39	19	135.8	590.6	0.0002	46	9	141.7	575.0	0.0004	37	25
130.0	610.2	0.0003	83	9	135.9	590.6	0.0002	48	8	141.8	575.0	0.0004	66	14
130.1	610.1	0.0003	43	17	136.0	590.5	0.0002	36	11	141.9	574.9	0.0004	58	16
130.2	610.1	0.0003	72	10	136.1	590.5	0.0009	43	46	142.0	574.8	0.0004	56	17
130.3	610.0	0.0008	51	36	136.2	590.3	0.0046	57	178	142.1	574.8	0.0004	59	16
130.4	609.8	0.0072	36	442	136.3	589.0	0.0076	44	384	142.2	574.7	0.0004	59	16
130.5	607.7	0.0069	49	316	136.4	587.8	0.0046	54	188	142.3	574.6	0.0004	60	15
130.6	607.6	0.0008	74	23	136.5	587.6	0.0014	55	57	142.4	574.6	0.0003	54	14
130.7	607.5	0.0008	46	37	136.6	587.4	0.0013	54	54	142.5	574.5	0.0003	53	14
130.8	607.3	0.0008	53	32	136.7	587.2	0.0013	64	45	142.6	574.5	0.0003	46	16
130.9	607.2	0.0008	62	28	136.8	587.0	0.0013	75	38	142.7	574.4	0.0003	80	9
131.0	607.1	0.0008	95	18	136.9	586.7	0.0013	49	59	142.8	574.3	0.0003	65	11
131.1	607.0	0.0008	38	45	137.0	586.5	0.0013	86	33	142.9	574.3	0.0003	53	14
131.2	606.8	0.0008	60	29	137.1	586.3	0.0013	73	39	143.0	574.2	0.0003	59	12
131.3	606.7	0.0007	83	18	137.2	586.1	0.0013	36	79	143.1	574.2	0.0003	83	9
131.4	606.6	0.0004	81	11	137.3	585.9	0.0013	76	38	143.2	574.1	0.0003	60	12
131.5	606.6	0.0003	54	11	137.4	585.7	0.0013	64	45	143.3	574.1	0.0003	60	12
131.6	606.5	0.0090	95	210	137.5	585.5	0.0013	53	54	143.4	574.0	0.0008	62	30
131.7	603.7	0.0138	72	427	137.6	585.3	0.0015	62	56	143.5	573.8	0.0041	61	147
131.8	602.1	0.0051	83	138	137.7	585.0	0.0014	58	55	143.6	572.7	0.0067	62	241
131.9	602.0	0.0003	73	10	137.8	584.8	0.0006	110	13	143.7	571.6	0.0067	59	253
132.0	602.0	0.0003	75	9	137.9	584.8	0.0002	55	8	143.8	570.6	0.0068	66	228
132.1	601.9	0.0003	70	10	138.0	584.8	0.0010	60	38	143.9	569.5	0.0065	57	256
132.2	601.9	0.0016	85	41	138.1	584.5	0.0019	83	51	144.0	568.4	0.0037	67	122
132.3	601.4	0.0020	62	74	138.2	584.1	0.0011	64	37	144.1	568.3	0.0010	54	41
132.4	601.2	0.0009	71	28	138.3	584.1	0.0001	56	3	144.2	568.1	0.0025	59	93
132.5	601.1	0.0005	67	18	138.4	584.1	0.0001	69	2	144.3	567.5	0.0024	64	84
132.6	601.1	0.0005	68	18	138.5	584.1	0.0008	59	31	144.4	567.3	0.0007	48	32
132.7	601.0	0.0005	62	20	138.6	583.8	0.0034	70	107	144.5	567.3	0.0018	71	55
132.8	600.9	0.0005	54	22	138.7	583.0	0.0033	88	83	144.6	566.8	0.0019	53	82
132.9	600.8	0.0010	58	38	138.8	582.8	0.0013	35	79	144.7	566.6	0.0006	50	25
133.0	600.6	0.0027	57	107	138.9	582.6	0.0012	51	51	144.8	566.6	0.0003	67	9
133.1	599.9	0.0030	57	118	139.0	582.4	0.0035	68	116	144.9	566.6	0.0022	59	82
133.2	599.6	0.0012	60	44	139.1	581.5	0.0097	58	372	145.0	565.9	0.0037	54	153
133.3	599.5	0.0003	58	13	139.2	579.3	0.0072	87	184	145.1	565.4	0.0025	60	92
133.4	599.5	0.0003	61	13	139.3	579.2	0.0008	57	31	145.2	565.1	0.0016	53	65
133.5	599.4	0.0003	66	12	139.4	579.0	0.0013	75	38	145.3	564.9	0.0016	45	78
133.6	599.4	0.0018	60	65	139.5	578.7	0.0025	70	80	145.4	564.6	0.0016	54	64
133.7	598.8	0.0044	70	140	139.6	578.2	0.0019	80	52	145.5	564.4	0.0021	47	100
133.8	597.9	0.0048	121	88	139.7	578.1	0.0005	47	22	145.6	563.9	0.0037	47	174
133.9	597.3	0.0028	72	88	139.8	578.1	0.0013	68	44	145.7	563.2	0.0025	54	105
134.0	597.0	0.0044	71	138	139.9	577.7	0.0041	53	173	145.8	563.1	0.0003	39	20
134.1	595.9	0.0072	75	214	140.0	576.8	0.0032	55	130	145.9	563.1	0.0003	65	12
134.2	594.7	0.0047	66	158	140.1	576.7	0.0004	33	30	146.0	563.0	0.0007	50	32
134.3	594.4	0.0021	82	57	140.2	576.6	0.0004	68	15	146.1	562.8	0.0016	31	112
134.4	594.0	0.0027	65	94	140.3	576.5	0.0007	57	26	146.2	562.5	0.0020	99	46
134.5	593.5	0.0031	72	97	140.4	576.4	0.0009	53	37	146.3	562.2	0.0018	42	96
134.6	593.0	0.0031	70	99	140.5	576.2	0.0009	48	41	146.4	561.9	0.0010	34	62
134.7	592.5	0.0031	78	89	140.6	576.1	0.0008	75	25	146.5	561.9	0.0003	49	13
134.8	592.0	0.0031	58	121	140.7	576.0	0.0008	50	36	146.6	561.8	0.0003	47	14
134.9	591.5	0.0027	41	145	140.8	575.8	0.0008	57	32	146.7	561.8	0.0003	48	14
135.0	591.1	0.0021	98	48	140.9	575.7	0.0008	44	41	146.8	561.7	0.0003	40	16
135.1	590.8	0.0011	40	61	141.0	575.6	0.0008	49	37	146.9	561.7	0.0003	50	13
135.2	590.8	0.0002	69	6	141.1	575.5	0.0007	47	33	147.0	561.6	0.0003	36	18

Table E.1. HYDRAULIC DATA continued

RM*	$Z^\dagger$	$S^\S$	$w^\#$	Ω^{**}	RM*	$Z^\dagger$	$S^\S$	$w^\#$	Ω^{**}	RM*	$Z^\dagger$	$S^\S$	$w^\#$	Ω^{**}
147.1	561.6	0.0003	51	13	153.0	549.8	0.0005	35	35	158.9	539.9	0.0004	51	19
147.2	561.5	0.0003	44	15	153.1	549.7	0.0005	47	26	159.0	539.8	0.0004	48	20
147.3	561.5	0.0003	51	13	153.2	549.6	0.0029	48	135	159.1	539.7	0.0012	58	46
147.4	561.4	0.0003	45	14	153.3	548.8	0.0028	41	151	159.2	539.4	0.0026	64	92
147.5	561.4	0.0003	38	17	153.4	548.7	0.0002	44	10	159.3	538.9	0.0033	52	141
147.6	561.3	0.0003	39	17	153.5	548.7	0.0039	57	152	159.4	538.3	0.0026	54	106
147.7	561.3	0.0003	48	14	153.6	547.5	0.0043	59	163	159.5	538.0	0.0011	59	43
147.8	561.2	0.0016	40	91	153.7	547.3	0.0010	59	37	159.6	538.0	0.0004	53	19
147.9	560.8	0.0046	43	235	153.8	547.1	0.0009	38	55	159.7	537.9	0.0004	48	20
148.0	559.8	0.0033	48	154	153.9	547.0	0.0009	66	31	159.8	537.8	0.0004	62	15
148.1	559.7	0.0005	45	23	154.0	546.8	0.0007	43	34	159.9	537.8	0.0004	55	17
148.2	559.6	0.0005	43	24	154.1	546.8	0.0003	36	20	160.0	537.7	0.0004	52	19
148.3	559.5	0.0005	48	22	154.2	546.7	0.0002	37	15	160.1	537.6	0.0004	48	20
148.4	559.5	0.0005	55	20	154.3	546.7	0.0002	31	18	160.2	537.6	0.0004	36	27
148.5	559.4	0.0006	66	20	154.4	546.7	0.0002	61	9	160.3	537.5	0.0004	45	21
148.6	559.3	0.0007	58	26	154.5	546.6	0.0002	37	15	160.4	537.4	0.0004	36	27
148.7	559.2	0.0007	51	29	154.6	546.6	0.0002	37	15	160.5	537.3	0.0004	52	18
148.8	559.1	0.0007	61	25	154.7	546.5	0.0002	50	11	160.6	537.3	0.0004	47	20
148.9	558.9	0.0007	44	34	154.8	546.5	0.0011	40	62	160.7	537.2	0.0023	64	81
149.0	558.8	0.0005	46	26	154.9	546.2	0.0013	47	62	160.8	536.5	0.0030	73	91
149.1	558.8	0.0004	57	15	155.0	546.1	0.0004	57	17	160.9	536.2	0.0009	56	37
149.2	558.7	0.0004	43	20	155.1	546.0	0.0003	43	14	161.0	536.2	0.0002	68	5
149.3	558.7	0.0004	47	18	155.2	546.0	0.0003	56	11	161.1	536.2	0.0002	58	6
149.4	558.6	0.0004	49	17	155.3	546.0	0.0003	44	13	161.2	536.2	0.0002	73	5
149.5	558.5	0.0004	63	14	155.4	545.9	0.0021	54	84	161.3	536.1	0.0002	33	10
149.6	558.5	0.0042	53	180	155.5	545.3	0.0030	44	149	161.4	536.1	0.0002	71	5
149.7	557.2	0.0102	61	373	155.6	545.0	0.0018	52	77	161.5	536.1	0.0002	68	5
149.8	555.2	0.0100	41	545	155.7	544.7	0.0024	60	91	161.6	536.1	0.0004	69	13
149.9	553.9	0.0043	58	162	155.8	544.2	0.0020	39	115	161.7	536.0	0.0021	67	69
150.0	553.8	0.0007	52	32	155.9	544.1	0.0006	62	23	161.8	535.4	0.0021	59	80
150.1	553.7	0.0007	56	29	156.0	544.0	0.0005	57	19	161.9	535.3	0.0005	61	17
150.2	553.6	0.0007	56	29	156.1	543.9	0.0005	52	21	162.0	535.3	0.0002	53	9
150.3	553.5	0.0007	38	43	156.2	543.8	0.0005	57	19	162.1	535.2	0.0002	68	7
150.4	553.3	0.0007	49	32	156.3	543.7	0.0005	65	17	162.2	535.2	0.0002	49	10
150.5	553.2	0.0007	43	35	156.4	543.7	0.0005	44	25	162.3	535.2	0.0002	50	9
150.6	553.1	0.0007	40	36	156.5	543.6	0.0005	59	19	162.4	535.1	0.0002	54	9
150.7	553.0	0.0007	38	38	156.6	543.5	0.0008	51	34	162.5	535.1	0.0002	55	8
150.8	552.9	0.0007	36	41	156.7	543.3	0.0024	53	98	162.6	535.1	0.0002	58	8
150.9	552.8	0.0007	49	30	156.8	542.7	0.0030	58	113	162.7	535.0	0.0002	58	8
151.0	552.7	0.0007	51	29	156.9	542.4	0.0012	56	48	162.8	535.0	0.0010	53	43
151.1	552.6	0.0007	40	37	157.0	542.3	0.0001	51	5	162.9	534.7	0.0018	62	65
151.2	552.5	0.0007	49	30	157.1	542.3	0.0000	57	1	163.0	534.4	0.0010	57	40
151.3	552.4	0.0007	40	37	157.2	542.3	0.0000	45	1	163.1	534.4	0.0003	38	16
151.4	552.3	0.0007	39	38	157.3	542.3	0.0000	62	0	163.2	534.3	0.0003	46	13
151.5	552.2	0.0007	42	35	157.4	542.3	0.0000	44	1	163.3	534.3	0.0003	58	10
151.6	552.1	0.0007	50	29	157.5	542.3	0.0000	48	1	163.4	534.2	0.0003	32	19
151.7	552.0	0.0007	34	43	157.6	542.3	0.0006	56	23	163.5	534.2	0.0003	66	9
151.8	551.9	0.0007	59	25	157.7	542.1	0.0016	48	73	163.6	534.1	0.0003	72	8
151.9	551.8	0.0007	48	33	157.8	541.8	0.0012	60	43	163.7	534.1	0.0003	64	9
152.0	551.6	0.0007	39	40	157.9	541.8	0.0003	47	15	163.8	534.1	0.0003	60	10
152.1	551.5	0.0007	58	27	158.0	541.7	0.0003	46	16	163.9	534.0	0.0003	60	10
152.2	551.4	0.0007	57	28	158.1	541.7	0.0020	59	77	164.0	534.0	0.0003	61	10
152.3	551.3	0.0020	43	102	158.2	541.1	0.0021	63	73	164.1	533.9	0.0003	61	10
152.4	550.8	0.0033	59	124	158.3	541.0	0.0004	58	14	164.2	533.9	0.0003	72	8
152.5	550.2	0.0019	49	88	158.4	540.9	0.0004	49	17	164.3	533.8	0.0003	59	10
152.6	550.1	0.0005	43	28	158.5	540.9	0.0007	57	26	164.4	533.8	0.0015	60	55
152.7	550.1	0.0005	56	22	158.6	540.7	0.0022	55	90	164.5	533.4	0.0035	70	113
152.8	550.0	0.0005	56	21	158.7	540.2	0.0025	51	107	164.6	532.7	0.0023	73	70
152.9	549.9	0.0005	50	24	158.8	539.9	0.0010	60	36	164.7	532.6	0.0002	64	8

Table E.1. HYDRAULIC DATA continued

RM*	$Z^\dagger$	$S^\S$	$w^\#$	Ω^{**}	RM*	$Z^\dagger$	$S^\S$	$w^\#$	Ω^{**}	RM*	$Z^\dagger$	$S^\S$	$w^\#$	Ω^{**}
164.8	532.6	0.0002	64	8	170.8	525.7	0.0001	53	5	176.7	515.4	0.0021	126	37
164.9	532.5	0.0002	71	7	170.9	525.7	0.0001	68	4	176.8	514.7	0.0039	58	149
165.0	532.5	0.0003	27	23	171.0	525.7	0.0001	87	3	176.9	514.1	0.0022	133	37
165.1	532.5	0.0010	53	43	171.1	525.7	0.0001	75	3	177.0	514.0	0.0007	121	12
165.2	532.2	0.0009	71	29	171.2	525.7	0.0001	84	3	177.1	513.9	0.0007	140	11
165.3	532.2	0.0002	72	5	171.3	525.6	0.0018	92	43	177.2	513.8	0.0007	101	15
165.4	532.1	0.0001	71	5	171.4	525.1	0.0064	88	162	177.3	513.7	0.0012	121	23
165.5	532.1	0.0001	70	5	171.5	523.6	0.0079	68	257	177.4	513.4	0.0035	93	85
165.6	532.1	0.0001	83	4	171.6	522.5	0.0033	69	107	177.5	512.5	0.0034	104	72
165.7	532.1	0.0001	51	6	171.7	522.5	0.0003	116	5	177.6	512.3	0.0012	64	41
165.8	532.0	0.0001	74	4	171.8	522.5	0.0003	118	5	177.7	512.2	0.0009	151	13
165.9	532.0	0.0001	70	5	171.9	522.4	0.0003	53	12	177.8	512.0	0.0007	111	14
166.0	532.0	0.0001	61	5	172.0	522.4	0.0003	45	14	177.9	511.9	0.0003	78	9
166.1	532.0	0.0001	74	3	172.1	522.3	0.0003	139	4	178.0	511.9	0.0001	58	4
166.2	531.9	0.0000	79	1	172.2	522.3	0.0003	136	5	178.1	511.9	0.0001	93	2
166.4	531.9	0.0013	67	44	172.3	522.2	0.0003	54	11	178.2	511.9	0.0003	88	7
166.5	531.3	0.0048	79	136	172.4	522.2	0.0003	67	9	178.3	511.8	0.0005	85	13
166.6	530.4	0.0030	76	90	172.5	522.1	0.0003	58	11	178.4	511.7	0.0005	83	14
166.7	530.3	0.0004	70	14	172.6	522.1	0.0003	72	9	178.5	511.6	0.0005	87	14
166.8	530.3	0.0004	71	13	172.7	522.0	0.0003	83	7	178.6	511.6	0.0005	81	15
166.9	530.2	0.0004	38	25	172.8	522.0	0.0003	84	7	178.7	511.5	0.0005	68	17
167.0	530.1	0.0004	44	21	172.9	522.0	0.0003	119	5	178.8	511.4	0.0005	78	15
167.1	530.1	0.0004	45	21	173.0	521.9	0.0003	78	8	178.9	511.3	0.0005	75	16
167.2	530.0	0.0004	95	10	173.1	521.9	0.0003	73	8	179.0	511.2	0.0005	72	15
167.3	529.9	0.0004	86	11	173.2	521.8	0.0017	65	57	179.1	511.1	0.0004	85	12
167.4	529.8	0.0004	80	12	173.3	521.3	0.0034	61	125	179.2	511.1	0.0033	61	122
167.5	529.8	0.0004	70	13	173.4	520.7	0.0020	73	62	179.3	510.1	0.0097	84	255
167.6	529.7	0.0004	87	11	173.5	520.7	0.0002	93	5	179.4	508.0	0.0076	67	255
167.7	529.6	0.0004	61	15	173.6	520.6	0.0002	101	4	179.5	507.6	0.0022	68	71
167.8	529.6	0.0004	116	8	173.7	520.6	0.0002	56	8	179.6	507.3	0.0045	66	154
167.9	529.5	0.0006	76	18	173.8	520.6	0.0002	106	4	179.7	506.1	0.0066	40	367
168.0	529.4	0.0048	100	106	173.9	520.6	0.0002	60	7	179.8	505.1	0.0041	42	216
168.1	528.0	0.0053	86	138	174.0	520.5	0.0002	68	7	179.9	504.8	0.0024	62	87
168.2	527.7	0.0011	79	32	174.1	520.5	0.0002	57	8	180.0	504.3	0.0036	89	90
168.3	527.6	0.0004	89	9	174.2	520.5	0.0007	93	16	180.1	503.7	0.0039	48	180
168.4	527.6	0.0004	77	11	174.3	520.3	0.0025	94	59	180.2	503.1	0.0027	81	75
168.5	527.5	0.0004	55	15	174.4	519.7	0.0038	91	92	180.3	502.8	0.0019	81	53
168.6	527.4	0.0004	62	14	174.5	519.1	0.0038	78	108	180.4	502.5	0.0019	122	35
168.7	527.4	0.0004	124	7	174.6	518.4	0.0037	87	94	180.5	502.2	0.0019	53	81
168.8	527.3	0.0004	88	10	174.7	517.9	0.0020	62	71	180.6	501.8	0.0019	84	51
168.9	527.3	0.0004	64	13	174.8	517.8	0.0004	59	16	180.7	501.5	0.0027	75	80
169.0	527.2	0.0004	83	11	174.9	517.7	0.0004	114	8	180.8	501.0	0.0040	89	100
169.1	527.1	0.0004	84	12	175.0	517.7	0.0004	33	28	180.9	500.3	0.0026	102	56
169.2	527.0	0.0004	77	13	175.1	517.6	0.0004	66	14	181.0	500.2	0.0006	95	15
169.3	527.0	0.0004	79	13	175.2	517.5	0.0004	74	13	181.1	500.0	0.0006	61	23
169.4	526.9	0.0004	77	13	175.3	517.5	0.0004	58	16	181.2	499.9	0.0005	129	9
169.5	526.8	0.0004	81	12	175.4	517.4	0.0004	76	12	181.3	499.9	0.0004	62	14
169.6	526.8	0.0004	85	12	175.5	517.3	0.0004	67	14	181.4	499.8	0.0004	107	8
169.7	526.7	0.0004	75	13	175.6	517.3	0.0004	52	18	181.5	499.8	0.0004	112	7
169.8	526.6	0.0016	73	47	175.7	517.2	0.0017	63	59	181.6	499.7	0.0030	67	99
169.9	526.2	0.0020	79	57	175.8	516.7	0.0024	68	77	181.7	498.8	0.0041	73	127
170.0	526.0	0.0009	71	27	175.9	516.4	0.0016	47	78	181.8	498.4	0.0016	90	40
170.1	525.9	0.0003	60	11	176.0	516.2	0.0028	140	44	181.9	498.3	0.0005	82	14
170.2	525.9	0.0003	79	8	176.1	515.5	0.0024	147	36	182.0	498.2	0.0005	79	14
170.3	525.8	0.0002	75	6	176.2	515.4	0.0003	54	14	182.1	498.1	0.0005	60	19
170.4	525.8	0.0001	82	3	176.3	515.4	0.0001	68	3	182.2	498.1	0.0005	102	12
170.5	525.8	0.0001	70	4	176.4	515.4	0.0001	78	3	182.3	498.0	0.0009	111	17
170.6	525.8	0.0001	77	3	176.5	515.4	0.0001	87	2	182.4	497.8	0.0011	104	24
170.7	525.7	0.0001	72	4	176.6	515.4	0.0001	86	2	182.5	497.6	0.0011	83	31

Table E.1. HYDRAULIC DATA continued

RM*	Z†	S§	w#	Ω**	RM*	Z†	S§	w#	Ω**	RM*	Z†	S§	w#	Ω**
182.6	497.4	0.0011	114	22	188.5	486.3	0.0006	62	22	194.4	472.8	0.0018	65	60
182.7	497.2	0.0011	49	51	188.6	486.2	0.0006	81	17	194.5	472.5	0.0020	132	33
182.8	497.1	0.0011	145	17	188.7	486.1	0.0006	97	14	194.6	472.2	0.0027	117	52
182.9	496.9	0.0011	71	34	188.8	486.0	0.0006	53	26	194.7	471.6	0.0022	72	68
183.0	496.7	0.0021	104	46	188.9	485.9	0.0006	48	29	194.8	471.5	0.0011	107	23
183.1	496.2	0.0047	80	130	189.0	485.8	0.0006	109	13	194.9	471.2	0.0025	56	97
183.2	495.2	0.0039	97	90	189.1	485.7	0.0010	114	20	195.0	470.7	0.0027	51	119
183.3	494.9	0.0015	95	35	189.2	485.5	0.0014	90	34	195.1	470.4	0.0012	141	19
183.4	494.7	0.0013	52	54	189.3	485.2	0.0014	77	40	195.2	470.3	0.0006	91	15
183.5	494.5	0.0013	88	32	189.4	485.0	0.0014	102	30	195.3	470.2	0.0010	102	22
183.6	494.3	0.0013	136	21	189.5	484.8	0.0015	109	30	195.4	469.9	0.0021	138	34
183.7	494.1	0.0014	76	41	189.6	484.5	0.0031	48	143	195.5	469.5	0.0020	86	52
183.8	493.9	0.0017	69	54	189.7	483.8	0.0046	60	170	195.6	469.3	0.0012	84	31
183.9	493.6	0.0018	108	38	189.8	483.1	0.0046	66	153	195.7	469.1	0.0012	111	23
184.0	493.3	0.0019	109	39	189.9	482.3	0.0046	150	68	195.8	468.9	0.0012	62	42
184.1	493.0	0.0020	60	75	190.0	481.6	0.0027	158	38	195.9	468.7	0.0012	102	25
184.2	492.6	0.0020	76	59	190.1	481.5	0.0007	47	33	196.0	468.6	0.0012	119	22
184.3	492.3	0.0014	131	23	190.2	481.4	0.0005	131	9	196.1	468.4	0.0015	133	24
184.4	492.2	0.0006	57	24	190.3	481.3	0.0005	90	14	196.2	468.1	0.0018	81	49
184.5	492.1	0.0005	93	13	190.4	481.2	0.0005	113	11	196.3	467.8	0.0018	55	72
184.6	492.0	0.0006	59	22	190.5	481.1	0.0006	81	16	196.4	467.5	0.0014	94	34
184.7	491.9	0.0007	54	28	190.6	481.0	0.0010	64	34	196.5	467.3	0.0009	53	39
184.8	491.8	0.0007	108	15	190.7	480.8	0.0019	60	72	196.6	467.2	0.0007	60	27
184.9	491.7	0.0007	55	29	190.8	480.4	0.0025	83	67	196.7	467.1	0.0007	70	23
185.0	491.6	0.0007	92	17	190.9	480.0	0.0025	96	57	196.8	467.0	0.0007	76	21
185.1	491.5	0.0007	134	12	191.0	479.6	0.0016	90	41	196.9	466.9	0.0007	59	28
185.2	491.4	0.0007	96	16	191.1	479.5	0.0009	112	17	197.0	466.7	0.0007	86	19
185.3	491.2	0.0040	55	161	191.2	479.3	0.0009	71	27	197.1	466.6	0.0007	147	11
185.4	490.1	0.0040	78	114	191.3	479.2	0.0009	128	15	197.2	466.5	0.0007	66	24
185.5	490.0	0.0006	79	17	191.4	479.0	0.0009	114	17	197.3	466.4	0.0007	99	16
185.6	489.9	0.0005	104	11	191.5	478.9	0.0009	134	14	197.4	466.3	0.0007	119	14
185.7	489.8	0.0007	52	30	191.6	478.8	0.0007	45	36	197.5	466.2	0.0005	82	14
185.8	489.7	0.0010	81	28	191.7	478.7	0.0005	56	18	197.6	466.1	0.0002	104	4
185.9	489.5	0.0012	89	29	191.8	478.6	0.0003	74	10	197.7	466.1	0.0001	123	2
186.0	489.3	0.0012	98	26	191.9	478.6	0.0006	98	12	197.8	466.1	0.0001	120	2
186.1	489.1	0.0012	53	48	192.0	478.4	0.0015	142	23	197.9	466.1	0.0001	86	2
186.2	488.9	0.0010	105	20	192.1	478.1	0.0019	118	36	198.0	466.1	0.0001	66	3
186.3	488.8	0.0005	76	15	192.2	477.8	0.0012	53	52	198.1	466.0	0.0001	110	2
186.4	488.7	0.0003	65	10	192.3	477.7	0.0009	43	49	198.2	466.0	0.0001	95	2
186.5	488.7	0.0003	66	10	192.4	477.5	0.0009	85	25	198.3	466.0	0.0001	87	2
186.6	488.6	0.0003	77	8	192.5	477.4	0.0009	40	52	198.4	466.0	0.0013	78	38
186.7	488.6	0.0005	82	13	192.6	477.2	0.0009	65	31	198.5	465.6	0.0021	96	49
186.8	488.5	0.0009	90	21	192.7	477.1	0.0009	57	35	198.6	465.3	0.0025	91	60
186.9	488.3	0.0011	82	29	192.8	476.9	0.0009	91	22	198.7	464.8	0.0057	90	140
187.0	488.1	0.0008	86	20	192.9	476.8	0.0009	96	21	198.8	463.5	0.0067	91	162
187.1	488.1	0.0005	79	13	193.0	476.6	0.0013	83	35	198.9	462.6	0.0034	72	106
187.2	488.0	0.0004	84	12	193.1	476.4	0.0018	70	57	199.0	462.4	0.0016	98	37
187.3	487.9	0.0004	102	10	193.2	476.1	0.0023	46	111	199.1	462.1	0.0016	151	24
187.4	487.9	0.0004	57	17	193.3	475.6	0.0031	88	79	199.2	461.9	0.0015	86	40
187.5	487.8	0.0004	150	6	193.4	475.1	0.0030	144	46	199.3	461.6	0.0015	68	48
187.6	487.7	0.0004	114	8	193.5	474.7	0.0019	122	35	199.4	461.4	0.0015	57	58
187.7	487.7	0.0004	95	10	193.6	474.5	0.0013	73	40	199.5	461.2	0.0015	107	31
187.8	487.6	0.0004	79	12	193.7	474.2	0.0013	195	15	199.6	460.9	0.0013	95	31
187.9	487.5	0.0021	85	55	193.8	474.0	0.0013	120	24	199.7	460.7	0.0006	91	15
188.0	486.9	0.0026	72	81	193.9	473.8	0.0012	120	23	199.8	460.7	0.0001	51	4
188.1	486.7	0.0011	92	25	194.0	473.6	0.0012	112	24	199.9	460.7	0.0001	68	3
188.2	486.6	0.0006	111	12	194.1	473.4	0.0012	92	30	200.0	460.7	0.0001	109	2
188.3	486.5	0.0006	59	23	194.2	473.2	0.0012	69	39	200.1	460.7	0.0001	73	3
188.4	486.4	0.0006	65	21	194.3	473.0	0.0013	92	33	200.2	460.7	0.0001	87	2

Table E.1. HYDRAULIC DATA continued

RM*	$Z^\dagger$	$S^\S$	$w^\#$	Ω^{**}	RM*	$Z^\dagger$	$S^\S$	$w^\#$	Ω^{**}	RM*	$Z^\dagger$	$S^\S$	$w^\#$	Ω^{**}
200.3	460.6	0.0001	70	3	206.2	449.6	0.0023	126	41	212.1	433.7	0.0023	94	56
200.4	460.6	0.0001	119	2	206.3	449.2	0.0023	147	35	212.2	433.1	0.0044	60	162
200.5	460.6	0.0001	80	3	206.4	448.8	0.0023	106	49	212.3	432.3	0.0028	43	142
200.6	460.6	0.0001	84	2	206.5	448.5	0.0023	123	42	212.4	432.2	0.0008	54	35
200.7	460.6	0.0001	81	3	206.6	448.1	0.0020	68	66	212.5	432.0	0.0008	47	40
200.8	460.6	0.0001	91	2	206.7	447.8	0.0017	97	39	212.6	431.9	0.0008	39	49
200.9	460.6	0.0001	130	2	206.8	447.5	0.0017	99	38	212.7	431.8	0.0008	43	44
201.0	460.5	0.0001	115	2	206.9	447.3	0.0017	83	45	212.8	431.6	0.0008	64	27
201.1	460.5	0.0019	89	47	207.0	447.0	0.0017	78	48	212.9	431.5	0.0006	95	15
201.2	459.9	0.0040	100	89	207.1	446.7	0.0019	99	42	213.0	431.4	0.0005	45	27
201.3	459.2	0.0023	92	57	207.2	446.4	0.0023	145	35	213.1	431.3	0.0005	32	38
201.4	459.2	0.0003	129	5	207.3	446.0	0.0026	102	56	213.2	431.2	0.0005	87	14
201.5	459.1	0.0003	68	10	207.4	445.6	0.0022	99	50	213.3	431.2	0.0005	43	28
201.6	459.1	0.0003	132	5	207.5	445.3	0.0015	105	32	213.4	431.1	0.0005	55	22
201.7	459.0	0.0003	93	8	207.6	445.1	0.0012	41	66	213.5	431.0	0.0005	58	21
201.8	459.0	0.0010	108	20	207.7	444.9	0.0012	55	49	213.6	430.9	0.0005	56	22
201.9	458.7	0.0027	99	60	207.8	444.7	0.0012	53	50	213.7	430.8	0.0005	64	19
202.0	458.1	0.0025	105	52	207.9	444.5	0.0012	59	46	213.8	430.7	0.0005	66	18
202.1	457.9	0.0009	92	22	208.0	444.3	0.0012	77	35	213.9	430.6	0.0005	70	17
202.2	457.8	0.0007	51	29	208.1	444.1	0.0012	82	33	214.0	430.5	0.0005	85	14
202.3	457.7	0.0007	45	33	208.2	443.9	0.0012	131	20	214.1	430.4	0.0005	63	19
202.4	457.6	0.0007	147	10	208.3	443.7	0.0012	53	50	214.2	430.4	0.0005	68	18
202.5	457.5	0.0007	164	9	208.4	443.5	0.0010	113	20	214.3	430.3	0.0005	56	21
202.6	457.4	0.0008	86	22	208.5	443.4	0.0009	103	19	214.4	430.2	0.0005	47	25
202.7	457.2	0.0011	70	36	208.6	443.2	0.0009	84	24	214.5	430.1	0.0005	66	16
202.8	457.0	0.0012	65	42	208.7	443.1	0.0009	93	21	214.6	430.0	0.0003	109	7
202.9	456.8	0.0012	85	33	208.8	443.0	0.0009	79	25	214.7	430.0	0.0003	95	7
203.0	456.6	0.0012	128	20	208.9	442.8	0.0028	56	109	214.8	429.9	0.0003	56	11
203.1	456.5	0.0006	101	13	209.0	442.1	0.0050	52	214	214.9	429.9	0.0003	74	8
203.2	456.4	0.0001	88	2	209.1	441.2	0.0054	94	128	215.0	429.9	0.0003	64	10
203.3	456.4	0.0001	90	2	209.2	440.3	0.0054	34	355	215.1	429.8	0.0003	62	10
203.4	456.4	0.0001	79	2	209.3	439.5	0.0042	45	208	215.2	429.8	0.0004	69	13
203.5	456.4	0.0001	94	2	209.4	439.0	0.0024	51	104	215.3	429.7	0.0010	65	35
203.6	456.4	0.0003	105	6	209.5	438.7	0.0017	49	78	215.4	429.4	0.0015	68	50
203.7	456.3	0.0005	103	11	209.6	438.4	0.0017	124	31	215.5	429.2	0.0015	82	41
203.8	456.2	0.0005	105	11	209.7	438.2	0.0017	68	56	215.6	428.9	0.0015	73	46
203.9	456.1	0.0005	108	11	209.8	437.9	0.0017	60	63	215.7	428.7	0.0015	54	62
204.0	456.1	0.0005	113	10	209.9	437.6	0.0016	82	43	215.8	428.5	0.0015	81	41
204.1	456.0	0.0005	99	12	210.0	437.4	0.0014	62	50	215.9	428.2	0.0009	87	24
204.2	455.9	0.0007	98	15	210.1	437.2	0.0013	70	42	216.0	428.2	0.0004	49	19
204.3	455.8	0.0037	67	123	210.2	436.9	0.0012	56	48	216.1	428.1	0.0004	83	11
204.4	454.7	0.0043	74	131	210.3	436.8	0.0008	120	16	216.2	428.0	0.0004	85	11
204.5	454.4	0.0011	106	23	210.4	436.7	0.0006	54	27	216.3	428.0	0.0004	92	10
204.6	454.3	0.0002	79	5	210.5	436.6	0.0006	61	24	216.4	427.9	0.0004	73	13
204.7	454.3	0.0002	95	4	210.6	436.5	0.0006	55	26	216.5	427.8	0.0004	72	13
204.8	454.3	0.0002	94	4	210.7	436.4	0.0006	65	22	216.6	427.8	0.0004	101	9
204.9	454.2	0.0002	105	4	210.8	436.3	0.0006	110	13	216.7	427.7	0.0004	84	11
205.0	454.2	0.0007	110	15	210.9	436.2	0.0007	61	24	216.8	427.6	0.0004	73	13
205.1	454.0	0.0023	124	41	211.0	436.0	0.0008	57	30	216.9	427.6	0.0004	67	14
205.2	453.5	0.0063	187	75	211.1	435.9	0.0009	59	33	217.0	427.5	0.0006	59	24
205.3	452.0	0.0070	130	121	211.2	435.8	0.0009	46	43	217.1	427.4	0.0009	59	34
205.4	451.2	0.0026	123	47	211.3	435.6	0.0009	65	30	217.2	427.2	0.0010	66	33
205.5	451.1	0.0012	84	32	211.4	435.5	0.0009	55	36	217.3	427.0	0.0011	59	40
205.6	450.8	0.0027	60	99	211.5	435.3	0.0018	51	80	217.4	426.9	0.0038	61	139
205.7	450.3	0.0019	70	59	211.6	434.9	0.0033	80	91	217.5	425.8	0.0065	79	183
205.8	450.2	0.0004	170	6	211.7	434.3	0.0028	100	62	217.6	424.8	0.0065	86	167
205.9	450.1	0.0004	58	17	211.8	434.0	0.0012	48	55	217.7	423.7	0.0052	93	124
206.0	450.1	0.0005	56	22	211.9	433.9	0.0006	44	29	217.8	423.1	0.0025	37	147
206.1	450.0	0.0015	75	44	212.0	433.8	0.0006	64	21	217.9	422.9	0.0022	68	73

Table E.1. HYDRAULIC DATA continued

RM*	$Z^{\dagger}$	$S^{\S}$	$w^{\#}$	Ω^{**}	RM*	$Z^{\dagger}$	$S^{\S}$	$w^{\#}$	Ω^{**}	RM*	$Z^{\dagger}$	$S^{\S}$	$w^{\#}$	Ω^{**}
218.0	422.4	0.0028	60	105	223.3	410.2	0.0011	54	45	228.6	395.0	0.0011	53	48
218.1	422.0	0.0012	63	43	223.4	410.1	0.0007	153	11	228.7	394.8	0.0011	47	54
218.2	422.0	0.0001	72	4	223.5	410.0	0.0024	103	53	228.8	394.6	0.0011	69	37
218.3	422.0	0.0001	70	4	223.6	409.3	0.0057	64	200	228.9	394.4	0.0011	40	63
218.4	422.0	0.0001	76	4	223.7	408.2	0.0038	92	92	229.0	394.2	0.0037	46	181
218.5	421.9	0.0001	71	4	223.8	408.1	0.0003	37	19	229.1	393.2	0.0067	101	149
218.6	421.9	0.0001	65	4	223.9	408.1	0.0003	51	14	229.2	392.1	0.0062	64	216
218.7	421.9	0.0001	52	5	224.0	408.0	0.0003	45	15	229.3	391.2	0.0038	45	187
218.8	421.9	0.0001	57	5	224.1	408.0	0.0003	62	11	229.4	390.8	0.0024	61	88
218.9	421.9	0.0001	51	5	224.2	407.9	0.0003	37	19	229.5	390.5	0.0024	64	84
219.0	421.9	0.0001	52	5	224.3	407.9	0.0003	60	12	229.6	390.1	0.0024	70	76
219.1	421.8	0.0002	89	6	224.4	407.8	0.0003	64	11	229.7	389.7	0.0024	44	121
219.2	421.8	0.0017	50	78	224.5	407.8	0.0003	53	13	229.8	389.3	0.0024	43	123
219.3	421.3	0.0027	72	84	224.6	407.7	0.0003	71	10	229.9	388.9	0.0019	53	82
219.4	420.9	0.0013	66	45	224.7	407.7	0.0003	68	10	230.0	388.7	0.0010	42	52
219.5	420.8	0.0003	82	9	224.8	407.6	0.0003	48	14	230.1	388.6	0.0005	63	18
219.6	420.8	0.0003	42	18	224.9	407.6	0.0003	68	10	230.2	388.5	0.0005	42	26
219.7	420.7	0.0003	83	9	225.0	407.5	0.0003	72	10	230.3	388.4	0.0013	53	57
219.8	420.7	0.0009	89	23	225.1	407.5	0.0003	65	11	230.4	388.1	0.0020	44	99
219.9	420.4	0.0017	72	54	225.2	407.4	0.0003	69	10	230.5	387.8	0.0010	33	67
220.0	420.1	0.0018	88	45	225.3	407.4	0.0003	61	11	230.6	387.8	0.0002	45	12
220.1	419.9	0.0009	102	20	225.4	407.3	0.0003	59	12	230.7	387.7	0.0013	50	57
220.2	419.8	0.0003	113	6	225.5	407.3	0.0004	95	10	230.8	387.4	0.0059	64	206
220.3	419.8	0.0003	110	6	225.6	407.2	0.0007	73	20	230.9	385.8	0.0096	48	442
220.4	419.7	0.0026	128	46	225.7	407.0	0.0013	66	45	231.0	384.3	0.0053	46	258
220.5	418.9	0.0053	80	147	225.8	406.7	0.0066	87	171	231.1	384.1	0.0007	43	37
220.6	418.0	0.0055	95	130	225.9	404.9	0.0101	104	215	231.2	384.0	0.0004	38	23
220.7	417.1	0.0043	67	142	226.0	403.5	0.0060	77	174	231.3	384.0	0.0004	51	18
220.8	416.7	0.0018	81	48	226.1	403.0	0.0033	73	101	231.4	383.9	0.0004	34	26
220.9	416.6	0.0005	88	13	226.2	402.4	0.0033	65	112	231.5	383.8	0.0004	37	24
221.0	416.5	0.0015	75	43	226.3	401.9	0.0033	50	148	231.6	383.8	0.0004	37	24
221.1	416.1	0.0022	75	65	226.4	401.4	0.0033	63	117	231.7	383.7	0.0006	40	31
221.2	415.8	0.0016	85	41	226.5	400.8	0.0033	53	140	231.8	383.6	0.0019	37	111
221.3	415.6	0.0012	58	47	226.6	400.3	0.0033	64	116	231.9	383.1	0.0030	59	113
221.4	415.4	0.0012	74	37	226.7	399.8	0.0033	60	123	232.0	382.6	0.0019	56	74
221.5	415.2	0.0012	71	38	226.8	399.2	0.0033	63	116	232.1	382.5	0.0006	57	24
221.6	415.0	0.0012	89	30	226.9	398.7	0.0021	74	62	232.2	382.4	0.0016	36	102
221.7	414.8	0.0021	86	54	227.0	398.6	0.0009	63	33	232.3	382.0	0.0048	50	213
221.8	414.3	0.0034	74	103	227.1	398.4	0.0009	43	48	232.4	380.9	0.0048	49	215
221.9	413.7	0.0025	69	81	227.2	398.3	0.0009	51	41	232.5	380.5	0.0018	56	72
222.0	413.5	0.0009	58	35	227.3	398.1	0.0009	79	26	232.6	380.3	0.0009	34	61
222.1	413.4	0.0006	94	15	227.4	398.0	0.0009	33	63	232.7	380.2	0.0009	48	44
222.2	413.3	0.0006	85	16	227.5	397.8	0.0009	58	36	232.8	380.0	0.0009	35	59
222.3	413.2	0.0006	144	10	227.6	397.7	0.0009	56	37	232.9	379.9	0.0009	43	48
222.4	413.1	0.0006	74	19	227.7	397.5	0.0009	64	33	233.0	379.7	0.0009	47	44
222.5	413.0	0.0006	93	15	227.8	397.4	0.0014	41	75	233.1	379.6	0.0009	48	40
222.6	412.9	0.0006	109	13	227.9	397.1	0.0021	45	104	233.2	379.4	0.0008	52	35
222.7	412.8	0.0008	94	20	228.0	396.7	0.0023	48	108	233.3	379.3	0.0008	30	60
222.8	412.6	0.0041	74	122	228.1	396.3	0.0023	60	85	233.4	379.2	0.0008	61	30
222.9	411.5	0.0042	102	92	228.2	396.0	0.0023	52	98	233.5	379.0	0.0008	38	47
223.0	411.3	0.0019	48	90	228.3	395.6	0.0020	59	74	233.6	378.9	0.0008	63	28
223.1	410.9	0.0025	80	70	228.4	395.3	0.0014	78	39	233.7	378.8	0.0025	53	103
223.2	410.5	0.0020	67	67	228.5	395.1	0.0011	58	44	233.8	378.1	0.0045	49	205

Table E.1. HYDRAULIC DATA continued

RM*	$Z^\dagger$	$S^\S$	$w^\#$	Ω^{**}	RM*	$Z^\dagger$	$S^\S$	$w^\#$	Ω^{**}	RM*	$Z^\dagger$	$S^\S$	$w^\#$	Ω^{**}
233.9	377.3	0.0039	58	151	234.3	376.0	0.0014	40	79	234.7	374.8	0.0002	46	11
234.0	376.9	0.0029	46	142	234.4	375.5	0.0029	79	80	234.8	374.8	0.0002	33	16
234.1	376.4	0.0026	18	331	234.5	375.0	0.0021	42	112	234.9	374.8	0.0002	29	33
234.2	376.0	0.0013	21	141	234.6	374.9	0.0007	49	30					

*River miles referenced to Lees Ferry, AZ. Glen Canyon = negative values, Grand Canyon = positive values.

[†]Pre-dam water's surface elevation of the Colorado River (m).

[§]Channel gradient (m/m).

[#]Channel width (m).

**Unit stream power, calculated as: $\Omega = (\gamma QS)/w$; where Ω is the stream power per unit of bed area (watt/m^2), γ is the specific weight of water (N/m^3), Q is water discharge (m^3/s), S is channel gradient (m/m), and w is channel width (m).